ABSTRACT

MOYER, ALISON ELIZABETH. What is a Fossil? Modeling and Testing the Preservation of Original Tissues in the Rock Record: Keratinous and Other Biologically Derived Materials. (Under the direction of Mary H. Schweitzer).

Fossils preserved with associated soft tissues have been reported since the 1800s, but most have not been rigorously studied at the microscopic and molecular level. This dissertation research focuses on keratinous fossil remains as well as the role of microbes mediating preservation. I tested the *general hypothesis* that if 'soft' (non-biomineralized) structures are preserved in fossils then microscopic structures and proteins found in similar extant tissues should be detectable using methods routinely applied to modern tissues.

Feathers, an evolutionary novelty, are critical to our understanding of the origin of birds. Fossilized feathers have recently been the focus of controversial research claiming that organismal color, and thus ecology, can be determined based on the shape of microbodies within these tissues, observed using scanning electron microscopy, and interpreted as 'melanosomes'. However, when originally observed in 1995, these microbodies were ascribed to bacteria involved in the degradation and/or preservation of these fossil feathers; to date, this hypothesis has not been eliminated. Therefore, in Chapter 2 I demonstrate that microbes can colonize modern feathers in patterns similar to the 'melanosomes' observed in fossil feathers. Because microbes and melanosomes overlap in shape and size, a microbial origin remains a viable hypothesis; thus scientists cannot assume a melanosome origin for all microbodies observed in fossil feathers, nor can these bodies be used to reliably ascribe overall color to the organisms that possess them.

In Chapters 3 and 4, the "melanosome vs. microbe" debate is reviewed in more detail. In Chapter 3, melanin production is differentiated between eukaryotes and prokaryotes, and assumptions underlying the assignment of color in fossil organisms are noted. We examine a fossil fish eyespot as a case study to demonstrate appropriate techniques (e.g. transmission electron microscopy (TEM) and time of flight secondary ion mass spectrometry) and suggested criteria for identifying fossil melanosomes. Shortly following this publication, the field of 'paleocolor' was reviewed; however this was replete with misinterpretations, and in Chapter 4 we respond with clarifications of these misinterpretations and overstatements. Additionally, we

address preservation potentials, the complexity of coloration in animals, and analytical methods which can aid in distinguishing between fossil microbes and melanosomes.

I also considered the relative preservation potentials of feather melanosomes and the keratinous matrix in which they are embedded. To directly test if keratin has a higher inherent preservation potential than melanosomes, I analyzed extant feathers exposed to varying temperatures and moisture conditions for up to 10 years, for the retention of microscopic and molecular components; results are in Chapter 5. Using TEM and immunochemical methods (employing an antibody custom made for this research), I show that even under the harshest conditions, microstructure was preserved, and keratin epitopes could be detected, but no melanosomes were observed. I further demonstrate the durability of keratin and confirm a previous study positing a filament collected from the dinosaur *Shuvuuia deserti* was the remnant of an early feather-like structure.

In Chapter 6, I extend my research to another type of keratinous fossil by analyzing a sample from *Citipati osmolskae*, an oviraptorid dinosaur preserved with purported claw sheath material. Electron microscopy demonstrated that the fossil sample retains micro- and ultrastructure similar to extant emu and ostrich claw sheath. Furthermore, *in situ* immunohistochemistry demonstrates localized, endogenous keratinous epitopes consistent with extant claw tissue.

Finally, because microbes have been posited to be actively involved in the preservation of feather, I chose to revisit the hypothesis that they also played a role in “soft tissues” of another type. We tested the hypothesis that previously reported blood vessels derived from dinosaur bone may have a microbial source. Using small cubes of bone in which all organics were removed, we showed that although biofilms will grow when nutrients are supplied, electron microscopy and immunochemical methods refute a biofilm origin of these structures.

In short, this research indicates keratinous remains are amenable to molecular paleontological studies and taphonomic experiments are needed to elucidate preservational mechanisms.

What is a Fossil? Modeling and Testing the Preservation of Original Tissues in the Rock Record: Keratinous and Other Biologically Derived Materials

by
Alison Elizabeth Moyer

A dissertation submitted to the Graduate Faculty of
North Carolina State University
in partial fulfillment of the
requirements for the degree of
Doctor of Philosophy

Zoology

Raleigh, North Carolina

2016

APPROVED BY:

_____	_____
Mary H. Schweitzer Committee Chair	Lindsay E. Zanno
_____	_____
Amy M. Grunden	Michael B. Goshe

_____
Roger H. Sawyer

DEDICATION

I would like to dedicate my doctoral dissertation to my loving and supportive family: Mom (Joyce Moyer), Dad (Ron E. Moyer Jr.), Sister (Jennifer Petrucelli), Brother (Ron E. Moyer III), Nephew (Parker Petrucelli), and Niece (Alexandra Petrucelli). Thank you for your constant support (of all varieties) and encouraging me to pursue my dreams, no matter how crazy they may seem. I would also like to dedicate this to the three family members I lost along the way: Aunt Donna, my Babci (Mary Zagorski) and Baby Alexander. Thank you for being a constant reminder of what *really* matters.

BIOGRAPHY

My name is Alison Elizabeth Moyer. I am from Langhorne, Pennsylvania. I am the daughter of Ronald (Jr.) and Joyce Moyer, sibling of Jennifer Petrucelli (married to Daniel Petrucelli) and Ronald Moyer III and Aunt of Parker and Alexandra Petrucelli. I was awarded a Bachelor's of Science degree from Drexel University (Philadelphia, PA) where I majored in biology with a concentration in paleontology and geology. I have always had an interest in the natural world which I started to explore at an early age at my family's summer home on the New Jersey side of the Delaware Bay. But my interest in dinosaurs was not sparked until I was a freshman at Drexel University where I met Dr. Kenneth Lacovara whom, in the same year, introduced me to Dr. Mary Schweitzer; they became my undergraduate advisor and graduate advisor, respectively. I began my paleontological career by excavating at a marl pit in Sewell, NJ (now the Rowan University Fossil Quarry). Shortly after, I embarked on an expedition with Dr. Lacovara and the rest of his team to the Santa Cruz Province of Patagonia, Argentina to dig up *Dreadnoughtus schrani*, one of the world's most complete massive dinosaurs ever discovered. After my undergraduate degree, I worked as a biology lab technician for my alma mater, Drexel University. I took what I was learning and the paleontology passion I discovered and decided I wanted to go to graduate school and study under Dr. Mary Schweitzer doing molecular paleontology and the type of research that captivated me back when I was a freshman.

ACKNOWLEDGMENTS

I would like to thank my advisor, Mary H. Schweitzer, and my other four committee members, Lindsay Zanno, Amy Grunden, Mike Goshe, and Roger Sawyer, for their mentorship, guidance, and encouragement during this research and my tenure as a graduate student. A sincere thank you to Megan (Wenxia) Zheng for helping me every day to acquire these data. I would also like to thank all my co-authors and collaborators including but not limited to Ken Lacovara, Matt Lamanna, Johan Lindgren, Johan Gren. Thank you to Luis Chiappe, Alan Titus, Mark Norell, Amy Davidson, Phil Currie, Vince Schneider, Ken Anderson (Poultry Unit at NCSU), Doug Czajka, Thomas Marrow for their contribution of fossil and extant samples for these studies. Thanks to Toby Tung, Sue Brumfield, and Jeanette Shipley-Phillips for their help with electron microscopy. I'd also like to thank all my fellow grad students and paleo-mates, Amanda Hale, Tim Cleland, Liz Johnson, Kate Dzikiewicz, Edwin Cadena, Tyler Bridges, Elena Schroeter, Khai Button, Susan Drymala, and Victoria Arbour for their helpful discussion and companionship. A special thank you to my roommates Kyle Dawson, Matt Blackmon, Sara Schultz, Ashley Hanes, Margaret Frey and Lilly. Thanks to my 'glam squad', Bonnie Garcia-Gloeckner, Sara Schultz, Tom Long, Nick Staeck, Vincent Cheng, Ken Lacovara, Doug Czajka. I'd like to thank my students for inspiring me. Thank you to all the faculty, staff and students in MEAS and Biology. To all my friends, including the OB squad and the BNQ gang, for their support and friendship. And of course a big thank you to my family, Mom, Dad, Jenn, Dan, Ronnie, Parker, Alex, grandparents, cousins, aunts, and uncles for their constant love and support!

TABLE OF CONTENTS

LIST OF TABLES viii
LIST OF FIGURES ix
CHAPTER 1: INTRODUCTION 1
Skin as an organ and its components 1
Evolution of alpha-keratin 3
Evolution of beta-keratin 3
Beta-keratin terminology 4
Beta-keratin and the evolution of the gene family 5
Evolutionary context of skin variants across taxa 6
Feathers as an evolutionary novelty 9
The fossil record of keratinous structures 10
Epidermal appendages in the fossil record 13
Alpha-keratin derivatives 13
Beta-keratin derivatives 13
Feathers 13
Modes of preservation of keratinous structures in the fossil record 15
Feathers 15
Claw sheaths 19
Beaks 20
Bony correlates of keratinous coverings 20
Methods 21
Criteria for endogeneity 22
Role of microbes in preservation 23
In bone 24
Other modes 26
Melanin 26
Actualistic taphonomy 27
Implications 28
References 29
CHAPTER 2: MELANOSOMES OR MICROBES: TESTING AN ALTERNATIVE HYPOTHESIS FOR THE ORIGIN OF MICROBODIES IN FOSSIL FEATHERS 54
Abstract 54
Results 55
Discussion 58
Methods 61
References 61
Acknowledgements 62
Author contributions 62
Additional information 62
Supplementary information 63
CHAPTER 3: INTERPRETING MELANIN-BASED COLORATION THROUGH DEEP TIME: A CRITICAL REVIEW 68
Abstract 68
Introduction 68

Vertebrate melanogenesis 69
Melanin synthesis in microorganisms 69
Melanin and melanosomes in the fossil record 70
Assumptions underlying assignment of colour to fossil organisms 70
Assumption 1: melanosomes are inherently resistant to degradation 70
Assumption 2: melanin pigments confer resistance to degradation 70
Assumption 3: fossil microbody shape and size are reliable indicators of colour 71
A way forward: integrated morphological and geochemical approaches 71
Case study: structural and molecular identification of fossil melanosomes ...71
Rationale for assignment of the fossil microbodies to remnant melanosomes 73
Summary 73
Data accessibility 73
Authors' contributions 73
Competing interests 73
Funding 73
Acknowledgements 74
References 74
Electronic supplementary material 77
Supplementary methods 79
Specimen details and reference materials 79
Scanning electron microscopy (SEM) 79
Transmission electron microscopy (TEM) 80
Time-of-flight secondary ion mass spectrometry (ToF-SIMS) 80
Infrared (IR) microspectroscopy 81
Additional information on molecular analyses 81
CHAPTER 4: MELANOSOMES AND ANCIENT COLORATION REEXAMINED: A RESPONSE TO VINTHER 2015 (DOI 10.1002/BIES.201500018) 93
Abstract 93
Introduction 93
The role of pigments in biology and evolution 93
What is the preservation potential of melanosomes, and how are the altered through geological time 94
Chemical characterization of the matrix in which presume melanosomes are embedded will support their identity 94
Have melanosomes been robustly differentiated from microbes? 95
Can microbody shape be used to determine color 96
Analytical methods may differentiate melanosomes (or melanin) and microbial biomarkers in exceptionally preserved fossils 97
Conclusions 99
Acknowledgements 100
References 100
CHAPTER 5: KERATIN DURABILITY HAS IMPLICATIONS FOR THE FOSSIL RECORD: RESULTS FROM A 10 YEAR FEATHER DEGRADATION EXPERIMENT 103

Abstract 103
Results 104
Discussion 107
Conclusions 111
Methods and materials 112
Transmission electron microscopy (TEM) 113
In situ immunohistochemistry (IHC) – Immunofluorescence (IF) 114
Antibody specificity controls 115
References 117
CHAPTER 6: MICROSCOPIC AND IMMUNOHISTOCHEMICAL ANALYSES OF THE CLAW OF THE NESTING DINOSAUR, *CITIPATI OSMOLSKAE* 133
Abstract 133
Introduction 133
Results 135
Discussion 137
Conclusions 139
Methods and materials 140
Scanning electron microscopy (SEM) coupled with energy dispersive X-ray spectroscopy (EDS) 140
Transmission electron microscopy 140
In situ immunohistochemistry (IHC) – Immunofluorescence (IF) 141
References 145
CHAPTER 7: TESTING THE HYPOTHESIS OF BIOFILM AS A SOURCE FOR SOFT TISSUE AND CELL-LIKE STRUCTURES PRESERVED IN DINOSAUR BONE 164
Abstract 164
Introduction 164
Results 167
Discussion 170
Materials and methods 175
Cotton blue staining 176
Inoculation and growth of biofilm in organic-free bone 176
Scanning electron microscopy (SEM) 176
Transmission electron microscopy (TEM) 176
Dinosaur materials 177
TEM of MOR 1125 vessels 177
In situ Immunohistochemistry (IHC) 177
Dinosaur bone petrographic section 178
Acknowledgements 178
Author Contributions 178
References 178
CHAPTER 8: SUMMARY 182
References 192

LIST OF TABLES

CHAPTER 2: MELANOSOMES OR MICROBES: TESTING AN ALTERNATIVE HYPOTHESIS FOR THE ORIGIN OF MICROBODIES IN FOSSIL FEATHERS

Table 1. SEM-EDS quantitative data for the fossil feather 60

CHAPTER 6: MICROSCOPIC AND IMMUNOHISTOCHEMICAL ANALYSES OF THE CLAW OF THE NESTING DINOSAUR, *CITIPATI OSMOLSKAE*

Table 1. SEM-EDS quantitative data for the emu claw (Figure 4), fossil *Citipati* claw (Figure 5), and the sediment associated with the fossil claw (Figure S2), in decreasing abundance 154

LIST OF FIGURES

CHAPTER 1: INTRODUCTION
Figure 1. Skin ultrastructure and layers 51
Figure 2. Hypothetical evolutionary sequence of formation and diversification of beta-keratins from an amniote ancestor in different non-avian sauropsid (reptile) groups 52
Figure 3. Evolution of avian beta-keratins from molecular dating (Bayesian analysis) using beta-keratins from a lizard, turtle, crocodile and chicken and zebra finch 53
CHAPTER 2: MELANOSOMES OR MICROBES: TESTING AN ALTERNATIVE HYPOTHESIS FOR THE ORIGIN OF MICROBODIES IN FOSSIL FEATHERS
Figure 1. Electron micrographs of modern *Gallus gallus* feathers and *Bacillus cereus* pure culture, compared with an SEM image of a fossil feather from published work 55
Figure 2. FE-SEM micrographs of biofilm overgrowth of extant feathers compared with published images of fossil feathers 56
Figure 3. SEM images of melanosomes from extant *Gallus gallus* feathers 56
Figure 4. TEM images of *Bacillus cereus*-treated black chicken feather 57
Figure 5. Images of the fossil feather ascribed to *Gansus yumenensis* (ANSP 23403) 58
Figure 6. High magnification image of the black region of the fossil feather 58
Figure 7. SEM-EDS data derived from the black fossil feather region 59
Figure 8. SEM-EDS data derived from the brown, basal part of the fossil feather 60
Supplementary Figure S1. SEM images of untreated and *Bacillus cereus* treated extant chicken feathers 63
Supplementary Figure S2. FESEM image of environmental biofilm grown on extant feather 64
Supplementary Figure S3. FESEM images of untreated, fresh-fractured guineafowl feather 64
Supplementary Figure S4. SEM images of the Gansus yumenensis feather (ANSP 23403) 65
CHAPTER 3: INTERPRETING MELANIN-BASED COLORATION THROUGH DEEP TIME: A CRITICAL REVIEW
Figure 1 72
Figure 2. Negative ion ToF-SIMS spectra collected from fossil microbodies located within the ‘eye spot’ of FUM-N-2268 (‘fossil microbodies’) and synthetic eumelanin 72
Supplementary figure S1. SEM micrographs of extant microbial biofilms 84
Supplementary figure S2. Peaks selected from a negative ion ToF-SIMS spectrum collected from microbodies located within the ‘eye spot’ of FUM-N-2268 85
Supplementary figure S3. Negative ion ToF-SIMS spectra acquired 86
Supplementary figure S4. Negative ion ToF-SIMS spectra obtained from fossil microbodies located within the ‘eye spot’ of FUM-N-2268 and three different melanin standards 87
Supplementary figure S5. High-resolution ToF-SIMS images showing different molecular components in a fossil microbody sample taken from the ‘eye spot’ of

FUM-N-2268 88
Supplementary figure S6. IR absorbance spectra of microbodies from the ‘eye spot’ of FUM-N-2268 (‘fossil microbodies’), synthetic pyomelanin and natural eumelanin 89
Supplementary figure S7. SEM micrograph of RPE melanosomes isolated from a Zebra obliquidens (*Astatotilapia latifasciata*) 90
CHAPTER 4: MELANOSOMES AND ANCIENT COLORATION REEXAMINED: A RESPONSE TO VINTHER 2015 (DOI 10.1002/BIES.201500018)
Figure 1. Transmission electron micrographs (TEM) showing co-existence of melanosomes (MN, arrows) and microbes (MB, arrows) in keratinous material 97
Figure 2. SEM images of degraded bird feathers (A–C) and snake skin 98
CHAPTER 5: KERATIN DURABILITY HAS IMPLICATIONS FOR THE FOSSIL RECORD: RESULTS FROM A 10 YEAR FEATHER DEGRADATION EXPERIMENT
Figure 1. Feathers after 10 year exposure to several different environmental conditions 122
Figure 2. Barb fragment from 350°C feather 123
Figure 3. TEM images of feathers from varied conditions 124
Figure 4. TEM images of 350°C feather fragments 125
Figure 5. Localization of antibody antigen (ab—ag) complexes *in situ* on feathers exposed to varied conditions 126
Figure 6. Localization of antibody antigen (ab—ag) complexes *in situ* on 350°C barb 127
Figure 7. Localization of antibody antigen (ab—ag) complexes *in situ* on *Shuvuuia deserti* (IGM 100/977) filament 128
Figure S1. Immunological staining results for the secondary antibody only (negative) controls of feathers exposed to varied conditions 129
Figure S2. Immunological staining results from the specificity controls of the primary antibody on extant tissue 130
Figure S3. Immunological staining results from human fingernail tissue 131
Figure S4. Immunological staining results from the inhibition control of the primary antibody on *S. deserti* tissue 132
CHAPTER 6: MICROSCOPIC AND IMMUNOHISTOCHEMICAL ANALYSES OF THE CLAW OF THE NESTING DINOSAUR, *CITIPATI OSMOLSKAE*
Figure 1. Fossil and extant claw material 150
Figure 2. SEM images of extant emu and *Citpati* claw material 151
Figure 3. SEM-EDS results for *Citipati* claw material 152
Figure 4. SEM-EDS results for emu claw tissue 153
Figure 5. TEM micrographs of ostrich claw tissue and *Citipati* claw material 155
Figure 6. Immunohistochemical staining results for ostrich claw and claw exposed to the custom-made antiserum 156
Figure S1. *Citipati osmolskae* specimen MDC-P 100/979 157
Figure S2. SEM-EDS results of sediment surrounding the claw material from *Citipati* 158
Figure S3. *Citipati* claw before and after EDTA demineralization 159
Figure S4**.** Immunohistochemical staining results 160
Figure S5. Primary antiserum specificity controls for ostrich claw 161

Figure S6. Primary antiserum specificity controls for *Citipati* tissue 162
Figure S7. Immunological staining results for decalcified ostrich bone 163
CHAPTER 7: TESTING THE HYPOTHESIS OF BIOFILM AS A SOURCE FOR SOFT TISSUE AND CELL-LIKE STRUCTURES PRESERVED IN DINOSAUR BONE
Figure 1. MOR 2598 vessels recovered after demineralization compared with a hyphal mat both stained with the fungal stain cotton blue 165
Figure 2. Biofilm growing on cow bone from which organics had been removed ..166
Figure 3. Biofilm growth compared to vessels from MOR 2967-C5-1.....167
Figure 4. SEM images of *B. cereus* and *S. epidermidis* 168
Figure 5. TEM images of biofilm recovered from modern bone from which organics had been removed, compared with representative vessels recovered from dinosaur bone 170
Figure 6. *In situ* immunohistochemistry of biofilms and dinosaur vessels exposed to polyclonal antibodies raised against actin, a cytoskeletal protein 171
Figure 7. In situ immunohistochemistry of biofilms and dinosaur vessels exposed to polyclonal antibodies raised against elastin, a highly conserved, robust protein found in vascular walls 172
Figure 8. Overlay and fluorescent images of *B. cereus, S. epidermidis, B. Canadensis* vessels and *T. rex* vessels exposed to antiserum raised against purified ostrich hemoglobin 173
Figure 9. Overlay and fluorescent images of *B cereus, S. epidermidis* biofilms, *B. canadensis* and *T. rex* vessels exposed to antibodies raised against peptidoglycan ..174
Figure 10. Histological ground sections of *T. rex* cortical bone and *B. canadensis* cortical bone 175
CHAPTER 8: SUMMARY
Figure 1. Feather degradation experiment that resulted in the production of a black 'film' under and surrounding both pigmented (reddish-brown and black) and unpigmented (white) chicken feathers 199
Figure 2. Feather degradation experiment that resulted in the degradation of the rachis before any other parts of the feather 200
Figure 3. Fossil skin samples from *Edmontosaurus annectens* (NCSM 23119) 201

CHAPTER 1 - Introduction

Bone and teeth are the most common vertebrate fossil materials to be represented in the rock record, most likely because these materials are biomineralized during life [1,2]. However, epidermally derived structures, including skin, hair, feathers, and the like, are often discovered in association with skeletons, despite not being fully biomineralized. These materials directly interact with the environment, and as a result are usually colonized by microbial populations in life; consequently, these structures are typically vulnerable to rapid decay. Nonetheless, fossils of originally keratinous structures have been discovered and documented since the 1840s [3] but with few exceptions (e.g., [4–8]) these structures have not been investigated at microscopic or molecular levels for the presence of endogenous organic material. In sauropsids (all extant and extinct members of reptilia (including birds) [9] *sensu* [10]), these structures are partially composed of the structural protein beta-keratin which is a rigid, hydrophobic and resistant molecule; thus fossils of epidermally derived tissues are good targets for molecular paleontological studies with the potential to elucidate evolutionary strategies in the extinct ancestors of today's extant archosaurs.

Skin as an organ and its composition

Skin is the largest vertebrate organ [11]. It is the first line of defense against the external environment, as well as the key means of maintaining homeostasis. This organ is arguably one of the most vital adaptations in vertebrate evolution. The skin of all vertebrates: piscine, amphibian, and all amniotes, is composed of a cornified multilayered epidermis which is separated from an underlying dermis by a basement membrane [12].

Resistant structural keratin proteins along with specialized tight junctions in the epithelium enabled terrestrial tetrapods to adapt to the harsh environment out of water. The epidermis is the thinnest and outermost layer of skin but is an animal's first line of defense and thus must be able to resist and respond to mechanical and physiological stress. It forms a barrier between the inside of the organism and the outside world and its primary function is to prevent water loss [13,14], allowing the organism to maintain homeostasis. Cornification (formation of a horny layer of skin from fully keratinized non-living epithelial cells [15]) of the epidermis was essential for providing a chemical and water barrier [15]. Cornification most likely coincided with the full transition of vertebrates to the land, because most amphibian skin is not cornified

[14–16]. In addition, because cornification results in a layer of dead cells, it is metabolically efficient to continually shed and repair this layer.

Besides keratins and other structural proteins, desmosomes play an important role in epidermal function as the intercellular molecular junctions between keratin intermediate filaments of adjacent cells [17] (Figure 1A). The cell-cell interactions rely on calcium-dependent transmembrane glycoproteins called cadherins [17]. Additionally, plakoglobin is a protein component of adhesive junctions and binds desmosomal cadherins [17]. Desmoplakin is another important protein in the desmosome structure and functions to anchor directly to keratin filaments [17]. Unlike desmosomes which function in cell-cell linkages, hemidesmosomes are the attachment sites for cell-extracellular matrix interactions via integrin molecules and the basement membrane [17]. These intercellular anchored intermediate filaments create an transcellular anastomosing network which resists mechanical stress [17].

The epidermis also contains melanocytes, specialized cells that produce melanin, a molecule responsible for skin pigmentation. Melanocytes are located in the stratum basale (basal layer), the deepest layer of the epidermis [11] (Figure 1B). Once the melanin is synthesized it is transferred to specialized organelles, melanosomes, which reside in keratinocytes. Unlike mammals and birds, which utilize melanocytes, cold-blooded animals (poikilotherms) capable of physiological color change synthesize melanin using melanophores, a special class of light-reflecting cells, chromatophores, containing various pigments [11,18,19]. In fact, in most organisms, the amount and distribution of pigment, and the pigment cells, are not permanent but tightly regulated by physiological changes induced by stimuli such as heat and light [20].

The dermis, a soft layer of living tissue composed of structural proteins such as collagen and elastin, is thicker than the epidermis [11]. The combination of these proteins, along with interstitial fluids, provides flexibility and support to skin. The dermis is also vascularized and contains cells and tissues responsible for sensory and communication functions. In addition to various keratinous and non-keratinous proteins and vessels, the integument is surrounded by fat and muscle tissue [21].

The dominant protein in the outer skin layers (epidermis) is keratin, a hydrophobic, rigid structural protein. Keratin is encoded by two separate gene families, alpha and beta, that are evolutionarily related. Alpha-keratin is expressed in nearly all vertebrates, supporting an early origin and the hypothesis that this family of proteins evolved first [22].

Evolution of alpha-keratin

Alpha-keratins are intracellular proteins with a coiled-coil alpha-helix conformation, derived from intermediate filaments originating from the cytoskeleton [23–25]. The presence of alpha-keratin in all vertebrates implies the precursor protein originated before the divergence of vertebrate lineages. It has been proposed that alpha-keratin is derived from two genes present in the ancestor of all extant vertebrates [22]. Tetrapod alpha-keratins are arranged in two large gene clusters. When expressed, type I keratin molecule (acidic) and one type II molecule (basic) form obligatory heterodimers, resulting in 40-70 kDa sized proteins [24].

Alpha-keratins are comprised of an alpha-helical central rod forming 8-10nm filaments [27]. The matrix in which these intermediate filaments are embedded is fibrous and composed of keratin-associated proteins. Members of the alpha-keratin family are expressed differentially; hair, nails hooves, claws, baleen, quills, etc. are composed of ‘hard alpha-keratins, and skin and epithelium are composed of ‘soft alpha-keratins’ [28]. These differ primarily in the amount of cysteine containing sulfur and thus disulfide bonds, that is responsible for varying hardness between these structures [29].

Evolution of beta-keratin

There are two hypotheses for the origin of beta-keratin in the amniote lineage (illustrated in Figure 2, adapted from [30]). Following traditional terminology, if all sauropsids express beta-keratin this would include the stem ‘reptiles’ (Captorhinids) within Amniota. Therefore early synapsids, the ‘mammal-like reptiles’ (Pelycosaurs), would have expressed beta-keratin, presumably with a scaly integument, which was subsequently lost in therapsids [14,31]. More parsimoniously, beta-keratin expression arose in the sauropsid lineage after the synapsid-sauropsid split ~310 million years ago giving rise to the scaly reptiles [32]. It has been proposed that mammalian histidine-rich proteins in the keratinous matrix in the epidermis of therapsids, provided a thick outer layer to protect against the harsh terrestrial environment [29]. Whether all synapsids relied on a cornified integument composed of alpha-keratin only or whether the early synapsids along with the sauropsids had a cornified integument (and potentially other integumentary appendages) composed of beta-keratin and alpha-keratin depends when beta-keratin evolved.

One of the hypotheses for the origin of beta-keratin is that mutations occurred in the ancestral alpha-keratins, perhaps resulting in proline enrichments [33]. A recent study provided

data supporting the divergence of beta-keratin from its common ancestor (presumably alpha-keratin) in the Permian, about 278 million years ago (See Figure 3, adapted from [34]). This corresponds to the diversification of amniotes and the emergence of the ancestral lineage of extant sauropsids. Molecular data also suggests that avian beta-keratins diverged from the archosaurian ancestral gene family approximately 216 million years ago, and that feather beta-keratins diverged from the basal avian beta-keratins 143 million years ago (see Figure 3 from [34]). All extant avian beta-keratins were present by the Early Cretaceous [34]. Therefore, the utility of studying the molecular preservation of beta-keratin not only contributes to phylogenetic resolution but also to temporal placement.

Beta-keratin terminology

Despite the common and long-term use of the term "beta-keratin", in several recently published studies, the beta-keratins are referred to as 'corneous (or feather) beta proteins' [33,35–37]. It is argued that the term 'keratin' is only appropriate for the proteins derived from intermediate filaments (the alpha-keratins). Most define keratins are a class of tough and fibrous structural proteins which form *filaments* in the epidermis. Beta-keratins are a family of monomeric proteins united by the possession of a ~32 amino acid residue region rich in hydrophobic residues and contained within a beta-pleated sheet secondary structure. This results in the mature protein forming ~3nm filaments with a hydrophobic core in quaternary structure (compared to the much larger ~8-10nm alpha-keratin filaments) [26,38,39]. Thus, keratin is appropriate for both gene products, and will be used in this dissertation to refer to both alpha- and beta-keratin.

The ambiguity in naming this protein family arises from its chromosomal location and its association with other non-keratinous corneous proteins. Those in support of abandoning the term beta-keratin argue that the structural proteins of the outermost layers of mammalian and sauropsid epidermis are all derived from the epidermal differentiation complex (EDC) [35] gene cluster and therefore the term beta-keratin misleads because it does not suggest ancestry or homology with keratins according to the Gene Nomenclature Committee [35]. Furthermore, the EDC gene cluster on microchromosome 25 [35], is not located near the gene clusters responsible for alpha-keratins [22]. Additionally, there are other corneous proteins expressed by the EDC that associate with the sauropsid beta-keratins such as loricrin, involucrin, and small proline-rich proteins, cornulin, trichohyalin, and filaggrin and therefore collectively should be termed

corneous proteins [35,40]. However, unlike these other corneous proteins, beta-keratins form filaments, similar to the intermediate filament keratins as defined above. Nearly all studies, including those by the scientists in disagreement, use the term beta-keratin (and alpha-keratin), and therefore will be used throughout this review.

Beta-keratin and the evolution of the gene family

The beta-keratins can be divided based on their differences in mass. The beta-keratins with a molecular weight range of ~14-25 kD, which are co-expressed with alpha-keratins, make up claws, scales and beaks of sauropsids [41,42]. The lower molecular weight beta-keratin (~10.5 kDa) is the structural protein comprising 80%-90% of feathers [41,43], and is thought to have arisen from a deletion event of four peptides each comprised of 13 amino acids in the ancestral scale protein [44]. Based on its X-ray diffraction diagram, beta-keratin is composed of chains of twisted pleated-sheets in a non-uniform (both parallel and anti-parallel) direction [38,39,45]. Beta-keratins form filaments which are influenced by a hydrophobic core; this region is highly conserved and likely functions as the site for polymerization of the proteins [39,46,47].

Among sauropsids, crocodilians and birds demonstrate the highest beta-keratin sequence homology [33,34,48]. A 20 amino acid residue has been characterized that is highly conserved in the beta-keratins of all avian and crocodilian epidermal appendages [48] (termed the “core box by Alibardi (e.g. [29])) but which contains considerable variability in other sauropsids. This suggests that this conserved region arose in the common ancestor of archosaurs. Biochemical and morphological studies suggest feathers may be derived from an asymmetric scale present in the ancestor of all archosaurs [48,49]. Although the evolution of feathers from non-avian sauropsid scales was proposed almost 50 years ago [50] based on morphology, the data to support *genetic* homology between beta-keratin genes of bird feathers and non-avian sauropsids was originally suggested through separation of non-cross-reacting antisera of alpha- and beta-keratins by one-dimensional polyacrylamide gel electrophoresis [48]. In this immunohistochemical study, antisera made against soluble keratins from feathers reacted with both feather and non-avian sauropsid scale tissues, indicating that scales and feathers express similar proteins [48].

Genes encoding scale beta-keratins are thought to be the most basal members of the beta-keratin protein family among archosauria, and have the widest distribution in integumentary structures [25,43]. Beta-keratins expressed in claw sheaths share an ancestor with scale proteins, both of which are basal to feather keratins [25]. Recent studies show feather keratins are the most

derived of the four avian keratin subfamilies: keratinocytes, scale, claw and feather beta-keratins [25,34,46]. All beta-keratin genes are coded primarily on microchromosomes 25 and 27 [25,33].

Feather keratins incorporate a reduced number of glycine-tyrosine residues relative to the keratins of claw and skin [32,33]. Conversely, the non-feather beta-keratins are enriched in glycine proline, and tyrosine. Unlike beak, scale and claw keratins, feather keratins form bundles oriented parallel to each other, allowing for the structural formation of barbs and barbules. An epitope, 23 amino acid sequence (VGSTTSAAVGSILSEEGVPINSG) specific to feather keratin has been characterized [51,52]. It is not only expressed in the embryonic epidermis of a developing feather but also chick and zebra finch scutate scale, and embryonic epidermis of alligator, further supporting the homology of these proteins within archosauria [51,52].

Evolutionary context of skin variants across taxa

Unlike other vertebrates, living (non-cornified) epidermal cells interact directly with the environment in fish [53]. Studies predict keratinous skin evolved with the cartilaginous fishes [54], and consisted primarily of type I alpha-keratins, compared to the type I and type II alpha-keratins expressed by two gene clusters of terrestrial vertebrates [55]. Piscine skin is covered in mucous which functions primarily as an antimicrobial system but also decreases resistance in the water [12]. Osmotic pressure and physical forces are therefore the two main stresses for fish, which have evolved overlapping calcified dermal scales that penetrate the epidermis, micro-ridges on scales, an extracellular cuticle, and orthogonal arrangement patterns of dermal collagen as adaptations to these stresses [53]. The presence of epidermal mucus production is retained in amniotes and is the first matrix to which keratin filaments are exposed [56].

Amphibians are unique among living vertebrates in that their skin serves as a respiratory organ. As animals that transition between water and land, amphibians express a fish-like epidermis covered with mucus in their aquatic environment but a sauropsid-like, cornified epidermis in terrestrial environments [15]. The major integumentary adaptation between the transition from fish to amphibians was the corneous cell envelope which allowed for the stratification and cornification of the outer integumentary layers [16,31]. This alone was not a barrier to water loss; basal amniotes required further enhancements in their integument to adapt to a fully terrestrial lifestyle.

Land vertebrates have cornified skin which is impermeable to water and pathogens [12]. The integument of true amniotes was enhanced with the expression of keratin-associated proteins

or matrix proteins (e.g., filaggrin and trichohyalin), which, together with keratin, form a resistant corneous layer that prevents water loss as required for life in terrestrial environments [15,31]. The basal amniote lineage split into two clades, therapsids and synapsids, and each evolved a different strategy for dealing with the harsh terrestrial conditions. Alpha-keratin expression further diversified within synapsids eventually resulting in hair, fur, and cornified appendages (e.g. hooves, nails) in mammals [14,29].

In sauropsids, cornification was accomplished through the expression of beta-keratin. A recent study provides data suggesting beta-keratin diverged from its common ancestor, hypothesized to be alpha-keratin as discussed above, ~278 million years ago [34]. This divergence corresponds to the Permian period when diversification of amniotes took place [22,29,31].

The outer skin layer, stratum corneum, of non-avian sauropsids and a small portion of avian skin (see below) is tough and composed primarily of beta-keratin which overlays softer layers composed of alpha-keratin [29,33,51]. Non-avian sauropsids have two different skin morphologies. In one, scales overlap (such as in snakes lizards) and in the other scales do not overlap (such as crocodiles). Lepidosaurs, non-avian sauropsids with overlapping scales, express alternating outer cornified layers of alpha and beta-keratin [16,29,57]. In non-avian sauropsids without an overlapping scaled integument, each scale is separated by a hinge region. This hinge region consists of primarily alpha-keratin and provides flexibility to the rigid scale texture (composed of beta-keratin) [37,58–62].

While non-avian sauropsid skin incorporates beta-keratin in the epidermis and epidermal appendages covering the entire animal (with the exception of some lizards and snakes [33]), avian skin is less cornified and only certain regions are composed of beta-keratin [63,64]. These include claw sheaths and beaks, which express both alpha and beta-keratin and feathers, unique because in mature form consist almost entirely of beta-keratin, constituting approximately 80%-90% of the feather [43,65,66]. It is important to note that alpha-keratin has been detected in embryonic development and growth of feathers [36,67,68], suggesting it is important for proper development of feathers. However, upon complete cornification, only beta-keratin is detected supporting that it comprises most of the feather and may even mask alpha-keratin detection [58].

In the avian integument, featherless skin (apteric regions) express primarily alpha-keratin [15,69] as well as the reticulate scales on the posterior side of the leg, except for one beta-keratin

protein during development (See below). The overlapping, plate-like scutate and scutellate scaled skin on the anterolateral surface of the leg and foot is composed of beta-keratin in the outermost layers, similar to overlapping scales of lepidosaurs [29]. However, the beta-keratin isolated from avian scutate scales is not homologous to the beta-keratin in the scales of their non-avian sauropsid ancestors, but rather appears to be more closely related to feather beta-keratin [51,70]. Studies have suggested that the ancestral state for modern birds is feathered legs, which is suppressed in most modern birds [51,71,72]. This was demonstrated through gene manipulation experiments in which molecular manipulations were made in limb identity in birds resulting in the growth of feathers on their legs [71].

In a recent study, it was recognized that although the relationship between feathers and avian scutate scales was the center of many studies, the relationship between these and avian reticulate scales and crocodilian scales [49], was less well understood. These scientists performed *in situ* immunofluorescence experiments to detect and observe patterns of beta-catenin, a transduction signaling molecule expressed during the development of various epidermal structures across many taxa including mammals, in developing chicken feathers, scutate scales, reticulate scales and alligator scales. Homology between these structures had previously been proposed based on the presence or absence of an epidermal placode (a thickening of the epidermis where these derived structures will form [49]); however the results from these experiments are controversial ([49] and the references therein). This is in part because alligator scales, avian reticulate scales and scales of squamates do not form from an epidermal placode. This study observed the expression of beta-catenin during development of these structures and sought to alleviate the controversy by using molecular expression techniques. The authors found that nuclear beta-catenin is expressed in similar patterns early in development of feathers, avian scutate scales and alligator scales, but not in avian reticulate scales. The sharing of similar genetic expression among these structures suggests that these developmental stages are homologous and may have all evolved from an ancestral archosaurian scale. Although no nuclear beta-catenin was expressed in reticulate scales [49], it was expressed in the basal cells prior to the formation of the scales, and the authors propose that the formation of an epidermal placode may actually be observed as the entire region (the footpad) which does not form cellular restrictions for the scales as observed for scutate and alligator scales. Therefore they propose two

scenarios for the evolution of reticulate scales: 1) they are related to the ancestral archosaurian scale but lost the beta-catenin expression, or 2) they evolved independently [49].

A study by Wu et. al. 2015 mapped the expression of alpha- and beta-keratins in these same structures [73]. Unlike all previous studies which failed to detect beta-keratin in avian reticulate scales, this study identified the expression of a keratinocyte beta-keratin (KTN13) in a developing reticulate scale[42].

Both the ungual sheath of claws and ramphotheca of beaks in sauropsids are epidermally derived structures that contain mechanoreceptors and are important morphological features specialized for the lifestyle of the animal such as locomotion and feeding. Claw sheaths are modified scales [74]. Therefore, their formation and growth patterns are similar to typical scale growth patterns. There are slight differences in claws among varying taxa (e.g., development and shape), however in general, formation results from the elongation of a terminal scale at the distal end of the terminal phalanx [74]. It extends more distally and laterally on the dorsal surface (unguis) than ventral (sub-unguis) [74]. The outer, dorsal surface accumulates layers of beta-keratin creating a resistant stratum corneum [74]. On the other hand, the ventral surface is comprised mostly of alpha-keratin [74]. Amphibian and mammalian claw sheaths are composed only of alpha-keratins (and keratin associated proteins) and not derived from scales, therefore are not homologous with sauropsid claws [74].

Ramphothecas of sauropsids are hardened horny sheaths comprised of beta-keratin at the end of the snout covering underlying bone and soft tissue. They are formed by outgrowth of the beak mesenchyme and then covered by the epidermally derived beta-keratinous sheath, the ramphotheca [14].

Feathers as an evolutionary novelty

Feathers are an evolutionary novelty, present only in avian and non-avian dinosaurs. The presence of fossil feathers from the Jurassic (e.g. *Anchiornis* [75] and *Archaeopteryx* [76]) that are morphologically similar to modern pennaceous flight feathers indicate that these complex structures evolved by ~160 million years ago. Although their capability of powered flight has been debated [77–79], most studies conclude that the earliest taxa bearing pennaceous feathers were not capable of powered flight [77,80,81]). Prum and Brush (1999) suggest evolution of feathers as novelty structures through a series of hierarchical transitions starting with a hollow tubular structure [82,83], an idea supported by developmental processes observed in extant

feathers. Other scientists hypothesize that feathers evolved from archosaurian scales [33,51,58], and support this hypothesis with morphological and biochemical data. See below for a more in depth discussion of feather evolution.

The fossil record of keratinous structures

Skin contains phylogenetically informative features, and expresses evolutionary novelties (e.g. hair, feathers). Thus, when preserved, skin informs on many aspects of the paleobiology of extinct organisms. A cornified integument evolved early in vertebrate evolution and extant animals provide limited insight to the evolutionary stages of integumentary development since the emergence of this lineage in the Cambrian (~ 525 million years ago); therefore by studying epidermally derived structures of extinct organisms and learning how they, along with skin, have changed over time, not only will we add a large piece to the evolutionary puzzle, but we begin to understand how animals respond to different and changing environments.

Because the epidermis is primarily composed of keratin, a hydrophobic, structural protein, and is essentially dead tissue, it presumably has a higher preservation potential than the underlying dermis. Therefore, when specimens are reported to preserve with skin, what is observed is likely some trace of the outermost epithelial layer, the epidermis, and often the scale pattern, regardless of mode of preservation.

Fossil skin impressions have been described in scientific literature as early as 1841 from the “footmark” of an extinct animal found in the Late Triassic deposits (New Red Sandstone) of the Connecticut River Valley [3,84]. Hitchcock made the observation that “no trace of any organic matter could be perceived occupying the cavity or mould” [3]. Conventional wisdom still follows this logic, regarding skin fossils as true impressions, or imprints in the sediment; implying no original soft tissue was incorporated into the rock record [2]. Thus, the preservation of endogenous organic matter in skin fossils has remained largely untested, despite the excavation and collection of exceptionally preserved [2] specimens throughout the years (i.e. “mummified” dinosaurs [6,85]).

There are several types of skin fossils differing in preservational modes and thus the potential for preserving varying material. The most common types of skin fossils reported in the scientific literature are impression, compression, or cast and mold fossils (e.g. [2,85–87]). Impressions and cast and mold fossils indicate that the skin of the extinct organism became fossilized as an impression (a negative image) in the sediment surrounding the dead animal,

presuming the actual soft tissue was not preserved in the fossilization process. Compression fossils, often resulting in part and counterpart, are formed by a physical compression of the original tissue and therefore suggest the soft tissue plays a role in the preservation process and endogenous organics may or may not be preserved [2].

To date, most remnants of fossil skin have been described as *impressions* (e.g. [2,86–91]). In this mode, the skin is not preserved, but rather what remains is an imprint of the skin in the sediment, similar to a footprint. Alternatively, the impression could be in a matrix other than sediment, such as a mineral precipitation or fossilized biofilm. For a fossil to be a true impression, it should be consistent in texture and composition with the sediment or matrix preserving the impression. However, a brief review of the literature illustrating dinosaur skin fossils indicates many of these impression fossils differ in color and texture than the underlying sediment, and are often observed as a discolored 'film', suggesting they are not true impressions. (See Chapter 8 for a brief discussion of preliminary data from fossil *Edmontosaurus* (NCSM 23119) skin).

When the fossil skin is observed as a 2-dimensional 'film' on the sediment, it implies the skin has been preserved as a compression fossil, similar to the carbonaceous film preservation of feathers ([92] discussed below). There are two hypothetical sources from what the film is derived: 1) original skin tissue altered by low-grade metamorphism [2,93,94] or 2) overgrowth of biofilm participating in the diagenesis of the carcass [2,95], which may also mediate and incorporate mineral deposition (See Role of Microbes discussion below). It is likely the biochemical interactions between the decomposing tissue and the surrounding sediment particles play a part in skin preservation. This could be elucidated by taphonomic experiments. Compression skin fossils are observed as a brown-black film with scale patterns such as in many of the exceptionally preserved specimens, including birds and lizards, of the Jehol Biota [96].

The other type of skin fossils is a cast (and subsequently also a mold), which results in 3-dimensional (3-D) preservation. The cast of the skin must be made in some matrix, and it has been proposed this matrix may be sediment interacting with a biofilm that is also able to mediate mineral precipitation [95]. It is presumed that no original skin tissue partook in preservation, therefore no skin persists; however this has not been tested. One of the most well recognized examples of 3-D dinosaur skin preserved as a cast is the embryonic skin with detailed scale patterns from sauropod eggs from the Auca Mahuevo site in Patagonia, Argentina [97–99]. One

of these embryonic skin samples was sectioned, and it was proposed that osteoderms could be observed underlying scale tubercles with potential organics preserved but chemical analyses have not yet been performed [2].

Most dinosaur skin fossils are found associated with duck-billed dinosaurs (hadrosaurs) [86–88]. However, skin has been noted in other ornithischians (e.g., [100–103]), including *Kulindadromeous* [104], a triceratops [105], *Psittacosaurus* [103], and a stegosaur [106], and more rarely in theropods [107–109]. Exceptionally preserved wing membranes of pterosaurs have also been documented [110,111]. No fossilized skin has been documented for early non-dinosaurian dinosauromorphs [89], therefore studying dinosaurian skin fossils are important for understanding the evolution of the integument, scale patterns and epidermal novelties. It should be noted that fossilized skin is not limited to terrestrial environments. There have been discoveries of ichthyosaurs, plesiosaur, fish and sea turtles with skin preserved ([8,112] and the references therein). All of these specimens have skin preserved as a brown-black film similar to what has been described for carbonized compression fossils.

A study in 2014 by Davis [87] sought to understand why and what the most important factors are in the increased preservation of hadrosaur skin relative to other taxa by compiling a dataset derived from the literature composed of details about each skin fossil, then subjecting these data to a statistical analysis. This study suggests that rather than taphonomic or collection bias, their population size or depositional environment, the reason there are more hadrosaurian skin fossils is because of some ‘intrinsic’ feature of the taxa. He proposes tougher/thicker skin. However, there are many publications that investigate the biogeochemistry of soil microbiology and what happens to the activity and products of microbes in various sediment types, which is not accounted for or discussed in this study. For example, it is known that charged clay particles adsorb enzymes, rendering them inactive [2,93,113], and proteolytic enzymes in mudflat sediments are pH and temperature sensitive [114]. Therefore, skin decomposition may be potentially hindered in these environments. Subsequently, although hadrosaurian skin may have histologically possessed a characteristic that aided in preservation, I argue it is likely that the lithology and depositional environment play an important role as well [89]. As mentioned in this chapter, and discussed below, such a study would greatly benefit from actualistic experiments involving skin degradation of various taxa in varying depositional environments similar to the dinosaurs with skin preserved.

In addition to fossilized skin remains in sedimentary rock, skin has been fossilized in amber from the Oligocene/Miocene [115], Eocene [116–118] and Cretaceous [119–121], typically observed still covering an entirely preserved carcass, usually a lizard or gecko. The oldest example is a lizard from the Lower Cretaceous of Lebanon [122]. These fossils are preserved in pristine detail making them ideal for comparative anatomy and evolutionary studies, but because of the chemical alteration induced by amber preservation [123], there have been no successful molecular studies.

Epidermal appendages in the fossil record

Alpha-keratin derivatives

In addition to the integument, keratins makeup many types of epidermal appendages and other skin derivatives. Alpha-keratin is the main structural protein in nails, hair, hooves, and horns in mammals [26], and the baleen of whales [124]. In sauropsids, alpha and beta-keratins are co-expressed in scales, claws and beaks as well as the plastron and carapace of turtles [48].

To my knowledge, except in younger permafrost specimens which are not comparable to Mesozoic fossils, no tissues composed of ‘soft’ alpha-keratin only, e.g. mammalian skin, have been preserved. Similar to avian apteric skin, alpha-keratin comprising skin contains less disulfide bridges than the alpha-keratins making up the ‘harder’ structures such as nails and hair [28], making it less resistant to degradation and is thus probably a factor in its preservation potential. Consequently, structures composed of ‘hard’ alpha-keratin, which incorporates more disulfide bonds than the ‘softer’ alpha-keratin [28], have been observed in the rock record. Fossil mammalian hair, as early as the Jurassic, has been preserved as carbonized impressions surrounding a skeleton ([125,126] and the references therein), as casts and impressions in coprolites [127], and in amber [125].

Beta-keratin derivatives:

Feathers

Paleontological discoveries of fossil feathers have been growing over the last couple decades, prominently from China, and have begun to shed light on the evolutionary stages of feathers. The most basic feather structure was suggested by Prum and Brush, and based upon developmental studies to be a single hollow tubular filament [83,128]. Around the same time, similar structure(s) associated with non-avian dinosaurs were described in the fossil record.

The most primitive feather described, often called a ‘protofeather’, is a small filament-like (non-branching) and presumably hollow structure as seen in *Sinosauropteryx*, a compsognathid theropod [129] and *Beipiaosaurus*, a therizinosauroid [130], from the Early Cretaceous of China. These structures are observed as a halo of “fuzz” along the back and tail of *Sinosauropteryx*, which the authors suggest surrounded the whole body [129]. The scientists initially describing both of these specimens provided evidence that the structures were hollow, possibly with some branching at the tips [129,130]. The filaments observed in *Beipiaosaurus* were similar to but longer than those of *Sinosauropteryx*, and unlike in *Sinosauropteryx* directly contacted the ulna [130]. The evolutionary importance of these specimens was that it provided the first direct indication of primitive feather-like structures in non-avian dinosaurs, providing additional support to the theropod ancestry of birds and suggesting that similar feathers or feather-like structures were present in taxa most closely related to birds. In addition, these animals were obviously not capable of flight (feathers were more simplistic than asymmetric vaned flight feathers [130]); therefore it could confidently be presumed that feather-like structures evolved prior to flight and thus performed some other function ([131] and the references within). This idea was supported by later finds of more feathered dinosaur specimens with feather morphologies representing various transitional stages of complexity as predicted by the model put forth by Brush and Prum [14,132,133].

Protoarchaeopteryx and *Caudipteryx* are early diverging oviraptorosaurian dinosaurs possessing primitive feathers [134,135]; all three taxa were found in China [134] and are dated to the Early Cretaceous, therefore it is older than *Sinosauropteryx* but younger than *Archaeopteryx*. The feathers on *Protoarchaeopteryx* are described as symmetric contour and plumulaceous downy feathers and also retrices (tail feathers) and thus are all more complex (and more similar to the feathers observed in *Archaeopteryx*) than the integumentary structures of *Sinosauropteryx* [134].

Some of the most remarkable feathered dinosaurs discovered have been those described with ‘hind-wings’, or rather feathered hindlimbs, such as *Microraptor gui* [136], *Anchiornis huxleyi* [137] and *Yi qi* (even more unique due to its bat-like forewings) [138]. These findings supported scientists’ earlier hypothesis that extinct ancestors of modern birds likely were adorned with feathered hindlimbs as discussed above.

The changes in the epidermis leading to the formation of a visible protruding tubular (filament) structure occur at the microscopic level [70]. Therefore, it has been argued that there are no fossils demonstrating the transition from scales to feathers [139] either because those structures do not preserve or because these changes are not observable in fossils.

Fossils of *Archaeopteryx* show that complex feathers that are morphologically similar to flight feathers, asymmetrically vaned pennaceous feathers, evolved by at least ~150 million years. The "protofeather" structures are described from specimens found in the Yixian formation in China which is Early Cretaceous in age, 120-130 million years old. Therefore, although phylogenetic studies classify these specimens with "protofeathers", or filamentous unbranched feathers, as more primitive than *Archaeopteryx*, temporally these species lived *after* more complex feathers have already evolved.

It must be noted that most often what is observed in the fossil record of birds is the preservation of feather material along with the skeleton, but not the actual skin of the animal. This may be the result of degradation of the mature, softer apteric integument made of alpha-keratin [140] which is less resistant to decay compared to either mineralized bone or beta-keratinous feathers. This remains to be tested and can only be verified through taphonomic experiments.

Modes of preservation of keratinous structures in the fossil record:

I start by discussing the most complex and evolutionarily derived of the epidermally derived keratinous structures, feathers, because they are: 1) the most plentiful of the fossils originally composed of keratin, 2) more taxonomically widespread, i.e. found in more taxa than are skin or beak fossils, and 3) are the focus of the succeeding four chapters of my dissertation (Chapters 2-5).

Feathers

Over the past two decades fossil feathers have been, and continue to be, the focus of many paleontological discoveries [141] and have been found in a variety of environments, including amber [92,142] and ash [143]. However, most fossil feathers have been preserved in lacustrine environments [89] and are described as 'carbonized' impressions [92].

In 1995, Davis and Briggs published on the fossilization of feathers, and proposed a correlation between environment and preservation. They suggested that different processes are involved during the fossilization of feathers in different depositional settings. They proposed five

different modes of preservation may exist for feather fossilization [92]. These include: 1.) Carbonized traces in mudstones (lacustrine settings). These are by far the most common mode observed in the fossil record (e.g. [144–147] and references within [92]). It is in this type of fossil feathers the authors observed what they interpreted as bacteria and their associated glycocalyx using electron microscopy, suggesting a role for microbes in their preservation [92] (See Discussion below). 2.) Bacterial autolithification. This was described as preservation by bacteria-mediated biomineralization of soft tissue producing a "shadow" surrounding the animal [148]. 3.) Bacterial imprinting was proposed as the mechanism for preserving *Archaeopteryx* feather(s) where the feather morphology is preserved as lithified bacteria, but no remaining organic material from the feather remains (unlike potentially in the carbonized mode of preservation) [92]. 4.) The fourth preservational mode of feathers is in amber from terrestrial settings [92,142]. These are suggested to preserve the most detail, because it is the only mode to preserve the feather as their true 3-dimensional (3-D) structure. 5.) Coprolites in marine settings are the fifth mode of preservation described in which the fossil feathers persist as 3-D molds formed from the precipitation of apatite followed by degradation of the feather . This has only been reported in coprolites from Miocene marine deposits [149].

More recently, in 2008, a novel mode of fossil feather preservation was proposed; that the bacteria (biofilm) observed in the fossil feathers were instead the remnants of pigment containing organelles, melanosomes, and therefore " […] most fossil feathers are preserved as melanosomes […]" [150] implying that the keratinous feather is degraded or at least partially degraded and the melanosome organelles remain in the shape/pattern of the feather. In the years following the initial melanosome hypothesis paper, a number of studies were published by various authors reporting similar observations in other fossil specimens of feathers [145,150–157] and marine 'reptiles' [8,158]. With the exception of a select few studies (primarily on non-feather structures), most reported on the morphology alone and used differences in the shape of the melanosomes to infer original color, as well as behavior and physiology, without ever ruling out the original bacteria hypothesis. Additionally, most of these studies that argued for the preferential preservation of melanosomes because melanin conferred resistance did not actually report bodies, but rather empty "moulds" remaining in a uncharacterized matrix that they argued were left after the melanosomes degraded [138,153,156,157].

The fossil melanosome studies have relied on the untested assumption that the microstructures were undoubtedly color-imparting organelles, despite bacteria and melanosomes being identical in shape size. Therefore in 2014, we published a study testing the hypothesis that bacteria can and will grow on extant feathers in a pattern similar to that observed for purported fossil melanosomes [159] (Chapter 2). Modern feathers were exposed to the biofilm-forming organism, *Bacillus cereus*, and an environmental pond inoculum, then observed to visualize how the biofilm grew on the feathers. This study demonstrated that bacteria will colonize the surface of feathers and grow in patterns similar to the patterns described for fossil melanosomes, including leaving behind impressions in a matrix. They were the same size and shape as melanosomes and therefore impossible to distinguish based on morphology alone, and we recommended caution in ascribing all microbodies observed in fossil feathers to melanosomes without additional chemical data. Furthermore, there are many factors contributing to the coloration of feathers, including other pigments, hormones, diet, or even the presence or absences of feather colonizing bacteria that affect color expression [160,161]. It is recognized in the literature that determining all the factors influencing the color of extant feathers is a complex process and the coloration imparted by melanin can only be completed with confidence if the melanin gradients are analyzed along the entire feather [162]. Therefore one must question the robustness of color determination in extinct taxa when only a few sample points, with a micrometer-sized focal plane, are used to determine the color of a feather or entire animal.

Because of the persistent controversy regarding this debate [163], we published a review addressing melanin production in both eukaryotic and prokaryotic organisms, conflicts in the literature with assigning all microbodies associated with vertebrate remains to melanosomes, the robustness and limitations of the methods used to conclude a melanosome origin and used a case study of a fossil fish eye, to outline the scientific process that, in our opinion, should be followed in analyzing and interpreting fossil melanosome/melanin studies [164] (Chapter 3). In this manuscript we also investigate the underlying assumptions that are problematic in the melanosome hypothesis.

Shortly after our review was published (Chapter 3), Vinther et al. published a review of the ‘field of paleo-color’ [165]. This paper misrepresented published data, was incompletely cited, and did not address the literature comprehensively, so we wrote a detailed response reviewing the potential of microbes to preserve and differences in the location, texture,

distribution, and preservation potential of these two alternatives [166] (Chapter 4). In this rebuttal we addressed many of the oversights by Vinther, including the preservation potential of bacteria and fossil bacteria, and the viability of the microbial hypothesis for the origin of microbodies, or more often the 'mouldic impressions', observed in fossil feathers [166]. In addition, the complexity of color and how melanosome morphology is not enough to interpret organismal color was discussed.

To date, despite being the focus of many paleontological studies, only one study has rigorously analyzed a purported fossil feather at the molecular level [4] to test the hypothesis that it was microscopically and molecularly similar to modern feathers (but see [7] for a study on melanin preservation in fossil feathers). The sample was from *Shuvuuia deserti*, an alvarezsaurid dinosaur from the Late Cretaceous of Mongolia [167]. Small fibers, white in nature with a hollow center, were observed in close association with the cervical region of the skeleton. Analyses confirmed the structure retained feather-like microscopic and molecular characteristics using electron microscopy, time of flight secondary ion mass spectrometry, and immunochemical methods. I repeated the immunochemical analyses on this same sample using the custom-antiserum I had made to analyze keratinous structures (Chapters 5-6). I achieved the same results as in the 1999 study, using a different antibody, further supporting the endogeneity of the positive signal for the retention of keratin epitopes.

The study repeating the experiment on the *Shuvuuia* filament also included the investigation of the microscopic and molecular preservation of modern partridge feathers that had been buried in sediment collected from a dinosaur site and subjected to different conditions and temperatures for up to 10 years (Chapter 5). It has been argued in several of the fossil melanosome papers that the keratin matrix of the feathers was completely degraded [150,152,156], despite reporting the presence of fossil melanosomes in a matrix without an indication as to what that matrix is. One of the criteria we proposed for determining whether the microbodies are melanosomes is to test the matrix, because if they are melanosomes the matrix should be feather keratin. If they are bacteria, that matrix would be the EPS of the biofilm. Interestingly, after 10 years at 350°C, recognizable feather structures still remained, although the color and texture had clearly changed, approximating more closely what we see in most fossil feathers than in the control feather stored dry and covered. They were fragmentary, shiny black structures, sometimes with remnant barbs (See Figures 1 and 2 in Chapter 5). Rather than being

completely destroyed under these harsh conditions, transmission electron microscopy revealed the retention of the honeycomb-like microstructure comprising the pith of a rachis or barb. No structures consistent with melanosomes were observed in any of the samples from the 350°C condition, however using *in situ* immunohistochemical testing, we were able to demonstrate that the structures still weakly cross-reacted to the beta-keratin antibody, providing evidence for the persistence of keratinous epitopes despite being subjected to harsh conditions for an extended period of time. These results support the hypothesis that keratin protein outlasts melanosomes (But see below for discussion on melanin). Additionally, these experiments demonstrate the appropriateness of beta-keratin as a target molecule for preservation, and a tool to address the melanosome vs. microbe debate.

Claw Sheaths

The keratinous sheath covering the claws of many terrestrial organisms form another source for preservation of these epidermally derived tissues in the rock record. As mentioned above, entire organisms (e.g. gecko, anole, lizard) have been found encased in fossilized amber. Therefore, the presence of claw material, as stated in a recent publication [119], is presumed in at least some of these specimens. However, to my knowledge, there have only been two reports of the preservation of the actual 'horny sheaths' of dinosaur claws in the literature [168,169]. Often, rather than the presence of claw material, publications report the 'impression' of a keratinous sheath (e,g. [170]). Alternatively, its presence is not mentioned or noted, but examination of published images of fossil dinosaurs (avian and non-avian) indicates there is a three-dimensional hard structure, distinct from the surrounding sediment, extending beyond the ungual(s) in these specimens where a keratinous claw would be expected (e.g. [136]).

To my knowledge, samples from only two specimens, the raptorial bird *Rahonavis ostromi* [5] and the oviraptorid *Citipati osmolskae* [171,172] (Chapter 6), have been analyzed to determine if the purported soft tissue preservation was endogenous claw material. In both studies, electron microscopy as well immunohistochemical analyses were employed to test the hypothesis that the structures observed were indeed the remains of the original keratinous sheath. This was successfully demonstrated by comparing analogous structures from extant taxa to ancient samples. These structures retained micro- and ultrastructure similar to modern avian claw sheath material. Additionally, custom-made antibodies were used to demonstrate that epitopes similar to extant beta-keratinous tissues were present in these fossil tissues.

Beaks

Fossils retaining remnants of original ramphotheca structure are the rarest of keratinous fossils. What is more often reported than remnant tissue with appropriate microsctructure is a mold infilling of the beak comb, the region between the underlying bone and the ramphotheca, or keratinous horny covering. Indeed, empirical evidence of a beak, rather than just descriptions as provided by Cope in 1883 [173] and others in the early 1900s [174,175] (due to destruction of the bill molds during excavation and/or preparation), was discussed in 1970 by William Morris in a specimen of *Anatosaurus annectens* (LACM 23502) [176]. In this specimen, siltstone encased the premaxilla of the skull in a 'vertically fluted' and 'undulating' pattern suggesting it had preserved a mold of the interior surface of the overlying beak [176]. Morris discussed the descriptions from all the papers reporting hadrosaur beak structures up until 1970, and concludes that it was apparent some misinterpreted their observations. He further notes that although they all agree on some form of a beak-like structure on the upper jaw; disagreement remained regarding the presence of a beak on the lower jaw. Morris reports no evidence for the presence of a beak on the lower jaw, but Cope (1883) describes a horny beak on both the upper and lower jaw; however it is not clear based on Cope's description whether or not the structures are soft tissue remains or an internal mold as described by Morris.

In 2001, Norell et al. reported on soft tissue preservation of beaks in two ornithimimid specimens [177]. They observed what they interpret as traces of preserved soft tissues from a keratinous ramphotheca, extending several millimeters inferiorly and superiorly from the premaxilla and dentary, respectively. The purported soft tissue differs in appearance and texture from the underlying bone and surrounding sediment. They also report, in a second specimen, the preservation of columnar structures which are presumed to represent lamellae from the interior surface of the beak, and which resemble the tooth-like lamellae observed in modern anseriforms. Although location and similarity to extant organisms certainly suggest these fossil structures are the remains of a keratinous beak, only microscopic and molecular analyses can confirm their origin.

Bony correlates of keratinous coverings

The presence of a keratinous structures covering claws and beaks is inferred using Extant Phylogenetic Bracketing [178]. Additionally, paleontologists have relied on bony correlates to infer the presence of claws [179], a keratinous beak in dinosaurs [177,180–182], and horny frill

coverings in ceratopsians [183,184]. This is often observed as a pitted appearance or rugosity on the bones directly underlying the keratinous beak or claw as a result of vascularization [177] and the soft tissue participating in adhering to the underlying bone. The presence of these structures in both groups of extant archosaurs, birds and crocodiles, combined with the observation of bony correlates lend strong support to this hypothesis.

Methods

The number of techniques that can be used to study the molecular preservation of keratinous fossils is currently limited when compared to bone fossils, which can be subjected to extraction methods and other suites of methods [185]. However, with continuing efforts in sample preparation techniques and with advancing technologies, it is certain more methods will become suitable for molecular paleontological studies of keratinous tissues.

Before any manipulation of the specimen to collect a sample for analyses, it must first be photodocumented and all possible information collected, especially when destructive analyses will be performed. This may include utilizing CT imaging to capture the appearance of the specimen prior to sampling. Photodocumentation also applies to the sample collected from the specimen prior to being subjected to destructive analyses.

Unlike fossil bone [186], keratinous fossils are often observed and collected in minute quantities and therefore require strategic experimental planning. However, since obtaining approval for destructive analyses is often difficult, developing assays that yield maximum information from minimal sample should facilitate the approval for such analyses.

Surface techniques that only minimally damage a specimen should be applied first to collect preliminary data assessing the potential of exceptional preservation. Such methods include scanning electron microscopy (SEM), which generates a 3D image of the topography of the sample, and time of flight secondary ion mass spectrometry (ToF-SIMS), which generates an ion spectrum unique to the sample [158,185]. Although these techniques are minimally damaging, one must consider and account for potential contamination. These methods are sensitive; therefore anything the surface has come in contact with can be a source of contamination and has the potential to interfere with analyses, particularly problematic for ToF-SIMS. This can be minimized by sampling freshly exposed areas.

After non-destructive analyses are performed, methods that require ‘destructive’ analyses can be employed. To reduce the amount of sample required, a small (less than 1mm) fragment

can be embedded in LR white medium, which is amenable to both transmission electron microscopy (TEM) and *in situ* immunohistochemical (IHC) analyses [186]. Sections can be cut from the same embedded sample to the necessary thickness for each type of analysis. TEM generates 2D images of the cross-section of the sample, providing micro- and ultrastructure details on a sub-nanometer scale [185]. *In situ* IHC gives specific information on the type of protein epitopes present in a sample as well as where they are localized allowing identification of exogenous contamination [186]. If endogenous, signal should only be seen within tissues, while exogenous contaminant would not be so localized.

Elemental analyses (energy dispersive X-ray spectroscopy, EDX or EDS) can be coupled with both SEM and TEM to provide qualitative information about the elemental makeup of the sample or sample area of interest. The quantitative data that are produced are relative because they depend on the number of X-rays detected, which varies with each sample run, surface topography and charging.

Criteria for endogeneity

After confirming exceptional preservation of a specimen by gross observation (e.g. articulation, persistence of structures not expected to preserve (e.g. macroscopic 'soft tissues' like feathers)), microscopic and molecular methods are employed to analyze characteristics of the samples. Only by comparing fossil tissues to similar extant tissues, can their origin or source be interpreted. Additionally, all samples and materials are stored and experiments are conducted in separate lab spaces to minimize the possibility of cross-contamination from modern materials.

The criteria for assessing endogeneity should be determined before experimentation begins and should be based upon what is known of the chemical physical and molecular make up of homologous extant tissues. 1. Ancient samples must retain microstructure and molecular fingerprints similar to their extant comparisons. 2. Multiple techniques, each testing for different features should be used collectively to support an endogenous origin. 3. Appropriate controls must be included for there to be confidence in the results and conclusions. These include a positive and negative control, usually modern tissue and sediment, respectively. 4. The fossil sample being tested should retain characteristics of the modern tissue, and should not be detected in the surrounding sediment.

Indeed, assigning criteria and acquiring the necessary data are not without challenges. No matter how high of a resolution an instrument can obtain, the source of the structures being

observed cannot be asserted without doubt. This is in part because diagenesis alters the organic matter which can result in features overlapping in resemblance, rendering it impossible to be certain that the structures accurately reflect the starting material. This is one of the many reasons taphonomic experiments are important for such studies. Fossils must be compared with similar modern tissues, however often the modern samples have not been characterized (this is particularly the case for molecular databases).

I employed the following criteria for keratinous fossils. The features that support endogeneity are: 1) an epidermally derived structure associated with the fossil and/or skeleton (Note: the first *Archaeopteryx* fossil was an isolated feather [187,188] and not associated with skeletal material, therefore any conclusions made from studying that fossil, such as color interpretation [155] must be met with caution because the organism who possessed that feather is not able to be identified with certainty [187].), 2) microstructure(s) consistent with the specific analogous extant tissue used for comparison (e.g. 3nm beta-keratin filaments), 3) molecular signal also consistent with extant tissue (e.g. positive IHC signal using anti-beta-keratin antibodies).

Role of microbes in preservation

It is well known that microbes are the primary agents of organic decay and decomposition [189]. But the participation of microbes in the preservation, especially exceptional preservation, of fossils is not as well understood. Nonetheless, the role of microbes, particularly microbially-mediated mineralization, has been the focus of several reviews and studies investigating both the fossilization of bacteria (autolithification) [190–197] and the role of bacteria in the fossilization of other organisms [198–206].

Most microorganisms occur in the natural world as biofilms, an aggregate of the organisms, and surrounded by the EPS matrix they secrete. This EPS accounts for over 90% of the dry mass [207–209] of the biofilm. The EPS is comprised of proteins and (poly) saccharides which create a ‘sticky’ medium that allows the biofilm and the organisms within to adhere to solid or liquid substrates [210,211]. These molecules impart a negative charge to both the cells and the biofilm making them highly reactive. Thus biofilms are good facilitators of biologically mediated mineral precipitation and absorption of nutrients and metals [211,212].

To preserve fossils in an exceptional manner, tissues must be stabilized before they decay [205,213,214]. Stabilization can occur by mineral precipitation on tissues, and it has been shown

that microbes facilitate this precipitation orders of magnitude more rapidly than it can occur abiotically [215]. Although microbes are known to facilitate mineralization, sometimes no microbial traces can be detected in fossil samples [213]. However, there are many instances where remnants of bacteria are observed in fossils, including but not limited to in a pterosaur crest [216], dinosaur coprolites [196], an Oligocene tadpole from Enspel [191], soft tissue of a Miocene frog [217], and a fetal horse [218]. Not to mention many of the fossils that have been recovered from the Messel shale (e.g., [190,201,219]).

The modes of microbially-mediated preservation that have been proposed include mineralization of the tissues themselves and/or the biofilms encasing them. The most documented is authigenic mineralization which is the rapid *in situ* deposition of minerals facilitated by the bacteria present during initial stages of decay [1,220,221]. What results is often a morphological replica of the organism (rather than permineralization or replacement) [213,222]. An example is the rapid phosphatization of the soft tissues of numerous fossils (e.g., [197,206,223]). Phospatization may occur in conjunction with calcium carbonate concretions where the phosphatized fossil serves as a substrate for the concretion, resulting in the exceptional 3-D preservation [221]. This has been referred to as ‘the Medusa effect’ or ‘instant fossilization’ because the carcass essentially turns to ‘stone’ and the deposition of mineral must occur before the animal is buried and before it decomposes [221]. This may also occur at the molecular level, where the mineral replaces the soft tissue [221]. Fossilization may also occur as only an impression of the organism in the surrounding biofilm due to early cementation with the surrounding sediment, followed by degradation of all original tissue [1,202].

Despite being well-documented in the paleontological literature, the mechanisms of these microbially-mediated mineralization processes remain to be elucidated. This can only be understood by performing actualistic taphonomic experiments in the lab which is possible because of the rapidity of these reactions (Discussed more below).

In bone

Archaeological and paleontological research has acknowledged microbial attack and infiltration of bone [224,225]. Because microbes, both prokaryotic (e.g. bacteria) and eukaryotic (e.g. fungi) are certainly among the primary agents of degradation of soft tissue and bone, but also are proposed to play a role in fossilization, then what exactly are fossils? And how is complete degradation evaded?

When soft tissues structures were first recovered and described from dinosaur bone, two hypotheses were put forth to address their origin: microbial [226] vs. endogenous [227–231]. Peterson et al. (2010) demonstrated a possible role for biofilms in exceptional preservation that resulted in retention of original soft tissue and/or endogenous biomolecules of such structures in fossils [203]. They performed a taphonomic experiment analyzing the growth and morphology of environmental biofilms on extant chicken and alligator bone and compared these results to fossil bone from the Hell Creek Formation (late Cretaceous) before and after demineralization. They used both whole and fractured extant bone and placed them in the different zones (and therefore different conditions) in a natural sink hole. From their study they proposed a mode of preservation which involves biofilm growth inside the pores of bone which subsequently prevents it from degradation early in decomposition; they call this process 'microbial masonry'.

The overarching conclusion of this paper is that exceptional preservation is more likely to occur in un-fractured bones perhaps by the process called "microbial masonry". Based on what is known about biofilm growth and the data presented in their paper, they propose that early in diagenesis, microorganisms would infiltrate bone through the surface openings, using the external bone and related soft tissue as nutrients. During their own growth, EPS secretions, and ultimate degradation, these microbes create microenvironments inside the bone, which then mineralize to virtually "seal off" the more interior soft tissue, leading to preservation. This "sealing off" phenomenon and creating microenvironments has been proposed on a larger scale (e.g., encasement of a carcass) [197,232].

Although we didn't investigate aspects of mineralization, we did choose to revisit and test the alternative hypothesis, proposed in 2008, that the vessel-like structures uncovered from dinosaur bones [227] were biofilm [226] and not endogenous to the dinosaur (Chapter 7). To do this, we first had to demonstrate that biofilm would invade bone from which all original organics were removed (as this is presumed to be the case for dinosaur bone based on conventional wisdom [233]), because this had not been demonstrated. We subjected small pieces (several millimeters) of bone which the organics had been removed, to biofilm forming organisms, *Bacillus cereus* and *Staphylococcus aureus.* These were placed in nutrient broth for two weeks (Chapter 7) after which time biofilm growth was observed on the surface of the bone. The mineral matrix was then removed with a calcium chelator to visualize the biofilm structures. Upon removal of the mineral matrix, it could be observed that the biofilms infiltrated the pores

of the bone, superficially mimicking the anastomosing network of vasculature; however any manipulation resulted in the rapid and complete disintegration of the biofilms. Electron microscopy illustrated distinct differences in the ultrastucture between the biofilm and dinosaur vessels, liberated from bone through chelation of calcium minerals. Additionally, *in situ* immunochemical methods demonstrated specific antigen retrieval. Biofilm structures only reacted with bacteria-specific antibodies and did not cross react with eukaryotic antibodies that bound the vessels. Likewise, the vessel-like structures did not bind the bacteria-specific antibodies. These results showed, using both electron microscopy and molecular techniques, that the structures recovered from fossil dinosaur bone do not support a biofilm origin; the alternative hypothesis of a microbial origin is not supported, rather an endogenous source is strengthened.

Other modes

Melanin

Melanin is a universal pigment molecule found in nearly all living organisms [234], from prokaryotic and eukaryotic microorganisms to complex vertebrates. Its ubiquity, photoprotective properties [18,235,236], and ability to scavenge free radicals [234,236–238] indicates it's probably one of the oldest biomolecules on earth. Its conformation and structure is not yet fully characterized due to the complexity of polymerization preventing it to be broken into monomeric units, heterogeneity in structure, and insolubility [234,239]. The melanin molecules consists of various functional groups (carboxylic acids, hydroxyls, and amines), allowing the molecule to participate in binding of various metals [240,241]. Various aspects of melanin pigmentation are environmentally influenced, such as oxidation states and ion exchange with metals [234]. Important for taphonomic studies, the microbes involved in organic degradation can also produce melanin [242,243].

In the past several years, melanin preservation has been the focus of many paleontological studies. Although melanin, an uncharacterized polymeric molecule [123], inherently has a high preservation potential, making it amenable to molecular paleontological studies, this has likely been fueled by the battery of fossil feather papers reporting the preservation of pigment-containing melanosomes. However, many of the studies rely on the assumption that melanin is preserved based on the presumption that the structures preserved are indeed melanosomes. This is circular reasoning.

In studies with data indicating the preservation of melanin, there still remains a viable question; is the melanin endogenous to the specimen or prokaryotic in origin? In samples of tissues which would have had had high concentrations of melanin in life (e.g. a fish eye [164] or squid ink [244]), it is more parsimonious to interpret the detected melanin fingerprint(s) as endogenous. However, in specimens which may or may not have been melanized in life (e.g. feathers) and because microorganisms produce melanin and are present in degradation (and preservation) of fossils, a microbial origin cannot be eliminated without testing.

Regardless of the origin, because of the characteristics of melanin and its inherent preservation potential, one could propose that the presence of melanin plays a role in the preservation of the soft tissues possibly through a process such as 'melanin leaching', as suggested by preliminary data from a taphonomic experiment (J. Lindgren, personal communication). Therefore, even when melanosomes are not observed, such as described in Chapter 5, melanin may still remain but dispersed throughout the remaining structure. This remains to be rigorously tested and analyzed using a preexisting set of criteria that account for chemical changes accruing during diagenesis.

Actualistic Taphonomy

The rapidity of reactions necessary to arrest degradation, thus allowing for the preservation of labile tissues and molecules, implies that they are capable of being reproduced in a lab while monitoring early diagenetic processes that may result in stabilization. Because preservation is clearly affected by burial environments [92], the interaction of bacteria with the surrounding environment immediately after the death of the animal is a crucial step in the preservation of fossils. This suggests that a mechanism for preservation at the molecular level can be identified, and supports previous and counterintuitive observations that microbes are agents of preservation as well as decay.

Actualistic experiments are amenable to hypothesis testing and will provide the data necessary for assessing the role of microbes (and their constituents) in preservation of soft tissues. If bacteria significantly influence the exceptional preservation in actualistic experiments then these findings can be used to model modes and mechanisms of preservation of exceptional fossils. If microbes facilitate preservation such that original molecules (and their diagenetic products) are preserved, this has many implications including predicting the type of environment that favors such preservation.

Implications

My research has laid the foundation for additional studies. I address suggestions for future work in the chapter summarizing these data (Chapter 8). Studying keratinous fossils at the microscopic and molecular level has implications for several aspects of paleontology including evolutionary (phylogenetic) relationships, biomechanics and ecology.

Keratinous structures are adapted and utilized for the lifestyle of the animal, e.g., feeding locomotion, display. Therefore scientists can infer aspects of behavior and biomechanics as well the ecology of the animal based upon the characteristics of these epidermally derived structures, all traits we cannot infer from studying bony elements alone.

Studying keratinous fossils at the molecular level will elucidate evolutionary relationships (dinosaur to bird transitions) and also provide temporal resolution of the protein family, which remains uncertain. Divergence times of the different types of beta-keratins have been estimated [34,43,46], but without sufficient resolution to determine unequivocally which avian and non-avian dinosaurs were expressing which type of beta-keratin. This is especially applicable to the evolution of 'flight' feathers and the evolution of powered flight. These questions can only be answered by studying fossils. For example, it is possible that the feathers of dinosaurs in the late Jurassic, such as *Archaeopteryx* and *Anchiornis*, were expressing an ancestral form of feather beta-keratin, estimated to have evolved ~157 million years ago [34,46].

The study of feather degradation also has the potential to provide useful data to the industry of poultry science and all disciplines involved in the initiative to rid of feather waste in a sustainable and eco-friendly way. Every year, billions of kilograms of feather waste are generated [245]. Because of their resistance to decomposition, waste elimination is challenging. Most methods currently employed are expensive and include incineration or landfill burial, which result in pollution or used in poor quality animal feed [245]. There are obvious concerns with these methods, especially the release of greenhouse gases. Therefore, by studying the decomposition and also preservation of feathers with the intent to elucidate the natural mechanisms involved, this knowledge can be applied to feather waste research to help determine how to more effectively and naturally deal with eliminating feather waste.

References

1. Briggs, D. E. G. 2003 The role of decay and mineralization in the preservation of soft-bodied fossils. *Annu. Rev. Earth Planet. Sci.* **31**, 275–301. (doi:doi:10.1146/annurev.earth.31.100901.144746)
2. Schweitzer, M. H. 2011 Soft Tissue Preservation in Terrestrial Mesozoic Vertebrates. *Annu. Rev. Earth Planet. Sci.* **39**, 187–216. (doi:doi:10.1146/annurev-earth-040610-133502)
3. Hitchcock, E. 1841 *Final Report on the Geology of Massachusetts: In Four Parts: I. Economical Geology. II. Scenographical Geology. III. Scientific Geology. IV. Elementary Geology. With an Appended Catalogue of the Specimens of Rocks and Minerals in the State Collection, Vol*. J.S. & C. Adams. [cited 2014 Jul. 10].
4. Schweitzer, M. H., Watt, J. A., Avci, R., Knapp, L., Chiappe, L., Norell, M. & Marshall, M. 1999 Beta-keratin specific immunological reactivity in feather-like structures of the Cretaceous Alvarezsaurid, Shuvuuia deserti. *J. Exp. Zool.* **285**, 146–157. (doi:10.1002/(sici)1097-010x(19990815)285:2<146::aid-jez7>3.0.co;2-a)
5. Schweitzer, M. H., Watt, J. A., Avci, R., Forster, C. A., Krause, D. W., Knapp, L., Rogers, R. R., Beech, I. & Marshall, M. 1999 Keratin Immunoreactivity in the Late Cretaceous Bird Rahonavis ostromi. *J. Vertebr. Paleontol.* **19**, 712–722.
6. Manning, P. L. et al. 2009 Mineralized soft-tissue structure and chemistry in a mummified hadrosaur from the Hell Creek Formation, North Dakota (USA). *Proc. Biol. Sci.* **276**, 3429–37. (doi:10.1098/rspb.2009.0812)
7. Lindgren, J. et al. 2015 Molecular composition and ultrastructure of Jurassic paravian feathers. *Sci. Rep.* **5**, 13520. (doi:10.1038/srep13520)
8. Lindgren, J. et al. 2014 Skin pigmentation provides evidence of convergent melanism in extinct marine reptiles. *Nature* (doi:10.1038/nature12899)
9. Huxley, T. 1864 The Structure and Classification of the Mammalia. *Med. Times Gaz.*
10. Goodrich, E. S. 1916 On the Classification of the Reptilia. *Proc. R. Soc. B Biol. Sci.* **89**, 261–276. (doi:10.1098/rspb.1916.0012)
11. Haslam, I. S., Roubos, E. W., Mangoni, M. L., Yoshizato, K., Vaudry, H., Kloepper, J. E., Pattwell, D. M., Maderson, P. F. A. & Paus, R. 2014 From frog integument to human skin: dermatological perspectives from frog skin biology. *Biol. Rev. Camb. Philos. Soc.* **89**,

618–55. (doi:10.1111/brv.12072)

12. Rakers, S., Gebert, M., Uppalapati, S., Meyer, W., Maderson, P., Sell, A. F., Kruse, C. & Paus, R. 2010 'Fish matters': the relevance of fish skin biology to investigative dermatology. *Exp. Dermatol.* **19**, 313–24. (doi:10.1111/j.1600-0625.2009.01059.x)
13. Strasser, B., Mlitz, V., Hermann, M., Rice, R. H., Eigenheer, R. A., Alibardi, L., Tschachler, E. & Eckhart, L. 2014 Evolutionary origin and diversification of epidermal barrier proteins in amniotes. *Mol. Biol. Evol.* **31**, 3194–205. (doi:10.1093/molbev/msu251)
14. Wu, P., Hou, L., Plikus, M., Hughes, M., Scehnet, J., Suksaweang, S., Widelitz, R. B., Jiang, T. X. & Chuong, C. M. 2004 Evo-Devo of amniote integuments and appendages. *Int. J. Dev. Biol.* **48**, 249–270. (doi:10.1387/ijdb.15272390)
15. Alibardi, L. 2006 Structural and Immunocytochemical Characterization of Keratinization in Vertebrate Epidermis and Epidermal Derivatives. *Int. Rev. Cytol.* **253**, 177–259. (doi:10.1016/S0074-7696(06)53005-0)
16. Alibardi, L. 2003 Adaptation to the land: The skin of reptiles in comparison to that of amphibians and endotherm amniotes. *J. Exp. Zool. B. Mol. Dev. Evol.* **298**, 12–41. (doi:10.1002/jez.b.24)
17. Green, K. J. & Jones, J. C. 1996 Desmosomes and hemidesmosomes: structure and function of molecular components. *FASEB J.* **10**, 871–81.
18. Wasmeier, C., Hume, A. N., Bolasco, G. & Seabra, M. C. 2008 Melanosomes at a glance. *J Cell Sci* **121**, 3995–3999. (doi:10.1242/jcs.040667)
19. Ligon, R. A. & McCArtney, K. L. 2016 Biochemical regulation of pigment motility in vertebrate chromatophores : A review of physiological color change mechanisms. *Curr. Zool.* **In Press**, 1–29.
20. d'Ischia, M. et al. 2013 Melanins and melanogenesis: methods, standards, protocols. *Pigment Cell Melanoma Res.* **26**, 616–633. (doi:10.1111/pcmr.12121)
21. Aufderheide, A. C. 2011 Soft tissue taphonomy: A paleopathology perspective. *Int. J. Paleopathol.* **1**, 75–80. (doi:10.1016/j.ijpp.2011.10.001)
22. Vandebergh, W. & Bossuyt, F. 2012 Radiation and functional diversification of alpha keratins during early vertebrate evolution. *Mol Biol Evol* **29**, 995–1004. (doi:msr269 [pii]10.1093/molbev/msr269 [doi])
23. Fuchs, E. 1995 Keratins and the skin. *Annu. Rev. Cell Dev. Biol.* **11**, 123–53.

(doi:10.1146/annurev.cb.11.110195.001011)

24. Moll, R., Divo, M. & Langbein, L. 2008 The human keratins: biology and pathology. *Histochem Cell Biol* **129**, 705–733. (doi:10.1007/s00418-008-0435-6 [doi])
25. Greenwold, M. & Sawyer, R. 2010 Genomic organization and molecular phylogenies of the beta (beta) keratin multigene family in the chicken (Gallus gallus) and zebra finch (Taeniopygia guttata): implications for feather evolution. *BMC Evol. Biol.* **10**, 148.
26. Fraser, R. D. B., MacRae, T. P. & Rogers, G. E. 1972 *Keratins: their composition, structure, and biosynthesis*. Springfield, Ill.: Thomas.
27. Carver, W. E. & Sawyer, R. H. 1988 Avian scale development: XI. Immunoelectron microscopic localization of alpha and beta keratins in the scutate scale. *J Morphol* **195**, 31–43. (doi:10.1002/jmor.1051950104 [doi])
28. Marshall, R. C., Orwin, D. F. G. & Gillespie, J. M. 1991 Structure and biochemistry of mammalian hard keratin. *Electron Microsc. Rev.* **4**, 47–83. (doi:10.1016/0892-0354(91)90016-6)
29. Alibardi, L., Toni, M. & Dalla Valle, L. 2007 Hard cornification in reptilian epidermis in comparison to cornification in mammalian epidermis. *Exp. Dermatol.* **16**, 961–976. (doi:10.1111/j.1600-0625.2007.00609.x)
30. Alibardi, L. 2007 Microscopic analysis of lizard claw morphogenesis and hypothesis on its evolution. *Acta Zool.* **89**, 169–178. (doi:10.1111/j.1463-6395.2007.00312.x)
31. Maderson, P. F. A. 2003 Mammalian skin evolution: a reevaluation. *Exp. Dermatol.* **12**, 233–236. (doi:10.1034/j.1600-0625.2003.00069.x)
32. Alibardi, L. 2007 Cell organization of barb ridges in regenerating feathers of the quail: implications of the elongation of barb ridges for the evolution and diversification of feathers. *Acta Zool.* **88**, 101–117. (doi:10.1111/j.1463-6395.2007.00257.x)
33. Alibardi, L., Dalla Valle, L., Nardi, A. & Toni, M. 2009 Evolution of hard proteins in the sauropsid integument in relation to the cornification of skin derivatives in amniotes. *J. Anat.* **214**, 560–586. (doi:10.1111/j.1469-7580.2009.01045.x)
34. Greenwold, M. J. & Sawyer, R. H. 2011 Linking the molecular evolution of avian beta (β) keratins to the evolution of feathers. *J. Exp. Zool. Part B Mol. Dev. Evol.* **316B**, 609–616. (doi:10.1002/jez.b.21436)
35. Holthaus, K. B. et al. 2015 Comparative genomics identifies epidermal proteins associated

with the evolution of the turtle shell. *Mol. Biol. Evol.* , msv265. (doi:10.1093/molbev/msv265)

36. Strasser, B., Mlitz, V., Hermann, M., Tschachler, E. & Eckhart, L. 2015 Convergent evolution of cysteine-rich proteins in feathers and hair. *BMC Evol. Biol.* **15**, 82. (doi:10.1186/s12862-015-0360-y)
37. Alibardi, L. 2015 Immunolocalization of sulfhydryl oxidase in reptilian epidermis indicates that the enzyme participates mainly to the hardening process of the beta-corneous layer. *Protoplasma* **252**, 1529–36. (doi:10.1007/s00709-015-0782-9)
38. Fraser, R. D. B. & Parry, D. A. D. 2008 Molecular packing in the feather keratin filament. *J. Struct. Biol.* **162**, 1–13.
39. Fraser, R. D. & Parry, D. A. 2011 The structural basis of the filament-matrix texture in the avian/reptilian group of hard beta-keratins. *J Struct Biol* **173**, 391–405. (doi:S1047-8477(10)00289-3 [pii]10.1016/j.jsb.2010.09.020 [doi])
40. Alibardi, L. 2015 Review: mapping epidermal beta-protein distribution in the lizard Anolis carolinensis shows a specific localization for the formation of scales, pads, and claws. *Protoplasma* (doi:10.1007/s00709-015-0909-z)
41. Gregg, K. & Rogers, G. E. 1986 Feather Keratin: Composition, Structure and Biogenesis. In *Biology of the integument* (eds J. Bereiter-Hahn A. G. Maltosy & K. S. Richards), pp. 667–694. Berlin: Springer-Verlag.
42. Wu, P. et al. 2015 Topographical mapping of α- and β-keratins on developing chicken skin integuments: Functional interaction and evolutionary perspectives. *Proc. Natl. Acad. Sci.* **112**, E6770–E6779. (doi:10.1073/pnas.1520566112)
43. Greenwold, M. J., Bao, W., Jarvis, E. D., Hu, H., Li, C., Gilbert, M., Zhang, G. & Sawyer, R. H. 2014 Dynamic evolution of the alpha (α) and beta (β) keratins has accompanied integument diversification and the adaptation of birds into novel lifestyles. *BMC Evol. Biol.* **14**, 249. (doi:10.1186/s12862-014-0249-1)
44. Gregg, K., Wilton, S. D., Parry, D. a & Rogers, G. E. 1984 A comparison of genomic coding sequences for feather and scale keratins: structural and evolutionary implications. *EMBO J.* **3**, 175–178.
45. Fraser, R. D. B., MacRae, T. P., Parry, D. A. D. & Suzuki, E. 1969 The structure of β-keratin. *Polymer (Guildf).* **10**, 810–826.

46. Greenwold, M. J. & Sawyer, R. H. 2013 Molecular evolution and expression of archosaurian β-keratins: diversification and expansion of archosaurian β-keratins and the origin of feather β-keratins. *J. Exp. Zool. B. Mol. Dev. Evol.* **320**, 393–405. (doi:10.1002/jez.b.22514)
47. Fraser, R. D. B. & Parry, D. A. D. 2011 The structural basis of the two-dimensional net pattern observed in the X-ray diffraction pattern of avian keratin. *J. Struct. Biol.* **176**, 340–349. (doi:10.1016/j.jsb.2011.08.010)
48. Sawyer, R., Glenn, T. & French, J. 2000 The expression of beta (β) keratins in the epidermal appendages of reptiles and birds. *Am. …* **539**, 530–539.
49. Musser, J. M., Wagner, G. P. & Prum, R. O. 2015 Nuclear β-catenin localization supports homology of feathers, avian scutate scales, and alligator scales in early development. *Evol. Dev.* **17**, 185–194. (doi:10.1111/ede.12123)
50. Maderson, P. F. A. 1972 When? Why? and How? Some Speculations on the Evolution of the Vertebrate Integument. *Integr. Comp. Biol.* **12**, 159–171. (doi:10.1093/icb/12.1.159)
51. Sawyer, R. H. & Knapp, L. W. 2003 Avian skin development and the evolutionary origin of feathers. *J. Exp. Zool. Part B Mol. Dev. Evol.* **298B**, 57–72. (doi:10.1002/jez.b.26)
52. Sawyer, R. H., Glenn, T. C., French, J. O. & Knapp, L. W. 2005 Developing Antibodies to Synthetic Peptides Based on Comparative DNA Sequencing of Multigene Families. In *Methods in Enzymology* (eds A. Z. Elizabeth & H. R. Eric), pp. 636–652. Academic Press.
53. Hawkes, J. W. 1974 The structure of fish skin. *Cell Tissue Res.* **149**, 147–158. (doi:10.1007/BF00222270)
54. Schaffeld, M., Höffling, S. & Jürgen, M. 2004 Sequence, evolution and tissue expression patterns of an epidermal type I keratin from the shark Scyliorhinus stellaris. *Eur. J. Cell Biol.* **83**, 359–368. (doi:10.1078/0171-9335-00395)
55. Zimek, A. & Weber, K. 2005 Terrestrial vertebrates have two keratin gene clusters; striking differences in teleost fish. *Eur. J. Cell Biol.* **84**, 623–35. (doi:10.1016/j.ejcb.2005.01.007)
56. Alibardi, L. 2001 Keratinization in the epidermis of amphibians and the lungfish: comparison with amniote keratinization. *Tissue Cell* **33**, 439–49. (doi:10.1054/tice.2001.0198)
57. Toni, M., Valle, L. D. & Alibardi, L. 2007 Hard (Beta-)keratins in the epidermis of

reptiles: composition, sequence, and molecular organization. *J Proteome Res* **6**, 3377–3392. (doi:10.1021/pr0702619 [doi])

58. Alibardi, L. & Toni, M. 2008 Cytochemical and molecular characteristics of the process of cornification during feather morphogenesis. *Prog. Histochem. Cytochem.* **43**, 1–69. (doi:10.1016/j.proghi.2008.01.001)
59. Maderson, P. F. A., Rabinowitz, T., Tandler, B. & Alibardi, L. 1998 Ultrastructural contributions to an understanding of the cellular mechanisms involved in lizard skin shedding with comments on the function and evolution of a unique lepidosaurian phenomenon. *J. Morphol.* **236**, 1–24. (doi:10.1002/(SICI)1097-4687(199804)236:1<1::AID-JMOR1>3.0.CO;2-B)
60. Alexander, N. 1970 Comparison of α and β keratin in reptiles. *Zeitschrift für Zellforsch. und Mikroskopische …* **165**, 153–165.
61. O'Guin, W. M. & Sawyer, R. H. 1982 Avian scale development: VIII. Relationships between morphogenetic and biosynthetic differentiation. *Dev. Biol.* **89**, 485–492. (doi:10.1016/0012-1606(82)90336-0)
62. Prin, F. & Dhouailly, D. 2004 How and when the regional competence of chick epidermis is established: feathers vs. scutate and reticulate scales, a problem en route to a solution. *Int. J. Dev. Biol.* **48**, 137–148. (doi:10.1387/ijdb.15272378)
63. Alibardi, L. 2005 Keratinization in crocodilian scales and avian epidermis : evolutionary implications for the origin of avian apteric epidermis. *Belgian J. Zool.* **135**, 9–20.
64. Alibardi, L. 2013 Immunolocalization of alpha-keratins and feather beta-proteins in feather cells and comparison with the general process of cornification in the skin of mammals. *Ann. Anat.* **195**, 189–98. (doi:10.1016/j.aanat.2012.08.005)
65. Fujii, T. & Li, D. 2008 Preparation and properties of protein films and particles from chicken feather citation export. *J. Biol. Macromol.* **8**, 48–55.
66. Stettenheim, P. R. 2000 The Integumentary Morphology of Modern Birds—An Overview. *Am. Zool.* **40**, 461–477. (doi:10.1093/icb/40.4.461)
67. Ng, C. S. et al. 2012 The chicken frizzle feather is due to an alpha-keratin (KRT75) mutation that causes a defective rachis. *PLoS Genet* **8**, e1002748. (doi:10.1371/journal.pgen.1002748 [doi]PGENETICS-D-11-02513 [pii])
68. Meyer, W. & Baumgartner, G. 1998 Embryonal feather growth in the chicken. *J. Anat.*

193, 611–616. (doi:10.1046/j.1469-7580.1998.19340611.x)

69. Alibardi, L. & Toni, M. 2006 Cytochemical, biochemical and molecular aspects of the process of keratinization in the epidermis of reptilian scales. *Prog. Histochem. Cytochem.* **40**, 73–134. (doi:10.1016/j.proghi.2006.01.001)
70. Sawyer, R. H., Rogers, L., Washington, L., Glenn, T. C. & Knapp, L. W. 2005 Evolutionary origin of the feather epidermis. *Dev. Dyn.* **232**, 256–267. (doi:10.1002/dvdy.20291)
71. Domyan, E. T. et al. 2016 Molecular shifts in limb identity underlie development of feathered feet in two domestic avian species. *Elife* **5**, 1–21. (doi:10.7554/eLife.12115)
72. Zheng, X., Zhou, Z., Wang, X., Zhang, F., Zhang, X., Wang, Y., Wei, G., Wang, S. & Xu, X. 2013 Hind wings in Basal birds and the evolution of leg feathers. *Science* **339**, 1309–12. (doi:10.1126/science.1228753)
73. Wu, P. et al. 2015 Topographical mapping of α- and β-keratins on developing chicken skin integuments: Functional interaction and evolutionary perspectives. *Proc. Natl. Acad. Sci.* **112**, E6770–E6779. (doi:10.1073/pnas.1520566112)
74. Alibardi, L. 2009 Claw development and cornification in the passeraceous bird zebrafinch (Taeniatopygia guttata castanotis). *Anat. Sci. Int.* **84**, 189–99. (doi:10.1007/s12565-009-0015-4)
75. Hu, D., Hou, L., Zhang, L. & Xu, X. 2009 A pre-Archaeopteryx troodontid theropod from China with long feathers on the metatarsus. *Nature* **461**, 640–643. (doi:http://www.nature.com/nature/journal/v461/n7264/suppinfo/nature08322_S1.html)
76. Mayr, G., Pohl, B., Hartman, S. & Peters, D. S. 2007 The tenth skeletal specimen of Archaeopteryx. *Zool. J. Linn. Soc.* **149**, 97–116. (doi:10.1111/j.1096-3642.2006.00245.x)
77. Nudds, R. L. & Dyke, G. J. 2010 Narrow Primary Feather Rachises in Confuciusornis and Archaeopteryx Suggest Poor Flight Ability. *Science* **328**, 887–889. (doi:10.1126/science.1188895)
78. Paul, G. S. 2010 Comment on "Narrow Primary Feather Rachises in Confuciusornis and Archaeopteryx Suggest Poor Flight Ability" *Science* **330**, 320–320. (doi:10.1126/science.1192963)
79. Nudds, R. L. & Dyke, G. J. 2010 Response to Comments on "Narrow Primary Feather Rachises in Confuciusornis and Archaeopteryx Suggest Poor Flight Ability"

Science **330**, 320–320. (doi:10.1126/science.1193474)

80. Foth, C., Tischlinger, H. & Rauhut, O. W. M. 2014 New specimen of Archaeopteryx provides insights into the evolution of pennaceous feathers. *Nature* **511**, 79–82. (doi:10.1038/nature13467)
81. Feo, T. J. et al. 2015 Barb geometry of asymmetrical feathers reveals a transitional morphology in the evolution of avian flight. *Proc. R. Soc. B Biol. Sci.* **282**, 20142864–20142864. (doi:10.1098/rspb.2014.2864)
82. Prum, R. O. 1999 Development and evolutionary origin of feathers. *J. Exp. Zool.* **285**, 291–306. (doi:10.1002/(sici)1097-010x(19991215)285:4<291::aid-jez1>3.0.co;2-9)
83. Prum, R. O. & Brush, A. H. 2002 The evolutionary origin and diversification of feathers. *Q. Rev. Biol.* **77**, 261–295.
84. Edward Hitchcock 1848 An Attempt to Discriminate and Describe the Animals That Made the Fossil Footmarks of the United States, and Especially of New England. In *Memoirs of the American Academy of Arts and Sciences*, pp. 129–256.
85. Osborn, H. F. 1911 A dinosaur mummy. *Am. Museum J.* , 7–11.
86. Bell, P. R. 2012 Standardized Terminology and Potential Taxonomic Utility for Hadrosaurid Skin Impressions: A Case Study for Saurolophus from Canada and Mongolia. *PLoS One* **7**, e31295.
87. Davis, M. 2012 Census of dinosaur skin reveals lithology may not be the most important factor in increased preservation of hadrosaurid skin. *Acta Palaeontol. Pol.* **59**, 601–605. (doi:10.4202/app.2012.0077)
88. Herrero, L. & Farke, A. a 2010 Hadrosaurid Dinosaur Skin Impressions from the Upper Cretaceus Kaiparowits Formation of Southern Utah, USA. *PalArch's J. Vertebr. Palaeontol.* **7**, 1–7.
89. Barrett, P. M., Evans, D. C. & Campione, N. E. 2015 Evolution of dinosaur epidermal structures. *Biol. Lett.* **11**, 20150229–20150229. (doi:10.1098/rsbl.2015.0229)
90. Czerkas, S. 1994 The History and Interpretations of Sauropod Skin Impressions. *GAIA* , 173–182.
91. Paik, I. S., Kim, H. J. & Huh, M. 2010 Impressions of dinosaur skin from the Cretaceous Haman Formation in Korea. *J. Asian Earth Sci.* **39**, 270–274. (doi:10.1016/j.jseaes.2010.02.015)

92. Davis, P. G. & Briggs, D. E. G. 1995 Fossilization of feathers. *Geology* **23**, 783–786. (doi:10.1130/0091-7613(1995)023<0783:fof>2.3.co;2)
93. Butterfield, N. J. 1990 Organic Preservation of Non-Mineralizing Organisms and the Taphonomy of the Burgess Shale. *Paleobiology* **16**, 272–286.
94. Butterfield, N. J. 2003 Exceptional Fossil Preservation and the Cambrian Explosion. *Integr. Comp. Biol.* **43**, 166–177. (doi:10.1093/icb/43.1.166)
95. Carpenter, K. 2007 How to make a fossil: Part 2 - dinosaur mummies and other soft tissue. *J. Paleontol. Sci.* **1**, 1–10. (doi:JPS.C.07.0001)
96. Benton, M. J., Zhonghe, Z., Orr, P. J., Fucheng, Z. & Kearns, S. L. 2008 The remarkable fossils from the Early Cretaceous Jehol Biota of China and how they have changed our knowledge of Mesozoic life. *Proc. Geol. Assoc.* **119**, 209–228. (doi:10.1016/S0016-7878(08)80302-1)
97. Chiappe, L. M., Coria, R. A., Dingus, L., Jackson, F., Chinsamy, A. & Fox, M. 1998 Sauropod dinosaur embryos from the Late Cretaceous of Patagonia. *Nature* **396**, 258–261.
98. Coria, R. A. & Chiappe, L. M. 2007 Embryonic Skin from Late Cretaceous Sauropods (Dinosauria) of Auca Mahuevo, Patagonia, Argentina. *J. Paleontol.* **81**, 1528–1532. (doi:10.1666/05-150.1)
99. Grellet-Tinner, G. 2005 Membrana Testacea of Titanosaurid Dinosaur Eggs from Auca Mahuevo (Argentina): Implications for Exceptional Preservation of Soft Tissue in Lagerstatten. *J. Vertebr. Paleontol.* **25**, 99–106. (doi:10.1671/0272-4634(2005)025[0099:mtotde]2.0.co;2)
100. Ji, S. & Bo, H. 1998 Discovery of the Psittacosaurid skin impressions and its significance. *Geol. Rev.* **44**, 603–606.
101. Godefroit, P., Sinitsa, S. M., Dhouailly, D., Bolotsky, Y. L., Sizov, A. V., McNamara, M. E., Benton, M. J. & Spagna, P. 2014 A Jurassic ornithischian dinosaur from Siberia with both feathers and scales. *Science* **345**, 451–455. (doi:10.1126/science.1253351)
102. Martill, D. M., Batten, D. J. & Loydell, D. K. 2000 A new specimen of the thyreophoran dinosaur cf. Scelidosaurus with soft tissue preservation. *Palaeontology* **43**, 549–559. (doi:10.1111/j.0031-0239.2000.00139.x)
103. Mayr, G., Peters, D. S., Plodowski, G. & Vogel, O. 2002 Bristle-like integumentary structures at the tail of the horned dinosaur Psittacosaurus. *Naturwissenschaften* **89**, 361–

5. (doi:10.1007/s00114-002-0339-6)

104. Godefroit, P., Cau, A., Dong-Yu, H., Escuillie, F., Wenhao, W. & Dyke, G. 2013 A Jurassic avialan dinosaur from China resolves the early phylogenetic history of birds. *Nature* **advance on**. (doi:10.1038/nature12168http://www.nature.com/nature/journal/vaop/ncurrent/abs/nature12168.html#supplementary-information)
105. Larson, P., Larson, M., Ott, C. & Bakker, R. 2007 Skinning a Triceratops. In *Journal of Vertebrate Paleontology*, pp. 104A. Soceity of Vertebrate Paleontology.
106. Christiansen, N. A. & Tschopp, E. 2010 Exceptional stegosaur integument impressions from the Upper Jurassic Morrison Formation of Wyoming. *Swiss J. Geosci.* **103**, 163–171. (doi:10.1007/s00015-010-0026-0)
107. Briggs, D. E. G., R., W. P., Perez-Moreno, B. P., Sanz, J. L. & Fregenal-Martinez, M. 1997 The mineralization of dinosaur soft tissue in the Lower Cretaceous of Las Hoyas, Spain. *J. Geol. Soc. London.* **154**, 587–588. (doi:10.1144/gsjgs.154.4.0587)
108. Rauhut, O. W. M., Foth, C., Tischlinger, H. & Norell, M. A. 2012 Exceptionally preserved juvenile megalosauroid theropod dinosaur with filamentous integument from the Late Jurassic of Germany. *Proc. Natl. Acad. Sci.* (doi:10.1073/pnas.1203238109)
109. van der Reest, A. J., Wolfe, A. P. & Currie, P. J. 2016 A densely feathered ornithomimid (Dinosauria: Theropoda) from the Upper Cretaceous Dinosaur Park Formation, Alberta, Canada. *Cretac. Res.* **58**, 108–117. (doi:10.1016/j.cretres.2015.10.004)
110. Martill, D. M. & Unwin, D. M. 1989 Exceptionally well preserved pterosaur wing membrane from the Cretaceous of Brazil. *Nature* **340**, 138–140. (doi:10.1038/340138a0)
111. Wang, X. 2002 A nearly completely articulated rhamphorhynchoid pterosaur with exceptionally well-preserved wing membranes and ?hairs? from Inner Mongolia, northeast China. *Chinese Sci. Bull.* **47**, 226. (doi:10.1360/02tb9054)
112. Martill, D. M. 1995 An ichthyosaur with preserved soft tissue from the Sinemurian of southern England. *Palaeontology* **38**, 897–903.
113. Garwood, G. A., Mortland, M. M. & Pinnavaia, T. J. 1983 Immobilization of glucose oxidase on montmorillonite clay: hydrophobic and ionic modes of binding. *J. Mol. Catal.* **22**, 153–163.
114. Mayer, L. M. 1989 Extracellular proteolytic enzyme activity in sediments of an intertidal

mudflat. *Limnol. Oceanogr.* **34**, 973–981. (doi:10.4319/lo.1989.34.6.0973)

115. Rieppel, O. 1980 Green anole in Dominican amber. *Nature* **286**, 486–487. (doi:10.1038/286486a0)
116. Poinar, G. O. & Cannatella, D. C. 1987 An upper eocene frog from the dominican republic and its implication for Caribbean biogeography. *Science* **237**, 1215–6. (doi:10.1126/science.237.4819.1215)
117. Bauer, A. M., Böhme, W. & Weitschat, W. 2005 An Early Eocene gecko from Baltic amber and its implications for the evolution of gecko adhesion. *J. Zool.* **265**, 327–332. (doi:10.1017/S0952836904006259)
118. Borsuk-BiĄnicka, M., Lubka, M. & BÓhme, W. 1999 A lizard from Baltic amber (Eocene) and the ancestry of the crown group lacertid. *Acta Palaeontol. Pol.* **44**, 349–38.
119. Daza, J. D., Stanley, E. L., Wagner, P., Bauer, A. M. & Grimaldi, D. A. 2016 Mid-Cretaceous amber fossils illuminate the past diversity of tropical lizards. *Sci. Adv.* **2**, e1501080–e1501080. (doi:10.1126/sciadv.1501080)
120. Perrichot, V. & Néraudeau, D. 2005 Reptile skin remains in the Cretaceous amber of France. *Comptes Rendus Palevol* **4**, 47–51. (doi:10.1016/j.crpv.2004.11.009)
121. Grimaldi, D. A., Engel, M. S. & Nascimbene, P. C. 2002 Fossiliferous Cretaceous Amber from Myanmar (Burma): Its Rediscovery, Biotic Diversity, and Paleontological Significance. *Am. Museum Novit.* **3361**, 1–71. (doi:10.1206/0003-0082(2002)361<0001:FCAFMB>2.0.CO;2)
122. Arnold, E. N., Azar, D., Ineich, I. & Nel, A. 2002 The oldest reptile in amber: a 120 million year old lizard from Lebanon. *J. Zool.* **258**, 7–10. (doi:10.1017/S0952836902001152)
123. Stankiewicz, B. A., Poinar, H. N., Briggs, D. E. G., Evershed, R. P. & Poinar, G. O. 1998 Chemical preservation of plants and insects in natural resins. *Proc. R. Soc. B Biol. Sci.* **265**, 641–647. (doi:10.1098/rspb.1998.0342)
124. Szewciw, L. J., de Kerckhove, D. G., Grime, G. W. & Fudge, D. S. 2010 Calcification provides mechanical reinforcement to whale baleen alpha-keratin. *Proc. Biol. Sci.* **277**, 2597–605. (doi:10.1098/rspb.2010.0399)
125. Vullo, R., Girard, V., Azar, D. & Néraudeau, D. 2010 Mammalian hairs in Early Cretaceous amber. *Naturwissenschaften* **97**, 683–7. (doi:10.1007/s00114-010-0677-8)

126. Martin, T., Marugán-Lobón, J., Vullo, R., Martín-Abad, H., Luo, Z.-X. & Buscalioni, A. D. 2015 A Cretaceous eutriconodont and integument evolution in early mammals. *Nature* **526**, 380–4. (doi:10.1038/nature14905)
127. Meng, J. & Wyss, A. R. 1997 Multituberculate and other mammal hair recovered from Palaeogene excreta. *Nature* **385**, 712–4. (doi:10.1038/385712a0)
128. Prum, R. O. 1999 Development and evolutionary origin of feathers. *J. Exp. Zool.* **285**, 291–306. (doi:10.1002/(SICI)1097-010X(19991215)285:4<291::AID-JEZ1>3.0.CO;2-9)
129. Chen, P., Dong, Z. & Zhen, S. 1998 An exceptionally well-preserved theropod dinosaur from the Yixian Formation of China. *Nature* **391**, 147–152.
130. Xu, X., Tang, Z. & Wang, X. 1999 A therizinosauroid dinosaur with integumentary structures from China. *Nature* **399**, 350–354. (doi:http://www.nature.com/nature/journal/v399/n6734/suppinfo/399350a0_S1.html)
131. Lowe, C. B., Clarke, J. A., Baker, A. J., Haussler, D. & Edwards, S. V. 2015 Feather Development Genes and Associated Regulatory Innovation Predate the Origin of Dinosauria. *Mol. Biol. Evol.* **32**, 23–28. (doi:10.1093/molbev/msu309)
132. Xu, X., Zhou, Z., Dudley, R., Mackem, S., Chuong, C.-M., Erickson, G. M. & Varricchio, D. J. 2014 An integrative approach to understanding bird origins. *Science* **346**, 1253293–1253293. (doi:10.1126/science.1253293)
133. Chen, C.-F., Foley, J., Tang, P.-C., Li, A., Jiang, T. X., Wu, P., Widelitz, R. B. & Chuong, C. M. 2015 Development, regeneration, and evolution of feathers. *Annu. Rev. Anim. Biosci.* **3**, 169–95. (doi:10.1146/annurev-animal-022513-114127)
134. Qiang, J., Currie, P. J., Norell, M. A. & Shu-An, J. 1998 Two feathered dinosaurs from northeastern China. *Nature* **393**, 753–761. (doi:http://www.nature.com/nature/journal/v393/n6687/suppinfo/393753a0_S1.html)
135. Brush, A. H. 2000 Evolving a Protofeather and Feather Diversity. *Am. Zool.* **40**, 631–639. (doi:10.1668/0003-1569(2000)040[0631:EAPAFD]2.0.CO;2)
136. Xu, X., Zhou, Z., Wang, X., Kuang, X., Zhang, F. & Du, X. 2003 Four-winged dinosaurs from China. *Nature* **421**, 335–340.
137. Xu, X., Zhao, Q., Norell, M., Sullivan, C., Hone, D., Erickson, G., Wang, X., Han, F. & Guo, Y. 2009 A new feathered maniraptoran dinosaur fossil that fills a morphological gap in avian origin. *Sci. Bull.* **54**, 430–435. (doi:10.1007/s11434-009-0009-6)

138. Xu, X. et al. 2015 A bizarre Jurassic maniraptoran theropod with preserved evidence of membranous wings. *Nature* **521**, 70–73. (doi:10.1038/nature14423)
139. Maderson, P. F. A. & Alibardi, L. 2000 The Development of the Sauropsid Integument: A Contribution to the Problem of the Origin and Evolution of Feathers. *Am. Zool.* **40**, 513–529. (doi:10.1093/icb/40.4.513)
140. Knapp, L. W., Shames, R. B., Barnes, G. L. & Sawyer, R. H. 1993 Region-specific patterns of beta keratin expression during avian skin development. *Dev. Dyn.* **196**, 283–290. (doi:10.1002/aja.1001960411)
141. Persons, W. S. & Currie, P. J. 2015 Bristles before down: A new perspective on the functional origin of feathers. *Evolution (N. Y).* **69**, 857–862. (doi:10.1111/evo.12634)
142. Mckellar, R. C., Chatterton, B. D. E., Wolfe, A. P. & Currie, P. J. 2011 A Diverse Assemblage of Late Cretaceous dinosaur and bird feathers from Canadian amber. *Science* **333**, 1619–1622. (doi:10.1126/science.1203344)
143. Jiang, B., Harlow, G. E., Wohletz, K., Zhou, Z. & Meng, J. 2014 New evidence suggests pyroclastic flows are responsible for the remarkable preservation of the Jehol biota. *Nat. Commun.* **5**, 3151. (doi:10.1038/ncomms4151)
144. Benton, M. J., Zhonghe, Z., Orr, P. J., Fucheng, Z. & Kearns, S. L. 2008 The remarkable fossils from the Early Cretaceous Jehol Biota of China and how they have changed our knowledge of Mesozoic life. Presidential Address, delivered 2nd May 2008. *Proc. Geol. Assoc.* **119**, 209–228. (doi:10.1016/S0016-7878(08)80302-1)
145. Knight, T. K., Bingham, P. S., Lewis, R. D. & Savrda, C. E. 2011 Feathers of the Ingersoll Shale, Eutaw Formation (Upper Cretaceous), Eastern Alabama: the Largest Collection of Feathers From North American Mesozoic Rocks. *Palaios* **26**, 364–376. (doi:10.2110/palo.2010.p10-091r)
146. Foth, C. 2012 On the identification of feather structures in stem-line representatives of birds: Evidence from fossils and actuopalaeontology. *Palaontologische Zeitschrift* **86**, 91–102. (doi:10.1007/s12542-011-0111-3)
147. Zhang, F. & Zhou, Z. 2000 A Primitive Enantiornithine Bird and the Origin of Feathers. *Science* **290**, 1955–1959. (doi:10.1126/science.290.5498.1955)
148. Wuttke, M. 1983 'Weichteil-Erhaltung' durch lithifizierte Mikroorganismen bei mittel-eozänen Vetebraten aus den Ölschiefern der 'Grube Messel' bei Darmstadt.pdf.

Senckenbergiana lethaea **64**, 509–527.

149. Wetmore, A. 1943 The occurrence of feather impressions in the Miocene deposits of Maryland. *Auk* **60**, 440–441.
150. Vinther, J., Briggs, D. E. G., Prum, R. O. & Saranathan, V. 2008 The colour of fossil feathers. *Biol. Lett.* **4**, 522–525. (doi:10.1098/rsbl.2008.0302)
151. Clarke, J. A., Ksepka, D. T., Salas-Gismondi, R., Altamirano, A. J., Shawkey, M. D., D'Alba, L., Vinther, J., DeVries, T. J. & Baby, P. 2010 Fossil Evidence for Evolution of the Shape and Color of Penguin Feathers. *Science* **330**, 954–957. (doi:10.1126/science.1193604)
152. Vinther, J., Briggs, D. E. G., Clarke, J., Mayr, G. & Prum, R. O. 2010 Structural coloration in a fossil feather. *Biol. Lett.* **6**, 128–131. (doi:10.1098/rsbl.2009.0524)
153. Li, Q., Gao, K. Q., Vinther, J., Shawkey, M. D., Clarke, J. A., D'Alba, L., Meng, Q., Briggs, D. E. & Prum, R. O. 2010 Plumage color patterns of an extinct dinosaur. *Science* **327**, 1369–1372. (doi:science.1186290 [pii]10.1126/science.1186290 [doi])
154. Zhang, F., Kearns, S. L., Orr, P. J., Benton, M. J., Zhou, Z., Johnson, D., Xu, X. & Wang, X. 2010 Fossilized melanosomes and the colour of Cretaceous dinosaurs and birds. *Nature* **463**, 1075–1078. (doi:http://www.nature.com/nature/journal/v463/n7284/suppinfo/nature08740_S1.html)
155. Carney, R. M., Vinther, J., Shawkey, M. D., D'Alba, L. & Ackermann, J. 2012 New evidence on the colour and nature of the isolated Archaeopteryx feather. *Nat. Commun.* **3**, 637. (doi:10.1038/ncomms1642)
156. Li, Q. et al. 2012 Reconstruction of Microraptor and the Evolution of Iridescent Plumage. *Science* **335**, 1215–1219. (doi:10.1126/science.1213780)
157. Li, Q., Clarke, J. a, Gao, K. Q., Zhou, C. F., Meng, Q., Li, D., D'Alba, L. & Shawkey, M. D. 2014 Melanosome evolution indicates a key physiological shift within feathered dinosaurs. *Nature* **507**, 350–353. (doi:10.1038/nature12973)
158. Lindgren, J., Uvdal, P., Sjövall, P., Nilsson, D. E., Engdahl, A., Schultz, B. P. & Thiel, V. 2012 Molecular preservation of the pigment melanin in fossil melanosomes. *Nat Commun* **3**, 1–7. (doi:http://www.nature.com/ncomms/journal/v3/n5/suppinfo/ncomms1819_S1.html)
159. Moyer, A. E., Zheng, W., Johnson, E. a, Lamanna, M. C., Li, D.-Q., Lacovara, K. J. &

Schweitzer, M. H. 2014 Melanosomes or microbes: testing an alternative hypothesis for the origin of microbodies in fossil feathers. *Sci. Rep.* **4**, 4233. (doi:10.1038/srep04233)

160. Hill, G. E. & McGraw, K. J. 2006 *Bird Coloration: Function and evolution*. Harvard University Press.
161. Matthew D. Shawkey, Shreekumar R. Pillai, Geoffrey E. Hill, Lynn M. Siefferman & Sharon R. Roberts 2007 Bacteria as an Agent for Change in Structural Plumage Color: Correlational and Experimental Evidence. *Am. Nat.* **169**, S112–S121. (doi:10.1086/510100)
162. McGraw, K. J. 2006 Mechanics of Melanin-Based Coloration. In *Bird Coloration: Mechanisms and measurements* (eds G. E. Hill & K. J. McGraw), pp. 243–294. London: Harvard University Press.
163. Vinther, J. 2015 Fossil melanosomes or bacteria? A wealth of findings favours melanosomes: Melanin fossilises relatively readily, bacteria rarely, hence the need for clarification in the debate over the identity of microbodies in fossil animal specimens. *Bioessays* **38**, 220–5. (doi:10.1002/bies.201500168)
164. Lindgren, J. et al. 2015 Interpreting melanin-based coloration through deep time: a critical review. *Proc. R. Soc. B Biol. Sci.* **282**, 20150614. (doi:10.1098/rspb.2015.0614)
165. Vinther, J. 2015 A guide to the field of palaeo colour: Melanin and other pigments can fossilise: Reconstructing colour patterns from ancient organisms can give new insights to ecology and behaviour. *BioEssays* **37**, 643–656. (doi:10.1002/bies.201500018)
166. Schweitzer, M. H., Lindgren, J. & Moyer, A. E. 2015 Melanosomes and ancient coloration re-examined: A response to Vinther 2015 (DOI 10.1002/bies.201500018). *BioEssays* , n/a–n/a. (doi:10.1002/bies.201500061)
167. Chiappe, L. M., Norell, M. A. & Clark, J. M. 1998 The skull of a relative of the stem-group bird Mononykus. *Nature* **392**, 275–278. (doi:10.1038/32642)
168. Xu, X., Wang, X.-L. & Wu, X.-C. 1999 A dromaeosaurid dinosaur with a filamentous integument from the Yixian Formation of China. *Nature* **401**, 262–266. (doi:http://www.nature.com/nature/journal/v401/n6750/suppinfo/401262a0_S1.html)
169. Xu, X. & Zhang, F. 2005 A new maniraptoran dinosaur from China with long feathers on the metatarsus. *Naturwissenschaften* **92**, 173–177. (doi:10.1007/s00114-004-0604-y)
170. Zanno, L. E. & Sampson, S. D. 2005 A New Oviraptorosaur (Theropoda, Maniraptora)

from the Late Cretaceous (Campanian) of Utah. *J. Vertebr. Paleontol.* **25**, 897–904.

171. Norell, M. A., Clark, J. M., Chiappe, L. M. & Dashzeveg, D. 1995 A nesting dinosaur. *Nature* **378**, 774–776. (doi:10.1038/378774a0)
172. Clark, J. M., Norell, M. & Chiappe, L. M. 1999 An oviraptorid skeleton from the late Cretaceous of Ukhaa Tolgod, Mongolia, preserved in an avianlike brooding position over an oviraptorid nest. *Am. Museum Novit.* **3265**, 1–36.
173. Cope, E. D. 1883 On the Characters of the Skull in the Hadrosauridæ. *Proc. Acad. Nat. Sci. Philadelphia* **35**, 97–107.
174. Sternberg, C. M. 1935 Hooded hadrosaurs of the Belly River series of the Upper Cretaceous: A comparison with descriptions of new species. *Nat. Mus. Bull* **77**, 1–37.
175. Versluys, J. 1923 Der Schadel des Skelettes von Trachodon annectens im Senkenberg. *Abh. Senckenb. Naturf. Ges* **38**, 1–19.
176. Morris, W. J. 1970 Hadrosaurian dinosaur bills – morphology and function. *Contrib. Sci. Los Angeles Cty. Museum Nat. Hist.* **193**, 1–14.
177. Norell, M. A., Makovicky, P. J. & Currie, P. J. 2001 Palaeontology. The beaks of ostrich dinosaurs. *Nature* **412**, 873–874. (doi:10.1038/35091139 [doi]35091139 [pii])
178. Witmer, L. M. 1995 The extant phylogenetic bracket and the importance of reconstructing soft tissues in fossils. In *Functional Morphology in Vertebrate Paleontology*, pp. 19–33.
179. Horner, J. R. & Marshall, C. 2002 Keratinous covered dinosaur skulls. In *Journal of Vertebrate Paleontology*,
180. Lautenschlager, S., Witmer, L. M., Altangerel, P. & Rayfield, E. J. 2013 Edentulism, beaks, and biomechanical innovations in the evolution of theropod dinosaurs. *Proc. Natl. Acad. Sci. U. S. A.* **110**, 20657–62. (doi:10.1073/pnas.1310711110)
181. Ostrom, J. H. 1961 Cranial Morphology of the Hadrosaurian Dinosaurs of North America. *Bull. Am. Museum Nat. Hist.* **122**, 33–186.
182. Hieronymus, T. L. & Witmer, L. M. 2010 Homology and Evolution of Avian Compound Rhamphothecae. *Auk* **127**, 590–604. (doi:10.1525/auk.2010.09122)
183. Sereno, P. C., Shichin, C., Zhengwu, C. & Chenggang, R. 1988 Psittacosaurus meileyingensis (Ornithischia: Ceratopsia), a new psittacosaur from the Lower Cretaceous of northeastern China. *J. Vertebr. Paleontol.* **8**, 366–377. (doi:10.1080/02724634.1988.10011725)

184. Horner, J. R. & Goodwin, M. B. 2008 Ontogeny of cranial epi-ossifications in Triceratops. *J. Vertebr. Paleontol.* **28**, 134–144. (doi:10.1671/0272-4634(2008)28[134:OOCEIT]2.0.CO;2)
185. Schweitzer, M. H., Avci, R., Collier, T. & Goodwin, M. B. 2008 Microscopic, chemical and molecular methods for examining fossil preservation. *Comptes Rendus Palevol* **7**, 159–184. (doi:10.1016/j.crpv.2008.02.005)
186. Zheng, W. & Schweitzer, M. H. 2012 Chemical analyses of fossil bone. In *Forensic Microscopy for Skeletal Tissues: Methods and Protocols, Methods in Molecular Biology* (ed L. S. Bell), pp. 153–72. [cited 2015 Mar. 23]. (doi:10.1007/978-1-61779-977-8_10)
187. Griffiths, P. J. 1996 The Isolated Archaeopteryx Feather. *Archaeopteryx* , 1–26.
188. von Meyer, H. 1861 Archaeopterix lithographica (Vogel-Feder) und Pterodactylus von Solenhofen. *N. Jb. Geol. Paläont. Mh. Jahr.* , 678–679.
189. Dent, B. B., Forbes, S. L. & Stuart, B. H. 2004 Review of human decomposition processes in soil. *Environ. Geol.* **45**, 576–585. (doi:10.1007/s00254-003-0913-z)
190. Liebig, K., Westall, F. & Schmitz, M. 1996 A study of fossil microstructures from the Eocene Messel Formation using transmission electron microscopy. *N. Jb. Geol. Pala¨ont. Mh* **4**, 218–231.
191. Toporski, J. K. W., Steele, A., Westall, F., Avci, R., Martill, D. M. & McKay, D. S. 2002 Morphologic and spectral investigation of exceptionally well-preserved bacterial biofilms from the Oligocene Enspel formation, Germany. *Geochim. Cosmochim. Acta* **66**, 1773–1791.
192. Westall, F. 1999 The nature of fossil bacteria: A guide to the search for extraterrestrial life. *J. Geophys. Res. Planets* **104**, 16437–16451. (doi:10.1029/1998je900051)
193. Toporski, J. K. W., Steele, A., Westall, F., Thomas-Keprta, K. L. & McKay, D. S. 2002 The Simulated Silicification of Bacteria— New Clues to the Modes and Timing of Bacterial Preservation and Implications for the Search for Extraterrestrial Microfossils. *Astrobiology* **2**, 1–26. (doi:10.1089/153110702753621312)
194. Westall, F., Boni, L. & Guerzoni, E. 1995 The experimental silicification of microorganisms. *Palaeontology* **48**, 495–528.
195. Wierzchos, J., Sancho, L. G. & Ascaso, C. 2005 Biomineralization of endolithic microbes in rocks from the McMurdo Dry Valleys of Antarctica: implications for microbial fossil

formation and their detection. *Environ. Microbiol.* **7**, 566–75. (doi:10.1111/j.1462-2920.2005.00725.x)

196. Hollocher, T. C., Chin, K., Hollocher, K. T. & Kruge, M. A. 2001 Bacterial Residues in Coprolite of Herbivorous Dinosaurs: Role of Bacteria in Mineralization of Feces. *Palaios* **16**, 547–565. (doi:10.1669/0883-1351(2001)016<0547:bricoh>2.0.co;2)
197. Martill, D. M. & Wilby, P. R. 1994 Lithified prokaryotes associated with fossil soft tissues from the Santana Formation (Cretaceous) of Brazil. *Kaupia* , 71–77.
198. Dunn, K. A., McLean, R. J. C., Upchurch, G. R. . J. & Folk, R. L. 1997 Enhancement of leaf fossilization potential by bacterial biofilms. *Geology* **25**, 1119–1122. (doi:10.1130/0091-7613(1997)025)
199. Sagemann, J., Bale, S. J., Briggs, D. E. G. & Parkes, R. J. 1999 Controls on the formation of authigenic minerals in association with decaying organic matter: an experimental approach. *Geochim. Cosmochim. Acta* **63**, 1083–1095. (doi:http://dx.doi.org/10.1016/S0016-7037(99)00087-3)
200. Raff, E. C. et al. 2008 Embryo fossilization is a biological process mediated by microbial biofilms. *Proc. Natl. Acad. Sci.* (doi:10.1073/pnas.0810106105)
201. Franzen, J. L. 1985 Exceptional Preservation of Eocene Vertebrates in the Lake Deposit of Grube Messel (West Germany). *Philos. Trans. R. Soc. B Biol. Sci.* **311**, 181–186. (doi:10.1098/rstb.1985.0150)
202. Gehling, J. G. 1999 Microbial Mats in Terminal Proterozoic Siliciclastics: Ediacaran Death Masks. *Palaios* **14**, 40–57.
203. Peterson, J. E., Lenczewski, M. E. & Scherer, R. P. 2010 Influence of Microbial Biofilms on the Preservation of Primary Soft Tissue in Fossil and Extant Archosaurs. *PLoS One* **5**, e13334.
204. Iniesto, M., Lopez-Archilla, A. I., Fregenal-Martinez, M., Buscalioni, A. D. & Guerrero, M. C. 2013 Involvement of Microbial Mats in Delayed Deca: An Experimental Essay on Fish Preservation. *Palaios* **28**, 56–66. (doi:10.2110/palo.2011.p11-099r)
205. Raff, R. A., Andrews, M. E., Pearson, R. L., Turner, F. R., Saur, S. T., Thomas, D. C., Eagan, J. L. & Raff, E. C. 2014 Microbial Ecology and Biofilms in the Taphonomy of Soft Tissues. *Palaios* **29**, 560–569. (doi:10.2110/palo.2014.043)
206. Wilby, P. R., Briggs, D. E. G., Bernier, P. & Gaillard, C. 1996 Role of microbial mats in

the fossilization of soft tissues. *Geology* **24**, 787–790. (doi:10.1130/0091-7613(1996)024)

207. Wingender, J., Neu, T. R. & Flemming, H. C. 1999 *Microbial Extracellular Polymeric Substances: Characterization, Structure, and Function*. Heidelberg, Germany: Springer.
208. Flemming, H.-C. & Wingender, J. 2010 The biofilm matrix. *Nat. Rev. Microbiol.* **8**, 623–633. (doi:10.1080/0892701031000072190)
209. Pacton, M., Fiet, N. & Gorin, G. E. 2007 Bacterial Activity and Preservation of Sedimentary Organic Matter: The Role of Exopolymeric Substances. *Geomicrobiol. J.* **24**, 571–581. (doi:10.1080/01490450701672042)
210. Wijman, J. G. E., de Leeuw, P. P. L. A., Moezelaar, R., Zwietering, M. H. & Abee, T. 2007 Air-liquid interface biofilms of Bacillus cereus: formation, sporulation, and dispersion. *Appl. Environ. Microbiol.* **73**, 1481–8. (doi:10.1128/AEM.01781-06)
211. Krumbein, W. E., Paterson, D. M. & Zavarzin, G. A. 2003 *Fossil and recent biofilms - a natural history of life on earth*.
212. Bhaskar, P. V. & Bhosle, N. B. 2006 Bacterial extracellular polymeric substance (EPS): A carrier of heavy metals in the marine food-chain. *Environ. Int.* **32**, 191–198. (doi:10.1016/j.envint.2005.08.010)
213. Briggs, D. E. G. 1995 Experimental taphonomy. *Palaios* **10**, 539–550. (doi:10.2307/3515093)
214. Briggs, D. E. & Kear, A. J. 1993 Fossilization of soft tissue in the laboratory. *Science* **259**, 1439–1442. (doi:10.1126/science.259.5100.1439)
215. Daniel, J. C. & Chin, K. 2010 The Role of Bacterially Mediated Precipitation in the Permineralization of Bone. *Palaios* **25**, 507–516. (doi:10.2110/palo.2009.p09-120r)
216. Pinheiro, F. L., Horn, B. L. D., Schultz, C. L., De Andrade, J. A. F. G. & Sucerquia, P. A. 2012 Fossilized bacteria in a Cretaceous pterosaur headcrest. *Lethaia* **45**, 495–499. (doi:10.1111/j.1502-3931.2012.00309.x)
217. McNamara, M. E., Orr, P. J., Kearns, S. L., Alcala, L., Anadon, P. & Penalver Molla, E. 2009 Soft-tissue Preservation in Miocene Frogs from Libros, Spain: Insights into the Genesis of Decay Microenvironments. *Palaios* **24**, 104–117. (doi:10.2110/palo.2008.p08-017r)
218. Franzen, J. L., Aurich, C. & Habersetzer, J. 2015 Description of a Well Preserved Fetus of the European Eocene Equoid Eurohippus messelensis. *PLoS One* **10**, e0137985.

(doi:10.1371/journal.pone.0137985)

219. Liebig, K. 1997 *Fossil Microorganisms from the Eocene Messel Oil Shale of Southern Hesse, Germany*. Heidelberg, Germany.
220. Martill, D. M. 1990 Macromolecular resolution of fossilized muscle tissue from an elopomorph fish. *Nature* **346**, 171–172. (doi:10.1038/346171a0)
221. Martill, D. M. 1989 The Medusa effect: instantaneous fossilization. *Geol. Today* , 201–205.
222. Wilby, P. R., Briggs, D. E. G., Bernier, P. & Gaillard, C. 1996 Role of microbial mats in the fossilization of soft tissues. *Geology* **24**, 787–790. (doi:10.1130/0091-7613(1996)024<0787:rommit>2.3.co;2)
223. Wilby, P. R. & Briggs, D. E. G. 1997 Taxonomic trends in the resolution of detail preserved in fossil phosphatized soft tissues. *Geobios* **30**, 493–502. (doi:10.1016/S0016-6995(97)80056-3)
224. Jans, M. M. E., Nielsen-Marsh, C. M., Smith, C. I., Collins, M. J. & Kars, H. 2004 Characterisation of microbial attack on archaeological bone. *J. Archaeol. Sci.* **31**, 87–95. (doi:http://dx.doi.org/10.1016/j.jas.2003.07.007)
225. Collins, M. J. et al. 2002 The survival of organic matter in bone: a review. *Archaeometry* **44**, 383–394. (doi:10.1111/1475-4754.t01-1-00071)
226. Kaye, T. G., Gaugler, G. & Sawlowicz, Z. 2008 Dinosaurian Soft Tissues Interpreted as Bacterial Biofilms. *PLoS One* **3**, 1–7. (doi:10.1371/journal.pone.0002808)
227. Schweitzer, M. H., Wittmeyer, J. L., Horner, J. R. & Toporski, J. K. 2005 Soft-Tissue Vessels and Cellular Preservation in Tyrannosaurus rex. *Science* **307**, 1952–1955.
228. Schweitzer, M. H., Suo, Z., Avci, R., Asara, J. M., Allen, M. A., Arce, F. T. & Horner, J. R. 2007 Analyses of Soft Tissue from Tyrannosaurus rex Suggest the Presence of Protein. *Science* **316**, 277–280. (doi:10.1126/science.1138709)
229. Schweitzer, M. H., Wittmeyer, J. L. & Horner, J. R. 2007 Soft tissue and cellular preservation in vertebrate skeletal elements from the Cretaceous to the present. *Proc. R. Soc. B Biol. Sci.* **274**, 183–197. (doi:10.1098/rspb.2006.3705)
230. Asara, J. M., Schweitzer, M. H., Freimark, L. M., Phillips, M. & Cantley, L. C. 2007 Protein Sequences from Mastodon and Tyrannosaurus Rex Revealed by Mass Spectrometry. *Science* **316**, 280–285. (doi:10.1126/science.1137614)

231. Mary Higby, S., Johnson, C., Zocco, T. G., Horner, J. R. & Starkey, J. R. 1997 Preservation of Biomolecules in Cancellous Bone of Tyrannosaurus rex. *J. Vertebr. Paleontol.* **17**, 349–359.
232. Martill, D. M. 1988 Preservation of fish in the Cretaceous Santana Formation of Brazil. *Palaeontology* **31**, 1–18.
233. Trueman, C. N. & Martill, D. M. 2002 The long–term survival of bone: the role of bioerosion. *Archaeometry* **44**, 371–382. (doi:10.1111/1475-4754.T01-1-00070)
234. Solano, F. 2014 Melanins: Skin Pigments and Much More—Types, Structural Models, Biological Functions, and Formation Routes. *New J. Sci.* , 1–28. (doi:10.1155/2014/498276)
235. Simon, J. D., Hong, L. & Peles, D. N. 2008 Insights into Melanosomes and Melanin from Some Interesting Spatial and Temporal Properties†. *J. Phys. Chem. B* **112**, 13201–13217. (doi:10.1021/jp804248h)
236. Riley, P. A. 1997 Melanin. *Int. J. Biochem. Cell Biol.* **29**, 1235–1239. (doi:10.1016/S1357-2725(97)00013-7)
237. Agodi, A., Stefani, S., Corsaro, C., Campanile, F., Gribaldo, S. & Sichel, G. 1996 Study of a melanic pigment of Proteus mirabilis. *Res. Microbiol.* **147**, 167–174. (doi:10.1016/0923-2508(96)80216-6)
238. Meredith, P. & Sarna, T. 2006 The physical and chemical properties of eumelanin. *Pigment Cell Res.* **19**, 572–594. (doi:10.1111/j.1600-0749.2006.00345.x)
239. Wakamatsu, K. & Ito, S. 2002 Advanced Chemical Methods in Melanin Determination. *Pigment Cell Res.* **15**, 174–183. (doi:10.1034/j.1600-0749.2002.02017.x)
240. Turick, C. E., Tisa, L. S. & Caccavo, F. 2002 Melanin production and use as a soluble electron shuttle for Fe(III) oxide reduction and as a terminal electron acceptor by Shewanella algae BrY. *Appl. Environ. Microbiol.* **68**, 2436–44.
241. Liu, Y., Hong, L., Kempf, V. R., Wakamatsu, K., Ito, S. & Simon, J. D. 2004 Ion-exchange and adsorption of Fe(III) by Sepia melanin. *Pigment Cell Res.* **17**, 262–9. (doi:10.1111/j.1600-0749.2004.00140.x)
242. Gospodaryov D. & Lushchak V. 2011 Some Properties of Melanin Produced By Azotobacter Chroococcum and Its Possible Application in Biotechnology. *Biotechnol. Acta* **4**, 61–69.

243. Plonka, P. M. & Grabacka, M. 2006 Melanin synthesis in microorganisms--biotechnological and medical aspects. *Acta Biochim. Pol.* **53**, 429–443. (doi:20061329 [pii])
244. Glass, K. et al. 2012 Direct chemical evidence for eumelanin pigment from the Jurassic period. *Proc. Natl. Acad. Sci.* **109**, 10218–10223.
245. Sahoo, D. K., Das, A., Thatoi, H., Mondal, K. C. & Mohapatra, P. K. Das 2012 Keratinase production and biodegradation of whole chicken feather keratin by a newly isolated bacterium under submerged fermentation. *Appl. Biochem. Biotechnol.* **167**, 1040–51. (doi:10.1007/s12010-011-9527-1)
246. Kottke, M. D., Delva, E. & Kowalczyk, A. P. 2006 The desmosome: cell science lessons from human diseases. *J. Cell Sci.* **119**, 797–806. (doi:10.1242/jcs.02888)

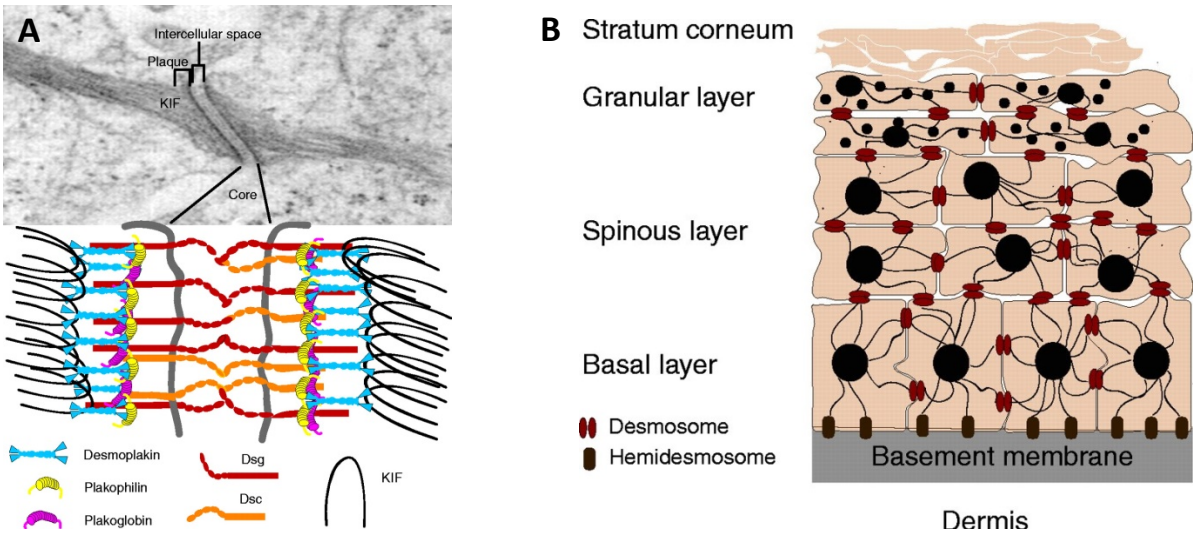

Figure 1. Skin ultrastructure and layers. A) Schematic and electron micrograph of a desmosome, a type of junctional complex that aids in cell-to-cell adhesion in between skin cells (keratinocytes). Plakoglobin mediates interactions between the cadherins (Dsg and Dsc) and desmoplakin, Desmoplakin binds directly to the keratin intermediate filaments (KIF). B) Simplistic schematic of skin layers (human). Desmosomes connect keratin filaments at cell-to-cell sites, whereas hemidesmosomes anchor them to the basement membrane. Modified from [246].

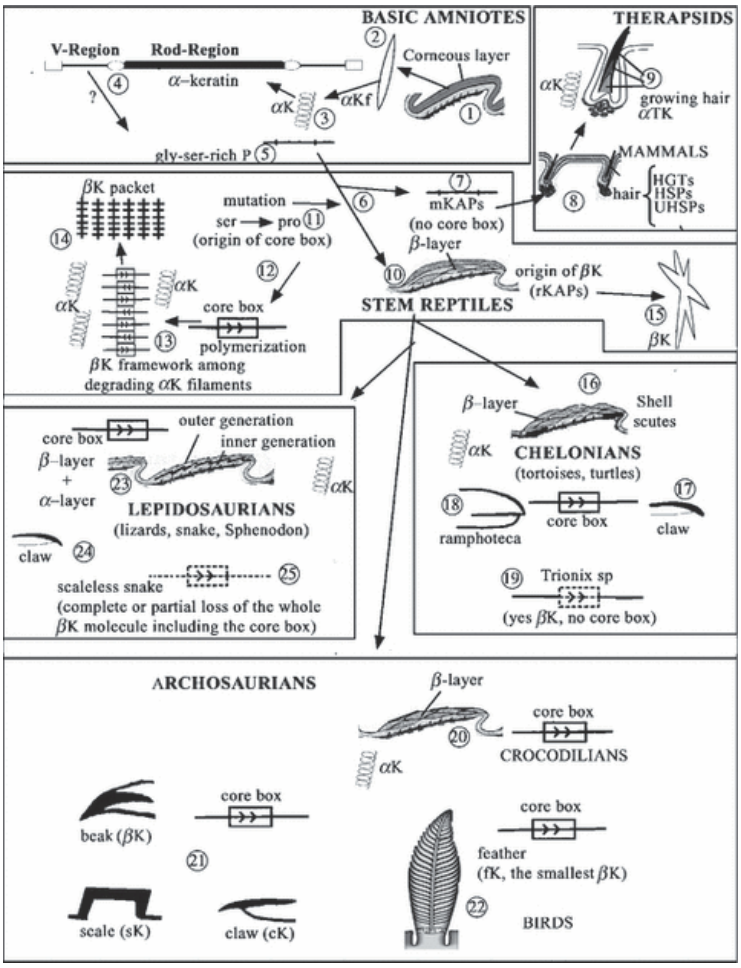

Figure 2. Hypothetical evolutionary sequence of formation and diversification of beta-keratins from an amniote ancestor in different non-avian sauropsid (reptile) groups. (1-3) The stratum corneum of ancestral amniotes contained alpha-keratin filaments. When the initial diversification of diapsids/anapsids from synapsids occurred (6) the glycine-serine-rich proteins (4-5) underwent a different fate in therapsids (7-9) no double-strand central region was formed, therefore no beta-keratins. In the reptilian lineage that originated the stem reptiles (10) a mutation central region of glycine-rich proteins may have originated proline (11–12). The double strand central region made possible polymerization of beta-keratin filaments and association with alpha-keratin filaments (13-14). In the lineage leading to chelonians, beta-keratins with central region were also formed in scutes, claws and ramphotheca (16–18). The central region might have been later lost in *Trionix* (softshelled turtle) (19). In the lineage of diapsids beta-keratins with their central regions further diversified in archosaurians (20–22) and lepidosaurians (23–25). In archosaurians and lepidosaurians beta-keratins with their central regions diversified in scales, claws, and in those of the beak and feathers in birds. Note: KAPS is a term used by Alibardi and are keratin associated proteins which in the text are referred to as matrix proteins. Also the 'core box' is the highly conserved central domain of beta-keratin. Modified from [29].

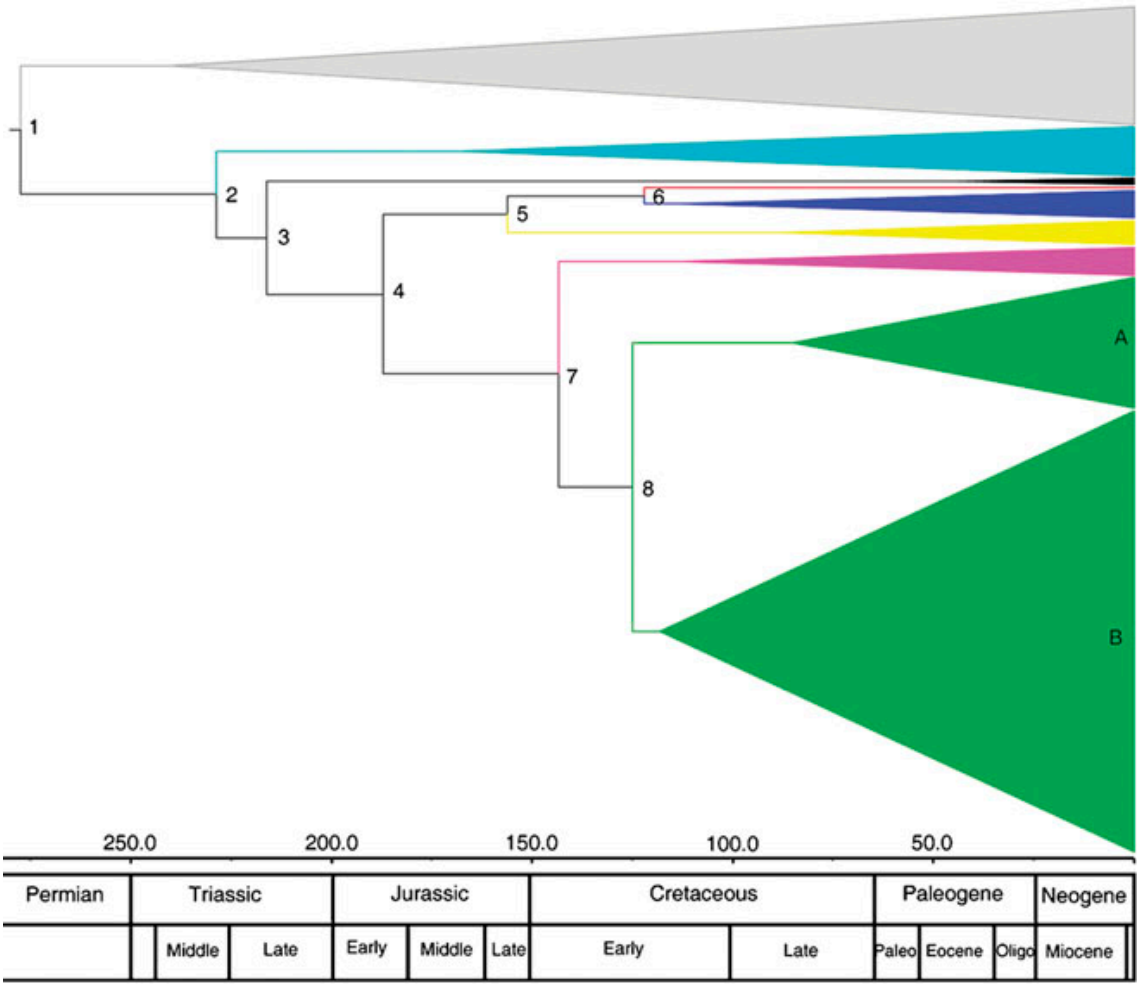

Figure 3. Evolution of avian beta-keratins from molecular dating (Bayesian analysis) using beta-keratins from a lizard, turtle, crocodile and chicken and zebra finch. Squamata (grey), Testudines (teal), Crocodylia (black), Beta-keratin from keratinocytes (red), Scale (blue), Claw (yellow), Feather-like (magenta), Feather (A green- chromosome 2, B green – microchromosome 25 and 27). Adapted from [34].

CHAPTER 2 - Melanosomes or Microbes: Testing an Alternative Hypothesis for the Origin of Microbodies in Fossil Feathers

SCIENTIFIC REPORTS

OPEN

SUBJECT AREAS:
SCANNING ELECTRON MICROSCOPY
TRANSMISSION ELECTRON MICROSCOPY
PALAEONTOLOGY
BACTERIA

Received
13 June 2013

Accepted
28 January 2014

Published
5 March 2014

Correspondence and requests for materials should be addressed to A.E.M. (aemoyer@ncsu.edu)

Melanosomes or Microbes: Testing an Alternative Hypothesis for the Origin of Microbodies in Fossil Feathers

Alison E. Moyer[1], Wenxia Zheng[1], Elizabeth A. Johnson[2], Matthew C. Lamanna[3], Da-qing Li[4], Kenneth J. Lacovara[5] & Mary H. Schweitzer[1,6]

[1]Department of Marine, Earth and Atmospheric Sciences, North Carolina State University, Raleigh, NC 27695, [2]Physical and Life Sciences Department, Colorado Northwestern Community College, Craig, CO, 81625, [3]Section of Vertebrate Paleontology, Carnegie Museum of Natural History, Pittsburgh, PA 15213, [4]Gansu Geological Museum, Lanzhou, Gansu, China, 730030, [5]Department of Biodiversity, Earth and Environmental Science, Drexel University, Philadelphia, PA 19104, [6]North Carolina Museum of Natural Sciences, Raleigh, NC, 27601.

Microbodies associated with fossil feathers, originally attributed to microbial biofilm, have been reinterpreted as melanosomes: pigment-containing, eukaryotic organelles. This interpretation generated hypotheses regarding coloration in non-avian and avian dinosaurs. Because melanosomes and microbes overlap in size, distribution and morphology, we re-evaluate both hypotheses. We compare melanosomes within feathers of extant chickens with patterns induced by microbial overgrowth on the same feathers, using scanning (SEM), field emission (FESEM) and transmission (TEM) electron microscopy. Melanosomes are always internal, embedded in a morphologically distinct keratinous matrix. Conversely, microbes grow across the surface of feathers in continuous layers, more consistent with published images from fossil feathers. We compare our results to both published literature and new data from a fossil feather ascribed to *Gansus yumenensis* (ANSP 23403). 'Mouldic impressions' were observed in association with both the feather and sediment grains, supporting a microbial origin. We propose criteria for distinguishing between these two microbodies.

In 1995, approximately 1 μm long elongate microbodies were observed on the surface of fossilized feathers from the Eocene of Messel (Germany), Oligocene of Cereste (France) and Jurassic Solnhofen Limestone (Germany)[1] using scanning electron microscopy (SEM). These microstructures were proposed to represent mineralized microorganisms and the glycocalyx they secrete, and, based upon this interpretation, a new mode of fossilization was proposed[1]. This was further supported by the observation of similar microbodies associated with fish, mammals and other material in the same deposit, and a microbial origin for these has not been disputed[2,3]. However, a decade after their discovery, the microbodies associated with fossil feathers were reinterpreted as eukaryotic melanosomes[4]; intracellular, membrane-bound organelles where melanin pigment is synthesized and stored[5]. Because melanosomes vary in morphology in extant feathers[6], it was additionally proposed that color could be inferred in fossil feathers solely on the *shape* of these structures; round indicating red and brown hues and oblate indicating black and/or grey[4,7–13]. Finally, aspects of behavior, physiology and ecology were posited for avian and non-avian dinosaurs[4,7–12] based solely upon these morphological data.

Bacteria and the extracellular polymeric substances (EPS) they secrete are known to fossilize[14,15]. Because bacterial cells contain a cell wall composed of resistant, cross-linked peptidoglycan polymers[16], they are hypothesized to have greater preservation potential than eukaryotic intracellular organelles[17], protected only by a lipid bilayer. The fossil record contains many examples of fossilized bacteria and biofilms[2,15,18,19], and some processes leading to their preservation have been elucidated in the lab[20]. Fossilization of intracellular organelles is extremely rare, even when cell-like microstructures retaining transparency and flexibility persist[21–23], but morphologies consistent with organelles have been noted[24]. Whether these represent molecule for molecule replacement in mineral or original components cannot be determined without chemical data. Because melanosomes and microbes overlap in shape and size, differentiating between the two is critical for supporting hypotheses of behavior[7], evolutionary significance[9,10], and/or ecology[11] in extinct organisms.

Because intracellular organelles are definitive evidence for a eukaryotic source, it is imperative to differentiate between melanin and melanosomes before proposing far-reaching interpretations of color, habitat, niche and

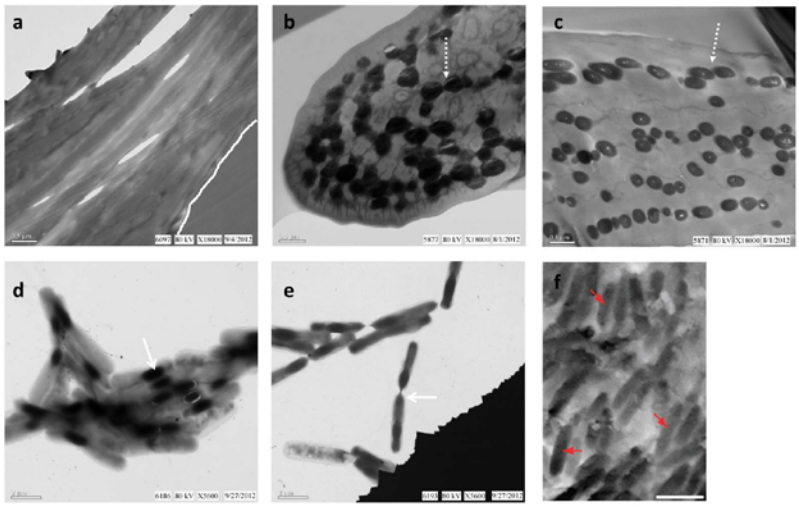

Figure 1 | Electron micrographs of modern *Gallus gallus* feathers and *Bacillus cereus* pure culture, compared with an SEM image of a fossil feather from published work. Chicken feathers were sectioned, stained, and viewed in transmission EM as described (see Methods). Melanosomes are observed (dashed arrow) in brown (b) and black (c) feathers but are absent in similarly prepared white feathers (a) (contact between feather and embedding medium delineated by white line in (a)). (d) Aggregation of *B. cereus* cells containing electron opaque internal endospores (arrow). (e) Two endospore-containing *B. cereus* cells aligned and connected (arrow), prepared and stained as described (see Methods). (f) SEM image of isolated feather of Jurassic bird *Archaeopteryx* with "[…] melanosomes (arrows) preserved […] as moulded imprints" (scale bar: 1 μm). Reprinted by permission from Macmillan Publishers Ltd: [NATURE COMMUNICATIONS][7], copyright (2012).

lifestyle. ***Melanin*** is an organic pigment derived from tyrosine residues[6] that are highly cross-linked and resistant to degradation. *Both* eukaryotes and prokaryotes produce melanin pigments, the basic structural unit of which is unknown[25]. ***Melanosomes*** are membrane-bound intracellular organelles within specialized cells called melanocytes where melanin pigments are polymerized by enzymes and stored[5]. Melanosomes have also been referred to as melanin 'granules'[26], a term more appropriate to describe irregular clusters of the melanin pigment regardless of source. During maturation of keratinous pigmented tissues, including skin, hair, and feathers, melanosomes are transferred from melanocytes to keratin-producing cells, where they become embedded *within* the keratinous matrix[6]. While melanin chemistry confers high preservation potential to the *pigment*[27], this resistance to degradation has not been shown to extend to the membrane-bound organelles containing pigment grains. In fact, melanosomes are related to lysosomes, organelles producing enzymes involved in autolytic degradation[5], therefore indicating a predisposition for rapid degradation. Finally, ***bacteria*** are prokaryotic organisms that may or may not secrete an enzyme-rich exopolymeric substance that facilitates bacterial adherence to a substrate and that may assist in degradative processes[28]. Melanosomes, as membrane-bound organelles, are not produced by bacteria, although many do produce and utilize the pigment melanin[29].

Data presented in previously published works describing fossil material have not eliminated either a eukaryotic melanosome or prokaryotic biofilm source for the microbodies associated with fossil feathers; thus, both hypotheses remain valid. We conducted actualistic experiments on extant feathers to test the hypothesis that microbodies observed in fossil feathers are more consistent with melanosomes than degrading bacteria colonizing the surface. We incubated extant feathers with either a naturally occurring microbial population (see Methods) or a pure culture of biofilm-forming *Bacillus cereus*, leaving some feathers untreated as controls. We used both pigmented (black and brown) and non-pigmented (white, lacking melanosomes) feathers and compared differences in distribution and morphology between microbes and melanosomes with published data for fossil feathers. We also examined a Chinese fossil feather using SEM-EDX to visualize microbodies or 'mouldic impressions' similar to those observed in previous studies of fossil feathers.

Results

Figure 1 shows that electron-dense melanosomes are visible using transmission electron microscopy (TEM) and are embedded within the keratinous matrix of both pigmented feathers (Fig. 1b, c), but are lacking in white feathers (Fig. 1a). These distinct bodies appear either elongate or round, depending on cutting aspect, but rarely overlap, are often separated, and are always completely surrounded by the keratinous matrix of the feather. Conversely, cells from cultured, endospore-forming *B. cereus* are external to the feather (Fig. 1d) and are more similar in size, shape, distribution and location to previously published work on fossil melanosomes in side by side comparisons (Fig. 1f[7], reprinted with permission).

Field emission-scanning electron microscopy (FESEM) images of guineafowl feathers incubated with pond inoculum (Fig. 2a and b) show microbial growth on the surface of the feather. Microbial bodies are dense and overlapping, form a virtually continuous mat across the feather *surface* and follow feather contours (Supplementary Fig. S2), in contrast to the relatively less abundant and non-overlapping distribution of melanosomes depicted in Fig. 1. In some regions, microbial bodies demonstrate a high degree of alignment (Fig. 2a, arrows), similar to patterns ascribed to fossil melanosomes (Figure 2d[13] and e[7], republished with permission). Also see Fig. 1b in Vinther *et al.* (2008) and Fig. 1c and e in Vinther *et al.* (2010).

It was previously noted that purported melanosomes are easier to observe in degraded fossil feathers[4,13], but we show that microbial cells can also be removed from their EPS, leaving 'mouldic impressions' (Fig. 2b) similar to those noted in fossil feathers (Fig. 2c[13], reprinted with permission)[7,10,13]. We propose that because microbes and their EPS are participants in degradation, it is more parsimonious to attribute these bodies to microbial overgrowth than to

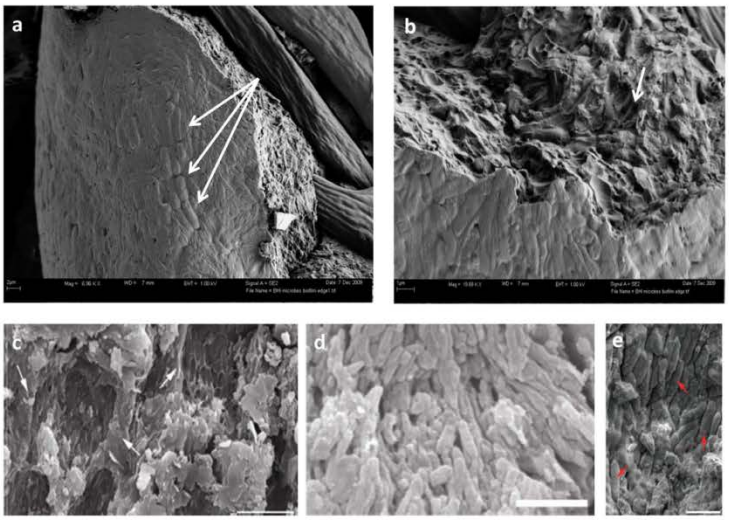

Figure 2 | FE-SEM micrographs of biofilm overgrowth of extant feathers compared with published images of fossil feathers. (a) Guineafowl feathers exposed to naturally occurring culture show strong alignment of microbial cells (arrows). (b) Higher magnification of biofilm edge in (a) showing where bacteria cells have been eliminated from the surrounding matrix (arrow), leaving voids similar to those figured in (c), which were identified as "[…] eumelanosomes preserved as moulds inside small areas that are separated from each other by anastomosing ridges of degraded feather (at arrows in c)" (scale bar: 5 μm). Reprinted by permission from Macmillan Publishers Ltd: [NATURE][13], copyright (2010). (d) "Strongly aligned, closely spaced, eumelanosomes preserved as solid bodies," in *Confuciusornis* feathers (scale bar: 2 μm). Reprinted by permission from Macmillan Publishers Ltd: [NATURE][13], copyright (2010). (e) "melanosomes (arrows)" figured in Carney *et al.* 2012 (scale bar: 1 μm). Reprinted by permission from Macmillan Publishers Ltd: [NATURE COMMUNICATIONS][7], copyright (2012).

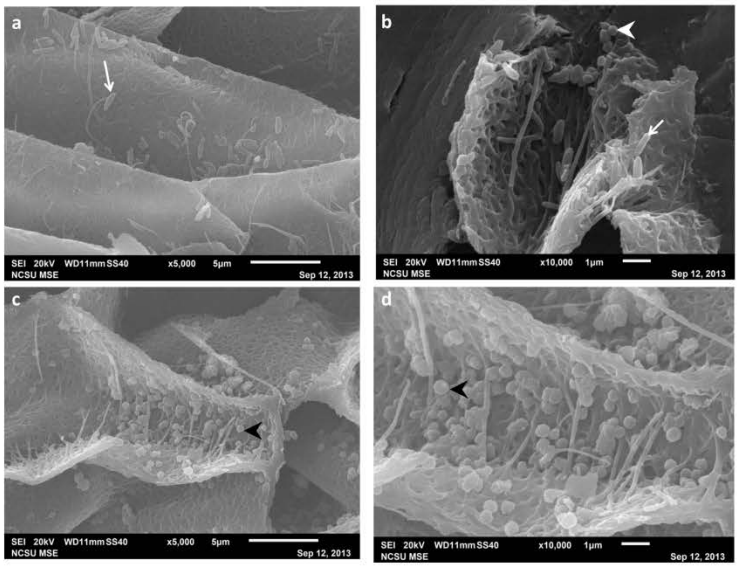

Figure 3 | SEM images of melanosomes from extant *Gallus gallus* feathers. Black (a,b) and brown (c,d) chicken feathers sectioned longitudinally. (b) Although the feather is visually black, both ovate eumelanosomes (arrow) and round phaeomelanosomes (arrowhead) are present. (c) Phaeomelanosomes (arrowhead) are also observed in the brown feather. (d) Melanosomes exhibit unsmooth, granular surfaces. Using this method, like those observed in TEM, melanosomes appear randomly oriented, rather than in dense mats as reported for fossils (see text). Considerable size variation (e.g. ~.5 μm–~2 μm for the eumelanosomes) is observed between all melanosomes.

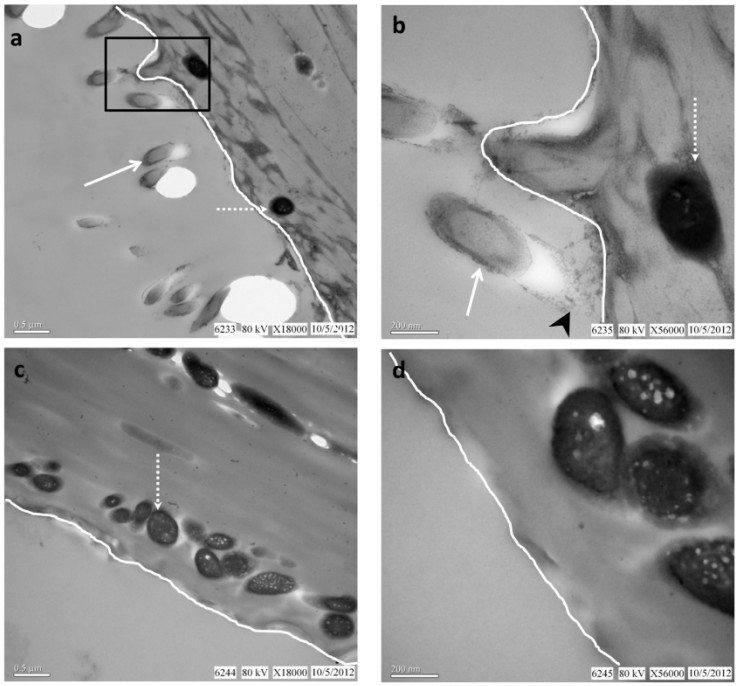

Figure 4 | TEM images of *Bacillus cereus*-treated black chicken feather. Stained (a,b) and unstained (c,d) TEM images of feather are compared. Feathers were incubated with cultured *B. cereus* for three days (See SI for details). (a) Superficial *B. cereus* cells (arrow) extending from the barb surface (white line; feather tissue is to the right). Melanosomes (dashed arrow) are *always* internal to the feather surface, sparsely distributed and non-overlapping. (b) Higher magnification of boxed area in (a) shows interaction (arrowhead) of bacteria (arrow) with barb surface (white line). White dashed arrow depicts internal, electron-opaque melanosome. Without staining, (c) bacteria are not visible on the external surface, as they are not normally electron-opaque, in contrast with easily visualized, internal, electron-opaque melanosomes (dashed arrow). The melanin pigment is inherently electron dense; no staining is necessary. (d) Enlarged image of unstained section in (c) shows vacuoles associated with internal melanosomes, as has been noted previously[4]. Keratinous matrix completely surrounds melanosomes, making them difficult to image in SEM without additional treatment.

melanosome exposure, and that these cannot be differentiated from melanosomes embedded in a keratinous matrix without chemical data.

We have examined many modern pigmented feathers (at least 20) prepared by fresh fracture, cryofracture, and/or sectioning in multiple planes, but definitively identifying melanosomes under SEM is not trivial. Consistent with other observations[10,30,31], we found that, in most cases, modern feathers must be treated to reduce or remove keratin before melanosomes embedded within the matrix are visible; alternatively, feathers embedded in resin and longitudinally sectioned[10] allow visualization under SEM. Without treatment, melanosomes were seen in only one feather after fresh fracturing (Supplementary Fig. S3). Melanosomes in extant chicken feathers are more sparse and have a non-overlapping distribution (Fig. 1b and c) compared to bacteria (Fig. 1d and e) when both are viewed in TEM. Furthermore, under our experimental conditions, microbes grew across the surfaces of the feathers in densely packed layers, more similar to what have been presented as fossil melanosomes than to in situ melanosomes in TEM sections of modern feathers. Never were melanosomes observed in whole mounts of extant feathers, as has been reported for visualization of fossil feather melanosomes, nor were they observed without extensive manipulation.

Following the protocol in Li et al. 2010, we were able to observe melanosomes in longitudinally-sectioned black and brown chicken feather barbs. We observed both morphological types of melanosomes, eumelanosomes (oblate) and phaeomelanosomes (round) in the black feather (Fig. 3b). Only phaeomelanosomes, displaying unsmooth, granular surfaces, were observed in the brown feather (Fig. 3c and d). All melanosomes detected by this method vary in size and appear to be randomly oriented. They are sparse and non-uniform in distribution, never occurring in dense mats or closely spaced, as described for the microbodies in fossil feathers[9,11,13,32,33].

Microbial bodies are easily distinguished from melanosomes in extant feathers, because they are not electron-dense and because melanosomes are always internal and embedded in the keratinous matrix while microbes are present as surface overgrowth[11] (Fig. 2a, b and Supplementary Fig. S1). Additionally, their electron-dense nature makes melanosomes visible in both stained and unstained sections (Fig. 4), while microbes are only clearly visible after heavy metal staining (Fig. 4a and b).

We also examined an isolated fossil feather (Fig. 5) (ANSP 23403) collected from the Xiagou Formation (Lower Cretaceous) in northwestern Gansu Province, China, and ascribed to the bird *Gansus yumenensis*[34,35]. As reported in other work[7–10,13,32] 'mouldic impressions' (Fig. 6) were observed associated with the fossil feather. Although the feather exhibited regions of different color (black apically (Fig. 5a), brown more basally (Fig. 5b)) the 'mouldic impressions' did not differ in type or distribution between the black and brown regions. In addition, these impressions were also observed on sediment grains (the identity of which is confirmed by EDS (Fig. 7))

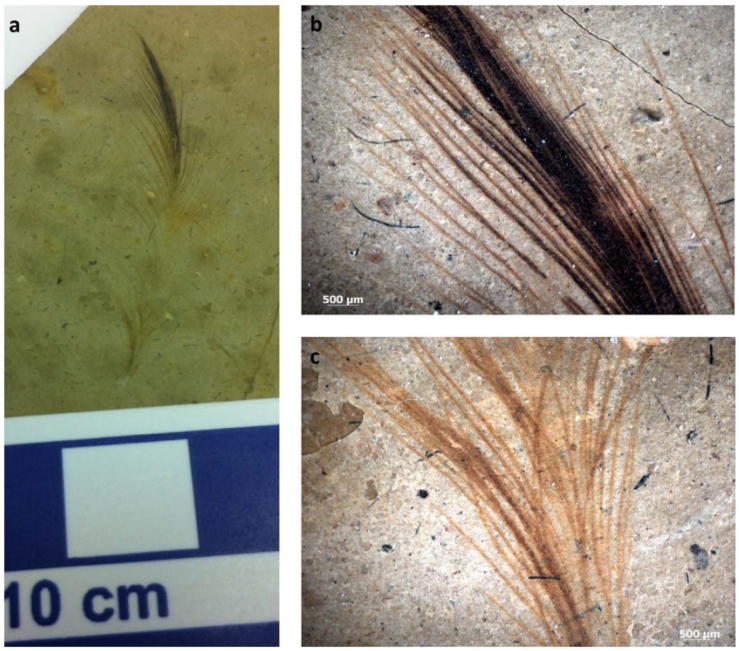

Figure 5 | Images of the fossil feather ascribed to *Gansus yumenensis* (ANSP 23403). (a) Photograph of the isolated feather from the Xiagou Formation showing varying color pattern; black at the top, and red-brown toward the base. It is beyond the scope of this paper to determine whether this apparent color variation reflects the actual biological color of the feather or taphonomic alteration. (b,c) Higher magnification images of the dense black distal region (b) and the finer, brown proximal region.

superficially associated with the feather. Because the sediment grains are clearly not part of the feather structure, yet retain 'mouldic impressions', a microbial origin for these impression structures is favored.

SEM-EDS analysis revealed that the fossil feather (Fig. 7 and 8) is composed primarily of C and Fe, although quantitative data from the brown portion (Fig. 8) indicates a reduced amount of C compared to the black region (Fig. 7) (see Table 1 for quantitative elemental data). The sedimentary matrix surrounding the feather, as well as the sediment grains observed associated with the fossil material, are composed primarily of O, Si and Al.

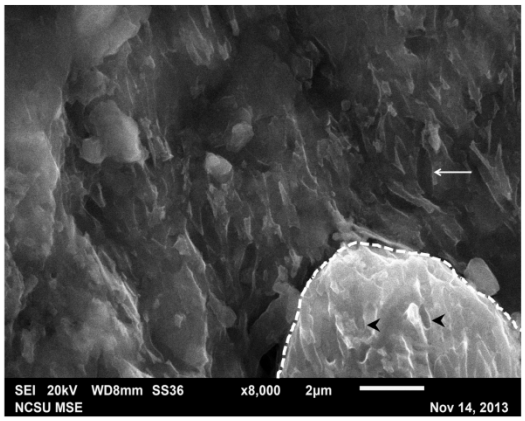

Figure 6 | High magnification image of the black region of the fossil feather. 'Mouldic impressions' (~1–1.5 µm) co-localize to both the fossil feather (arrow) and the sediment grains (arrowheads) intimately associated with but superficial to the fossil. The sediment grain is encircled by the dashed line.

Discussion

We evaluate statements used by others to support a melanosome origin for microbodies in fossil feathers, and put forth alternative interpretations equally supported by the same data. **(1.) Localization of microbodies to 'dark' and absence from 'light' regions of one fossil feather support a melanosome origin**[4]. Three hypotheses exist to explain the striped patterning of the fossil feather reported in Vinther et al. 2008. First, the original feather, in life, was also striped, with melanosomes distributed in the colored regions of the feather and no melanosomes in the uncolored parts, and the fossils preserve this original pattern. Second, microbial overgrowth on the surface of the feather is distributed according to the relatively more nutrient-rich pigmented feather regions over unpigmented areas[36]. Third, microbes preferentially colonized and completely degraded those feather regions most easily broken down (e.g. unpigmented)[37,38]; thus were no longer present in these regions during fossilization, but continued to act on the more resistant, melanin-containing regions. **(2.) Densely packed and aligned/organized layers support a melanosome origin (Fig. 2c–e)**[7,13]. Recently published research indicates original melanosome geometry and distribution are altered with heat and pressure[31], diagenetic processes affecting fossils, and that have not been taken into account in previous research claiming melanosome morphology in fossil feathers reflects their original color.

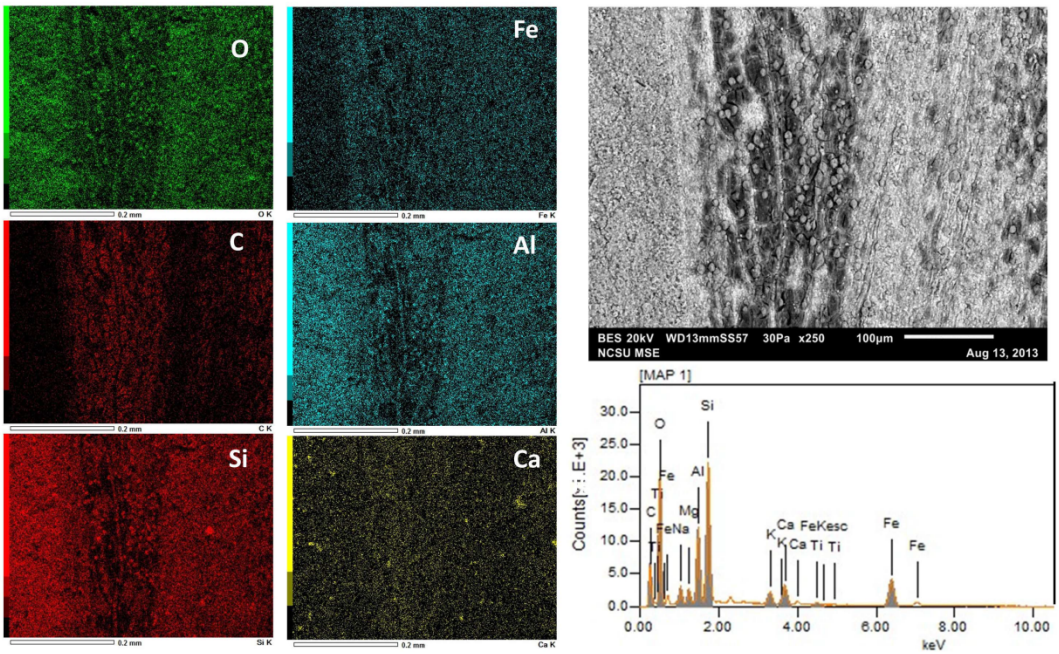

Figure 7 | SEM-EDS data derived from the black fossil feather region. The six dominant elements (~95% of detected electrons) are presented in order of decreasing abundance by weight percent. Elemental map and quantitative data (Table 1) suggest the fossil feather is composed primarily of C although Fe is also abundant. In contrast, Al is localized to the sediments and not in the feather. The surrounding sediment is composed primarily of O and Si which is consistent with previous analyses[32]. The data demonstrate that the ~8 µm-sized spheres shown in Fig. S4 are composed of O and Si, consistent with sediment grains and not part of the original feather structure.

Data presented here show microbial overgrowth is dense and can be aligned, whereas internal melanosomes are more sparsely distributed and relatively random in orientation as observed in both SEM and TEM. Our data show this description is more consistent with biofilm overgrowth (Fig. 2a, b) than melanosomes (Fig. 1b and c). In addition, bacteria can align (Fig. 1e, 2a, and Supplementary Fig. S1c2) and follow the contours of a feather (Supplementary Fig. S2) in layers. Unlike most bacteria, which usually exhibit more uniform and smooth cell surfaces[39,40], melanosomes, as observed in a previous study[26], are not smooth, but rather have bumpy and non-uniform surfaces (Fig. 3b and d). Because bacteria have a tough cell wall external to the plasma membrane[41], this granular topography[26] may be more difficult to observe in melanin-containing bacteria than in eukaryotic melanosomes. This remains to be tested. **(3.) Elements consistent with melanin, including Ca^{2+}, Cu^{2+} and $Zn^{2,43-44}$, are associated with feathers and thus support a melanosome origin.** However, these biomarkers are also used and/or sequestered by bacteria[45,46], including common soil bacteria and other microorganisms, and are also part of the sedimentary environment. These microorganisms are also capable of synthesizing melanin[29], thus elemental data alone cannot be used to discriminate microbes from melanosomes.

Our examination of the fossil feather ascribed to *Gansus yumenensis* showed no microbodies of any type, but did reveal 'mouldic impressions' (Fig. 6) similar to those described in previous studies. However, these impressions did not vary between black and brown regions of the feather, and were also observed on sediment grains (Fig. 6) (confirmed with EDS data) associated with the fossil. Therefore, because sediment grains do not contain melanosomes, it more parsimonious to propose these 'mouldic impressions' represent a microbial origin (remnant EPS) than intracellular structures derived from the original feather. A very similar image was presented in Barden et al. 2010 (Fig. 1H) but elemental data were not mapped, so identification as a sediment grain cannot be confirmed in their paper. Visual, textural (Fig. 5 and Fig. S4), and elemental data (Fig. 7 and 8 and Table 1) from the fossil feather suggest differential diagenetic processes acting on the different regions of the feather. The reason for these differences is beyond the scope of this paper and requires additional studies.

Pending the identification of definitive molecular or chemical signals unique to either melanosomes or microbes in extant feathers that are likely to persist across geological time, distinguishing microbes from melanosomes in fossils may be difficult. Until new data are presented, we propose the following criteria to support a melanosome origin for microbodies associated with fossil feathers: 1) a taphonomic mechanism must be demonstrated for removing resistant keratin while leaving the intracellular organelles intact; 2) electron-dense material should be localized to the microbodies using TEM-EELS (TEM coupled with energy loss spectroscopy) or TEM-EDX; 3) melanosome-specific (e.g. cargo proteins[5]) or bacteria-specific (e.g., peptidoglycans[16]) biomolecules should be localized to the structures to eliminate the alternative, using in situ surface techniques (e.g., time of flight secondary ion mass spectrometry (TOF-SIMS[42])), or other softer mass spectrometry imaging methods.

The 'mouldic impressions' described in fossil feathers imply that the microbodies were once present, and subsequently degraded from an amorphous material that retained the impression through fossilization. Therefore, if the structures are melanosomes, this material

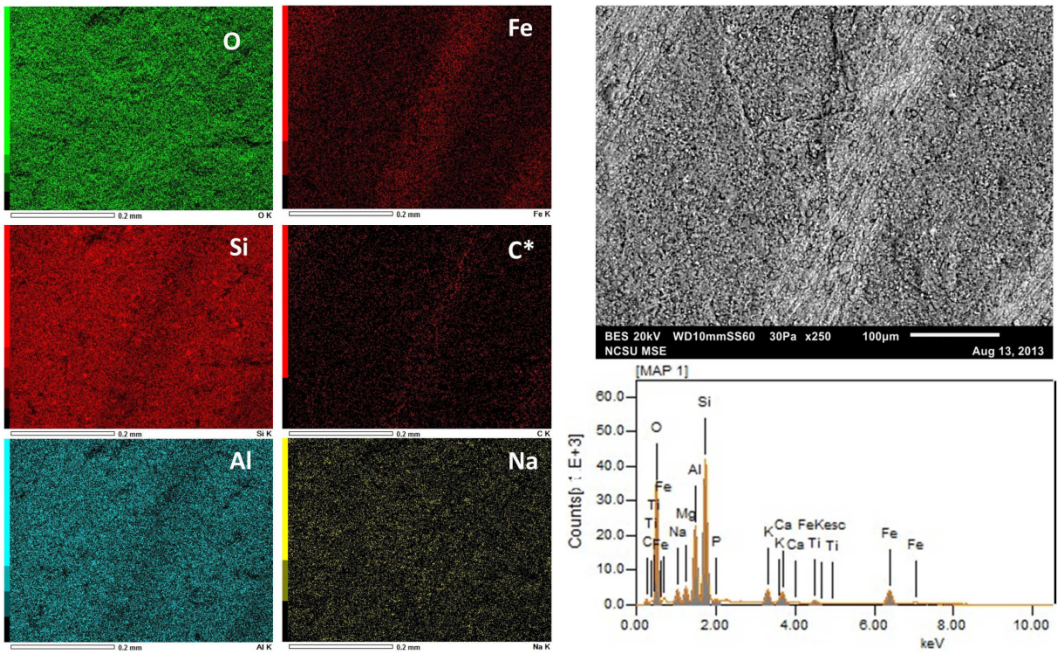

Figure 8 | SEM-EDS data derived from the brown, basal part of the fossil feather. The six dominant elements (~93% of detected electrons) are presented in order of decreasing abundance by weight percent. See Table 1 for the quantitative data. Carbon is denoted with an asterisk because it was not auto-detected by the instrument and was manually inserted. Although this basal portion of the fossil is also dominated by Fe and C, as above, the quantitative data indicate the C is greatly decreased in abundance relative to the black portion.

should resemble β-keratin, because the β-keratin matrix of feathers is highly resistant to degradation[47]. β-keratin is a rigid structural protein comprising ~80% of the organic matrix of mature feathers[48]. Its multiple cross-links, twisted-pleated-sheet tertiary structure and hydrophobic amino acid composition[49] confer high preservation potential to structures comprised of this protein[50]. Mammals do not produce β-keratin[51], thus common contamination by human keratins can be easily recognized. If microbial, the material should retain microbial-specific biomarkers in the environment immediately surrounding these microbodies.

Some papers state the keratin matrix is completely degraded in fossil feathers and no feather structure remains[4,9,11,13], but fail to state what material, then, retains 'mouldic impressions'. If feather structure is not preserved, how is the object identifiable as a fossil feather, and how has a biofilm source been eliminated? The presence or absence of keratin has not been tested in any fossil feather purporting to contain melanosomes. Yet, the melanosome hypothesis posits that melanosomes are preserved 'in life position'. Modern feather melanosomes ('in life') are *always* embedded in a keratinous matrix, thus the 'mouldic impressions' cited by many in support of the melanosome hypothesis are assumed to be made in the original keratinous matrix of the feather, an assumption that has never been tested.

It should be noted that handling history and full depositional description are often not included in studies purporting to recover fossil melanosomes. Excavation of a fossil feather as part and counterpart could be interpreted differently than a feather collected as a whole specimen. This information is critical for determining where these microbodies are localized (ie. inside versus on the surface of the feather).

More importantly, even if irrefutable data support a melanosome origin for microbodies in a given fossil, imparting color to the entire organism, or even the entire feather, based upon their presence cannot be inferred. *All* melanized feathers in extant birds contain *both* eumelanin and phaeomelanin[6]; it is the relative *abundances* of these two melanins that determine the expressed color of a pigmented feather[6]. Claiming a 'red-orange' or 'black-grey' color for entire fossil organisms based upon identification of round or elongate morphologies is overly simplistic, because in living birds, pigment molecules of multiple types are employed to confer hues of brown, red, orange, etc.[6]. Coloration of feathers is complex, the result of expression of more than one type of pigment (e.g. porphyrins, carotenoids)[6], which may be more labile, with lower preservation potential, than the relatively resistant melanins. Without preservation of all pigments originally employed, original organismal color cannot be interpreted with accuracy.

The initially proposed hypothesis of a microbial origin[1] for these microstructures observed in multiple fossilized feathers, as well as other fossil material from the Messel deposits[2,3] has not been refuted,

Table 1 | SEM-EDS quantitative data for the fossil feather. Both black (Fig. 7) and brown (Fig. 8) regions of the feather are presented as weight (ms%) and molar (mol%) percentages in decreasing abundance. * indicates element not auto-detected by instrument

Black	ms%	mol%	Brown	ms%	mol%
O	37.92	41.36	O	45.29	57.03
C	28.06	40.76	Si	19.12	13.72
Si	10.99	6.83	Al	9.53	7.11
Fe	9.90	3.09	Fe	8.39	3.03
Al	5.75	3.72	C*	7.30	12.24
Ca	2.20	0.96	Na	2.59	2.27

or indeed addressed, with data presented in previous studies, but is supported by the data we present herein. The present data do *not* support the melanosome hypothesis for these fossilized microstructures. Morphology alone is insufficient to distinguish between a melanosome and/or microbial origin, but data that capitalize on distinct chemical differences between melanosomes and microbes are needed to support one hypothesis over the other. With the exception of one fossil feather study where the chemical data are not of high resolution[52], the only in-depth chemical data presented for microbodies in the fossil record that seem to support a melanosome origin are derived from marine[42,52–54] rather than terrestrial environments, where preservational conditions are very different than the lacustrine environments from which most feathers have been recovered[1]. Additionally, geochemical data from fossil feather 'melanosomes' are compared only with that derived from extant melanosomes; microbes are not included in the comparative data[50].

Furthermore, because the *shape* of melanosomes has been used to interpret color[4,7–11] and behavior[9,11] in extinct animals, distinguishing melanosomes from microbes is critical to acceptance or rejection of these hypotheses. As McGraw warned "[…] it is wise to withhold classification of a color as partially or wholly melanin-based before the appropriate biochemical tests are conducted"[6]. How much more should this caution be applied to extinct organisms?

Methods

Feather and microbial preparations. A culture from an environmental sample of pond water (Bozeman, Montana) was grown in brain heart infusion broth (BHI) on pigmented feathers taken from *Numida meleagris* prepared using aseptic techniques. Biofilms were air dried, coated with ~5 Å of iridium, and visualized using FESEM (Zeiss Supra 55VP).

Pigmented and non-pigmented chicken feathers (*Gallus gallus domesticus*) were collected from the Poultry Teaching Unit at North Carolina State University. (All experiments involving live vertebrates were performed in accordance with relevant guidelines and regulations of North Carolina State University.) Primary and secondary flight feathers were plucked and placed in clean Ziploc® bags. Feathers were incubated in 5% tryptic soy broth inoculated with *Bacillus cereus* (ATTC 14579) for three days at room temperature with agitation, then fixed in 10% formalin. Feathers of each type were reserved in 10% formalin without inoculation and used as negative controls.

Fossil feather specimen. For more information on the geologic context of the fossil feather specimen (ANSP 23403) ascribed to *Gansus yumenensis* see the Supplementary Methods section online.

Scanning electron microscopy (SEM) and SEM with energy dispersive x-ray spectroscopy (SEM-EDX). For whole mount/surface analysis, *G. gallus* feathers were gently washed in E-pure water and air dried.

To view melanosomes, approximately ~1 mm sections were taken from *G. gallus* feathers, and washed in phosphate buffered saline, dehydrated in two changes of 70% ethanol for 30 minutes with rocking followed by a one hour incubation of (2 : 1) LR white: 70% ethanol. Samples were then incubated for one hour each in two changes of 100% LR white, followed by a third incubation overnight. Feathers were placed in gelatin capsules with the long axis parallel to the length of the capsule, filled with LR white and covered to exclude oxygen. Resin was polymerized for 24 hours at 60°C. A Leica EMUC6 ultra-microtome with a Diatome 45° knife was used to cut 5 and 10 μm longitudinal (parallel to long axis of the barb) sections.

Samples were mounted on double-sided carbon tape and imaged using a JEOL JSM-6010LA analytical SEM controlled by JEOL InTouchScope version 1.05A software. Some images (Fig. 3 and Supplementary Fig. S1b1, b3, c2 and c3) were captured after applying a 3–6 nm gold/palladium coating. All EDS data of the uncoated fossil feather sample were collected at 20 kV accelerating voltage, a working distance of 10 mm and for 100–120 seconds.

Transmission electron microscopy (TEM). Samples for TEM were prepared as described above for visualizing melanosomes in SEM. One sample of *B. cereus*-treated black chicken feather was embedded directly in LR white following fixation, eliminating all dehydration and penetration steps (Fig. 4). Cross sections were taken at 90 nm with a diamond knife on a Leica EMUC6 ultra-microtome, mounted on 200 mesh copper grids, and imaged using an Erlangshen ES1000W Model 785 TEM coupled to a CCD 11Megapixel High-speed Digital Camera, and analyzed using Gatan Microscopy Suite (GMS) software. Some sections were stained with 15% methanolic uranyl acetate and Reynolds' lead citrate (Fig. 1a–c and Fig. 4a–b).

Images of *B. cereus* were obtained from culture growth as indicated above, diluted by 50% and applied directly to a Formvar-coated 200 mesh nickel grid followed by negative staining with 1% phosphotungstic acid (Fig. 1d) or 0.5% uranyl acetate (Fig. 1e).

1. Davis, P. G. & Briggs, D. E. G. Fossilization of feathers. *Geology* **23**, 783–786 (1995).
2. Liebig, K., Westall, F. & Schmitz, M. A study of fossil microstructures from the Eocene Messel Formation using transmission electron microscopy. *N. Jb. Geol. Paläont. Mh.* **4**, 218–231 (1996).
3. Franzen, J. L. Exceptional preservation of Eocene vertebrates in the lake deposit of Grube Messel (West Germany). *Philos. Trans. R. Soc. B Biol. Sci.* **311**, 181–186 (1985).
4. Vinther, J., Briggs, D. E. G., Prum, R. O. & Saranathan, V. The colour of fossil feathers. *Biol. Lett.* **4**, 522–525 (2008).
5. Marks, M. S. & Seabra, M. C. The melanosome: membrane dynamics in black and white. *Nat. Rev. Mol. Cell Biol.* **2**, 738–748 (2001).
6. McGraw, K. J. in *Bird Color. Mech. Meas.* (Hill, G. E. & McGraw, K. J.) 243–294 (Harvard University Press, 2006).
7. Carney, R. M., Vinther, J., Shawkey, M. D., D'Alba, L. & Ackermann, J. New evidence on the colour and nature of the isolated *Archaeopteryx* feather. *Nat. Commun.* **3**, 637 (2012).
8. Clarke, J. A. *et al.* Fossil evidence for evolution of the shape and color of penguin feathers. *Science* **330**, 954–957 (2010).
9. Li, Q. *et al.* Reconstruction of *Microraptor* and the evolution of iridescent plumage. *Science* **335**, 1215–1219 (2012).
10. Li, Q. *et al.* Plumage color patterns of an extinct dinosaur. *Science* **327**, 1369–1372 (2010).
11. Vinther, J., Briggs, D. E. G., Clarke, J., Mayr, G. & Prum, R. O. Structural coloration in a fossil feather. *Biol. Lett.* **6**, 128–131 (2010).
12. Li, Q. *et al.* Melanosome evolution indicates a key physiological shift within feathered dinosaurs. *Nature*; doi:10.1038/nature12973 (2014).
13. Zhang, F. *et al.* Fossilized melanosomes and the colour of Cretaceous dinosaurs and birds. *Nature* **463**, 1075–1078 (2010).
14. Pacton, M., Fiet, N. & Gorin, G. E. Bacterial activity and preservation of sedimentary organic matter: the role of exopolymeric substances. *Geomicrobiol. J.* **24**, 571–581 (2007).
15. Westall, F. *et al.* Early Archean fossil bacteria and biofilms in hydrothermally-influenced sediments from the Barberton greenstone belt, South Africa. *Precambrian Res.* **106**, 93–116 (2001).
16. Vollmer, W., Blanot, D. & De Pedro, M. A. Peptidoglycan structure and architecture. *FEMS Microbiol. Rev.* **32**, 149–167 (2008).
17. Westall, F. The nature of fossil bacteria: a guide to the search for extraterrestrial life. *J. Geophys. Res. Planets* **104**, 16437–16451 (1999).
18. Liebig, K. *Fossil Microorganisms from the Eocene Messel Oil Shale of Southern Hesse, Germany.* (1997).
19. Toporski, J. K. W. *et al.* Morphologic and spectral investigation of exceptionally well-preserved bacterial biofilms from the Oligocene Enspel Formation, Germany. *Geochim. Cosmochim. Acta* **66**, 1773–1791 (2002).
20. Westall, F., Boni, L. & Guerzoni, E. The experimental silicification of microorganisms. *Palaeontology* **48**, 495–528 (1995).
21. Cadena, E. & Schweitzer, M. Variation in osteocytes morphology vs bone type in turtle shell and their exceptional preservation from the Jurassic to the present. *Bone* **51**, 614–620 (2012).
22. Schweitzer, M. H., Wittmeyer, J. L., Horner, J. R. & Toporski, J. K. Soft-tissue vessels and cellular preservation in *Tyrannosaurus rex*. *Science* **307**, 1952–1955 (2005).
23. Schweitzer, M. H. *et al.* Biomolecular characterization and protein sequences of the Campanian hadrosaur *B. canadensis*. *Science* **324**, 626–631 (2009).
24. Henwood, A. Exceptional preservation of dipteran flight muscle and the taphonomy of insects in amber. *Palaios* **7**, 203–212 (1992).
25. d'Ischia, M. *et al.* Melanins and melanogenesis: methods, standards, protocols. *Pigment Cell Melanoma Res.* **26**, 616–633 (2013).
26. Simon, J. D., Hong, L. & Peles, D. N. Insights into melanosomes and melanin from some interesting spatial and temporal properties *J. Phys. Chem. B* **112**, 13201–13217 (2008).
27. Hollingworth, N. T. J. & Barker, M. J. in *Process. Foss.* (Donovan, S. K.) 105–119 (Columbia University Press, 1991).
28. Flemming, H.-C. & Wingender, J. The biofilm matrix. *Nat. Rev. Microbiol.* **8**, 623–633 (2010).
29. Plonka, P. M. & Grabacka, M. Melanin synthesis in microorganisms—biotechnological and medical aspects. *Acta Biochim Pol* **53**, 429–443 (2006).
30. Field, D. J. *et al.* Melanin concentration gradients in modern and fossil feathers. *PLoS One* **8**, e59451 (2013).
31. McNamara, M. E., Briggs, D. E. G., Orr, P. J., Field, D. J. & Wang, Z. Experimental maturation of feathers: implications for reconstructions of fossil feather colour. *Biol. Lett.* **9**, 1–6 (2013).
32. Barden, H. E. *et al.* Morphological and geochemical evidence of eumelanin preservation in the feathers of the Early Cretaceous bird, *Gansus yumenensis*. *PLoS One* **6**, e25494 (2011).
33. Knight, T. K., Bingham, P. S., Lewis, R. D. & Savrda, C. E. Feathers of the Ingersoll Shale, Eutaw Foramtion (Upper Cretaceous), eastern Alabama: the largest collection of feathers from North American Mesozoic rocks. *Palaios* **26**, 364–376 (2011).
34. Ma, F. *Late Mesozoic fossil fishes from the Jiuquan Basin of Gansu Province, China.* 118 (Ocean Press, 1993).

35. You, H. *et al.* A nearly modern amphibious bird from the Early Cretaceous of northwestern China. *Science* **312**, 1640–1643 (2006).
36. Grande, J. M., Negro, J. J. & Torres, M. J. The evolution of bird plumage colouration: a role for feather-degrading bacteria? *Ardeola* **51**, 375–383 (2004).
37. Goldstein, G. *et al.* Bacterial degradation of black and white feathers. *Auk* **121**, 656–659 (2004).
38. Gunderson, A. R., Frame, A. M., Swaddle, J. P. & Forsyth, M. H. Resistance of melanized feathers to bacterial degradation: is it really so black and white? *J. Avian Biol.* **39**, 539–545 (2008).
39. Brinkmann, V. *et al.* Neutrophil extracellular traps kill bacteria. *Science* **303**, 1532–1535 (2004).
40. Gaill, F., Desbruyères, D. & Prieur, D. Bacterial communities associated with "Pompei worms" from the East Pacific rise hydrothermal vents: SEM, TEM observations. *Microb. Ecol.* **13**, 129–139 (1987).
41. Schleifer, K. H. & Kandler, O. Peptidoglycan types of bacterial cell walls and their taxonomic implications. *Bacteriol. Rev.* **36**, 407–477 (1972).
42. Lindgren, J. *et al.* Molecular preservation of the pigment melanin in fossil melanosomes. *Nat. Commun.* **3**, 1–7 (2012).
43. Wogelius, R. A. *et al.* Trace metals as biomarkers for eumelanin pigment in the fossil record. *Science* **333**, 1622–1626 (2011).
44. McGraw, K. J. Melanins, metals, and mate quality. *Oikos* **102**, 402–406 (2003).
45. Waldron, K. J. & Robinson, N. J. How do bacterial cells ensure that metalloproteins get the correct metal? *Nat. Rev. Microbiol.* **7**, 25–35 (2009).
46. White, C., Wilkinson, S. C. & Gadd, G. M. The role of microorganisms in biosorption of toxic metals and radionuclides. *Int. Biodeterior. Biodegrad.* **35**, 17–40 (1995).
47. Brandelli, A., Daroit, D. & Riffel, A. Biochemical features of microbial keratinases and their production and applications. *Appl. Microbiol. Biotechnol.* **85**, 1735–1750 (2010).
48. Fujii, T. & Li, D. Preparation and properties of protein films and particles from chicken feather citation export. *J. Biol. Macromol.* **8**, 48–55 (2008).
49. Fraser, R. D. B. & Parry, D. A. D. Molecular packing in the feather keratin filament. *J. Struct. Biol.* **162**, 1–13 (2008).
50. Manning, P. L. *et al.* Synchrotron-based chemical imaging reveals plumage patterns in a 150 million year old early bird. *J. Anal. At. Spectrom.* **28**, 1024–1030 (2013).
51. Sawyer, R. H. & Knapp, L. W. Avian skin development and the evolutionary origin of feathers. *J. Exp. Zool. Part B Mol. Dev. Evol.* **298B**, 57–72 (2003).
52. Lindgren, J. *et al.* Skin pigmentation provides evidence of convergent melanism in extinct marine reptiles. *Nature* doi:10.1038/nature12899 (2014).
53. Glass, K. *et al.* Direct chemical evidence for eumelanin pigment from the Jurassic Period. *Proc. Natl. Acad. Sci.* **109**, 10218–10223 (2012).
54. Glass, K. *et al.* Impact of diagenesis and maturation on the survival of eumelanin in the fossil record. *Org. Geochem.* **64**, 29–37 (2013).

Acknowledgments

We thank the NCSU Poultry Education Unit, Toby Tung and the NCSU Materials Science and Engineering Department and Jeanette Shipley-Phillips and the NCSU Veterinary School Imaging Center. We also thank Amy Grunden, Lindsay Zanno and Timothy Cleland for their discussion and editorial comments. This research is supported by the National Science Foundation Graduate Research Fellowship (DGE-1252376) to A.E.M. and the David and Lucille Packard Foundation to M.H.S. Any opinion, findings, and conclusions or recommendations expressed in this material are those of the authors and do not necessarily reflect the views of the National Science Foundation.

Author contributions

A.E.M., E.A.J. and W.Z. performed data collection and research. D.L. and M.C.L. collected and described specimens of *Gansus yumenensis*. K.J.L. provided the geologic description of the *Gansus* site and performed initial analyses on the fossil specimen. A.E.M. and M.H.S. wrote the manuscript.

Additional information

Supplementary information accompanies this paper at http://www.nature.com/scientificreports

Competing financial interests: The authors declare no competing financial interests.

How to cite this article: Moyer, A.E. *et al.* Melanosomes or Microbes: Testing an Alternative Hypothesis for the Origin of Microbodies in Fossil Feathers. *Sci. Rep.* **4**, 4233; DOI:10.1038/srep04233 (2014).

Melanosomes or Microbes: Testing an Alternative Hypothesis for the Origin of Microbodies in Fossil Feathers

Authors: Alison E. Moyer[1*], Wenxia Zheng, Elizabeth A. Johnson, Matthew C. Lamanna, Da-Qing Li, Kenneth J. Lacovara, Mary H. Schweitzer

Supplementary Information:

Figures S1-S4 and Methods

Supplementary Materials:

Figures

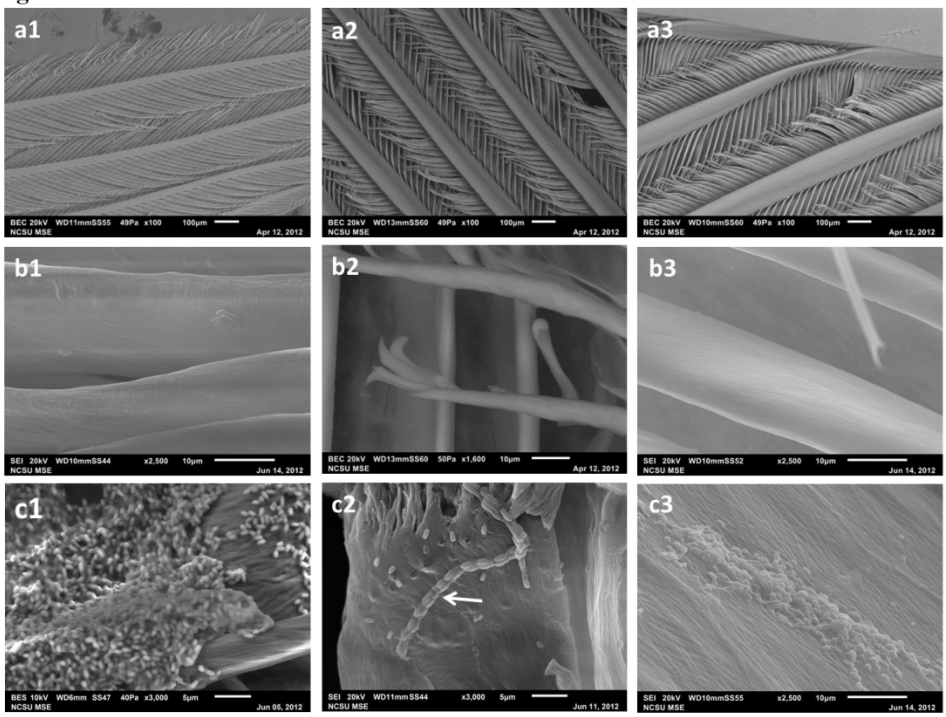

Supplementary Figure S1. SEM images of untreated and *Bacillus cereus* treated extant chicken feathers. Low (**a**) and high (**b**) magnification of untreated feathers. Feathers incubated with *Bacillus cereus* (**c**) for three days, then dried and imaged as described. Columns (**1**), (**2**), and (**3**) are white feather, brown feather, and black feather respectively. (**c1-c3**) show feather surfaces with microbial overgrowth. (**c2**) shows that *B. cereus* cells (arrow) are capable of strong alignment on feather surfaces, a feature ascribed only to melanosomes in the literature. Images b1, b3, c2 and c3 were captured after the specimens were gold coated (see Methods).

[1]Department of Marine, Earth and Atmospheric Sciences, North Carolina State University, Raleigh, NC 27695.
*Correspondence to aemoyer@ncsu.edu.

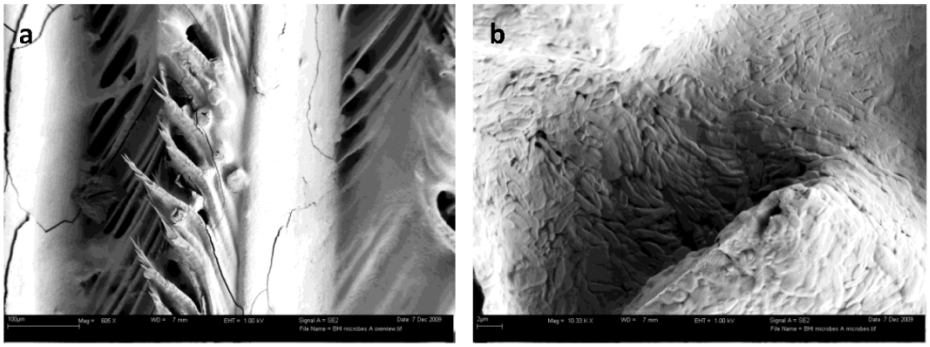

Supplementary Figure S2. FESEM image of environmental biofilm grown on extant feather. Low magnification (**a)** shows overgrowth draping individual barbs. High (**b**) magnification of closely packed bacterial cells that cover and follow the contours of a guineafowl (*N. meleagris*) feather.

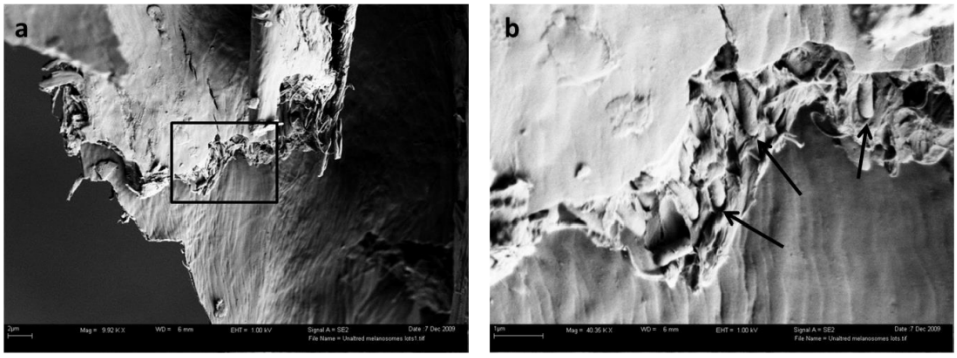

Supplementary Figure S3. FESEM images of untreated, fresh-fractured guineafowl feather. (**a**) Low magnification of the fractured feather. (**b**) Higher magnification of the boxed area in (a). Melanosomes (arrows) are sparse and embedded deep within the interior of the feather.

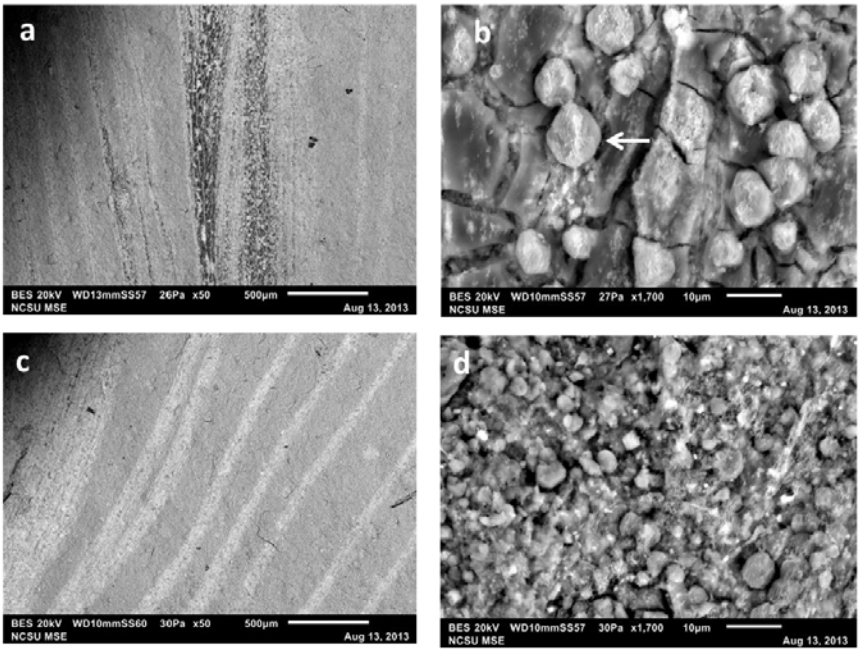

Supplementary Figure S4. SEM images of the *Gansus yumenensis* feather (ANSP 23403). The distal, black region, **(a,b)** and the brown proximal, or basal part **(c,d)** visualized using SEM. In back scatter mode, atomic differences distinguish the feather from the surrounding sediments **(a,c)** in lower magnifications. At higher magnifications, textural differences are observed. The black region **(b)** exhibits a smooth film-like appearance with ~8µm sized sediment grains. EDS data identify principle element composition of these grains to be sediment, distinct from the feather itself. See Fig. 7 and 8. A grainer texture with smaller sediment grains are observed in the brown region of the fossil **(d)**.

Methods:

Geologic context of fossil feather ascribed to *Gansus yumenensis* (ANSP 23403)

Location—The study area is located on provincial land in the Changma Basin, on the northern flank of the Qilian Mountains (the northernmost extent of the Tibetan-Qinghai Plateau) in far northwestern Gansu Province, China.

Sedimentology—The basin is ringed by near-vertically tilted exposures of sedimentary rocks of the Lower Cretaceous Xiagou Formation, providing extensive fossiliferous outcrops. The formation consists of lacustrine shales[1] and sandy lakeshore deposits. All known fossils come from the shale units. At its base, the local section contains about 45 m of deep-water lacustrine sediment. Fine grain size and thin laminae at this level indicate a quiescent environment in which plants, insects, and fishes were often preserved. From 45 m to 50 m above the base, depositional conditions alternated between deep-water and shallower lacustrine environments, as evidenced by layers of disturbance ripples. This lake margin facies contains the lower of the two known *Gansus*-producing quarries, as well as fossil plants, insects, and turtles. Above 50 m, sediments record a number of expansions and contractions of the lake margin, during which conditions rapidly fluctuated between shallow water and nearshore states. Matrix-rich conglomerates, graded sandstones, and symmetrically rippled cross-laminated sandstones represent the latter condition. The upper *Gansus*-producing quarry, from 51 m to 54 m above the base, contains layers of shallow lacustrine shale alternating with massive to rippled sandstones deposited along the lakeshore. The abrupt facies changes at 60 m and 63 m, from shale to matrix-rich conglomerate, are typical of lakes with steep margins[2] and record the delivery of coarse clastics via fluvial or mass-wasting processes to the lake margin. The lakeshore sandstones also contain oscillatory ripples characteristic of wave-dominated lakes. The substantial fetch required to generate an active littoral zone indicates the presence of a sizable lake. Thus, the sedimentology of this section shows a deep lake, shallowing at this location, with steep margins set widely apart leading down to sandy beaches. This depositional setting corresponds well with the interpretation of *Gansus yumenensis* as an amphibious bird[3].

Geochronology—The Xiagou Formation is Early Cretaceous in age[4, 5]. Suarez et al. (2013)[6] have refined the age of the Xiagou Formation lacustrine beds to the early Aptian stage based on carbon isotope chemostratigraphy.

References:

1. Ma, F. Late Mesozoic fossil fishes from the Jiuquan Basin of Gansu Province, China (Ocean Press, Beijing, 1993).
2. Link, M.H., Osborne, R.H. & Awramik, S.M. Lacustrine stromatolites and associated sediments of the Pliocene Ridge Route Formation, Ridge Basin, California. *Journal of Sedimentary Research* **48**, 143-157 (1978).
3. You, H.-l. et al. A Nearly Modern Amphibious Bird from the Early Cretaceous of Northwestern China. *Science* **312**, 1640-1643 (2006).
4. Hsü, J., Chiang, T.-c. & Young, H.-c. Sporo-pollen Assemblage and Geological Age of the Lower Xinminbu Formation of Chiuchuan, Kansu. *Journal of Integrative Plant Biology* **16**, 365-374 (1974).
5. Tang, F. et al. Biostratigraphy and palaeoenvironment of the dinosaur-bearing sediments in Lower Cretaceous of Mazongshan area, Gansu Province, China. *Cretaceous Research* **22**, 115-129 (2001).
6. Suarez, M.B., Ludvigson, G.A., González, L.A., Al-Suwaidi, A.H. & You, H.-L. Stable isotope chemostratigraphy in lacustrine strata of the Xiagou Formation, Gansu Province, NW China. *Geological Society, London, Special Publications* **382** (2013).

CHAPTER 3 - Interpreting melanin-based coloration through deep time: a critical review

PROCEEDINGS B

rspb.royalsocietypublishing.org

Review

Cite this article: Lindgren J *et al.* 2015 Interpreting melanin-based coloration through deep time: a critical review. *Proc. R. Soc. B* **282**: 20150614.
http://dx.doi.org/10.1098/rspb.2015.0614

Received: 17 March 2015
Accepted: 23 July 2015

Subject Areas:
palaeontology, molecular biology, evolution

Keywords:
bacteria, eumelanin, melanosome, pheomelanin, pyomelanin, vertebrate

Author for correspondence:
Johan Lindgren
e-mail: johan.lindgren@geol.lu.se

Electronic supplementary material is available at http://dx.doi.org/10.1098/rspb.2015.0614 or via http://rspb.royalsocietypublishing.org.

THE ROYAL SOCIETY PUBLISHING

Interpreting melanin-based coloration through deep time: a critical review

Johan Lindgren[1], Alison Moyer[3], Mary H. Schweitzer[1,3,4], Peter Sjövall[5], Per Uvdal[6,7], Dan E. Nilsson[2], Jimmy Heimdal[6], Anders Engdahl[6], Johan A. Gren[1], Bo Pagh Schultz[8] and Benjamin P. Kear[9,10]

[1]Department of Geology, and [2]Department of Biology, Lund University, 223 62 Lund, Sweden
[3]Department of Biological Sciences, North Carolina State University, Raleigh, NC 27695, USA
[4]North Carolina Museum of Natural Sciences, Raleigh, NC 27601, USA
[5]SP Technical Research Institute of Sweden, Chemistry, Materials and Surfaces, 501 15 Borås, Sweden
[6]MAX-IV laboratory, and [7]Chemical Physics, Department of Chemistry, Lund University, 221 00 Lund, Sweden
[8]MUSERUM, Natural History Division, 7800 Skive, Denmark
[9]Museum of Evolution, and [10]Palaeobiology Programme, Department of Earth Sciences, Uppsala University, 752 36 Uppsala, Sweden

Colour, derived primarily from melanin and/or carotenoid pigments, is integral to many aspects of behaviour in living vertebrates, including social signalling, sexual display and crypsis. Thus, identifying biochromes in extinct animals can shed light on the acquisition and evolution of these biological traits. Both eumelanin and melanin-containing cellular organelles (melanosomes) are preserved in fossils, but recognizing traces of ancient melanin-based coloration is fraught with interpretative ambiguity, especially when observations are based on morphological evidence alone. Assigning microbodies (or, more often reported, their 'mouldic impressions') as melanosome traces without adequately excluding a bacterial origin is also problematic because microbes are pervasive and intimately involved in organismal degradation. Additionally, some forms synthesize melanin. In this review, we survey both vertebrate and microbial melanization, and explore the conflicts influencing assessment of microbodies preserved in association with ancient animal soft tissues. We discuss the types of data used to interpret fossil melanosomes and evaluate whether these are sufficient for definitive diagnosis. Finally, we outline an integrated morphological and geochemical approach for detecting endogenous pigment remains and associated microstructures in multimillion-year-old fossils.

1. Introduction

The astonishing diversity of colour patterns seen in extant animals testifies to the important and multifunctional roles of melanin and other biological pigments (biochromes) in nature. Moreover, organic molecules (including eumelanin) can persist and be recognized over vast spans of geological time, and thereby evince crucial information about the history of life [1]. Preserved biochromes not only yield interpretations on the appearance of ancient organisms, but can also potentially elucidate their ecology and behaviour. They are therefore an insightful data source for resolving facets of palaeobiology and evolution.

For decades, scanning electron microscopy (SEM) and, more rarely, transmission electron microscopy (TEM) have been used to detect round to oblate microstructures (about 1–2 μm long) in exceptionally preserved vertebrate fossils (e.g. [2–5]). Until 2008, these minute bodies were interpreted as the remains of microorganisms that contribute to the decomposition of organic material (e.g. [4], but also see Voigt [6] and references therein). However, that year, Vinther *et al.* [7] re-described them as residual melanosomes: eukaryotic, melanin-containing cellular organelles, responsible in part for the coloration of integumentary structures, including skin, hair and feathers. They further suggested that the shape and arrangement of fossil melanosomes could be used to deduce plumage colours in ancient birds and non-avian dinosaurs [7], which led to inferences

about ecology and behaviour that have since been adopted by numerous studies (e.g. [8–10]).

Although information about the colour of extinct animals might provide important clues pertaining to lifestyles and habits, the reconstruction of specific tones and hues based on morphological evidence alone is not a straightforward process [11]. This is particularly pertinent when only SEM image data are considered, as these are demonstrably inadequate for discriminating between remnant melanosomes and pervasive bacteria [12]. Differentiation of melanosomes from microorganisms is necessary because they overlap in size, shape and distribution [12–14]. Moreover, microbes are always associated with decaying carcasses, and are known to fossilize as both organic (e.g. [15,16]) and inorganic traces (e.g. [17]). Another confounding issue is that microorganisms synthesize melanins [18,19], an ability that is most prevalent in bacteria inhabiting soil and marine environments [19]. Compounds arising from the degradation of melanic pigments have also been detected in microbial fossils, including fungal hyphae [20].

Defining colour from the shape of fossil microbodies (see [8,9]) has other limitations. Extant eumelanosomes (ellipsoidal organelles associated with dusky pigmentation [21], but also see below) can contain only eumelanin, but pheomelanosomes (spherical organelles associated with reddish pigmentation [21]) may not exist without a eumelanin complement [22]. Finally, the eumelanin-dominated eye pigments of vertebrates exhibit a random distribution of melanosome shapes that do not correlate with the type of melanin present [23,24].

Here, we address conceptual and methodological issues related to the interpretation of microbodies detected in fossilized animal tissues. As a framework, we briefly review melanosome formation in vertebrates (for brevity, we do not address invertebrate melanogenesis), focusing on physical and chemical properties of one of its main constituents: melanin. This moiety is thought to impart stability to the intracellular organelle, thereby enabling its preservation through deep time. Microbial melanization is also summarized for a practical character-based discrimination between fossil melanosomes and microorganismal cells. Our critical assessment of the methods commonly employed to identify fossil microstructures is intended to facilitate confident documentation and reduce the risk of insufficiently supported claims propagating in the literature.

2. Vertebrate melanogenesis

Structurally, melanins are heterogeneous biopolymers comprising a series of conjugated indole (resonant double-ring) moieties [25,26]. Several major melanin types exist in nature, but the most common are (dark brown-black) eumelanin and (red-yellow) pheomelanin [27]. Eumelanin is derived from enzyme-controlled oxidation of the amino acid tyrosine [28] to form a biochrome that is inherently resistant to degradation [25]; thus, its molecular structure is incompletely known [22,26]. Likewise, despite recognition that pheomelanin is produced from sulfur-containing benzothiazine units [28], its chemical structure is also not fully characterized [21].

In vertebrates, melanins are distributed through epidermal tissues and their derivatives, where the colour they impart plays important roles in social and predator–prey interactions, thermoregulation and ultraviolet (UV) protection [29,30]. In addition, internal organs and tissues, such as the liver, spleen, brain and inner ear, also contain melanin, which contributes to physiological processes and disease resistance [30, fig. 1].

The cellular site of melanin synthesis, storage and transportation is the melanosome—a membrane-bound organelle generated by melanocytes, melanophores and pigment-epithelial cells [29]. Melanosomes attain a broad range of sizes and shapes, ranging from sub-micrometre-sized spherical grains [21, fig. 2d] to elongate particles up to 4 μm long [31, fig. 2a]. Ellipsoidal forms are typically ascribed to eumelanosomes, whereas spherical structures are referred to pheomelanosomes (e.g. [21]). This subdivision of shape has been proposed to reflect the chemical composition of the type of melanin they contain ([21], but also see below).

Melanosome biogenesis follows four sequential stages (enumerated I–IV), where melanin deposition is initiated at stage III, and the organelle is fully melanized by stage IV [32, fig. 1a]. Polymerization of melanin within the developing melanosome results in the formation of granules (this term is inconsistently used in the literature, but we follow the definition of Simon & Peles [22] as a standard) on intraluminal fibrils, and continues until all other structures within the organelle are obliterated [28,33]. At this time (stage IV), the organelle is considered to be mature [22]. Fully grown melanin granules normally range from 10 to 30 nm in diameter [22,34,35]; however, larger grains up to 80 nm in diameter have been recorded within red human hair melanosomes [21]. The melanin granules cause the outer surface of the melanosomes to become rugose [36, figs 2 and 3], a characteristic trait that is most marked in spherical forms [23].

Whereas pure eumelanin is naturally occurring, pure pheomelanin has not yet been documented [22]. Instead, pheomelanosomes contain a mixture of eumelanin and pheomelanin [21,28,37]. Pheomelanin granules are thought to comprise a pheomelanin core surrounded by a eumelanin sheath (the casing model [22,38], but see Gorniak *et al.* [39] for a different interpretation), the thickness of which determines expressed colour, at least in iridal melanosomes [37].

3. Melanin synthesis in microorganisms

In addition to eumelanin and pheomelanin, bacteria and fungi also produce a third type of melanin, generically named allomelanin [18,40]. Allomelanins are synthesized from an array of sources and via different biochemical pathways. As a result, several major subtypes exist, the most ubiquitous being pyomelanin. Allomelanins usually form from nitrogen-free precursors and are hence devoid of this constituent (see Plonka & Grabacka [18] for a comprehensive review of melanin biosynthesis in microorganisms).

In contrast to vertebrates, whose melanogenesis is confined to specialized cellular organelles, melanin synthesis in fungi usually occurs within the cell wall [41,42]. Nonetheless, some fungal species deposit melanins intracellularly in the form of cytoplasmic bodies, whereas others secrete melanic pigments into the surrounding environment [43]. The melanized fungal cell wall is highly durable, and thus can be isolated by chemical treatments destructive to other cellular components [44]. The resulting melanin shells (often called melanin ghosts) are hollow, but retain both the shape and size of the original cells after degradation and removal of the non-melanized constituents [18,44]. Melanin ghosts are composed of tightly packed and occasionally laminated melanin granules between 30 and

150 nm in diameter [43,44]. These impart a nodular appearance to the external ghost wall [44, fig. 2], and are typically accompanied by diagnostic crater-like scars derived from the budding process ([44, fig. 5], [45, fig. 1]).

In prokaryotic organisms, melanogenesis normally occurs extracellularly, and hence most bacterial melanins form amorphous deposits when purified [18,46], although globular aggregates have been reported [47]. However, in some bacteria, melanins are localized to the cytoplasm and may appear as electron-dense spots [48, fig. 5e]. Melanin-like compounds have also been detected in bacterial endospore coats, where they probably protect the developing spore against harmful UV radiation (e.g. [49]).

4. Melanin and melanosomes in the fossil record

Reports describing fossil melanins and melanosomes have been published sporadically since the 1930s (e.g. [6,50,51]), yet the search for ancient melanic pigments only began in earnest in the late 2000s following the proposal that feather traces might infer evidence of original hues and shades [7,52]. Since then, a number of investigations have used chemical markers and presumed fossil melanosomes to explore aspects of the biology and ecology of extinct animals, including colour [8,9,53–57], behaviour [8,56] and physiology [10]. However, studies reporting remnant melanosomes have been met with controversy, and an alternative hypothesis has been put forth favouring a more conservative interpretation of the fossil microbodies as microbes colonizing the degrading tissues prior to burial [12,58]. Such criticism has sparked intense debate (see Edwards *et al.* [11] for review), that is further aggravated by the dearth of unequivocal molecular indicators for ancient melanic pigments, which thus far have only been recorded from cephalopod ink sacs [59,60], a fish 'eye spot' [61] and marine reptile integuments [56]. Indeed, most occurrences of fossil melanosomes reported so far (particularly in feathers) are based entirely on morphology, packing and distribution (e.g. [7–10, 52–54,62]), whereas chemical studies, with few exceptions (see above), have either been inconclusive (e.g. [14,63]) or lacking in specificity and/or relevant comparative material to rule out alternative hypotheses (e.g. [55,64,65]). Most critically, many alleged melanosomes occur only as imprints ('mouldic melanosomes' [53]), a preservation mode that implies preferential degradation of the bodies relative to the surrounding substrate [12]. To complicate matters further, impressions indistinguishable from those attributed to melanosomes are occasionally found also in clay minerals, on silica crystals, and other sedimentary grains associated with, but clearly distinct from, the fossilized tissue structures (e.g. [9,12,65]).

These conflicts highlight the need for clear and unambiguous criteria by which remnant melanosomes can be differentiated from microbial residues. Clearly, this is vital for any accurate inference of organismal colour and its subsequent influence on ancient behaviours or ecology. We therefore outline factors contributing to the preservation potential of both melanin and melanosomes, and evaluate published methodologies employed to identify fossil microbodies. We also propose an integrated structural and molecular approach to promote rigorous interpretation of fossil melanins and melanosomes in the future. Firstly, however, we address a series of untested assumptions regarding melanosome data derived from the vertebrate fossil record.

5. Assumptions underlying assignment of colour to fossil organisms

(a) Assumption 1: melanosomes are inherently resistant to degradation

Whereas melanosomes in living animals contain a variety of biomolecules in addition to melanins (including significant amounts of proteins and lipids [66, fig. 1]), only eumelanin has so far been confidently identified in fossil melanosomes [56,61]. This suggests that the fully melanized stage IV melanosomes have the greatest capacity for preservation given their internal architecture of densely aggregated melanin granules [56,61]. The cross-linked polymeric structure of the eumelanin macromolecule is most likely responsible for this survival in fossil form [56,61]. Support for this hypothesis has been gleaned from degradation experiments, which demonstrate the remarkable mechanical rigidity of the melanin framework and its ability to retain both the size and shape of hydrolysed melanosomes, even after the complete removal of proteins and lipids [31,66–68]. Yet despite this durability, melanin is still susceptible to breakdown via oxidative reactions [66] and by some enzymes [69]. Moreover, populations of specialized melanophages infest vertebrate tissues (e.g. [70,71]). These monocyte-derived cells engulf melanosomes and retain them within their cytoplasm where both organelles and pigments are degraded over relatively short spans of time (e.g. [70,71]). In accordance, melanin can disintegrate rapidly under natural conditions, and thus its architectural stability and chemical robustness do not unequivocally confer preservation potential over geological time.

(b) Assumption 2: melanin pigments confer resistance to degradation

Melanized epidermal tissues and their appendages are known to have increased resistance to physical abrasion relative to unmelanized ones (e.g. [69,72]). Melanin insolubility, imparted by abundant intramolecular cross-links, has been argued to contribute to the preservation of integumentary structures in fossils, and especially feathers (e.g. [54]). However, the assumption that melanin unanimously confers degradation resistance to the enclosing organelles, or the surrounding keratinous tissues, has not yet been rigorously tested. This is critical for evaluating the many published accounts on presumed melanosomes in fossils, because the majority of those specimens where expressed colour, physiology, behaviour or evolutionary significance have been proposed do not illustrate three-dimensional bodies, but rather derive data from ovoid to elongate imprints within an uncharacterized matrix (e.g. [8–10,54]). This observation implies that the microbodies decay more rapidly than does the surrounding matrix, thus challenging the idea that melanin confers decay resistance to the bodies. Because the attribution of these imprints to melanosomes rests on assumptions of their inherent durability, this assignment is called into question when only voids are present. Taphonomic experiments designed to test the relative resistance of melanosomes in keratin, keratin alone and microbial cells in extracellular polymeric substance (EPS) under varying conditions may present a possible method for addressing this issue.

(c) Assumption 3: fossil microbody shape and size are reliable indicators of colour

Statistical correlations support coherency between the shape and size of melanosomes in living epidermal tissues and the expression of melanin-derived colours (e.g. [8,9]). However, in addition to melanins, many other factors contribute to organismal coloration, including diet, light conditions, tissue structure, gender and co-expressed pigments [73,74]. Melanosomes occurring in skin and skin derivatives have also been statistically compared to microbodies (or more frequently their imprints) in fossil-associated material, and used to assign hues and colour patterns (e.g. [8,9]). However, with one exception [10], these extrapolations have failed to consider potential diagenetic alterations of these parameters in the matrix; instead, most studies have assumed the measured impressions to accurately reflect the shape and size of the original bodies (e.g. [57]). Nonetheless, maturation experiments on extant feathers designed to simulate the fossilization process have shown that melanosome size can be altered by increasing temperature and/or pressure [75]. Notably though, no consistent morphological modification has yet been documented in presumed fossil melanosomes, and it remains feasible that varying decompositional conditions, as well as mineralization might also effect structural change [60].

Another problem is the possibility that the supposed melanosome imprints could represent microbial cells preserved in mineralized EPS. Microorganismal EPS has high preservation potential because of its inherent affinity for mineral ions, and is thus likely to persist in the rock record [17]. Moreover, bacteria are ubiquitous in degrading organic matter and were undoubtedly present with all fossilized specimens. Imprints produced in the EPS when microbes degrade or are lost in other ways are consistent in virtually every aspect with those attributed to fossil melanosomes (electronic supplementary material, figure S1).

To further complicate matters, melanosomes in other pigmented tissues, such as the retina and choroid of the vertebrate eye, also vary widely in shape and size [23,76]. In these tissues at least, melanosome morphologies might additionally differ during ontogeny, yet the main melanin component is eumelanin regardless of melanosome shape and surface topography [23,76]. Microstructures comparable to those in modern vertebrate eyes are occasionally found in the orbital region of animal fossils (e.g. [61,77]), demonstrating that diverse ocular melanosome morphologies are not limited to extant taxa. Whether similar conditions apply to melanosomes derived from integumentary tissues has yet to be verified (it was recently discovered that similarly shaped melanosomes obtained from modern iridescent feathers have a highly variable chemistry [78]); however, the fact that diverse melanosome shapes occur in the eyes of ectothermic vertebrates suggests that factor(s) other than colour, energetics and physiology [8–10] can influence melanogenesis and the resulting melanosome morphologies.

Given the degree of morphological variation observed in living tissues, diagenetic factors and the co-expression of other pigments that may not persist in the fossil record, as well as the fact that a microbial source for most of these fossil microbodies and impressions has not been eliminated, we question the validity of reconstructing organismal colour based on the external structure of fossil microbodies alone and conclude that rigorous extant correlations with the same anatomical sources (i.e. comparing skin with skin and feathers with feathers) offer the only accurate paradigm for reliable interpretations.

6. A way forward: integrated morphological and geochemical approaches

The intrinsic resistance of melanin to degradation (except in the presence of cells/enzymes targeted specifically against it) and its preservation in fossils highlight significant potential for elucidating the biology of extinct organisms. Nevertheless, such interpretations are inherently equivocal, and further complicated by the fact that microbes: (1) overlap in size, shape and preservation potential with melanosomes; (2) can produce melanins; and (3) are innately associated with decaying organics [12]. Judicious elimination of alternative hypotheses for the origin of microbodies in fossils is therefore necessary prior to extrapolations of colour or function. While SEM imaging of external morphology and organisation provides a viable first step, it is not sufficient for a definitive diagnosis [12]. To augment morphology, higher resolution images should therefore be obtained from field emission gun scanning electron microscopy (FEG-SEM), which can reveal distinctive surface features, such as melanin granules (e.g. [56, fig. 2c]). TEM imaging can also yield complementary information about internal structures. Generally, microbial cells have an electron lucent core ([12, fig. 4], [79, figs 7, 9–13], [80, fig. 1]), as opposed to the electron opaque interior of mature melanosomes (see [61, electronic supplementary material, fig. S2], [81, fig. 3]). Exceptions do exist, however, such as hollow melanosomes [82] and solid, 'carbonized' bacteria [16, fig. 7c]. Therefore, for confident identification, chemical fingerprints of eumelanins, pheomelanins and/or their degradation products must be localized to the fossil microbodies (e.g. [56,59–61]). Ideally, these biomarkers should not occur only as trace metals because microbes and the EPS they secrete can concentrate metal ions from the environment [83]. Thus, elevated trace metal levels in fossilized animal tissues could be bacterially mediated [84,85] or artificially concentrated during diagenesis [11]. Furthermore, many enzymes employed by microbes to degrade keratinized tissues (including both white and pigmented feathers) are metalloenzymes that use a variety of metal ions which deposit on keratin surfaces during decomposition [86].

(a) Case study: structural and molecular identification of fossil melanosomes

To illustrate a proposed set of practical parameters for detecting endogenous pigment biomarkers and associated microstructures in an exemplary fossil, we undertook a series of stepwise microscopic and chemical analyses on microbodies obtained from the preserved 'eye' of a teleost fish (FUM-N-2268; MUSERUM) from the early Eocene of Denmark (figures 1 and 2; electronic supplementary material, figures S2–S6).

Initial macroscopic examination of the orbital residue showed a clearly delineated accumulation of a dense, brown substance that was superficially amorphous but distinct from the surrounding sediment in both texture and colour (figure 1*a*,*b*). FEG-SEM imaging revealed its composition to be a morphologically heterogeneous mass of spherical, oval and elongate bodies ranging from 0.2 to 3 µm in length (figure 1*c*,*d*). These structures were tightly

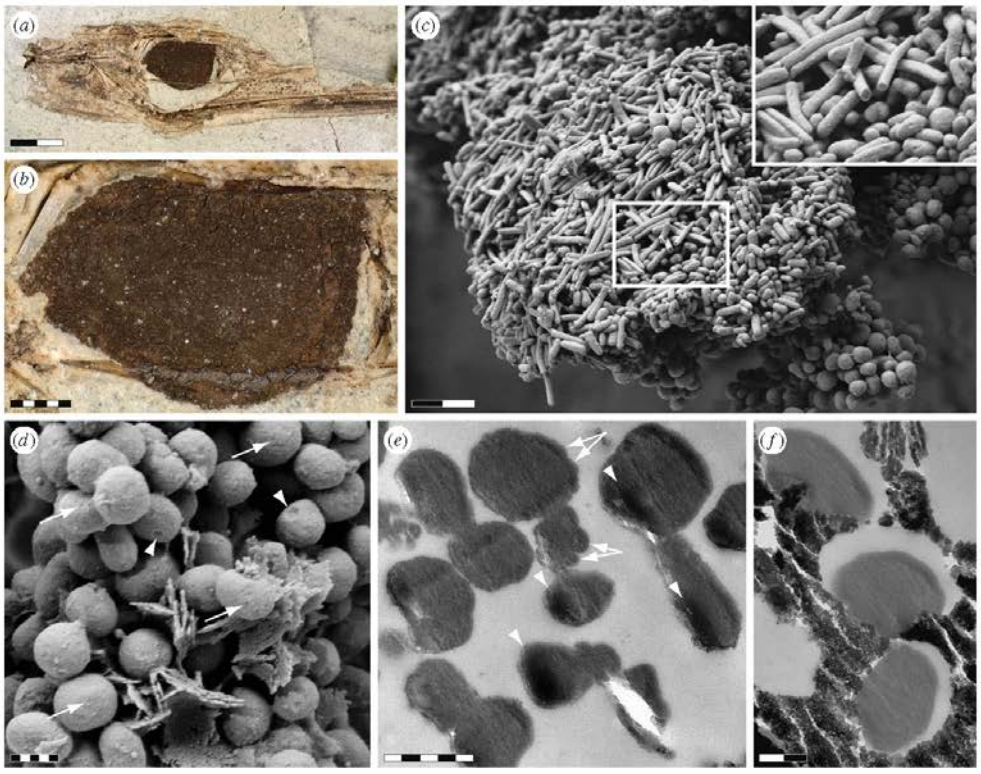

Figure 1. (*a*) Articulated skull of FUM-N-2268A. (*b*) Enlargement showing organic matter within the orbital cavity. (*c*) FEG-SEM micrograph of massed microbodies revealing morphological variation consistent with retinal melanosomes found in extant vertebrate eyes. Inset details elongate microbodies with homogeneous interior structure. (*d*) Surface pits (arrows) and depressions (arrowheads) on densely packed sub-spherical microbodies, the latter probably produced by diagenetic compression. Laminar structures are infiltrating sedimentary matrix. Note distinct size difference between moulds formed by diagenetic minerals and microbodies (see also *f*). (*e*) TEM micrograph of sectioned, unstained microbodies exposing external nodules (arrows) and electron-dense interior. Corrugated internal texture might be diagenetic; darker coloration (arrowheads) may represent replacement by inorganic material, possibly (based on ToF-SIMS data) iron sulfate. (*f*) TEM micrograph indicating diagenetic shrinkage of microbodies within the enclosing matrix. Scale bars: (*a*) 2 mm; (*b*) 500 µm; (*c*) 2 µm; (*d*,*e*) 500 nm; (*f*) 200 nm.

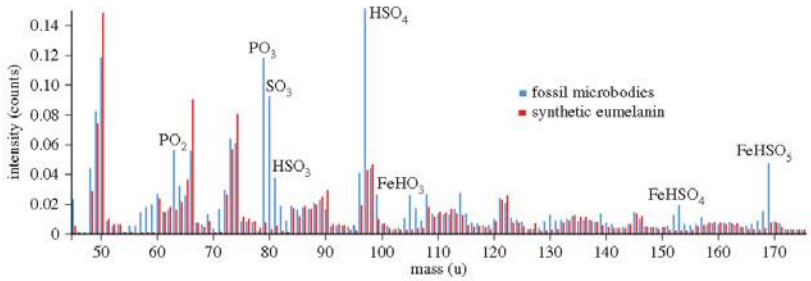

Figure 2. Negative ion ToF-SIMS spectra collected from fossil microbodies located within the 'eye spot' of FUM-N-2268 ('fossil microbodies') and synthetic eumelanin. Bars represent the integrated signal intensity at each nominal mass (the spectra are normalized to the sum intensity of the major eumelanin peaks). Peaks in the fossil spectrum that are not present in the eumelanin spectrum correspond to inorganic ions (as indicated), sulfur-containing organic ions (C_2HS at 57 u, CSN at 58 u and C_3SN at 82 u) and oxygen-containing organic ions ($C_2H_3O_2$ at 59 u and $C_3H_3O_2$ at 71 u), respectively.

packed but showed limited spatial overlap. Instead, some areas were characterized by stacks of rod-shaped microbodies (figure 1*c*), whereas other regions showed a predominance of globular forms (figure 1*d*). Superficially, the exterior surface of all microbodies appeared to be fairly smooth; however, closer inspection revealed a fine granular fabric incorporating randomly scattered pits (figure 1*d*—arrows) and depressions (figure 1*d*—arrowheads).

TEM imaging of sectioned microbodies exposed a corrugated, electron-dense interior (figure 1*e*,*f*). A darker coloration in

some areas could indicate replacement of the presumed organic matter (see below) by inorganic material (figure 1*e*—arrowheads). A notable size difference between natural moulds formed by precipitated minerals and the microbodies indicates that the latter may have contracted during the fossilization process (figure 1*d*,*f*).

Energy dispersive X-ray microanalysis (EDX) identified carbon as the primary constituent in the orbital residue, with minor contributions from other elements, such as sulfur.

ToF-SIMS analysis targeting the fossil microbodies yielded mass spectra consistent with comparative data from synthetic and natural eumelanins, but which excluded pheomelanin and pyomelanin as significant surface components (figure 2; electronic supplementary material, figures S2–S5). Deviations were identified as ionic constituents of the sedimentary matrix (including phosphate and sulfate), as well as iron sulfate and sulfur-containing organics (figure 2; electronic supplementary material, figure S2). The latter suggest diagenetic incorporation of sulfur into the eumelanin macromolecule [56,61], or alternatively represent derivatives from a minor pheomelanin component.

These data were corroborated by IR microspectroscopic measurements, which produced broad-band absorbance in the 900–1800 and 2500–3700 cm^{-1} regions, consistent with natural eumelanin (electronic supplementary material, figure S6).

(b) Rationale for assignment of the fossil microbodies to remnant melanosomes

The co-localization of melanin and microbodies in the 'eye spot' of FUM-N-2268 advocates a common source, but whether this is endogenous or exogenous remains to be determined. Alternative hypotheses exist: (1) the minute bodies could be the fossilized remains of ocular melanosomes preserved as melanin 'pseudomorphs' with a morphology replicating that of the original melanosomes; (2) they might also represent preserved invasive microbes and/or their spores; or (3) be a mixture of both endogenous and exogenous melanin sources.

To discriminate between these possibilities, we first tested for hollowness and the presence/absence of budding scars indicative of fungal melanin ghosts. TEM imaging accordingly showed that the FUM-N-2268 microbodies were solid, unlike melanin ghosts. Even though intracellular melanogenesis has been documented in some microorganisms, the process is toxic and potentially inhibitory to cell growth [48]. Hence, internal microbial melanins are restricted to either small spots or rare globular aggregates [43,48], inconsistent with the pattern observed in this sample. To the best of our knowledge, no extant microorganism undergoes cytoplasmic melanin production to such an extent that it obscures all other cellular details. Additionally, although shallow, circular depressions exist on the surface of some microbodies, they do not exhibit the typical characteristics of budding scars (see [44, fig. 5]). Instead, these marks are most likely diagenetic, being formed during compaction when the microbodies were pressed against one another.

EDX analysis detected carbon and sulfur in the 'eye' residue. These elements are components of melanin but also occur in bacterial biofilms [87]. Hence, they are insufficient to determine the affinity of the fossil microbodies. On the other hand, the predominance of eumelanin biomarkers in intimate association with the bodies (as evidenced by ToF-SIMS analysis) allows more confident determination. Eumelanin is the primary biochrome in vertebrate ocular melanosomes [76]. Moreover, modern vertebrate eyes contain a number of melanin-housing tissues, including the iris, retina and choroid [76]. Of these, the retinal pigment epithelium (RPE) is notable for its disparity in melanosome shapes and sizes (e.g. [24, fig. 1]). Furthermore, despite being located adjacent to one another, the various morphologies occur in functionally different parts of the RPE: rod-shaped forms proliferating in the apical processes wrapping the photoreceptor outer segments [88, fig. 6], and spherical forms dominating the basal cytoplasm immediately below the apical region [89]. Post-mortem degradation and subsequent collapse of the RPE and attendant tissues will inevitably result in a partial mixture of melanosome morphologies via stacking and/or close proximal packing (electronic supplementary material, figure S7), a distributional pattern consistent with that observed in FUM-N-2268. Conversely, if the fossil microbodies represent invading microorganisms, then multiple unrelated eumelanin-producing microbes, each with the ability to survive massive cytoplasmic melanin accumulation, must have independently colonized the orbital cavity during the decay of this fish. We deem this to be highly unlikely, and instead advocate a more parsimonious explanation of the microbodies as endogenous, being the fossilized remains of ocular melanosomes.

7. Summary

Organismal colour holds deep fascination because species recognition, gender differences and many other traits are intimately linked to pigmented epidermal tissues. There is no doubt that biochromes were, and are, an integral substrate for natural selection. Indeed, the various patterns, hues and shades that we observe today unquestionably also had equivalents in the distant past. Hence, characterizing pigments in extinct animals has enormous potential to shed light on evolutionary aspects of biology and ecology. Despite this, the study of colour through deep time is still very much in its infancy and can be impinged by numerous experimental pitfalls. Caution should therefore be exercised in this endeavour. Illuminating aspects of ancient organismal colour is achievable only by thorough evaluation of all plausible hypotheses. These remain valid until disproven and should not be swayed by popular opinion. Developing a comprehensive understanding of exceptional preservation processes through careful actualistic experiments must also be augmented by knowledge of diagenetic effects and how they potentially alter the morphology and chemistry of microbodies associated with decaying organics. Such approaches will ultimately facilitate more rigorous interpretations and reduce the risk of spectacular yet insufficiently supported claims propagating in the literature.

Data accessibility. FUM-N-2268 is deposited at MUSERUM. Additional supporting data can be accessed from the Department of Geology, Lund University.

Authors' contributions. J.L., A.M., M.H.S., D.E.N. and B.P.K. wrote the manuscript. J.L., A.M., P.S. and P.U. made the illustrations. J.L., A.M., P.S., P.U., J.H., A.E. and J.A.G. performed the analyses and interpreted the data. B.P.S. provided access to FUM-N-2268. All of the authors discussed the results and content of the manuscript.

Competing interests. We have no competing interests.

Funding. This research was supported by the Swedish Research Council, the Royal Physiographical Society in Lund and the Crafoord

Foundation to J.L., the David and Lucile Packard Foundation to M.H.S., and the US National Science Foundation to M.H.S. and A.M.

Acknowledgements. Carina Rasmussen isolated melanosomes from a zebra obliquidens. Ola Gustafsson assisted during the SEM and TEM analyses. Niels Christenson Bonde provided taxonomic information on FUM-N-2268. The micrographs in electronic supplementary material, figure S1, are credited to J. W. Costerton archives, courtesy MSU Center for Biofilm Engineering.

References

1. Briggs DEG, Summons RE. 2014 Ancient biomolecules: their origins, fossilization, and role in revealing the history of life. *Bioessays* **36**, 482–490. (doi:10.1002/bies.201400010)
2. Wuttke M. 1983 'Weichteil-Erhaltung' durch lithifizierte Mikroorganismen bei mittel-eozänen Vertebraten aus den Ölschiefern der 'Grube Messel' bei Darmstadt. *Senck. Leth.* **64**, 509–527.
3. Franzen JL. 1985 Exceptional preservation of Eocene vertebrates in the lake deposit of Grube Messel (West Germany). *Phil. Trans. R. Soc. Lond. B* **311**, 181–186. (doi:10.1098/rstb.1985.0150)
4. Davis PG, Briggs DEG. 1995 Fossilization of feathers. *Geology* **23**, 783–786. (doi:10.1130/0091-7613(1995)023<0783:FOF>2.3.CO;2)
5. Toporski JKW, Steele A, Westall F, Avci R, Martill DM, McKay DS. 2002 Morphologic and spectral investigation of exceptionally well-preserved bacterial biofilms from the Oligocene Enspel formation, Germany. *Geochim. Cosmochim. Acta* **66**, 1773–1791. (doi:10.1016/S0016-7037(01)00870-5)
6. Voigt E. 1988 Preservation of soft tissues in the Eocene lignite of the Geiseltal near Halle/S. *Cour. Forsch. Inst. Senck.* **107**, 325–343.
7. Vinther J, Briggs DEG, Prum RO, Saranathan V. 2008 The colour of fossil feathers. *Biol. Lett.* **4**, 522–525. (doi:10.1098/rsbl.2008.0302)
8. Li Q, Gao K-Q, Vinther J, Shawkey MD, Clarke JA, D'Alba L, Meng Q, Briggs DEG, Prum RO. 2010 Plumage color patterns of an extinct dinosaur. *Science* **327**, 1369–1372. (doi:10.1126/science.1186290)
9. Li Q *et al.* 2012 Reconstruction of *Microraptor* and the evolution of iridescent plumage. *Science* **335**, 1215–1219. (doi:10.1126/science.1213780)
10. Li Q, Clarke JA, Gao K-Q, Zhou C-F, Meng Q, Li D, D'Alba L, Shawkey MD. 2014 Melanosome evolution indicates a key physiological shift within feathered dinosaurs. *Nature* **507**, 350–353. (doi:10.1038/nature12973)
11. Edwards NP, Manning PL, Wogelius RA. 2014 Pigments through time. *Pigment Cell Melanoma Res.* **27**, 684–685. (doi:10.1111/pcmr.12271)
12. Moyer AE, Zheng W, Johnson EA, Lamanna MC, Li D-Q, Lacovara KJ, Schweitzer MH. 2014 Melanosomes or microbes: testing an alternative hypothesis for the origin of microbodies in fossil feathers. *Sci. Rep.* **4**, 4233. (doi:10.1038/srep04233)
13. Knight TK, Bingham PS, Lewis RD, Savrda CE. 2011 Feathers of the Ingersoll Shale, Eutaw Formation (Upper Cretaceous), eastern Alabama: the largest collection of feathers from North American Mesozoic rocks. *Palaios* **26**, 364–376. (doi:10.2110/palo.2010.p10-091r)
14. Barden HE, Wogelius RA, Li D, Manning PL, Edwards NP, van Dongen BE. 2011 Morphological and geochemical evidence of eumelanin preservation in the feathers of the Early Cretaceous bird, *Gansus yumenensis*. *PLoS ONE* **6**, e25494. (doi:10.1371/journal.pone.0025494)
15. Pacton M, Fiet N, Gorin G. 2006 Revisiting amorphous organic matter in Kimmeridgian laminites: what is the role of the vulcanization process in the amorphization of organic matter? *Terra Nova* **18**, 380–387. (doi:10.1111/j.1365-3121.2006.00702.x)
16. Preston LJ, Shuster J, Fernández-Remolar D, Banjerjee NR, Osinski GR, Southam G. 2011 The preservation and degradation of filamentous bacteria and biomolecules within iron oxide deposits at Rio Tinto, Spain. *Geobiology* **9**, 233–249. (doi:10.1111/j.1472-4669.2011.00275.x)
17. Westall F. 1999 The nature of fossil bacteria: a guide to the search for extraterrestrial life. *J. Geophys. Res.* **104**, 16 437–16 451. (doi:10.1029/1998JE900051)
18. Plonka PM, Grabacka M. 2006 Melanin synthesis in microorganisms—biotechnological and medical aspects. *Acta Biochim. Polon.* **53**, 429–443.
19. Gospodaryov D, Lushchak V. 2011 Some properties of melanin produced by *Azotobacter chroococcum* and its possible application in biotechnology. *Biotechnol. Acta* **4**, 61–69.
20. Beimforde C, Schäfer N, Dörfelt H, Nascimbene PC, Singh H, Heinrichs J, Reitner J, Rana RS, Schmidt AR. 2011 Ectomycorrhizas from a lower Eocene angiosperm forest. *New Phytol.* **192**, 988–996. (doi:10.1111/j.1469-8137.2011.03868.x)
21. Liu Y, Hong L, Wakamatsu K, Ito S, Adhyaru B, Cheng C-Y, Bowers CR, Simon JD. 2005 Comparisons of the structural and chemical properties of black and red human hair melanosomes. *Photochem. Photobiol.* **81**, 135–144. (doi:10.1562/2004-08-03-RA-259.1)
22. Simon JD, Peles DN. 2010 The red and the black. *Acc. Chem. Res.* **43**, 1452–1460. (doi:10.1021/ar100079y)
23. Zareba M, Szewczyk G, Sarna T, Hong L, Simon JD, Henry MM, Burke JM. 2006 Effects of photodegradation on the physical and antioxidant properties of melanosomes isolated from retinal pigment epithelium. *Photochem. Photobiol.* **82**, 1024–1029. (doi:10.1562/2006-03-08-RA-836)
24. Lopes VS, Wasmeier C, Seabra MC, Futter CE. 2007 Melanosome maturation defect in Rab38-deficient retinal pigment epithelium results in instability of immature melanosomes during transient melanogenesis. *Mol. Biol. Cell* **18**, 3914–3927. (doi:10.1091/mbc.E07-03-0268)
25. Riley PA. 1997 Melanin. *Int. J. Biochem. Cell Biol.* **29**, 1235–1239. (doi:10.1016/S1357-2725(97)00013-7)
26. Kaxiras E, Tsolakidis A, Zonios G, Meng S. 2006 Structural model of eumelanin. *Phys. Rev. Lett.* **97**, 218102-1–218102-4. (doi:10.1103/PhysRevLett.97.218102)
27. Banerjee A, Supakar S, Banerjee R. 2014 Melanin from the nitrogen-fixing bacterium *Azotobacter chroococcum*: a spectroscopic characterization. *PLoS ONE* **9**, e84574. (doi:10.1371/journal.pone.0084574)
28. Simon JD, Hong L, Peles DN. 2008 Insights into melanosomes and melanin from some interesting spatial and temporal properties. *J. Phys. Chem. B.* **112**, 13 201–13 217. (doi:10.1021/jp804248h)
29. Wasmeier C, Hume AN, Bolasco G, Seabra MC. 2008 Melanosomes at a glance. *J. Cell Sci.* **121**, 3995–3999. (doi:10.1242/jcs.040667)
30. Dubey S, Roulin A. 2014 Evolutionary and biomedical consequences of internal melanins. *Pigment Cell Melanoma Res.* **27**, 327–338. (doi:10.1111/pcmr.12231)
31. Broekhuyse RM, Kuhlmann ED, Winkens HJ. 1993 Experimental autoimmune anterior uveitis (EAAU). III. Induction by immunization with purified uveal and skin melanins. *Exp. Eye Res.* **56**, 575–583. (doi:10.1006/exer.1993.1071)
32. Chen KG, Leapman RD, Zhang G, Lai B, Valencia JC, Cardarelli CO, Vieira WD, Hearing VJ, Gottesman MM. 2009 Influence of melanosome dynamics on melanoma drug sensitivity. *J. Natl. Cancer Inst.* **101**, 1259–1271. (doi:10.1093/jnci/djp259)
33. Ortolani-Machado CF, Freitas PF, Faraco CD. 2009 Melanogenesis in dermal melanocytes of Japanese silky chicken embryos. *Tissue Cell* **41**, 239–248. (doi:10.1016/j.tice.2008.11.005)
34. Liu Y, Simon JD. 2003 Isolation and biophysical studies of natural eumelanins: applications of imaging technologies and ultrafast spectroscopy. *Pigment Cell Res.* **16**, 606–618. (doi:10.1046/j.1600-0749.2003.00098.x)
35. Akazaki S *et al.* 2014 Three-dimensional analysis of melanosomes isolated from B16 melanoma cells by using ultra high voltage electron microscopy. *Microsc. Res.* **2**, 1–8. (doi:10.4236/mr.2014.21001)
36. Liu Y, Kempf VR, Nofsinger JB, Weinert EE, Rudnicki M, Wakamatsu K, Ito S, Simon JD. 2003 Comparisons of the structural and chemical properties of human hair eumelanin following enzymatic and acid/base extraction. *Pigment Cell Res.* **16**, 355–365. (doi:10.1034/j.1600-0749.2003.00059.x)
37. Peles DN, Hong L, Hu D-N, Ito S, Nemanich RJ, Simon JD. 2009 Human iridal stroma melanosomes

of varying pheomelanin contents possess a common eumelanic outer surface. *J. Phys. Chem. B* **113**, 11 346–11 351. (doi:10.1021/jp904138n)

38. Agrup G, Hansson C, Rorsman H, Rosengren E. 1982 The effect of cysteine on oxidation of tyrosine, dopa, and cysteinyldopas. *Arch. Dermatol. Res.* **272**, 103–115. (doi:10.1007/BF00510400)
39. Gorniak T *et al.* 2014 Support and challenges to the melanosomal casing model based on nanoscale distribution of metals within iris melanosomes detected by X-ray fluorescence analysis. *Pigment Cell Melanoma Res.* **27**, 831–834. (doi:10.1111/pcmr.12278)
40. Solano F. 2014 Melanins: skin pigments and much more—types, structural models, biological functions, and formation routes. *N. J. Sci.* **2014**, 498276. (doi:10.1155/2014/498276)
41. Romero-Martinez R, Wheeler M, Guerrero-Plata A, Rico G, Torres-Guerrero H. 2000 Biosynthesis and functions of melanin in *Sporothix schenckii*. *Inf. Immunol.* **68**, 3696–3703. (doi:10.1128/IAI.68.6.3696-3703.2000)
42. Kizil'shtein LY, Shpitsgluz AL. 2014 The structure of fossil fungal spores based on the results of ion etching. *Solid Fuel Chem.* **48**, 81–84. (doi:10.3103/S0361521914020062)
43. Alviano CS, Farbiarz SR, de Souza W, Angluster J, Travassos LR. 1991 Characterization of *Fonsecaea pedrosoi* melanin. *J. Gen. Microbiol.* **137**, 837–844. (doi:10.1099/00221287-137-4-837)
44. Eisenman HC, Nosanchuk JD, Webber JBW, Emerson RJ, Camesano TA, Casadevall A. 2005 Microstructure of cell wall-associated melanin in the human pathogenic fungus *Cryptococcus neoformans*. *Biochemistry* **44**, 3683–3693. (doi:10.1021/bi047731m)
45. Nosanchuk JD, Casadevall A. 2003 The contribution of melanin to microbial pathogenesis. *Cell. Microbiol.* **5**, 203–223. (doi:10.1046/j.1462-5814.2003.00268.x)
46. Tarangini K, Mishra S. 2013 Production, characterization and analysis of melanin from isolated marine *Pseudomonas* sp. using vegetable waste. *Res. J. Eng. Sci.* **2**, 40–46.
47. Agodi A, Stefani S, Corsaro C, Camparile F, Gribaldo S, Sichel G. 1996 Study of melanic pigment of *Proteus mirabilis*. *Res. Microbiol.* **147**, 167–174. (doi:10.1016/0923-2508(96)80216-6)
48. Geng J, Yuan P, Shao C, Yu S-B, Zhou B, Zhou P, Chen X-D. 2010 Bacterial melanin interacts with double-stranded DNA with high affinity and may inhibit cell metabolism *in vivo*. *Arch. Microbiol.* **192**, 321–329. (doi:10.1007/s00203-010-0560-1)
49. McKenney PT, Driks A, Eichenberger P. 2013 The *Bacillus subtilis* endospore: assembly and functions of the multilayered coat. *Nat. Rev. Microbiol.* **11**, 33–44. (doi:10.1038/nrmicro2921)
50. Voigt E. 1936 Über das Haarkleid einiger Säugetiere aus der mitteleozänen Braunkohle des Geiseltales. *Nova Acta Leopoldina* **4**, 317–334.
51. Beyermann K, Hasenmaier D. 1973 Identifizierung 180 Millionen Jahre alten, wharscheinlich unverändert erhaltenen Melanins. *Zeitschrift Anal. Chem.* **266**, 202–205. (doi:10.1007/BF00428061)
52. Vinther J, Briggs DEG, Clarke J, Mayr G, Prum RO. 2010 Structural coloration in a fossil feather. *Biol. Lett.* **6**, 128–131. (doi:10.1098/rsbl.2009.0524)
53. Zhang F, Kearns SL, Orr PJ, Benton MJ, Zhou Z, Johnson D, Xu X, Wang X. 2010 Fossilized melanosomes and the colour of Cretaceous dinosaurs and birds. *Nature* **463**, 1075–1078. (doi:10.1038/nature08740)
54. Carney RM, Vinther J, Shawkey MD, D'Alba L, Ackermann J. 2012 New evidence on the colour and nature of the isolated *Archaeopteryx* feather. *Nat. Commun.* **3**, 637. (doi:10.1038/ncomms1642)
55. Manning PL *et al.* 2013 Synchrotron-based chemical imaging reveals plumage patterns in a 150 million year old early bird. *J. Anal. At. Spectrom.* **28**, 1024–1030. (doi:10.1039/c3ja50077b)
56. Lindgren J *et al.* 2014 Skin pigmentation provides evidence of convergent melanism in extinct marine reptiles. *Nature* **506**, 484–488. (doi:10.1038/nature12899)
57. Vinther J. 2015 A guide to the field of palaeo colour: melanin and other pigments can fossilise: reconstructing colour patterns from ancient organisms can give new insights to ecology and behaviour. *Bioessays* **37**, 643–656. (doi:10.1002/bies.201500018)
58. Schweitzer MH. 2011 Soft tissue preservation in terrestrial Mesozoic vertebrates. *Annu. Rev. Earth Planet. Sci.* **39**, 187–216. (doi:10.1146/annurev-earth-040610-133502)
59. Glass K *et al.* 2012 Direct chemical evidence for eumelanin pigment from the Jurassic period. *Proc. Natl Acad. Sci. USA* **109**, 10 218–10 223. (doi:10.1073/pnas.1118448109)
60. Glass K *et al.* 2013 Impact of diagenesis and maturation on the survival of eumelanin in the fossil record. *Org. Geochem.* **64**, 29–37. (doi:10.1016/j.orggeochem.2013.09.002)
61. Lindgren J, Uvdal P, Sjövall P, Nilsson DE, Engdahl A, Schultz BP, Thiel V. 2012 Molecular preservation of the pigment melanin in fossil melanosomes. *Nat. Commun.* **3**, 824. (doi:10.1038/ncomms1819)
62. Clarke JA, Ksepka DT, Salas-Gismondi R, Altamirano AJ, Shawkey MD, D'Alba L, Vinther J, DeVries TJ, Baby P. 2010 Fossil evidence for evolution of the shape and color of penguin feathers. *Science* **330**, 954–957. (doi:10.1126/science.1193604)
63. Barden HE, Bergmann U, Edwards NP, Egerton VM, Manning PL, Perry S, van Veelen A, Wogelius RA, van Dongen BE. 2015 Bacteria or melanosomes? A geochemical analysis of micro-bodies on a tadpole from the Oligocene Enspel Formation of Germany. *Palaeobio. Palaeoenv.* **95**, 33–45. (doi:10.1007/s12549-014-0177-5)
64. Wogelius RA *et al.* 2011 Trace metals as biomarkers for eumelanin pigment in the fossil record. *Science* **333**, 1622–1626. (doi:10.1126/science.1205748)
65. Egerton VM *et al.* 2015 The mapping and differentiation of biological and environmental signatures in the fossil remains of a 50 million year old bird. *J. Anal. At. Spectrom.* **30**, 627–634. (doi:10.1039/C4JA00395K)
66. Borovanský J, Elleder M. 2003 Melanosome degradation: fact or fiction. *Pigment Cell Res.* **16**, 280–286. (doi:10.1034/j.1600-0749.2003.00040.x)
67. Ohtaki N, Seiji M. 1971 Degradation of melanosomes by lysosomes. *J. Invest. Dermatol.* **57**, 1–5. (doi:10.1111/1523-1747.ep12292038)
68. Borovanský J, Hach P, Duchoň J. 1977 Melanosome: an unusually resistant subcellular particle. *Cell Biol. Int. Rep.* **1**, 549–554. (doi:10.1016/0309-1651(77)90093-5)
69. Goldstein G, Flory KR, Browne BA, Majid S, Ichida JM, Burtt Jr EH. 2004 Bacterial degradation of black and white feathers. *Auk* **121**, 656–659. (doi:10.1642/0004-8038(2004)121[0656:BDOBAW]2.0.CO;2)
70. Keefe JR. 1973 An analysis of urodelian retinal regeneration: III. Degradation of extruded melanin granules in *Notophthalmus viridescens*. *J. Exp. Zool.* **184**, 233–237. (doi:10.1002/jez.1401840208)
71. Kordylewski L. 1983 An ultrastructural study of the melanophages in the cerebrospinal fluid of the tadpoles of *Xenopus*. *J. Morph.* **176**, 315–324. (doi:10.1002/jmor.1051760305)
72. Gunderson AR, Frame AM, Swaddle JP, Forsyth MH. 2008 Resistance of melanized feathers to bacterial degradation: is it really so black and white? *J. Avian Biol.* **39**, 539–545. (doi:10.1111/j.0908-8857.2008.04413.x)
73. Jawor JM, Breitwisch R. 2003 Melanin ornaments, honesty, and sexual selection. *Auk* **120**, 249–265. (doi:10.1642/0004-8038(2003)120[0249:MOHASS]2.0.CO;2)
74. McGraw KJ. 2008 An update on the honesty of melanin-based color signals in birds. *Pigment Cell Melanoma Res.* **21**, 133–138. (doi:10.1111/j.1755-148X.2008.00454.x)
75. McNamara ME, Briggs DEG, Orr PJ, Field DJ, Wang Z. 2013 Experimental maturation of feathers: implications for reconstructions of fossil feather colour. *Biol. Lett.* **9**, 20130184. (doi:10.1098/rsbl.2013.0184)
76. Liu Y, Hong L, Wakamatsu K, Ito S, Adhyaru BB, Cheng C-Y, Bowers CR, Simon JD. 2005 Comparisons of the structural and chemical properties of melanosomes isolated from retinal pigment epithelium, iris and choroid of newborn and mature bovine eyes. *Photochem. Photobiol.* **81**, 510–516. (doi:10.1562/2004-10-19-RA-345.1)
77. Tanaka G *et al.* 2014 Mineralized rods and cones suggest colour vision in a 300 Myr-old fossil fish. *Nat. Commun.* **5**, 5920. (doi:10.1038/ncomms6920)
78. Liu SY, Shawkey MD, Parkinson D, Troy TP, Ahmed M. 2014 Elucidation of the chemical composition of avian melanin. *RSC Adv.* **4**, 40 396–40 399. (doi:10.1039/C4RA06606E)
79. Sergeev VN, Knoll AH, Grotzinger JP. 1995 Paleobiology of the Mesoproterozoic Billyakh Group, Anabar Uplift, northern Siberia. *Paleontol. Soc. Mem.* **1995**, 1–37.
80. Igisu M, Ueno Y, Shimojima M, Nakashima S, Awramik SM, Ohta H, Maruyama S. 2009 Micro-FTIR spectroscopic signatures of bacterial lipids in

Proterozoic microfossils. *Precambrian Res.* **173**, 19–26. (doi:10.1016/j.precamres.2009.03.006)

81. Pfeiffer CJ, Jones FM. 1993 Epidermal lipid in several cetacean species: ultrastructural observations. *Anat. Embryol.* **188**, 209–218. (doi:10.1007/BF00188213)
82. Eliason CM, Bitton P-P, Shawkey MD. 2013 How hollow melanosomes affect iridescent colour production in birds. *Proc. R. Soc. B* **280**, 20131505. (doi:10.1098/rspb.2013.1505)
83. Hitchcock AP, Dynes JJ, Lawrence JR, Obst M, Swerhone GDW, Korber DR, Leppard GG. 2009 Soft X-ray spectromicroscopy of nickel sorption in a natural river biofilm. *Geobiology* **7**, 432–453. (doi:10.1111/j.1472-4669.2009.00211.x)
84. Choi DW *et al.* 2006 Spectral, kinetic, and thermodynamic properties of Cu(I) and Cu(II) binding by methanobactin from *Methylosinus trichosporium* OB3b. *Biochemistry* **45**, 1442–1453. (doi:10.1021/bi051815t)
85. Choi DW *et al.* 2006 Spectral and thermodynamic properties of Ag(I), Au(III), Cd(II), Co(II), Fe(III), Hg(II), Mn(II), Ni(II), Pb(II), U(IV), and Zn(II) binding by methanobactin from *Methylosinus trichosporium* OB3b. *J. Inorg. Biochem.* **100**, 2150–2161. (doi:10.1016/j.jinorgbio.2006.08.017)
86. Gupta R, Ramnani P. 2006 Microbial keratinases and their prospective applications: an overview. *Appl. Microbiol. Biotechol.* **70**, 21–33. (doi:10.1007/s00253-005-0239-8)
87. Kühl M, Jørgensen BB. 1992 Microsensor measurements of sulfate reduction and sulfide oxidation in compact microbial communities of aerobic biofilms. *Appl. Environ. Microbiol.* **58**, 1164–1174.
88. Zang Q-X, Lu R-W, Messinger JD, Curcio CA, Guarcello V, Yao X-C. 2013 *In vivo* optical coherence tomography of light-driven melanosome translocation in retinal pigment epithelium. *Sci. Rep.* **3**, 2644.
89. Kim IT, Choi JB. 1998 Melanosomes of retinal pigment epithelium—distribution, shape, and acid phosphatase activity. *Korean J. Ophthalmol.* **12**, 85–91. (doi:10.3341/kjo.1998.12.2.85)

Electronic supplementary material

Interpreting melanin-based colouration through deep time: a critical review

Johan Lindgren[1], Alison Moyer[2], Mary H. Schweitzer[2,3], Peter Sjövall[4], Per Uvdal[5,6], Jimmy Heimdal[5], Anders Engdahl[5], Dan E. Nilsson[7], Johan A. Gren[1], Bo Pagh Schultz[8] and Benjamin P. Kear[9,10]

[1]Department of Geology, Lund University, 223 62 Lund, Sweden

[2]Department of Biological Sciences, North Carolina State University, Raleigh, NC 27695, USA

[3]North Carolina Museum of Natural Sciences, Raleigh, NC 27601, USA

[4]SP Technical Research Institute of Sweden, Chemistry, Materials and Surfaces, 501 15 Borås, Sweden

[5]MAX-IV laboratory, Lund University, 221 00 Lund, Sweden

[6]Chemical Physics, Department of Chemistry, Lund University, 221 00 Lund, Sweden

[7]Department of Biology, Lund University, 223 62 Lund, Sweden

[8]MUSERUM, Natural History Division, 7800 Skive, Denmark

[9]Museum of Evolution, Uppsala University, 752 36 Uppsala, Sweden

[10]Palaeobiology Programme, Department of Earth Sciences, Uppsala University, 752 36 Uppsala, Sweden

Author for correspondence: Johan Lindgren e-mail: johan.lindgren@geol.lu.se

Supplementary methods

(a) Specimen details and reference materials

To test our integrated approach, we selected a skeletally incomplete fossil Pipefish (Syngnathiformes; see Bonde [1] for systematics) collected from the Stolle Klint sea-cliffs on the Isle of Fur, in the Limfjord region of Denmark (figure 1*a*). This specimen was recovered and prepared without preservatives or consolidants. Its derivation from a siliceous mudstone interval between the Stolle Klint Clay (Ølst Formation) and Fur Formation constrains an early Eocene age (see Heilmann-Clausen *et al.* [2] for details). The fossil comprises both part (FUM-N-2268A; MUSERUM) and counterpart (FUM-N-2268B), and is 19 mm in maximum length. A localised brownish pigmentation (2.7 × 1.8 mm) is present within the orbital region of the skull (figure 1*a*,*b*). No other soft tissue traces are preserved.

As a comparative data set, analyses were undertaken on synthetic and natural variants of eumelanin, pheomelanin, several porphyrins, and three microbial mats (see details in Lindgren *et al.* [3,4]). We also examined a pyomelanin chemically derived via auto-oxidation of homogentisic acid (HGA; see Turick *et al.* [5] for methodology), as well as isolated melanosomes from the eyes of a teleost fish, Zebra obliquidens (*Astatotilapia latifasciata*).

(b) Scanning electron microscopy (SEM)

A small microbody sample was removed from the orbital pigment residue of FUM-N-2268 using a sterile scalpel. Basic elemental composition was determined via elemental mapping (1900 sec scanning time at 15 keV, 62.0 µA, 10 mm working distance) on a Hitachi S-3400N SEM. A similarly prepared sample was first subjected to ToF-SIMS analysis (see below). It was then coated with a ~ 15 nm thick layer of gold/palladium and examined on a Zeiss Supra 40VP FEG-

SEM (2 keV, 3–5 mm working distance. Everhart-Thornley secondary electron detector). To test the possible effects of diagenetic processes on morphology and distribution, comparative retinal melanosomes were isolated from a male Zebra obliquidens (methodology after Liu *et al.* [6]) and sputter-coated with gold for examination using a Hitachi SU3500 SEM.

(c) Transmission electron microscopy (TEM)

A small sample from FUM-N-2268 was embedded in EPON (Agar Scientific) for ultrathin sectioning (50 nm) in a Leica Ultracut UCT ultratome equipped with a glass knife. Sections were then mounted on copper grids and examined without staining at 80 kV in a JEOL JEM-1230 TEM.

(d) Time-of-flight secondary ion mass spectrometry (ToF-SIMS)

ToF-SIMS is a vacuum-based surface analysis technique that provides mass spectrometric data of the molecular content on sample surfaces. During analysis, a focussed beam of high-energy (primary) ions bombards the sample surface, which results in the emission of atoms, molecular fragments and intact molecules in the mass range up to 2000–3000 Da. The ionised fraction of the emitted particles is extracted into in a time-of-flight mass analyser, thereby producing mass spectra which provide detailed molecular information pertaining to the investigated surface. Furthermore, the spatial distribution of specific molecular components can be imaged by scanning the primary ion beam over the sample surface while simultaneously monitoring the signal intensity of selected ions representing compounds of interest. Although the signal intensity generally reflects the surface concentration of the monitored compounds, it may also depend on other factors, such as the chemical environment of the molecular components and topography of

93 the sample. These factors can complicate analyses, particularly those involving geological
94 samples, such as the fossil microbodies examined herein. For a more comprehensive discussion
95 regarding the utility of ToF-SIMS analysis in geoscience, see Thiel & Sjövall [7].
96 For this study, microbodies were removed from the orbital pigment residue of FUM-N-
97 2268 using a sterile scalpel and placed on double-sided tape. ToF-SIMS analyses in the static
98 SIMS mode were performed on a ToF-SIMS IV instrument (IONTOF GmbH) using 25 keV Bi_3^+
99 primary ions and low energy electron flooding for charge compensation (technique follows
100 Lindgren *et al.* [3,4]). High mass resolution data ($m/\Delta m \sim 5000$) were acquired at a spatial
101 resolution of ~ 3–4 µm, while high image resolution data (spatial resolution ~ 0.2–0.5 µm) were
102 obtained at a mass resolution of $m/\Delta m \sim 300$ (256 × 256 pixels in both cases). Because the
103 positive ion spectra showed strong interference from the sedimentary matrix signal, only
104 negative ion data were selected for presentation.
105
106 **(e) Infrared (IR) microspectroscopy**
107 Fossil microbodies, together with bone samples and sedimentary matrix were removed from
108 FUM-N-2268 using a sterile scalpel and placed on CaF_2 spectrophotometric windows (see details
109 in Lindgren *et al.* [3]). Infrared microspectroscopy was performed at the beamline D7, MAX-IV
110 laboratory, Lund University. This set-up combines a Hyperion 3000 microscope with a Bruker
111 IFS66/v FTIR spectrometer. The microscope was operated in transmission mode using a ×15
112 objective and apertures ranging from 20 × 20 to 170 × 170 µm.
113
114 **(f) Additional information on molecular analyses**

ToF-SIMS analysis yielded mass spectra consistent with those of synthetic and natural eumelanin standards (figure 2 and electronic supplementary material, figures S2–S4). Importantly, all major peaks in the eumelanin spectra were reproduced in the fossil spectra (including distinct peaks at 50, 66, 73, 74, 121, 122, 145, and 146 u), both with regard to relative intensity distribution (figure 2 and electronic supplementary material, figure S4) and precise mass position (electronic supplementary material, figure S2). Deviations represented ionic components of the sedimentary matrix (including phosphate and sulfate), as well as iron sulfate and sulfur-containing organics (figure 2 and electronic supplementary material, figure S2). The latter suggest possible diagenetic incorporation of sulfur into the melanin macromolecule [3,4], or alternatively the presence of small amounts of pheomelanin. High-resolution images of 'characteristic' ions representing different molecular compounds revealed that eumelanin was co-localised with sulfur-containing organics but also with sulfate, whereas silicate showed a complementary spatial distribution (electronic supplementary material, figure S5).

Further comparisons were made with natural pheomelanin (see Lindgren *et al.* [4] for details) and synthetic pyo- (HGA) melanin (electronic supplementary material, figures S2–S4). These evidenced a noticeable deviation of the pheomelanin spectrum from those of eumelanin and the fossil microbodies (particularly in the mass region above 100 u). There was also strong signal intensity in the pheomelanin spectrum from sulfur-containing fragment ions at 58 and 82 u (these were present only at low intensities in the fossil spectra). The observed pyomelanin spectrum, on the other hand, was similar to that of eumelanin (electronic supplementary material, figures S3,S4). However, since the molecular structure of HGA melanin is devoid of nitrogen [5], fragment ions containing this element are conspicuously absent from the pyomelanin spectrum (note weak signals at 50, 66, 74, 90, 122 and 146 u; electronic supplementary material,

138 figures S2*a*,S4). We therefore conclude that the strong signal intensity from nitrogen-containing
139 fragment ions in the fossil spectra likely indicates eumelanin as the primary organic constituent
140 of the microbody surfaces in the orbital pigment residue of FUM-N-2268.

141 This interpretation was further corroborated by IR microspectroscopic measurements,
142 which produced broad-band absorbance in the 900–1800 and 2500–3700 cm^{-1} regions, consistent
143 with natural eumelanin. In contrast, the pyomelanin spectrum manifested narrower and sharper
144 absorption bands in the 1300 1800 cm^{-1} region (electronic supplementary material, figure S6).
145
146
147
148
149
150
151
152
153
154
155
156
157
158
159
160

Supplementary figures

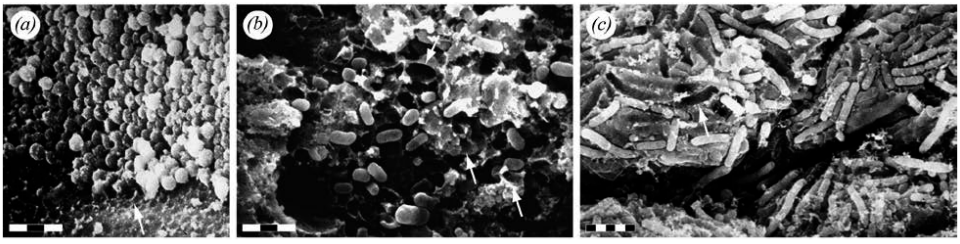

Supplementary figure S1. SEM micrographs of extant microbial biofilms, showing (*a*) spherical (*Staphylococcus aureus*), (*b*) rod-shaped (coccobacilli) and (*c*) elongate (*Proteus vulgaris*) bacteria. Note extensive EPS and distinct cellular imprints (arrows). The images are modified from Marrie *et al*. [8]: fig. 3 and Costerton *et al*. [9]: fig. 1c, and are republished with permission. Scale bars: (*a*,*b*) 3 μm; (*c*) 5 μm.

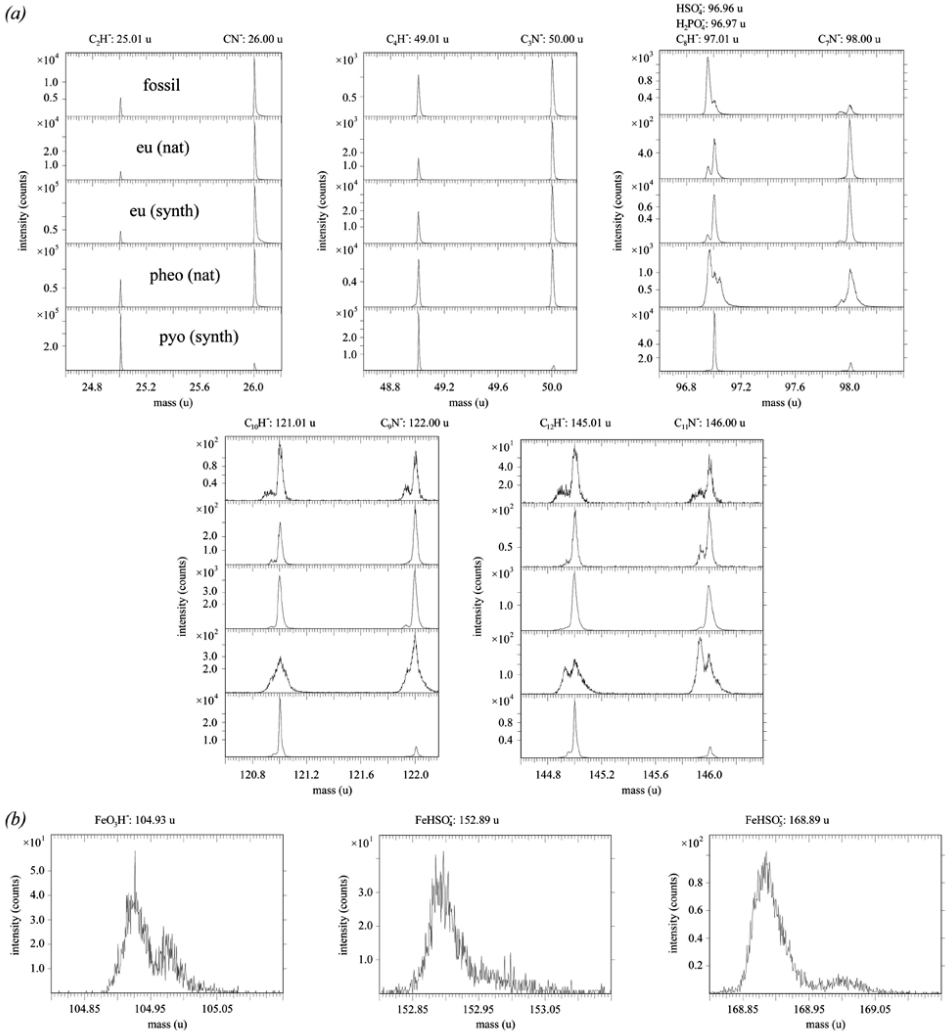

172

173 **Supplementary figure S2.** Peaks selected from a negative ion ToF-SIMS spectrum collected
174 from microbodies located within the 'eye spot' of FUM-N-2268 (recorded at high mass
175 resolution) representing (*a*) characteristic eumelanin and (*b*) iron-containing inorganic ions. The
176 assignment of each peak is indicated at the top of each panel together with the theoretical mass
177 of respective ion. In (*a*) the fossil microbody spectrum ('fossil' – top spectrum in all panels) is

presented together with spectra from natural ['eu (nat)'] and synthetic ['eu (synth)] eumelanin, natural pheomelanin ['pheo (nat)'], and synthetic pyomelanin ['pyo (synth)'] standards, respectively. Note the prominent sulfate peak in the fossil spectrum at 96.96 u, probably originating from sedimentary matrix (see also figure 2).

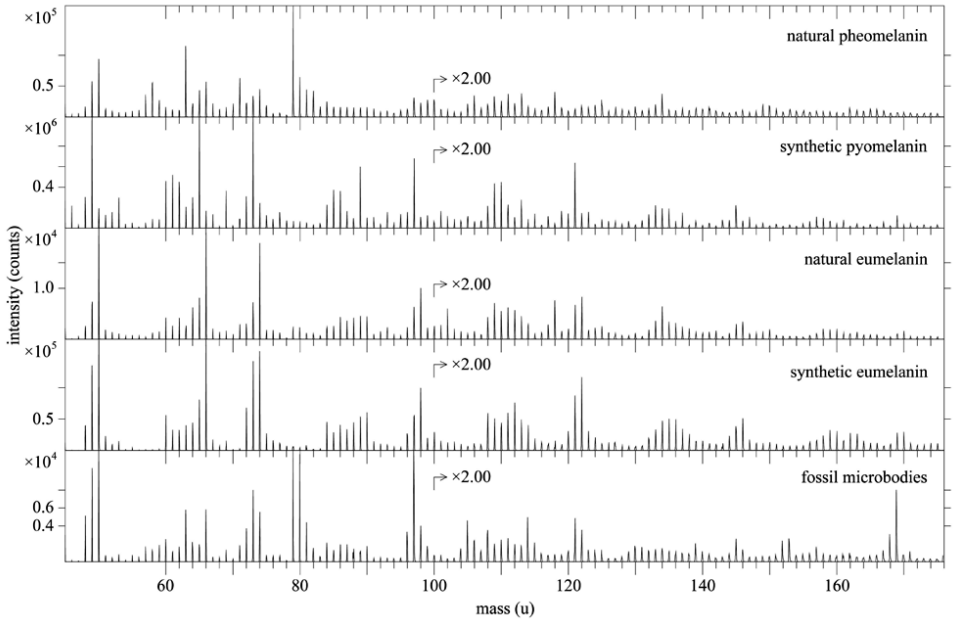

Supplementary figure S3. Negative ion ToF-SIMS spectra acquired from a natural pheomelanin sample (see Lindgren *et al*. [4] for details), pyomelanin synthesised from homogentisic acid, natural eumelanin from *Sepia officinalis*, synthetic eumelanin, and microbodies collected from the 'eye spot' of FUM-N-2268 (see also electronic supplementary material, figure S4).

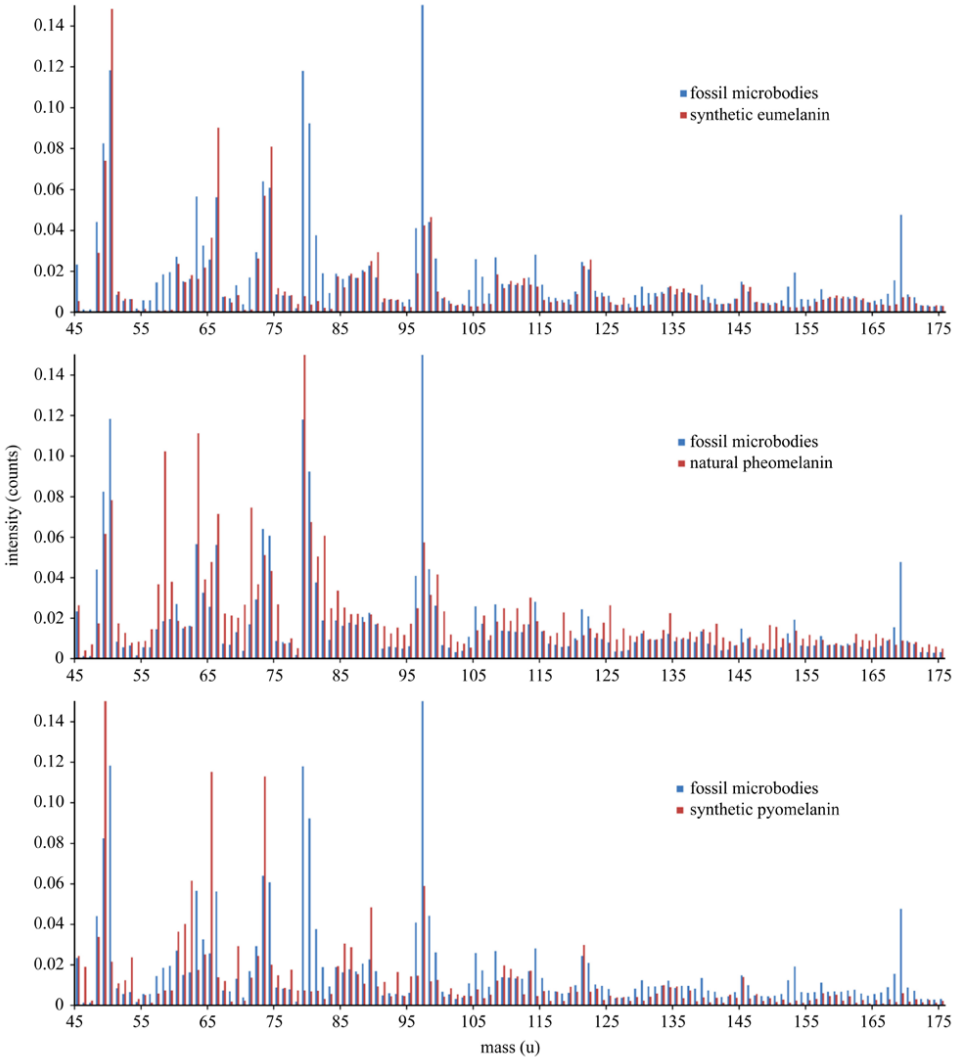

189

190 **Supplementary figure S4.** Negative ion ToF-SIMS spectra obtained from fossil microbodies
191 located within the 'eye spot' of FUM-N-2268 and three different melanin standards; i.e.,
192 synthetic eumelanin (top – same spectrum as in figure 2), natural pheomelanin (centre) and
193 synthetic pyomelanin (bottom). Note detailed agreement between the microbody and synthetic

eumelanin spectra, whereas the two other standards are considerably less compatible with the fossil material. Peaks in the microbody spectrum that are not present in the eumelanin one correspond to inorganic ions (as indicated in figure 2), sulfur-containing organic ions (C_2HS^- at 57 u, CSN^- at 58 u and C_3SN^- at 82 u) and oxygen-containing organic ions ($C_2H_3O_2^-$ at 59 u and $C_3H_3O_2^-$ at 71 u), respectively.

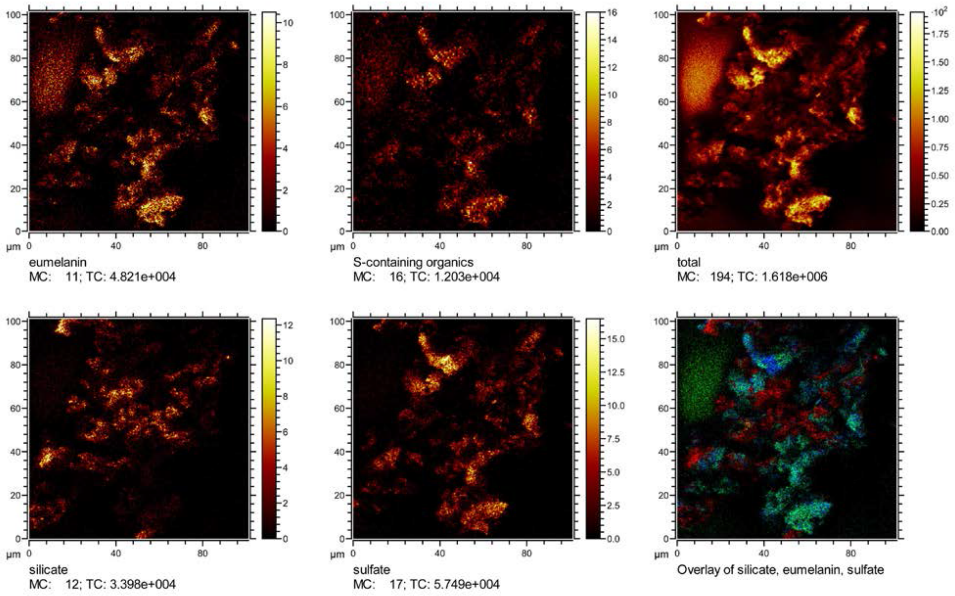

Supplementary figure S5. High-resolution ToF-SIMS images showing different molecular components in a fossil microbody sample taken from the 'eye spot' of FUM-N-2268. The images display the added signal intensity distribution from negative ions representing eumelanin (50 + 66 + 73 + 74 u), sulfur-containing organics (57 + 58 + 82 u), silicate (60 + 76 + 77 u), and sulfate (97 u). The total ion image depicts the added signal intensity from all negative ions in the

sample (the intensity mainly reflects the topography of the investigated surface). The overlay image shows silicate (red), eumelanin (green) and sulfate (blue). Field of view is 100 × 100 µm^2.

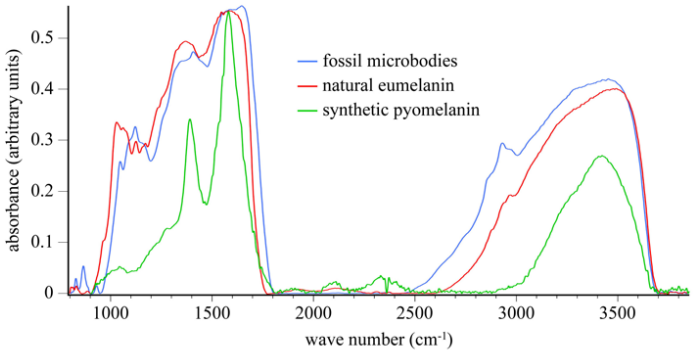

Supplementary figure S6. IR absorbance spectra of microbodies from the 'eye spot' of FUM-N-2268 ('fossil microbodies'), synthetic pyomelanin and natural eumelanin. The spectrum collected from the microbodies exhibits broad-band absorbance in the 900–1800 and 2500–3700 cm^{-1} regions, consistent with the eumelanin standard. The microbody and pyomelanin spectra were recorded in transmission mode using a ×15 objective, a single element (100 × 100 µm) MCT detector and a 40 × 40 (microbody) or a 20 × 20 µm (pyomelanin) aperture. The homogeneous natural eumelanin standard was recorded in off-line mode under identical conditions, although a 170 × 170 µm aperture was used for these measurements.

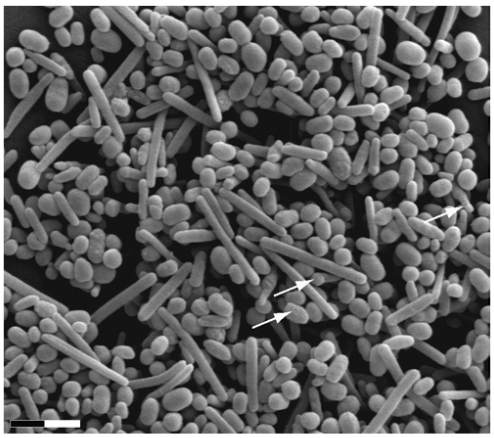

Supplementary figure S7. SEM micrograph of RPE melanosomes isolated from a Zebra obliquidens (*Astatotilapia latifasciata*). Note broad range of morphologies and sizes, random surface pits (arrows) and external nodules on some melanosomes. The organelles were isolated in 2011 and have since been stored at room temperature demonstrating retention of structural integrity even after four years of ambient conditions. Scale bar: 2 μm.

235 **Supplementary references**

236

237 1. Bonde NC. 1987 *Moler – its origin and its fossils, especially fishes*. Nykobing Mors: Morso
238 Bogtrykkeri.
239 2. Heilmann-Clausen C, Nielsen OB, Gersner F. 1985 Lithostratigraphy and depositional
240 environments in the upper Paleocene and Eocene of Denmark. *Bull. Geol. Soc. Denmark*
241 **33**, 287 323.
242 3. Lindgren J, Uvdal P, Sjövall P, Nilsson DE, Engdahl A, Schultz BP, Thiel V. 2012
243 Molecular preservation of the pigment melanin in fossil melanosomes. *Nat. Commun.* **3**,
244 824.
245 4. Lindgren J, Sjövall P, Carney RM, Uvdal P, Gren JA, Dyke G, Schultz BP, Shawkey MD,
246 Barnes KR, Polcyn MJ. 2014 Skin pigmentation provides evidence of convergent melanism
247 in extinct marine reptiles. *Nature* **506**, 484–488.
248 5. Turick CE, Tisa LS, Caccavo F, Jr. 2002 Melanin production and use as a soluble electron
249 shuttle for Fe(III) oxide reduction and as a terminal electron acceptor by *Shewanella algae*
250 BrY. *Appl. Environ. Microbiol.* **68**, 2436–2444.
251 6. Liu Y, Hong L, Wakamatsu K, Ito S, Adhyaru BB, Cheng C-Y, Bowers CR, Simon JD. 2005
252 Comparisons of the structural and chemical properties of melanosomes isolated from
253 retinal pigment epithelium, iris and choroid of newborn and mature bovine eyes.
254 *Photochem. Photobiol.* **81**, 510 516.
255 7. Thiel V, Sjövall P. 2011 Using time-of-flight secondary ion mass spectrometry to study
256 biomarkers. *Annu. Rev. Earth Planet. Sci.* **39**, 125–156.

257 8. Marrie TJ, Nelligan J, Costerton JW. 1982 A scanning and transmission electron microscopic
258 study of an infected endocardial pacemaker lead. *Circulation* **66**, 1339–1341.
259 9. Costerton W, Veeh R, Shirtliff M, Pasmore M, Post C, Ehrlich G. 2003 The application of
260 biofilm science to the study and control of chronic bacterial infections. *J. Clin. Invest.*
261 **112**, 1466–1477.

CHAPTER 4 - Melanosomes and ancient coloration reexamined: A response to Vinther 2015 (DOI 10.1002/bies.201500018)

Insights & Perspectives

Think again

Melanosomes and ancient coloration re-examined: A response to Vinther 2015 (DOI 10.1002/bies.201500018)

Mary H. Schweitzer[1)2)3)], Johan Lindgren[3)] and Alison E. Moyer[1)]*

Round to elongate microbodies associated with fossil vertebrate soft tissues were interpreted as microbial traces until 2008, when they were re-described as remnant melanosomes – intracellular, pigment-containing eukaryotic organelles. Since then, multiple claims for melanosome preservation and inferences of organismal color, behavior, and physiology have been advanced, based upon the shape and size of these microstructures. Here, we re-examine evidence for ancient melanosomes in light of information reviewed in Vinther (2015), and literature regarding the preservation potential of microorganisms and their exopolymeric secretions. We: (i) address statements in Vinther's recent (2015) review that are incorrect or which misrepresent published data; (ii) discuss the need for caution in interpreting "voids" and microbodies associated with degraded fossil soft tissues; (iii) present evidence that microorganisms are in many cases an equally parsimonious source for these "voids" as are remnant melanosomes; and (iv) suggest methods/criteria for differentiating melanosomes from microbial traces in the fossil record.

Keywords:
ancient color; fossil feather; melanin; melanosome; microbe; molecular paleontology; parsimony

DOI 10.1002/bies.201500061

[1)] Department of Biological Sciences, North Carolina State University, Raleigh, NC, USA
[2)] North Carolina Museum of Natural Sciences, Raleigh, NC, USA
[3)] Department of Geology, Lund University, Lund, Sweden

***Corresponding author:**
Mary H. Schweitzer
E-mail: mhschwei@ncsu.edu

Abbreviations:
EPS, exopolymeric substances; **FDB,** feather-degrading bacteria; **SEM,** scanning electron microscopy; **SR,** synchrotron radiation; **TEM,** transmission electron microscopy.

Introduction

The idea that we can somehow detect and determine hues and shades in extinct animals holds great appeal, in part because color is such a vital part of organismal function and ecology. As exciting as this possibility is, however, caution must be applied when inferring organismal color from fossils. This is particularly relevant when interpretations rely solely on the size and shape of minute microbodies posited as melanosomes (eukaryotic, melanin-containing intracellular organelles), or more often, the *impressions* of such bodies in an amorphous and uncharacterized matrix associated with vertebrate fossil remains. Presumed "fossil melanosomes" overlap completely with bacteria in size, shape, and morphology [1]. Moreover, microbes are widely distributed, ubiquitous in natural environments, and *always* associated with decaying organic matter. Bacteria, and the exopolymeric substances (EPS) they secrete, have high preservation potential and, in fact, have been shown to participate directly in processes resulting in "exceptional preservation" of vertebrate soft tissues (such as skin and feathers) in the fossil record [2].

The case for fossil melanosomes, and by extension ancient organismal color, is argued enthusiastically by Jakob Vinther in a recent BioEssays article [3]. However, several points made in this paper require clarifications, and a number of misstatements necessitate corrections. Here, we assess the arguments used by Vinther (and others) first, to identify these microbodies as melanosomes, and second, to propose overall organismal color based upon this identification. Only when all data are accurately presented and all viable hypotheses considered can interpretations of "paleocolor" be presented.

The role of pigments in biology and evolution

Biological pigments (biochromes) are acted upon by natural selection, and there is no doubt that pigmentation has played an important role in vertebrate evolution. Biochromes are produced by

virtually all classes of organisms [4], from bacteria (e.g. [5] and references therein) and fungi [6] to "higher" vertebrates [7–9]. Most pigments are associated with physiological functions other than coloration, and their presence in sediments has been used to trace the origin and radiation of numerous biological processes, such as photosynthesis [10]. Melanin, a ubiquitous biochrome, has photoprotective and antibacterial functions [4]. Intriguingly, some microorganisms produce this biochrome [11, 12], whereas others are efficient at breaking it down to use as a carbon source [6]. Porphyrin, a well-characterized biochrome, forms the functional units of hemoglobin, cytochrome, and chlorophyll; chlorophyll, one of the oldest biochromes [13, 14], is the site of photosynthesis. Thus both pigment groups are vital to the origin and evolution of life [10]. They also have high preservation potential [13], and are well represented in the fossil record [15, 16]. However, porphyrins, including heme, are *not* similar structurally or functionally to melanin, as erroneously stated by Vinther ([3], p. 6), except that both biomolecules bind metal ions. In fact, considering only one parameter, that of absorbance of ultraviolet/visible (UV/Vis) light, melanin absorbance spectra [17] differ greatly from those of porphyrin-containing pigments (e.g. [18]).

Contrary to claims by Vinther [3], the chemical characterization of fossil pigments, including those derived from microbes and/or plants [13], has a robust history. The study of fossil pigments in sedimentary environments began in earnest with work by Treibs in the 1930s [19], was expanded by Blumer [20] and others (e.g. [21]) in the next several decades, and is still ongoing (e.g. [22] and references therein). This field has hardly been "neglected" ([3], p.1); in fact, a cursory literature database search under "fossil pigment" yields hundreds of references from the late 1800s to the present.

What is the preservation potential of melanosomes, and how are they altered through geological time?

In fossil feathers, the size and shape of microbodies ascribed to remnant melanosomes have been used to infer color, physiology and other traits [23, 24], but the potential of melanosomes to retain primary characteristics without alteration has not been rigorously tested (but see [25]). Although melanin pigment is resistant to degradation [26], few data exist to suggest that this resistance confers without change to intracellular organelles containing this biochrome. Vinther's (2015) statement ([3], p. 3) that "organic residues in fossil vertebrates are usually melanin-bearing structures such as integument, eyes, and certain internal organs" ([3], p. 3) may be generally correct, but one could argue that the molecular composition of keratin is at least as important as melanin in preserving epidermally derived structures such as skin, feathers, hair, and claw, because melanin and keratin can co-exist in these tissues. Additionally, this statement ignores digestive tract tissues [27], and blood vessels, osteocytes, and other cell-like components that retain original flexibility and transparency, as well as fibrous bone matrix microscopically and chemically consistent with collagen [28–33]. These are not associated with melanin, but have nonetheless been observed in multiple fossil specimens.

The "fossil melanosome" literature acknowledges that the "voids" associated with fossil feathers are "often larger than the melanosome itself" ([3], p. 5; [34], p. 4). This is accounted for by attributing diagenetic shrinkage to the bodies [3], but equally likely, the voids could have enlarged as a result of variations in temperature and pressure once the bodies were degraded. Size and morphology of melanosomes may also be affected by pH and other environmental factors (e.g. [35] and references therein; [25]). Nonetheless, if melanosomes are more susceptible to diagenetic shrinkage and other artefacts than is the matrix in which they are embedded, it can also be posited that they may be more easily degraded than the matrix as well. This is supported by the identification of primarily voids, not three-dimensional bodies, in many papers reporting fossil feather "melanosomes" (e.g. [23, 36–38]). On the other hand, reports of melanin granules in fossil squid ink sacs [39], and remnant melanosomes in fossil fish "eyes" [40, 41] and "skin" [42] present measurements of grains or bodies, not voids, and can chemically map eumelanin signatures to these microstructures [35, 39, 41, 42]. It should also be noted that these specimens derive from marine environments, where environmental chemistry and ion availability are different from those in non-marine settings, and this may influence preservation.

Chemical characterization of the matrix in which presumed melanosomes are embedded will support their identity

If the microbodies found associated with fossil feathers are melanosomes, then the matrix in which they are embedded should be remnant keratin. On the other hand, if the bodies are microbial in origin, then the matrix should be some type of EPS residue from which diagnostic biomarkers can be derived [43]. Contradicting claims in the fossil melanosome literature, Vinther states that "keratin does not preserve" ([3], p. 6). Nonetheless, in most reports of ancient "melanosomes," published images clearly support the presence of *some* kind of matrix (e.g. [23, 24, 38, 44]). Moreover, "voids" presented as evidence for melanosomes (and thus color) are *stated* to occur in a keratin matrix [24, 45], although no data have been presented to support this conclusion, and tests to identify remnant keratin have not been conducted, to the best of our knowledge. Instead, it is assumed that these voids represent melanosomes; thus the matrix must be keratin. This is circular reasoning. There is no proposed mechanism by which keratin can be replaced with another substance, yet retain "voids" as more accurate representatives of melanosomes than the microbodies themselves ([3], p.1) other than perhaps differential mineralization (i.e. keratin mineralizing more rapidly than do melanosomes), which has not yet been demonstrated for keratin in feathers (but see [46]). However, microbial EPS *does* mineralize rapidly [2, 47–49], and preserves voids within the mineralized matrix once the cells are degraded (see

below). In fact, voids in mineralized matrices of preserved biofilms, virtually identical to what is presented as evidence for some melanosome "voids," are recognized as a "typical" microbial fabric (e.g. [50]).

If both microbodies and matrix are preserved, tests can be conducted to chemically characterize the composition of both. Indeed, published data show that keratin is robust, and its molecular fingerprints can persist into the geological record [51, 52]. In addition to feathers, the presence of many keratin-derived structures in the rock record, including skin [42, 53–56], beak [57], hair [58–60], and claw sheaths [51, 61, 62] (and references therein), as well as ongoing experiments, support this conclusion. If the matrix depicted in association with "melanosomes" can be unambiguously assigned to keratin, and if animal melanin or its degradation products can be localized to the bodies, then any further arguments about their identity would be moot. However, this has not been demonstrated in most fossils where color is imparted to the organism. Additionally, although not conclusive, the relationship between microbodies and fossil feather material could also be addressed in part by TEM (see discussion in [63]), yet fossil "melanosomes" are rarely presented as TEM images, and to our knowledge, TEM is not routinely employed to analyze fossil feather structures (but see [46, 52]).

As some of the paleontologists who "have sought to understand which organic compounds might be preserved in…fossils and how to identify them" ([3], p. 1), we have proposed, described, and utilized many methods by which one could accomplish this task (e.g. [64, 65]), but with few notable exceptions (e.g. [35, 39, 41, 42, 46, 66]) few chemical or molecular methods have been employed by scholars claiming melanosome preservation.

Have melanosomes been robustly differentiated from microbes?

Vinther's claim ([3], p. 6) that "the old bacterial paradigm [has been] put to rest" is not supported by data or the literature, which indeed testifies to the pervasiveness and robustness of microbes in the fossil record. Given the ubiquity of microorganisms in any environment, and in particular, their association with decaying organic matter (including feathers and skin [67, 68]) a microbial hypothesis is still equally parsimonious overall to explain microbodies (and "voids") preserved in association with keratin-derived fossil material. Microbes are among the earliest life forms on earth, with the broadest global distribution ([43] and references therein), and contribute vastly more to earth's biomass than does any other organismal group [69]. Without a doubt, microbes were associated with the remains of decaying dinosaurs, as surely as they are in every environment on earth today. Thus, it is incumbent upon the researcher to show with quantitative data why these microbodies are *not* microbial before advancing other hypotheses. In most cases, this has not been done.

Vinther and others have erroneously focused on the "marked size differences" between microbes and melanosomes ([3], p. 6; [70]). However, microbes and melanosomes completely overlap in both size and shape. The smallest characterized microbes measure ~0.1–0.3 μm [71–73] and the largest, the giant sulfur bacterium *Thiomargarita namibiensis*, measures up to 1 mm [74]; however, most microorganisms average ~1–2 μm [75]. Similarly, melanosomes in vertebrate tissues range in size from "sub-micrometer" [76] to ~4 μm [77]. Furthermore, microbes are pervasive in virtually all environments, including those also associated with melanosomes (e.g. skin and feathers also, see Fig. 2). Hence, size and shape of either voids or microbodies are not conclusive evidence for melanosomes, and do not eliminate microbes as an alternative source for these data.

The statement "there is currently no evidence that bacteria fossilize as isolated three-dimensional bodies… bacteria are known as fossils, but as inclusions in cherts and organic biomarkers" ([3], p. 6) neglects the entire sub-discipline of geomicrobiology. For just a few examples of microbes preserved in three dimensions, in carbonate sediments, or in substrates other than chert, see [50, 59, 78–85] and references therein. Microbial body fossils are also frequently reported in amber or other resins (e.g. [86, 87]). In fact, a plethora of papers exist that document experimental "fossilization" of living microbes, and demonstrate the rapidity of these reactions (e.g. [2, 48, 88–92] and references therein). Additionally, mineralized EPS has been shown to retain "voids" of microbial bodies that are virtually identical in size and shape to those figured for "melanosomes" (e.g. [50] Figs. 4, 7; [81] Fig. 4; [93] Fig. 7).

Microbes have high preservation potential. The macromolecular components of bacterial cell walls, as well as the EPS they secrete, are highly reactive and negatively charged; they bind a host of metal ions, which encrust microbial cells and stabilize the EPS (e.g. [47, 48, 83, 89, 94–97] and references therein). This process is exceedingly efficient because of high surface area to volume ratios; mineralization confers resistance to deformation as well. Because microbes and the EPS they secrete actively participate in the precipitation of carbonates, phosphates and silicates [88, 91, 92, 98]; the role of microbes in the exceptional preservation of eukaryotic material is well documented (e.g. [99] and references therein; [2, 78, 79, 100, 101]) and has recently been posited as contributing to a mode of fossilization resulting in exceptionally preserved *Anchiornis* feathers preserved with microbodies and voids. The data support a mix of melanosome and microbial sources [46].

Although microbes participate in exceptional preservation, they are also the primary agents of organic decay [101]. They grow on surfaces, and between sediment–organic interfaces of degrading organic material [102]. It has been shown that microbes more readily colonize rough, hydrophobic surfaces than hydrophilic ones [103]; thus the naturally hydrophobic, branching, barbed surfaces of feathers are excellent substrates for microbial colonization. "Melanosomes" associated with fossil feathers are easily seen without sectioning in most samples, consistent with a superficial location, and are noted to be easier to visualize when feathers are more highly degraded [24, 45], yet the role of microbes in that degradation is not acknowledged.

Furthermore, feather-degrading bacteria (FDB) have been shown to colonize the feathers of virtually all living birds and have been posited to influence plumage characteristics, including color and hue, during evolution [104]. Thus, the difficulty in correlating melanosome density within fossil feathers because of "keratin collapse and condensation into a thinner layer" ([3], p. 4) may be equally explained by the post-mortem proliferation of FDB already existing on feather surfaces [104]. Without chemical data, the preservation of microorganisms within or outside of mineralized EPS is at least as well supported as melanosomes to explain microbodies (or "voids") associated with exceptionally preserved fossils, including feathers. Because of the ubiquity of microbes and their role in organic degradation, a microorganismal source is an equally parsimonious hypothesis for these fossil-associated microbodies and voids. Only when a microbial source has been ruled out by chemical means should the alternative melanosome hypothesis be considered.

To test the hypothesis that microbodies and voids associated with fossil feathers might be attributed with equal parsimony to microbes as to melanosomes, Moyer et al. [1] designed a "proof of concept" set of actualistic taphonomic experiments. The goal was to show that microbes and the EPS they secrete will overgrow feathers in a confluent arrangement similar to that portrayed as "melanosomes" in fossil feathers ([3] Fig. 2D). For these experiments *Bacillus cereus*, a bacterium on the larger end of the scale of microbial dimensions, was chosen because it is commonly available, well characterized, ubiquitous in soils and sediments, available in pure cultures, and known to produce a biofilm. The experiments were not, nor were they meant to be, representative of microorganisms in a natural environment with respect to cellular size. In fact, microbes in natural environments are smaller than the same species cultured in a laboratory, and it has been shown that soil microbes of smaller size are increasingly more difficult to culture, although they grow robustly in their natural environments [72]. Although using a pure culture of biofilm-producing organisms was important for experimental purposes, almost all naturally occurring microbes grow in mixed populations (e.g. [67, 68]), not pure cultures (Fig. 2E, F, G). Thus, a diversity of sizes and shapes are represented [72], consistent with what is reported in much of the "fossil melanosome" literature (e.g. [24]). The criticism of the size of microbes used in these experiments is not valid for these reasons. And, as mentioned above, naturally occurring microbes fall well within the reported size ranges for melanosomes.

Can microbody shape be used to determine color?

There are several problems associated with using the size and shape of presumed melanosomes to infer color, physiology, or behavior [24, 34, 38, 105], not the least of which is that overall coloration in living vertebrates is usually determined by co-expression of multiple pigments with differing preservation potentials [106]. It is noted that "melanosomes in iridescent feathers are also in some cases highly modified, and can be hollow, flattened, or disc-shaped" ([3], p. 3). Yet no criteria exist to differentiate between diagenetically and biologically modified shapes. Regardless, if melanosomes can be "modified" then how can one be certain that their preserved shapes "accurately reflect color?"

Briggs and Summons [107] are cited to support the shrinkage of melanosomes bodies to "loss of CO_2, CH_4, H_2O, and N_2" during burial and subsequent diagenetic maturation ([3], p. 5); however, the referred work discusses changes occurring when "sedimentary rocks are buried deeper in the earth's crust" and refers to molecular, not morphological change [107]. These authors also state that "a melanin biomarker would provide a test of its presence" ([107], p. 486). We agree completely, yet this has been demonstrated with high resolution in only a few of the many publications on fossil "melanosomes" [35, 39, 41, 42, 46], and most of these were conducted on marine specimens and skin samples [39, 41, 42], not feathers (but see [46]). Therefore, the alternative hypothesis of microbial remains is not eliminated in the majority of cases, particularly concerning feathers. Measuring the voids is proposed to be more accurate for determining original color because diagenesis may cause the bodies to shrink, whereas the "voids" retain their original dimensions ([3], p. 5–6). Because the factors affecting the microbodies of necessity affect the medium in which they are embedded, the shrinkage of the bodies while the voids retain original dimensions can only reasonably occur if the matrix is mineralized before the microbodies (see above). This has been shown to occur in biofilms (e.g. [50, 108, 109]), but such rapid post-mortem mineralization has not yet been demonstrated by taphonomic experimentation to occur in the keratin matrix relative to melanosomes embedded in it. Additionally, it is assumed that bodies from which no melanin can be detected are altered ([3], p. 5), based only on the lack of melanin signal. The alternative and equally viable hypothesis, i.e. that they are not melanosomes, but rather microbes, is not considered. If no animal melanin can be ascribed to fossil microbodies, they are equally likely to be microbial in origin. This was noted by Lindgren et al. [46]; studies on fossil plumage show, in some regions, bodies to which melanin signal is mapped, and in others, impressions both with, and without melanin signal. However, they posit that phosphatization must contribute to survival of fibril-like structures in that specimen, which may imply a bacterially mediated process ([78, 79] and references therein). This in turn could have implications for the interpretation of "voids" associated with fossil feathers ([23, 36, 110] and references therein), and allows the possibility that both melanosomes (containing detectable and mappable melanin signal) and microbes become intermingled in the degradation process (e.g. Fig. 1). This can be addressed through taphonomic experiments; in particular, experiments designed to determine the rate and conditions under which keratin could phosphatize.

According to Vinther, the ability to determine organismal color depends upon the shape of associated "melanosomes," yet he admits the "cause for this correlation between melanin chemistry and melanosome morphology still need clarification" ([3], p. 4). In fact, this correlation does not hold true for "melanosomes" associated with fossilized (or

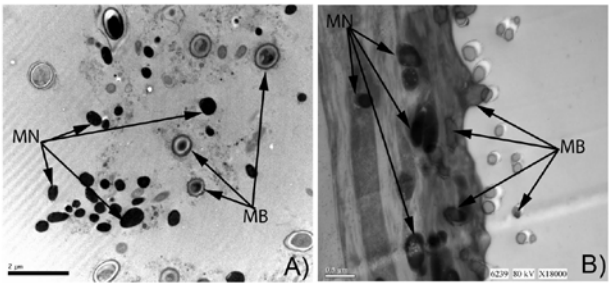

Figure 1. Transmission electron micrographs (TEM) showing co-existence of melanosomes (MN, arrows) and microbes (MB, arrows) in keratinous material. **A:** Unstained TEM showing electron-dense melanosomes and semi-translucent bacterial cells. The image was taken as part of an ongoing study where *Morelia* skin samples were allowed to decompose under various environmental conditions (see also Fig. 2). This particular sample had been decaying for 10 weeks in sea water prior to being photographed. **B:** Stained TEM image of black chicken feather which was incubated with *Bacillus cereus* for 3 days then chemically fixed; melanosomes are observed as electron dense microbodies embedded within the keratinous matrix of the feather, whereas the bacteria are the sub-micron electron translucent microbodies observed external to the feather. Some are interacting with the feather surface or immediately beneath the outermost cortex as degradation progressed.

extant) eye regions. Pheomelanin has not, to our knowledge, been chemically detected in retinal pigments of living organisms, yet if shape is the ultimate determinant, fossil (and extant) organisms had the full range of melanin types in their eyes, based upon observed morphologies of microbodies contained therein [63].

As Vinther noted ([3], p. 7–8), extant birds exhibit a range of colors beyond black, gray (eumelanosome determined), brown, or red (pheomelanosome determined); they also employ carotenoids and other pigments [9, 111], which may have been employed by Paraves and relatives expressing feathery integumentary structures (but see [112]). Furthermore, shape of melanosomes alone also does not account for the effect of diet [113], oxidation state of melanin within melanosomes [114], thickness of the melanin coat surrounding the pheomelanin core in pheomelanosomes (the "casing model" [115]), or influence of FDB on color and hue [104], all of which may affect the expression or penetrance of melanins in determining color without altering melanosomes shape. And, if pH affects the size of melanin granules [35], it is reasonable to propose that similar diagenetic conditions could also affect size and/or shape of melanosomes (as discussed above).

Vinther suggests that the density of melanosomes in these fossil feathers correlates with the relative observed brightness ([3], p.5); however, in living birds where both eu- and pheomelanin are expressed, neither brightness or hue can be directly correlated with the ratio of melanosomes expressing either pigment ([4] and references therein). On the other hand, it has been shown that the presence of microbes, including FDB, directly influences both hue and brightness in the feathers of extant birds [104].

Finally, color inferred for extinct organisms based upon "melanosomes" or, more often, "void" shape and dimensions, is used to posit behaviors, physiologies, and ecological niches [23, 36]. But because microbes can and do co-exist with pigment organelles (Fig. 1), caution must be employed before ascribing these traits to extinct organisms. For example, if statistics are done on samples that include microbial cells in addition to melanosomes, the inferences will inevitably be incorrect.

Analytical methods may differentiate melanosomes (or melanin) and microbial biomarkers in exceptionally preserved fossils

Because of the complete overlap between melanosomes and microbes in size, shape, distribution, and association with feathers (Fig. 2), only chemical methods can potentially distinguish between the two and thus should be incorporated into every study claiming melanosomes preservation [116]. Furthermore, to posit red or brown color for fossil organisms based only on the presence of round bodies is not supported, because conclusive evidence for pheomelanin has not yet, to the best of our knowledge, been demonstrated in fossil material, leaving only eumelanin and its diagenetic degradation products as potential chemical biomarkers. We propose that, because of the ambiguity in differentiating between ancient melanosomes and microbes based upon morphology and distribution of preserved microbodies, more than one line of evidence must be presented to support the presence of melanosomes in fossils, and the possibility of microbial source must likewise be eliminated through chemical means (see [63]); similar parameters were required to support the preservation of original soft tissues in dinosaur skeletal remains [28–30, 32]. This approach was also recently employed to study fossil feathers [46], and suggested both melanosome and microbial presence in fossil feathers.

Melanin is not well characterized chemically [115], but certain breakdown products can be identified that are causally linked to this biochrome. However, melanin is also produced by microbes [11, 12], so microbial melanin(s) arising from bacteria and fungi should be characterized and eliminated as a possibility. Time-of-flight secondary ion mass spectrometry (ToF-SIMS) is a powerful tool for melanosome investigation, because it can be conducted in situ on fossil samples, and can identify patterns consistent with melanin and map them to fossil microbodies [41]; however, this method is sensitive to surface and preparation artefacts. Other technologies that have been employed to characterize aspects of melanin chemistry can be used in tandem to support ToF-SIMS data. These include UV/Vis absorbance [115], electron paramagnetic resonance (EPR [115]), particle-induced X-ray Emission (PIXE) [117], or Raman spectroscopy [118, 119]. For a more in depth discussion of methodologies, applications, and limitations, see [32, 41, 63–65].

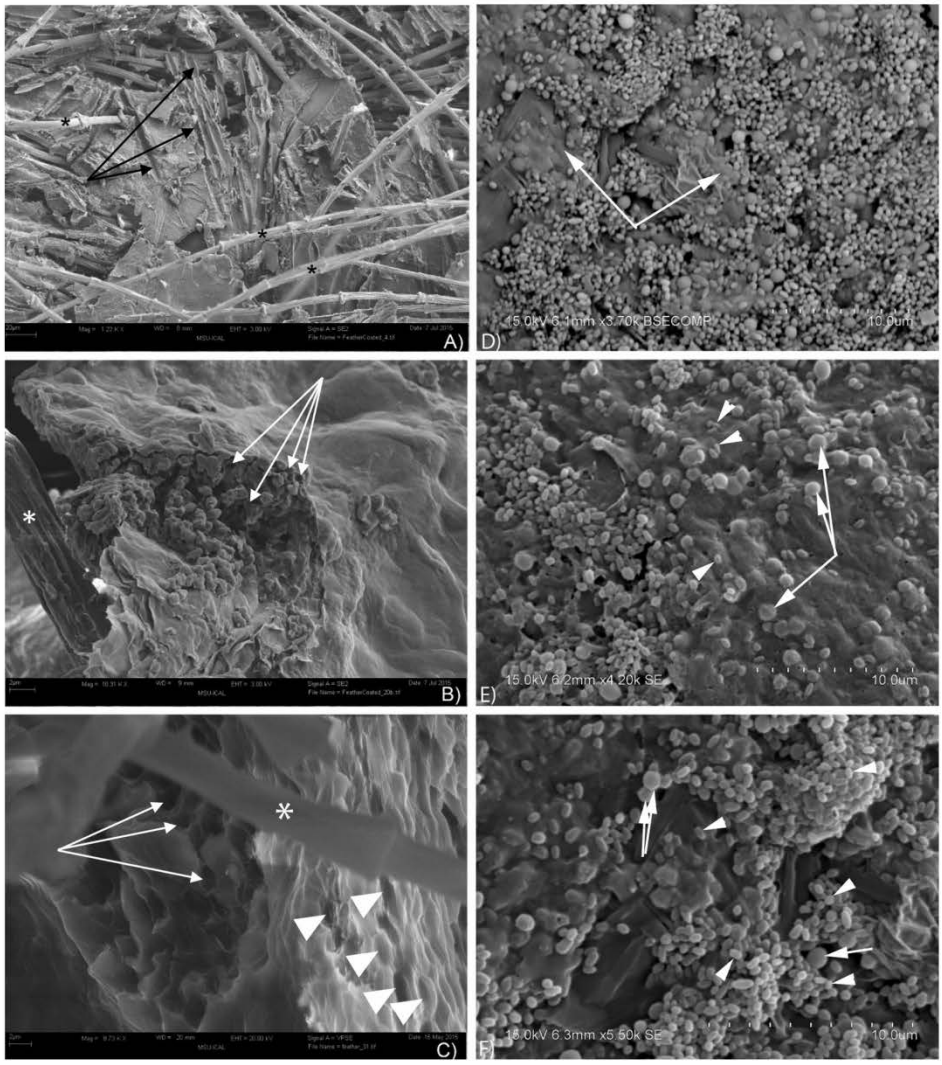

Figure 2. SEM images of degraded bird feathers (**A–C**) and snake skin (**D–G**). **A–C:** SEM images of feathers collected from a common pheasant (*Phasianus colchicus*) after undergoing natural degradation until all that remained were bone and feathers. Feathers in A, B, were coated with 40 nm iridium, C was uncoated. **A:** Barbules (*) both in three dimensions, and as "impressions" in the presumed biofilm matrix (arrows), showing that this microbially associated matrix is capable of retaining three-dimensional shapes as voids. **B:** Feather barbule (*) closely associated with superficial amorphous substance and associated microbodies. Voids can also be seen where no microbial bodies are present (arrows). **C:** Feathers from same bird, imaged uncoated and under variable pressure. Feather barbule (*) with region of what appear to be voids in an amorphous matrix. Note both randomly distributed (arrows) and aligned (arrowheads) voids in matrix. Melanosomes are embedded within keratin, whereas microbes are superficial; because these bodies and associated matrix were observed without sectioning or any other preparation, as described for similar analyses of fossil feather "melanosomes," it is most parsimonious to assume a microbial source for these structures. **D–F:** SEM images of microbes and secreted EPS recovered from sediments in which pigmented skin of the sea snake *Morelia* sp. was degraded. Skin from the specimen was placed in a tank containing normal seawater from Öresund, Sweden (salinity ~1.0–1.5%) and a fine grained, well-sorted quartz sand, also from the sea near Lund, on which the specimen was placed. The specimen was allowed to degrade for a period of ~10 weeks under low ambient light and ~20°C. **D:** Wide distribution of sizes and shapes of microbial bodies overgrowing skin and sediment in a confluent pattern. Arrow shows smooth contours of presumed microbial EPS. **E, F:** higher magnification of large, round (arrows) and smaller elongate (arrowhead) bodies, coexisting and closely associated with amorphous EPS. Note that elongate bodies are consistently smaller than 1 μm. Scale bars as indicated.

Morphologically, TEM should be required to support a hypothesis of melanosome presence. Mature melanosomes of extant organisms are completely filled with electron dense material, whereas microbes may have mineralized cell walls, but generally possess translucent interiors (Fig. 1, and reviewed in [63]). However, exceptions do exist, in that some fossil ("carbonized") microbes may be completely infilled ([120] Fig. 7c), and some melanosomes are hollow [121] so this type of analysis, alone, is not definitive.

Recently, synchrotron radiation (SR)-based studies have been employed to address the possibility of melanosome preservation (reviewed in [122]). These methods couple ultra-high energy X-rays with infrared light to obtain very high resolution elemental and molecular information, and can map signal changes to surfaces.

SR can map element distributions with high resolution, and this functionality has been applied to paleontological samples as a proxy for melanin distribution in fossil tissues (e.g. [123]). However, "organically bound" trace metals can arise from at least four sources: (i) through metals incorporated into pigments (Cu^{+2} or Fe^{+3}); (ii) proteins (e.g. high sulfur keratins, iron-containing hemoglobin, or myoglobin); (iii) bacterial metalloenzymes involved in the breakdown of keratin or other components [124, 125]; or (iv) metal ions from the depositional environment. Thus, elements mapped using SR can reflect either original pattern or diagenetic effects, and thus elemental detection, even at high resolution, cannot be used as the sole inference for ancient color patterns. However, SR provides the great advantage of being able to map these distributions across the whole sample, rather than the spatially very small regions examined in SEM, TEM, or histology, which are more commonly applied to fossil material [123].

Similarly, methods used in conjunction with SR, such as X-ray diffraction (XRD) or infrared spectroscopy (IR) are also limited. XRD is a bulk method for identifying dominant mineral phase of a substance, but does not yield molecular information and is not mappable; IR identifies functional groups and their environments, but cannot identify source molecules with confidence. For example, if a protein is present, it must, by definition, contain amide bonds, which can be identified using IR. However, IR cannot distinguish between amides from animal or microbial proteins, nor can it always reliably differentiate protein from other amide-containing materials such as glue or other polymers. However, when coupled to other methods, SR techniques can increase the accuracy of data interpretation.

Finally, taphonomic experiments designed to show degradation pathways for melanosomes, and their preservation potential relative to keratin in epidermal tissues must be conducted. Similarly, experiments can be designed to show mineralization pathways for the keratin matrix. These experimental data may reveal a pattern for melanosome degradation that leaves the keratin matrix intact [24], or show whether melanin can contribute to the exceptional preservation of normally labile materials such as feathers, even while the bodies are no longer present, as stated in the "ancient melanosome" literature [38]. Alternatively, experiments may show that feathers are rapidly colonized by microbes contained in an amorphous matrix, in which voids are retained when microbial bodies are removed. Figure 2 shows feathers recovered from a naturally degraded pheasant (*Phasianus colchicus*), examined using SEM. Amorphous material (Fig. 2A) capable of retaining impressions of feather barbules can be seen, and Fig. 2B shows a feather barbule, almost completely surrounded by microbodies (and impressions) in an amorphous matrix that is presumably microbial EPS. Figure 2C shows both randomly oriented (arrows) and highly aligned (arrowheads) voids within the amorphous matrix.

Taphonomic experiments also testify to the overlap in size and shape between microbodies and melanosomes. Figure 2E– G shows SEM images of microbes and EPS discretely associated with degrading skin from *Morelia* sp. Although no chemistry was done on these bodies, we assign them to microbes because: (1) they are superfical; (2) they are associated with surrounding sediments as well as degrading skin; and (3) they are closely associated with and embedded in an amorphous substance that likewise is not limited to the immediate tissues, but extends to the surrounding sediments as well as the degrading skin. A range of sizes and shapes can be seen, but most of the bodies visualized here are elongate, and less than 1 μm in length, consistent with reported data for fossil "melanosomes". Because melanosomes are embedded within a keratinous matrix while microbes and biofilm primarily colonize surfaces, and because no sectioning or preparation was done to either feathers or skin samples presented in Fig. 2, we propose that these voids and bodies represent microbial colonization; however, chemistry is needed to confirm this.

Conclusions

Microbodies are often associated with ancient soft tissue fossils, including those of dinosaurs. While the possibility exists that these are remnant color-containing intracellular organelles, an equally parsimonious hypothesis in many cases is that they represent traces of microorganisms involved in the decay and degradation of the originally organic remains. Microbes are present in every environment on the planet, and are always associated with degrading tissues. They colonize biological material and secrete enzymes to degrade it, some of which incorporate metal ions. Microbes also concentrate metal ions in the EPS. Another complicating factor is that microorganisms can also mix with melanosomes during degradation of melanin-containing tissues (Fig. 1). Thus, parsimony requires that a microbial hypothesis must be ruled out in order to claim melanosome presence, and this can only be achieved chemically, because of the complete overlap in size, morphology, and distribution between these two alternative sources. But even if melanosomes can be shown to persist on a case-by-case basis for feathers and other originally keratinous materials associated with vertebrate remains, the interpretation of organismal color requires consideration of numerous parameters, including diagenesis and presence of additional pigments, as well as factors affecting color that are not related to the shape and size of melanosomes. Finally, microbodies in a small region of the feather (i.e. what can fit in an electron

microscope chamber) do not necessarily indicate the pattern of the whole organism. Thus, shape and size of microbodies are not sufficient parameters on which to base hypotheses of original colors and color patterns.

Acknowledgments

We thank Wenxia Zheng for invaluable assistance and sample preparations, and L. Kirk, P. Stoodley, F.Westall, A. Grunden, and J. Toporski for discussions of microbial fossilization and microbially mediated mineral precipitation. This research was supported by funds from the National Science Foundation (INSPIRE to MHS: GRFP to AM); the David and Lucile Packard Foundation to MHS, and the Swedish Research Council, the Royal Physiographical Society in Lund, and the Crafoord foundation to J.L.

The authors have declared no conflicts of interest.

References

1. **Moyer AE, Zheng W, Johnson EA, Lamanna MC,** et al. 2014. Melanosomes or microbes: testing an alternative hypothesis for the origin of microbodies in fossil feathers. *Sci Rep* **4**: 4233.
2. **Sagemann J, Bale SJ, Briggs DEG, Parkes RJ.** 1999. Controls on the formation of authigenic minerals in association with decaying organic matter: an experimental approach. *Geochim Cosmochim Acta* **63**: 1083–95.
3. **Vinther J.** 2015. A guide to the field of palaeo colour. *BioEssays* **37**: 643–56.
4. **Solano F.** 2014. Melanins: skin pigments and much more-Types, structural models, biological functions, and formation routes. *New J Sci* **2014**: 1–28.
5. **Leavitt PR, Hodgson DA.** 2001. Sedimentary pigments. In Smol JP, Birks HJB, Last WM, eds; *Tracking Environmental Change Using Lake Sediments*. Dordrecht, the Netherlands: Kluwer Academic Publishers.
6. **Kutty SN, Lawman D, Singh ISB, Philip R.** 2013. Black yeasts from the slope sediments of Bay of Bengal: phylogenetic and functional characterization. *Mycosphere* **4**: 346–61.
7. **McGraw KJ, Wakamatsu K, Ito S, Nolan PM,** et al. 2004. You can't judge a pigment by its color: carotenoid and melanin content of yellow and brown feathers in swallows, bluebirds, penguins, and domestic chickens. *The Condor* **106**: 390–5.
8. **Bradbury MW, Fabricant JD.** 1988. Changes in melanin granules in the fox due to coat color mutations. *J Hered* **79**: 133–6.
9. **McGraw KJ, Toomey MB, Nolan PM, Morehouse NI,** et al. 2007. A description of unique fluorescent yellow pigments in penguin feathers. *Pigment Cell Res* **20**: 301–4.
10. **Kvenvolden KA, Hodgson GW.** 1969. Evidence for porphyrins in Early Precambrian Swaziland System sediments. *Geochim Cosmochim Acta* **33**: 1195–202.
11. **Cubo MT, Buendia-Claveria AM, Beringer JE, Ruiz-Sainz JE.** 1988. Melanin production by rhizobium strains. *Appl Environ Microbiol* **54**: 1812–7.
12. **Plonka PM, Grabacka M.** 2006. Melanin synthesis in microorganisms—biotechnological and medical aspects. *Acta Biochim Pol* **53**: 429–43.
13. **Meinschein WG, Barghoorn ES, Schopf JW.** 1964. Biological remnants in a Precambrian sediment. *Science* **145**: 262–3.
14. **Olson JM, Blankenship RE.** 2004. Thinking about the evolution of photosynthesis. *Photosynth Res* **80**: 373–86.
15. **Greenwalt DE, Goreva YS, Siljestrom SM, Rose T,** et al. 2013. Hemoglobin-derived porphyrins preserved in a Middle Eocene blood-engorged mosquito. *Proc Natl Acad Sci USA* **110**: 18496–500.
16. **Schweitzer MH, Marshall M, Carron K, Bohle DS,** et al. 1997. Heme compounds in dinosaur trabecular bone. *Proc Natl Acad Sci USA* **94**: 6291–6.
17. **Mosca L, Blarzino C, Coccia R, Foppoli C,** et al. 1998. Melanins from tetrahydroisoquinolines: spectroscopic characteristics, scavenging activity and redox transfer properties. *Free Radic Biol Med* **24**: 161–7.
18. **Palmer G.** 1983. Iron porphyrins. In Lever ABP, Gray HB, eds; *The Iron Porphyrins, Part II*. Reading, MA: Addison Wesley. p. 43–85.
19. **Treibs A.** 1936. Chlorophyll and hemin derivatives in organic materials. *Angew Chem* **49**: 682–6.
20. **Blumer M.** 1965. Organic pigments: their long-term fate. *Science* **149**: 722–6.
21. **Furlong ET, Carpenter R.** 1988. Pigment preservation and remineralization in oxic coastal marine sediments. *Geochim Cosmochim Acta* **52**: 87–99.
22. **Wolkenstein K.** 2015. Persistent and widespread occurrence of bioactive quinone pigments during post-Paleozoic crinoid diversification. *Proc Natl Acad Sci USA* **112**: 2794–9.
23. **Li Q, Clarke JA, Gao K-Q, Zhou C-F,** et al. 2014. Melanosome evolution indicates a key physiological shift within feathered dinosaurs. *Nature* **507**: 350–3.
24. **Zhang F, Kearns SL, Orr PJ, Benton MJ,** et al. 2010. Fossilized melanosomes and the colour of Cretaceous dinosaurs and birds. *Nature* **463**: 1075.
25. **McNamara ME, Briggs DEG, Orr PJ, Field DJ,** et al. 2013. Experimental maturation of feathers: implications for reconstructions of fossil feather colour. *Biol Lett* **9**: 1–6.
26. **Liu SY, Shawkey MD, Parkinson D, Troy TP,** et al. 2014. Elucidation of the chemical composition of avian melanin. *RSC Advances* **4**: 40396–9.
27. **Dal Sasso C, Signore M.** 1998. Exceptional soft-tissue preservation in a theropod dinosaur from Italy. *Nature* **392**: 383–7.
28. **Avci R, Schweitzer MH, Boyd R, Wittmeyer J,** et al. 2005. Preservation of bone collagen from the Late Cretaceous period studied by immunological techniques and atomic force microscopy. *Am Chem Soc* **21**: 3584–91.
29. **Schweitzer MH, Suo Z, Avci R, Asara JM,** et al. 2007. Analyses of soft tissue from Tyrannosaurus rex suggest the presence of protein. *Science* **316**: 277–80.
30. **Schweitzer MH, Wittmeyer JL, Horner JR, Toporski JK.** 2005. Soft-tissue vessels and cellular preservation in *Tyrannosaurus rex*. *Science* **307**: 1952–5.
31. **Schweitzer MH, Zheng W, Cleland TP, Bern M.** 2013. Molecular analyses of dinosaur osteocytes support the presence of endogenous molecules. *Bone* **52**: 414–23.
32. **Lindgren J, Uvdal P, Engdahl A, Lee AH,** et al. 2011. Microspectroscopic evidence of Cretaceous bone proteins. *PLoS ONE* **6**: e19445.
33. **Bertazzo S, Maidment SCR, Kallepitis C, Fearn S,** et al. 2015. Fibres and cellular structures preserved in 75-million-year-old dinosaur specimens. *Nat Commun* **6**: 7352.
34. **Carney RM, Vinther J, Shawkey MD, D'Alba L,** et al. 2012. New evidence on the colour and nature of the isolated Archaeopteryx feather. *Nat Commun* **3**: 637.
35. **Glass K, Ito S, Wilby PR, Sota T,** et al. 2013. Impact of diagenesis and maturation on the survival of eumelanin in the fossil record. *Org Geochem* **64**: 29–37.
36. **Li Q, Gao K-Q, Meng Q, Clarke JA,** et al. 2012. Reconstruction of Microraptor and the evolution of iridescent plumage. *Science* **335**: 1215–9.
37. **Xu X, Zheng X, Sullivan C, Wang X,** et al. 2015. A bizarre Jurassic maniraptoran theropod with preserved evidence of membranous wings. *Nature* **521**: 70–3.
38. **Li Q, Gao K-Q, Vinther J, Shawkey MD,** et al. 2010. Plumage color patterns of an extinct dinosaur. *Science* **327**: 1369–72.
39. **Glass K, Ito S, Wilby PR, Sota T,** et al. 2012. Direct chemical evidence for eumelanin pigment from the Jurassic period. *Proc Natl Acad Sci USA* **109**: 10218–23.
40. **Tanaka G, Parker AR, Hasegawa Y, Siveter DJ,** et al. 2014. Mineralized rods and cones suggest colour vision in a 300 Myr-old fossil fish. *Nat Commun* **5**: 5920.
41. **Lindgren J, Uvdal P, Sjovall P, Nilsson DE,** et al. 2012. Molecular preservation of the pigment melanin in fossil melanosomes. *Nat Commun* **3**: 824.
42. **Lindgren J, Sjovall RM, Uvdal P, Gren JA,** et al. 2014. Skin pigmentation provides evidence of convergent melanism in extinct marine reptiles. *Nature* **506**: 484–8.
43. **Brocks JJ, Pearson A.** 2005. Building the biomarker tree of life. *Rev Mineral Geochem* **59**: 233–58.
44. **Vitek NS, Vinther J, Schiffbauer JD, Briggs DEG,** et al. 2013. Exceptional three-dimensional preservation and coloration of an originally iridescent fossil feather from the Middle Eocene Messel Oil Shale. *Paläont Z* **87**: 493–503.
45. **Vinther J, Briggs DEG, Prum RO, Saranathan V.** 2008. The colour of fossil feathers. *Biol Lett* **4**: 522–5.
46. **Lindgren J, Sjövall P, Carney RM, Cincotta A,** et al. 2015. Molecular composition and ultrastructure of Jurassic paravian feathers. *Sci Rep* **5**: 13520.
47. **Ferris FG.** 2000. Microbe-metal interactions in sediments. In Riding RE, Awramik SM, eds; *Microbial Sediments*. Berlin-Heidelberg: Springer-Verlag. p. 121–6.
48. **Ferris FG, Fyfe WS, Beveridge TJ.** 1988. Metallic ion binding by *Bacillus subtilis*:

implications for the fossilization of microorganisms. *Geology* **16**: 149–52.
49. **Fortin D, Ferris FG, Beveridge TJ.** 1997. Surface-mediated mineral development by bacteria. *Rev Mineral* **35**: 161–80.
50. **Lozano RP, Rossi C.** 2012. Exceptional preservation of Mn-oxidizing microbes in cave stromatolites (El Soplao, Spain). *Sediment Geol* **255–256**: 42–55.
51. **Schweitzer MH, Watt JA, Avci R, Forster CA,** et al. 1999. Keratin immunoreactivity in the Late Cretaceous bird *Rahonavis ostromi*. *J Vertebr Paleontol* **19**: 712–22.
52. **Schweitzer MH, Watt JA, Avci R, Knapp L,** et al. 1999. Beta-keratin specific immunological reactivity in feather-like structures of the cretaceous alvarezsaurid, *Shuvuuia deserti*. *J Exp Zool* **285**: 146–57.
53. **Chiappe LM, Coria RA, Dingus L, Jackson F,** et al. 1998. Sauropod dinosaur embryos from the late Cretaceous of Patagonia. *Nature* **396**: 258–61.
54. **Manning PL, Morris PM, McMahon A, Jones E,** et al. 2009. Mineralized soft-tissue structure and chemistry in a mummified hadrosaur from the Hell Creek Formation, North Dakota (USA). *Proc Biol Sci* **276**: 3429–37.
55. **Lindgren J, Alwmark C, Caldwell MW, Fiorillo AR.** 2009. Skin of the Cretaceous mosasaur Plotosaurus: implications for aquatic adaptations in giant marine reptiles. *Biol Lett* **5**: 528–31.
56. **Evans SE, Wang Y.** 2010. A new lizard (Reptilia: Squamata) with exquisite preservation of soft tissue from the Lower Cretaceous of Inner Mongolia, China. *J Syst Palaeontol* **8**: 81–95.
57. **Norell MA, Makovicky PJ, Currie PJ.** 2001. Paleontology. The beaks of ostrich dinosaurs. *Nature* **412**: 873–4.
58. **Taru P, Backwell L.** 2013. Identification of fossil hairs in *Parahyaena brunnea* coprolites from Middle Pleistocene deposits at Gladysvale cave, South Africa. *J Archaeol Sci* **40**: 3674–85.
59. **Meng J, Wyss AR.** 1997. Multituberculate and other mammal hair recovered from Palaeogene excreta. *Nature* **385**: 712–4.
60. **Bonnichsen R, Hodges L, Ream W, Field K,** et al. 2001. Methods for the study of ancient hair: radiocarbon dates and gene sequences from individual hairs. *J Archaeol Sci* **28**: 775–85.
61. **Clark JM, Norell MA, Chiappe LM.** 1999. An oviraptorid skeleton from the Late Cretaceous of Ukhaa Tolgod, Mongolia, preserved in an avianlike brooding position over and oviraptorid nest. *Am Mus Novit* **3265**: 1–36.
62. **Norell MA, Clark JM, Chiappe LM, Dashzeveg D.** 1995. A nesting dinosaur. *Nature* **378**: 774–6.
63. **Lindgren J, Moyer AE, Schweitzer MH.** 2015. Interpreting melanin-based colouration through deep time: a critical review. *Proc R Soc B* **282**: 20150614.
64. **Schweitzer MH, Avci R, Collier TC, Goodwin MB.** 2008. Microscopic, chemical and molecular methods for examining fossil preservation. *Comptes Rendus Palevol* **7**: 159–84.
65. **Zheng W, Schweitzer MH.** 2012. Chemical analyses of fossil bone. In Bell LS, ed; *Forensic Microscopy for Skeletal Tissues Methods and Protocols*. Methods Mol Biol **915**: 153–72.
66. **Barden HE, Bergmann U, Edwards NP, Egerton VM,** et al. 2015. Bacteria or melanosomes? A geochemical analysis of micro-bodies on a tadpole from the Oligocene Enspel Formation of Germany. *Palaeobiodiversity and Palaeoenvironments* **95**: 33–45.
67. **Burtt EHJ, Ichida JM.** 1999. Occurrence of feather-degrading bacilli in the plumage of birds. *The Auk* **116**: 364–72.
68. **Ichida JM, Krizova L, LeFevre CA, Keener HM,** et al. 2001. Bacterial inoculum enhances keratin degradation and biofilm formation in poultry compost. *J Microbiol Meth* **47**: 199–208.
69. **Gould SJ.** 2004. The evolution of life on Earth. *Sci Am* **14**: 92–100.
70. **Carney RM, Molnar J, Updike E, Brown W,** et al. 2014. Archaeopteryx in 4-D. *J Vertebr Paleontol*, Program and Abstracts, 103.
71. **Cisar JO, Xu D-Q., Thompson J, Swaim W,** et al. 2000. An alternative interpretation of nanobacteria induced biomineralization. *Proc Natl Acad Sci USA* **97**: 11511–5.
72. **Portillo MC, Leff JW, Lauber CL, Fierer N.** 2013. Cell size distributions of soil bacterial and archaeal taxa. *Appl Environ Microbiol* **79**: 7610–7.
73. **Leuf B, Frischkorn KR, Wrighton KC, Holman H-YN,** et al. 2015. Diverse uncultivated ultra-small bacterial cells in groundwater. *Nat Commun* **6**: 6372.
74. **Schulz HN, Schulz HD.** 2005. Large sulfur bacteria and the formation of phosphorite. *Nature* **307**: 416–8.
75. **Katz A, Alimova A, Xu M, Rudolph E,** et al. 2003. Bacteria sized determination by elastic light scattering. *IEEE J Sel Top Quant Electr* **9**: 277–87.
76. **Liu Y, Hong L, Wakamatsu K, Ito S,** et al. 2005. Comparisons of the structural and chemical properties of melanosomes isolated from retinal pigment epithelium, iris and choroid of newborn and mature bovine eyes. *Photochem Photobiol* **81**: 510–6.
77. **Simon JD, Peles DN.** 2010. The red and the black. *Accounts Chem Res* **43**: 1452–60.
78. **Briggs DEG, Moore RA, Shultz JW, Schweigert G.** 2005. Mineralization of soft-part anatomy and invading microbes in the horseshoe crab Mesolimulus from the Upper Jurassic Lagerstätte of Nusplingen, Germany. *Proc Biol Sci* **272**: 627–32.
79. **Briggs DEG.** 2003. The role of decay and mineralization in the preservation of soft-bodied fossils. *Annu Rev Earth Planet Sci* **31**: 275–301.
80. **Duck LJ, Glikson M, Golding SG, Webb RE.** 2007. Microbial remains and other carbonaceous forms from the 3.24 Ga Sulphur Springs black smoker deposit, Western Australia. *Precambrian Res* **154**: 205–20.
81. **Gong Y, Xu R, Xie S, Huang X,** et al. 2007. Microbial and molecular fossils from the Permian Zoophycos in South China. *Sci China Ser D* **50**: 1121–7.
82. **Van Lith Y, Warthmann R, Vasconcelos C, McKenzie JA.** 2003. Microbial fossilization in carbonate sediments: a result of the bacterial surface involvement in dolomite precipitation. *Sedimentology* **50**: 237–45.
83. **Riding R.** 2000. Microbial carbonates: the geological record of calcified bacterial-algal mats and biofilms. *Sedimentology* **47**: 179–214.
84. **Westall F, de Wit MJ, Dann J, van der Gaast S,** et al. 2001. Early archean fossil bacteria and biofilms in hydrothermally-influenced sediments from the Barberton greenstone belt, South Africa. *Precambrian Res* **106**: 93–116.
85. **Folk RL.** 1999. Nanobacteria and the precipitation of carbonate in unusual environments. *Sediment Geol* **126**: 47–55.
86. **Martín-González A, Wierzchos J, Gutiérrez JC, Alonso J,** et al. 2009. Microbial Cretaceous park: biodiversity of microbial fossils entrapped in amber. *Naturwissenschaften* **96**: 551–64.
87. **Beimforde C, Schmidt AR.** 2011. Microbes in resinous habitats: a compilation from modern and fossil resins. In Reitner J, ed; *Advances in Stromatolite Geobiology*. Berlin: Springer-Verlag. p. 391–407.
88. **Castanier S, Le Metayer-Levrel G, Perthuisot J-P.** 1999. Ca-carbonates precipitation and limestone genesis—the microbiogeologist point of view. *Sediment Geol* **126**: 9–23.
89. **Westall F.** 2008. Morphological biosignatures in early terrestrial and extraterrestrial materials. *Space Sci Rev* **135**: 95–114.
90. **Dunn KA, McLean RJC, Upchurch GR, Folk RL.** 1997. Enhancement of leaf fossilization potential by bacterial biofilms. *Geology* **25**: 1119–22.
91. **Wierzchos J, Sancho LG, Ascaso C.** 2005. Biomineralization of endolithic microbes in rocks from the McMurdo Dry Valleys of Antarctica: implications for microbial fossil formation and their detection. *Environ Microbiol* **7**: 566–75.
92. **Westall F, Boni L, Guerzoni E.** 1995. The experimental silicification of microorganisms. *Palaeontology* **38**: 495–528.
93. **Spadafora A, Perri E, McKenzie JA, Vasconcelos C.** 2010. Microbial biomineralization processes forming modern Ca:Mg carbonate stromatolites. *Sedimentology* **57**: 27–40.
94. **Choi DW, Zea CJ, Do YS, Semrau JD,** et al. 2006. Spectral, kinetic, and thermodynamic properties of Cu(I) and Cu(II) binding by Methanobactin from *Methylosinus trichosporium* OB3b†. *Biochemistry* **45**: 1442–53.
95. **Tazaki K, Rafiqul IABM, Nagai K, Kurihara T.** 2003. FeAs2 biomineralization on encrusted bacteria in hot springs: an ecological role of symbiotic bacteria. *Can J Earth Sci* **40**: 1725–38.
96. **Ehrlich HL.** 1998. Geomicrobiology: its significance for geology. *Earth Sci Rev* **45**: 45–60.
97. **Beveridge TJ, Hughes MN, Lee H, Leung KT,** et al. 1997. Metal-microbe interactions: contemporary approaches. *Adv Microbial Physiol* **38**: 177–243.
98. **Braissant O, Cailleau G, Dupraz C, Verrecchia EP.** 2003. Bacterially induced mineralization of calcium carbonate in terrestrial environments: the role of exopolysaccharides and amino acids. *J Sediment Res* **73**: 485–90.
99. **Bottjer DJ.** 2005. Geobiology and the fossil record: eukaryotes, microbes, and their interactions. *Palaeogeogr Palaeoclimatol Palaeoecol* **219**: 5–21.
100. **Meyer DL, Milsom CV.** 2001. Microbial sealing in the biostratinomy of Uintacrinus Lagerstätten in the upper Cretaceous of Kansas and Colorado, USA. *Palaios* **16**: 535–46.
101. **Babcock LE, Leslie SA, Elliot DH, Stigall AL,** et al. 2006. The "Preservation Paradox": microbes as a key to exceptional fossil

preservation in the Kirkpatrick Basalt (Jurassic), Antarctica. *The Sedimentary Record* **4**: 4–8.

102. **Wijman JGE, de Leeuw PPLA, Moezelaar R, Zwietering MH**, et al. 2007. Air-liquid interface biofilms of Bacillus cereus: formation, sporulation, and dispersion. *Appl Environ Microbiol* **73**: 1481–8.
103. **Donlan RM.** 2002. Biofilms: microbial life on surfaces. *Emerg Infect Dis* **8**: 881–90.
104. **Gunderson AR, Forsyth MH, Swaddle JP.** 2009. Evidence that plumage bacteria influence feather coloration and body condition of eastern bluebirds *Sialia sialis*. *J Avian Biol* **40**: 440–7.
105. **Clarke JA, Ksepka DT, Salas-Gismondi R, Altamirano AJ**, et al. 2010. Fossil evidence for evolution of the shape and color of penguin feathers. *Science* **330**: 954–7.
106. **McGraw KJ.** 2006. *Bird Coloration: Mechanisms and Measurements*. London: Harvard University Press. p. 243–94.
107. **Briggs DEG, Summons RE.** 2014. Ancient biomolecules: their origins, fossilization, and role in revealing the history of life. *BioEssays* **36**: 482–90.
108. **Pesquero MD, Souza-Egipsy V, Alcala L, Ascaso C**, et al. 2013. Calcium phosphate preservation of faecal bacteria negative moulds in hyaena coprolites. *Acta Palaeontol Pol* **59**: 997–1005.
109. **Cacchio P, Ercole C, Cappuccio G, Lepidi A.** 2003. Calcium carbonate precipitation by bacterial strains isolated from a limestone cave and from a loamy soil. *Geomicrobiol J* **20**: 85–98.
110. **Vinther J, Briggs DEG, Clarke JA, Mayr G**, et al. 2010. Structural coloration in a fossil feather. *Biol Lett* **6**: 128–31.
111. **Shawkey MD, Hill GE.** 2005. Carotenoids need structural colours to shine. *Biol Lett* **1**: 121–4.
112. **Thomas DB, McGraw KJ, Butler MW, Carrano MT**, et al. 2014. Ancient origins and multiple appearances of carotenoid-pigmented feathers in birds. *ProcBiol Sci* **281**: 1–9.
113. **Meadows MG, Roudybush TE, McGraw KJ.** 2012. Dietary protein level affects iridescent coloration in Anna's hummingbirds, *Calypte anna*. *J Exp Biol* **215**: 2742–50.
114. **van Grouw H.** 2006. Not every white bird is an albino: sense and nonsense about colour aberrations in birds. *Dutch Birding* **28**: 79–89.
115. **Ito S, Wakamatsu K, d'Ischia M, Napolitano A**, et al. 2011. Structure of melanins. In Borovansky J, Riley PA, eds; *Melanins and Melanosomes: Biosynthesis, Structure, Physiological and Pathological Functions*. Weinheim, Germany: John Wiley & Sons. p. 167–85.
116. **Edwards NP, Manning PL, Wogelius RA.** 2014. Pigments through time. *Pigm Cell Melanoma Res* **27**: 684–98.
117. **Riquelme F, Alvarado-Ortega J, Ruvalcaba-Sil JL, Aguilar-Franco M**, et al. 2013. Chemical fingerprints and microbial biomineralization of fish muscle tissues from the Late Cretaceous Múzquiz Lagerstätte, Mexico. *Rev Mex Cienc Geol* **30**: 417–35.
118. **Marshall CP, Carter EA, Leuko S, Javaux EJ.** 2006. Vibrational spectroscopy of extant and fossil microbes: relevance for the astrobiological exploration of Mars. *Vib Spectrosc* **41**: 182–9.
119. **Marshall CP, Marshall AO.** 2010. The potential of Raman spectroscopy for the analysis of diagenetically transformed carotenoids. *Philos Trans A Math Phys Eng Sci* **368**: 3137–44.
120. **Preston LJ, Shuster J, Fernández-Remolar D, Banierjee NR**, et al. 2011. The preservation and degradation of filamentous bacteria and biomolecules within iron oxide deposits at Rio Tinto, Spain. *Geobiology* **9**: 233–49.
121. **Eliason CM, Bitton P-P, Shawkey MD.** 2013. How hollow melanosomes affect iridescent colour production in birds. *Proc Biol Sci* **280**: 1–7.
122. **Bergmann U, Manning PL, Wogelius RA.** 2012. Chemical mapping of paleontological and archeological artifacts with synchrotron X-Rays. *Annu Rev Analyt Chem* **5**: 361–89.
123. **Manning PL, Edwards NP, Wogelius RA, Bergmann U**, et al. 2013. Synchrotron-based chemical imaging reveals plumage patterns in a 150 million year old early bird. *J Anal At Spectrom* **28**: 1024–30.
124. **Gupta R, Ramnani P.** 2006. Microbial keratinases and their prospective applications: an overview. *Appl Microbiol Biotechnol* **70**: 21–33.
125. **Brandelli A, Daroit DJ, Riffel A.** 2010. Biochemical features of microbial keratinases and their production and applications. *Appl Microbiol Biotechnol* **85**: 1735–50.

CHAPTER 5 - Keratin durability has implications for the fossil record: results from a 10 year feather degradation experiment

Abstract

Keratinous 'soft tissue' structures (i.e. epidermally derived and originally non-biomineralized), include feathers, skin, claws, beaks, and hair. Despite their relatively common occurrence in the fossil record (second only to bone and teeth), few studies have addressed natural degradation processes that must occur in all organic material, including those keratinous structures that are incorporated into the rock record as fossils. Because feathers have high preservation potential and strong phylogenetic signal, in the current study we examine feathers subjected to different burial environments for a duration of ~10 years, using transmission electron microscopy (TEM) and *in situ* immunofluorescence (IF). We use morphology and persistence of specific immunoreactivity as indicators of preservation at the molecular and microstructural levels. We show that feather keratin is durable, demonstrates structural and microstructural integrity, and retains epitopes suitable for specific antibody recognition in even the harshest conditions. These data support the hypothesis that keratin antibody reactivity can be used to identify the nature and composition of epidermal structures in the rock record, and to address evolutionary questions by distinguishing between alpha- (widely distributed) and beta- (limited to sauropsids) keratin.

Introduction

Beta-keratins are structural proteins expressed in the epidermis and epidermally derived structures of extant 'reptiles' and birds (sauropsids) [1–3]. Beta-keratin proteins are comprised of a high percentage of cysteine, a sulfur-containing amino acid. Cysteine readily forms disulfide bonds, which confer rigidity [4,5] and provide enhanced resistance to degradation. Beta-keratins also incorporate multiple hydrophobic residues in their primary structure which exclude water [6], one of the primary effectors of early degradation of proteins [7].

Beta-keratin makes up 80-90% of a mature feather [8,9]. Some researchers suggest feather beta-keratin is a corneous beta protein [4,10,11], but because the majority of researchers still refer to this family of proteins as beta-keratins we employ the more common term in this manuscript.

The inherent preservation potential of tissues and structures comprised of beta-keratin is relatively high, as suggested by previous studies [12–15] and indicated by the vertebrate fossil record in which the third most abundant fossils (after bones and teeth) are keratin-derived

materials such as skin and feathers [16]. However, taphonomic studies are needed to understand the conditions leading to the arrest of degradation (and thus preservation) of these original 'soft tissues'.

Here we report results from a 10 year experiment examining the effect of different burial conditions on feather preservation. To limit the number of variables tested, isolated feathers from a single Hungarian partridge were buried in sands taken from the Judith River formation and kept in the following conditions: 1) placed in 60°C incubator, watered twice weekly for 6 months, then intermittently for a total of 3 years, then allowed to dry and kept undisturbed for the remaining 7 years (60°C); 2) covered in foil and placed in a 350°C dry oven used for sterilization of microbiology glassware (350°C); 3) the whole bird with remaining feathers was buried in a drainage channel near a mountain pond. Five feathers were placed covered, in a clean aluminum dish and kept covered at room temperature for 10 years as a control. We employed transmission electron microscopy (TEM) to analyze ultrastructural integrity. To test for preservation of keratin epitopes of the feathers, i*n situ* immunofluorescence (IF) was performed using a custom-made affinity purified polyclonal rabbit primary antiserum raised against feather proteins.

To test the relative durability of pigmented vs non-pigmented keratin we compared and contrasted both white and pigmented portions of feathers from the control and 60°C conditions. Original color was impossible to determine in the 350°C remains. Finally, to extend these findings to the fossil record, we reexamined a fiber from a ~75 million year old fossil specimen *Shuvuuia deserti*, previously studied in 1999, with the custom-made primary antiserum used in this study [12].

Results

After 10 years, optical microscopy and gross observation of Hungarian partridge (*Perdix perdix*) feathers showed considerable variation of feather structure between environments. No damage, degradation, or alteration of color or morphology was observed in control feathers kept covered at room temperature (Fig 1 A, B). Although the wet burial (60°C) feathers (Fig 1 C, D) retained color banding (Fig 1D arrows), the non-pigmented portions changed from white-beige to yellow, and the patterning observed in the control feathers (Fig 1A, B) appeared obscured in the 60°C feathers. Feathers showed obvious degradation and fraying (Fig 1C). Dry burial (350°C) feathers showed fragmentation and little original structure (Fig 1 E, F). These feathers were very fragile and fractured during collection and sampling. Feather remnants were

fragmentary and had altered from beige-white and brown to black, shiny, hollow fragments that persisted in three dimensions. Barb remains were identified in only a few cases (Fig 2A). The external cortex and internal pith of the barb can be observed in section (200nm) under transmitted light microscopy (Fig 2B). No original color could be detected in any of the 350°C feathers; feather pieces were similar to 'carbonized remains' observed in the rock record ([17] and the references therein), except preserved in three dimensions.

Ultrastructural features of the feathers were examined using TEM. No discernible differences in ultrastructure were observed between non-pigmented (Fig 3A) and pigmented (Fig 3C, D) regions of the control feather, except for the presence of melanosomes in the pigmented barb (Fig 3C) and barbule (Fig 3D). There were also no discernible differences in observed ultrastructure between the white barb of the control feather (Fig 3A) and the white barb from 60°C (Fig 3B). Electron-dense microbodies consistent with melanosomes were observed in the pigmented regions of both barbs and barbules in the control (Fig 3 C, D) and 60°C feathers (Fig 3E). The external cortex (Fig 3C arrow) and internal pith, with its characteristic honey-combed texture (Fig 3C) were observed in the pigmented barb of the control feather. The 60°C pigmented feather (Fig 3E) showed structural damage, as revealed by the scalloped texture of the feather margin. For both control and 60°C conditions, pigmented barbules demonstrated more melanosomes than cortices of the barb, as noted in the literature [18]. The melanosomes of the control feather were homogenously dense and electron opaque (Fig 3D arrow). In contrast, the microbodies in the barbule of the 60°C pigmented feather are less electron-dense, show apparent density differences relative to the control (Fig 3E arrowhead), and some are 'hollow' (Fig 3E arrow), suggesting partial degradation of these organelles.

Because the pith of the rachis (Fig 3F) is indistinguishable from the pith of a barb (Fig 3C) at the magnification and small sample area required by TEM, the absence of observed melanosomes in the 350°C feather (Fig 4A, B) may be attributed to: 1) degradation, 2) inadvertently sampling pith of barb or rachis which may not necessarily possess them, or 3) sampling regions of the feather that were originally lacking pigment. We sampled pith, but whether it derived from rachis or barb was not possible to determine. Therefore, a second feather fragment positively identified as a barb (Fig 2) was examined as well. Approximately eight fragments from the 350°C condition could be confidently identified as barbs. However, most recovered feather fragments resembled the shiny, black, nondescript pieces observed in Fig 1 (E,

F). Fig 4 shows external cortex at both lower (Fig 4C, arrow) and higher magnification (Fig 4D). Although microstructure (the outer cortex and honeycomb-like pith of the barb) is well preserved, no melanosomes are observed (see below for discussion).

To determine if the exceptional microstructural preservation extended to the molecular level, we employed i*n situ* immunofluorescence (IF) to test the durability of keratin epitopes under the various treatment conditions. Antibodies raised against extracts of purified feather keratin (see Methods) reacted with high specificity to all feathers tested, although binding avidity was variable. Antibody-antigen complexes, observed as green fluorescence color, strictly localized to the feather structures (Fig 5), and controls (no primary antibodies but all other conditions identical; S1 Fig) were consistently negative for binding. Intriguingly, epitope recognition was greater in the feathers treated in 60°C condition (Fig 5C, D) than in the control feather (Fig 5A, B).

Although a diffuse background signal can be seen in the 350°C feather pith (Fig 5E), the complete lack of binding in the control (no primary antibodies added) (Fig 5F and S1 Fig) supports specific localization of ab-ag complexes to feather tissues.

To test the hypothesis that pigmented feathers are more resistant to degradation than non-pigmented feathers, we compared white barbs (Fig 5 A and C) to brown barbs (Fig 5 B and D) within each condition. No differences in structure or binding avidity were observed between colored and white feather parts in both the control and 60°C experimental conditions.

Two pieces of feather from the 350°C condition were analyzed using IF. One piece was either barb or rachis (see above discussion) and one piece was definitively barb (see Fig 2). Although it was impossible to distinguish areas of original color in the feather treated for 10 years at 350°C, we were able to demonstrate weak positive binding of anti-feather antibodies localized to the tissues (Fig 5E and Fig 6 C, D). Fig 6 illustrates IF results on the feather fragment identified as a barb and shows the cortex as well as the inner pith of the barb. Antibody binding is localized to the cortex as well as the lattice structure of the pith just deep to the cortex (Fig 6 C, D). Control conditions where no primary antibodies were added, were completely without signal (Fig 5F, S1 Fig J, and Fig 6B). In both samples, background signal is observed as a green ‘glow’ (Fig 5E and Fig 6D) however binding of the primary antiserum is localized to the feather microstructure. These data support the preservation of some protein components,

correlating with the exceptional microstructural integrity, but positive signal is greatly decreased compared to the other conditions.

The specificity of our custom antibodies was further demonstrated through an inhibition study. When antibodies are incubated first with excess feather protein extract to block the binding sites of the antibodies, then exposed to tissue sections, binding is reduced or eliminated (S2 Fig C, D for modern and S4 Fig C, D for fossil), testifying to the specificity of antibody-antigen interactions.

To further test specificity, we incubated the antibodies with human fingernail, and no binding was observed; however an alpha-keratin antibody applied to human fingernail reacted positively, showing the nail expresses alpha-keratin epitopes (S3 Fig A-C). The lack of response of human nail to the custom antibody employed herein supports the specificity to tissues containing beta-keratin (S3 Fig D-F). As in previous experiments, adding only secondary antiserum, without specific primary antibodies, controls for non-specific binding of the secondary antibody to the tissues (S3 Fig G-I).

Discussion

Fossil remains originally comprised of keratin have been noted since the 1800s (e.g., [19,20]), but few studies have sought to elucidate the microstructure and composition of these structures, or the mechanisms leading to their preservation. Additionally, recent discoveries and analyses of fossil feathers ([21–26] and the references therein) illustrate the need to understand mechanisms leading to the preservation of these evolutionarily significant structures. In this long term study, we examined the microstructural and molecular preservation of modern feathers subjected to varying conditions, including high heat which has been suggested as a proxy for time (e.g. [27–30]), to directly test the stability of these materials.

The small size of the barbs/barbules allowed the entirety of the structures to be observed under electron microscopy and these parts are where melanosomes are concentrated; therefore barbs were analyzed preferentially over rachises when possible. We show that after several years at 60°C in a wet burial condition, original color is transformed macroscopically (Fig 1), and feather microstructure is also altered (Fig 3). Some of the melanosomes remain embedded in the keratinous matrix, but appear partially degraded, as revealed by a loss of internal electron-opaque material within the melanosomes. We conclude that the semi-translucent nature of melanosomes in these feathers is a result of partial degradation and not the ‘hollow melanosome’

morphology characterized in the literature in some species of birds [31,32] for the following reasons: 1) No hollow melanosomes were observed in the control feathers. 2) This observation appeared in feathers *only* after exposure to wet burial conditions at 60°C for several years.

The compositional and structural differences between families of keratin proteins is significant, and as mentioned previously, mammals do not express beta-keratins, while feathers have little to no detectable alpha-keratin in mature form [33–35]. Although degraded, beta-keratin epitopes comprising the feather were capable of being detected, and in fact, antibody signal appears greater in the partially degraded feather than in the feather kept at room temperature for the same duration. We hypothesize that this increased response to antibodies is due to a taphonomic degradation pathway, similar to enzyme degradation [36], where breakage of the intramolecular bonds results in the exposure of epitopes that would otherwise be blocked.

It has been proposed that melanized feathers are more durable than unpigmented ones [37,38]; therefore we also compared microstructural and molecular degradation between brown (pigmented) and white (non-pigmented) portions of feathers, when they could be distinguished. This resistance has been attributed to the durability of melanin, the primary (or dominant) biochrome in colored feathers. Gunderson et al. (2008) concluded that non-pigmented feathers are more susceptible to degradation, but our results do not support this under the conditions we employed. No obvious differences in structural integrity were observed under TEM between white and brown regions of the feathers. They also did not differ in antibody response, showing neither increased nor decreased fluorescent signal.

Immunohistochemistry is a powerful analytical method if appropriate controls are performed in parallel. For each sample tested using *in situ* IF in this study, we confirmed specificity of our antibody response by applying the secondary antibody only and no primary antiserum. If no binding was observed, this negates the possibility of spurious (or non-specific) binding of the secondary antibody, and showed that only the binding of the primary antibody to its specific epitope, retained in the tissue, resulted in a positive signal.

In addition to this negative control, we confirmed signal specificity using additional controls. These included inhibiting the primary antiserum by exposing it to an excess of purified antigen against which the antibody was raised prior to incubation with the tissue (S2 Fig). The protein then occupied the binding sites of the antibody such that they were no longer available to bind with the test sample. Antibodies with binding sites for other proteins or epitopes would not

be inhibited by beta-keratin proteins and would be free to bind fossil tissues. Therefore, signal should be reduced or completely lost in the inhibition test. Indeed, this control was negative for binding in the extant chicken feather tissue (S2 Fig C, D).

To control for non-specific binding of the primary antibody, we applied an irrelevant antibody (S2 Fig E, F), one to which no binding to the sample would be expected, while all other parameters were kept consistent. As we demonstrated, no signal should be observed in the presence of an irrelevant (i.e., not expected to recognize the epitopes in the test sample) antibody. Often, as in most analytical techniques, there is background signal; however signal above this background, as long as all parameters are kept consistent between sections being compared, is assigned to a positive and specific signal. In each case, the controls we employed were consistently negative for binding, supporting that all binding signal is specific to epitopes present in the samples tested.

Remarkably, even under the harshest conditions in this experiment, feather microstructure and immunoreactivity, consistent with the presence of durable epitopes of beta-keratin proteins comprising the feather matrix, were repeatedly demonstrated. Furthermore, although melanosomes were visible in both the room temperature control and 60^{o}C wet burial feathers, melanosomes were not observed in the dry burial at 350°C remains after ten years. This may be explained if: 1) beta-keratin is more resistant to degradation than the pigment-containing organelles, 2) we sampled rachises (except for the definitive barb in Fig 2), which were unpigmented in the control feathers, thus not expected to contain melanosomes in these specific feathers, or 3) the feather fragments analyzed for this condition were originally non-pigmented; however, the starting condition for these feathers were a mix of pigmented and unpigmented regions.

Data supporting molecular mechanisms that result in the preservation of these feathers under long-term degradation experiments is beyond the scope of this paper. However, we propose hypotheses for future testing that are suggested by our initial results. Rapid mineralization, usually microbially mediated, has been invoked as a primary agent for early stabilization of organic components before degradation can occur [39,40]. In this process, microbial overgrowth of decaying organics results in the secretion of exopolymeric substances (EPS) that are negatively charged [41,42], facilitating the deposition of positively charged mineral ions. However, this mechanism does not directly apply to this experiment, particularly to

the feather kept at 350°C, because it is doubtful that microbes would grow in such an environment. An alternative hypothesis is that these colored feathers underwent 'melanin leaching' during degradation [15]. Although we have no we have no morphological evidence for pigment containing melanosomes in any 350°C feather examined after this 10 year experiment, we propose that melanin pigment may have leached out of the organelles to disperse throughout the feather, acting as a fixative agent to prevent further degradation (J. Lindgren, pers. comm). This hypothesis is amenable to future testing.

In the recent literature, microbodies associated with fossil feathers have enthusiastically been ascribed to melanosomes. These structures are depicted in SEM (scanning electron microscopy) images as confluent, over-lapping structures ([25] and references therein). Contrary to those studies, the melanosomes observed in these partridge feathers, as well as chicken feathers from a previous study [43], were distinct and non-overlapping (Fig 3D) even after partial degradation (Fig 3E) and did not display the density and arrangement depicted in SEM images of structures purported to be melanosomes in fossil feathers. These contrasting observations illustrate the need for more taphonomic studies that explore the degradation of feathers and their microstructural components.

Because the data herein support the durability of keratin-derived structures as well as the persistence of original keratin epitopes under the harshest condition, the application of antibodies to identify and/or differentiate structures in the rock record is supported. Therefore we applied our antibodies to a specimen already shown to demonstrate microstructural and molecular preservation. In 1999, data were published to support the hypothesis that the fiber collected from the cervical region of the articulated *Shuvuuia deserti* specimen, an alvarezsaurid from Mongolia, was a feather-like structure [44]. These data included microscopic and immunohistochemical consistencies between the fossil and modern feather material [12]. Positive binding, localized to the *S. deserti* sample, was also observed using the custom-made primary antiserum employed in this study (Fig 7 A, B). The control condition, where no primary antibody was exposed to *S. deserti* fibers, but all other conditions kept identical to the test specimens, showed no signal (Fig 7 C, D and S4 Fig E, F). Furthermore, the inhibition control (discussed above), in which the primary antibody was applied after being exposed to extracted feather protein, resulted in a greatly reduced signal in the fossil tissue (S4 Fig C, D) compared to the positive control (S4 Fig A, B). This also testifies to the specificity of the signal to epitopes

consistent with beta-keratin. TEM images of the hollow, fossil fiber (refer to Fig 4 in [12]) demonstrated filaments 3nm in diameter, consistent in size with modern beta-keratin filaments [3]. No electron-dense microbodies consistent with melanosomes were observed, and the fibers were universally white *in situ*.

The positive binding observed in the fossil sample further demonstrates the specificity of our antibody as well as its potential to be used for paleontological studies. Repeating the results from the original study with a second and custom-made beta-keratin-specific antibody validates the previous results and attests to the endogeneity of the feather-like epitopes in an ancient sample. It also demonstrates the stability of a sample in LR white embedding medium at ambient conditions for many years. Finally no structures consistent with melanosomes were observed in this ancient specimen (see SEM and TEM results Fig 3 and 4 respectively in [12]), similar to the results from the 350°C condition in this study, but the preserved samples demonstrated microstructural and molecular integrity consistent with modern feathers.

Conclusions

Using heat as a proxy for time [27–30] we show that molecular and microstructural features of feathers comprised of beta-keratin proteins persist for long time periods under conditions harsher than most fossil material will endure; our data also support their persistence in the fossil record over exceedingly long time spans at milder conditions. Thus, beta-keratin proteins are exceptional target molecules for paleontological studies.

As previously mentioned, numerous studies of fossil feathers have recently interpreted small microstructures as color-imparting melanosomes, based in part on the resistance to degradation of the pigment melanin, but in modern feathers, melanosomes are embedded in a keratin matrix, which our data suggest should also preserve, and under our experimental conditions preserve better than melanosomes. If keratin protein is more resistant to degradation than melanosomes, which has not been identified in the previously published studies of ancient feather samples, alternative hypotheses of a microbial origin for these preserved microstructures remain. Because of the wide distribution of microbes [45], their association with all degrading organic matter (e.g. [40,46]), and their demonstrated longevity (e.g. [47]), microbes indeed may be a more parsimonious explanation for their source. Thus, a microbial hypothesis must be eliminated with chemical data before interpretations of ancient color can be made.

We show that immunohistochemistry is one technique that can detect keratin and may be used in future studies to differentiate between a keratinous and a microbial origin for these materials. Furthermore the durability of keratin in feathers may be extended to other keratinous structures in the rock record that may be studied by these techniques. Both epidermally derived keratinous structures and expressions of color are key innovations in evolutionary history, and certainly contribute to the success of ancient organisms. Characterizing taphonomic transitions will provide more accurate interpretations of ancient organisms and the world with which they interacted. Only by studying and observing these processes in the lab can we then make predictions and assumptions about the fossilization processes that took place millions of years ago.

Methods and materials

The Hungarian partridge used in this study was taken in a hunt from private land. The bird was donated to the study and the landowner is since deceased. The species is neither protected nor endangered and is quite plentiful on the Montana prairies. No permissions were required because the bird was taken by a private citizen and was not killed for this study.

Feathers from a single Hungarian partridge (*Perdix perdix*) with rust, grey and white wing feathers, and body feathers of grey to rust (Fig 1) were subjected to four environmental conditions spanning a 10 year observation period. Feathers were plucked from a fresh-killed bird, covered to exclude dust, and maintained unaltered at room temperature (control feathers). For the other three conditions, feathers from the same bird were buried in fine-grained Judith River (JR) sand collected from a dinosaur excavation site to maintain as much consistency as possible. The burial conditions were; 1) buried in saturated sand in a container with holes for draining, intermittently watered with distilled water (once daily to weekly on average), and incubated at 60°C for approximately 3 years, then allowed to dry and kept buried at RT for the remaining 7 years (wet burial), 2) buried in saturated sand, then baked at 350°C uninterrupted for 10 years (dry burial) and 3) the whole bird with attached feathers was placed in an ~1.5m hole in which ~6-8 inches (~15-20 cm) of JR sands were placed, then the bird carcass, then covered with remaining JR sands. The hole was dug in a drainage channel surrounded by rich peaty soil adjacent to a mountain pond (stream burial).

Temperature has been suggested in the literature to be a proxy for time in the degradation of organic molecules with the general trend that warmer and wetter conditions are detrimental to

molecule survival [27–30,48,49]. The temperatures employed in this study were chosen based on availability to instruments at a facility where temperature could be maintained for an extended period of time.

Upon completion of the experiment, all feathers were kept covered at room temperature until analysis. Although disarticulated bones from the fourth condition were recovered, no evidence of feathers remained. Barbs and barbules, rather than rachises, were sampled when possible for comparison between pigmented and unpigmented portions of the feathers.

Transmission electron microscopy (TEM)

Samples of feathers from the first three conditions of this taphonomic experiment, as well as a reddish-brown chicken feather and human fingernail (see Specificity Controls below), were collected and fixed in 10% neutral buffered formalin for a minimum of one hour at room temperature, followed by a PBS (phosphate-buffered saline) wash. From the control and 60°C wet burial conditions, white feather barbs and brown barbs were prepped and analyzed separately to assess any differences in degradation between pigmented and non-pigmented feathers. Samples were dehydrated in two changes of 70% ethanol, then incubated in (2:1) LR white: 70% ethanol to equilibrate, and infiltrated by incubating in three changes of LR white embedding medium. Each specimen and embedding medium were placed in a gelatin capsule, capped to exclude oxygen, and allowed to polymerize for 48 hours at 60°C. This embedding polymer was chosen because it is permeable, allowing penetration of antibodies (see below).

A piece of rachis from the 60°C wet burial condition was embedded in Spurr's medium to demonstrate that the internal pith structure of a rachis and barb are indistinguishable. The sample was fixed in a solution of formaldehyde and glutaraldehyde (4F:1G) overnight, rinsed with 0.1M PBS (pH 7.2), then post fixed with 1% osmium tetroxide in 0.1M PBS for 24 hours. After washing in PBS, the sample was serially dehydrated in acetone (30%, 50%, 70%, 90%, 100%) for 15 minutes at each concentration, then equilibrated in a graded series of Spurr's:acetone solutions (1:3 for 6 hours, 1:2 overnight, 1:1 for 3 hours and 3:1 for 3 hours). Following an overnight infiltration of the sample with pure Spurr's, the sample was embedded in a silicone mold and cured at 70°C for 48 hours.

Embedded feathers from each condition were sectioned to 90nm using a Leica EMUC6 ultra-microtome with a diamond knife, then mounted on 200 mesh copper grids and stained with 15% methanolic uranyl acetate and Reynold's lead citrate prior to imaging. Microstructure was

capable of being visualized without staining in the 350°C feather (Fig 4C, D). The feathers were imaged with a Zeiss Leo 912 TEM 100KV accelerating voltage with a Proscan 2048X2048 CCD (Olympus Soft Imaging System) (Fig 4 C, D) or an Erlangshen ES1000W Model 785 TEM coupled to a CCD 11Megapixel High-speed Digital Camera (Gatan Microscopy Suite (GMS) software) (Fig 3 and Fig 4 A, B).

In situ immunohistochemistry (IHC) - Immunofluorescence (IF)

Using the same LR white-embedded specimens sectioned for TEM (described above), 200nm sections were taken for IHC. Sections were transferred to a 6-well Teflon coated slide, dried on a plate warmer (45°C) and then allowed to fully dry overnight at 42°C.

The primary antiserum for this study is an affinity-purified, polyclonal rabbit anti-chicken feather antibody produced by Bio-Synthesis, Inc (Lot Number: AB1312-1). Except where specifically mentioned, all antibody tests reported here employ this custom-made antiserum. The immunogen was protein recovered from a white chicken primary flight feather, extracted with a buffer comprised of 20mM Tris-HCl (pH=8.5), 2.6 M thiourea, 5 M urea and 5% 2-mercaptoethanol (BME) [50]. One milliliter of the extracted protein solution was dialyzed (using 3500 MW snakeskin dialysis tubing) then resuspended in 15 mL PBS buffer (pH= 6.8). Two laboratory rabbits (BSYN 6733 & 6734) at Bio-Synthesis, Inc. were injected subcutaneously and intramuscularly, then boosted subcutaneously multiple times over 12 weeks. The final 12 week serum collection was purified using a protein-bounded affinity column to concentrate the antibody and remove non-specific components of the serum. Mature feathers are unique among keratinous structures in that approximately 80-90% of the protein is beta-keratin [8,9], therefore it can confidently be assumed the extracted protein used to immunize is primarily, if not entirely beta-keratin. Antibody reactivity (observed as green fluorescent signal) marks the presence of epitopes of feather beta-keratin expressed in tissues which are recognized by the antibody.

In situ IF was conducted to localize binding of the beta-keratin antibodies to epitopes within the feather samples. All incubations were performed at room temperature unless noted otherwise and separated by 2x5 minute washes using IHC phosphate buffered saline (PBS). To expose epitopes, sections were incubated for 15 min with 25 µg/µL Proteinase K in 1X PBS at 37˚C, followed by 3x10 minutes with 0.5 M ethylenediaminetetraacetic acid (EDTA) pH 8.0, which participates in antigen retrieval. Sections were incubated for 2x10 min with 1mg/mL $NaBH_4$, also an antigen retrieval method as well as to reduce autofluorescence, then with 4%

normal goat serum (NGS) in IHC PBS for four hours to block nonspecific binding sites. The primary antiserum was diluted in dilution buffer (1% bovine serum albumin (BSA), 0.1% cold fish skin gelatin, 0.5% Triton X-100, 0.05% sodium azide, 0.01M PBS (pH= 7.2-7.4)) at 1:100 dilution (unless otherwise noted), applied to all test samples and incubated overnight at 4°C. Controls consisting of identical tissues sectioned and treated as above were incubated with dilution buffer containing no primary antibodies in tandem with and under identical conditions as the test samples. This controlled for non-specific binding of secondary antibodies or detection agents.

After incubation with primary antiserum (or dilution buffer only), all remaining incubations were separated by two washes in PBS with 5% Tween20 wash buffer for 10 minutes, followed by two 10-minute washes in PBS to remove unbound antibody. All sections, including controls, were then incubated with secondary antibody (biotinylated goat anti-rabbit IgG(H+L) from Vector Laboratories, BA-1000, Lot-Y1228) diluted 1:500 in secondary dilution buffer (0.01M PBS (pH= 7.2), 0.05% Tween 20) for 2 hours. Fluorescein Avidin D (Vector laboratories, A-2001, Lot-W1124), diluted 1:1000 in secondary dilution buffer and incubated in darkness, was used to detect antibody-antigen complexes. Slides were mounted with Vectashield mounting media (Vector laboratories, H-1000, Lot-Y0417), coverslips applied, and sections visualized using a Zeiss Axioskop 2 plus biological microscope.

Images were captured using an AxioCam MRc 5 (Zeiss) with 10x ocular magnification on the Axioskop 2 plus using Axiovision software package (version 4.7.0.0). For each antibody test, all images were acquired with the same data acquisition parameters unless otherwise noted here. Control and 60°C feather images were collected at 30ms exposure and the 350°C images were captured at 100ms exposure. At 100ms, the control and 60°C images were over-exposed and therefore the exposure was reduced. All other data acquisition parameters were kept identical amongst the respective images. The images in Fig 6 of the 350°C barb were captured at the same magnification and exposure as the images of the other 350°C sample in Fig 5, however required minimally modified acquisition parameters because of slightly higher background signal.

Antibody specificity controls

In addition to the application of all buffers and solutions as above, but without primary antiserum applied (secondary antiserum only control), additional steps to control for non-specific binding and to demonstrate specificity of antigen retrieval were performed. This included the

application of the primary antiserum as described above, to which was added extracted chicken feather proteins (1:200 dilution in a protein solution with ~1.75 mg of protein determined using a Pierce® BCA protein assay kit (Thermo Scientific, Product# 23227, Lot# OI193596)) to block binding sites and inhibit incubating antibodies. Then, this primary antiserum (now blocked by the protein solution) was incubated with brown chicken feather. A second control for specificity included application of an irrelevant primary antibody (anti-human elastin (courtesy of R. Mecham), 1:500) not expected to have epitopes cross-reacting with feather antibodies.

To further demonstrate the specificity and application potential of our custom-made antibody, we tested it against fossil material from *Shuvuuia deserti* (IGM 100/977) [44] previously studied for the presence of feather-like structure and composition [12]. The same samples, already embedded and trimmed for sectioning, from the original study were used. In addition to maintaining consistency, this allowed for us to test the stability of an embedded sample remaining at ambient conditions for ~16 years. Tissues were prepped and immunohistochemical analyses performed identical to modern tissue (see Methods above) but in a separate lab with equipment and materials designated for working with ancient samples only. Thin sections (200nm) of *S. deserti* were tested against the anti-chicken feather antibody and a secondary antiserum only control was run in parallel. Images were captured at 80ms exposure and acquisition parameters were set to -.27 for brightness, 2.72 for contrast, 1.81 for gamma. Images were captured at the same magnification but altered acquisition parameters than modern sections because of different background signal. The antibody inhibition control, as described above for modern tissue, was also performed on a second sample of fossil tissue. These images were captures at the same exposure and magnification as the other fossil sample. However, the primary antiserum was applied at 1:200 dilution, to keep consistent with the inhibition dilution, and acquisition parameters were set to -.09 for brightness, 9.00 for contrast, 1.45 for gamma.

To show that our antiserum does not cross-react with alpha-keratin epitopes (thus refuting the hypothesis that *in situ* binding results from human contamination), human fingernail was embedded and sectioned as described above and used as antigen in identical experiments. Fingernail sections were exposed to our custom-made antiserum (1:200 dilution) as well as a polyclonal rabbit anti-alpha-keratin antibody (1:200 dilution) (provided by L. Knapp).

To demonstrate repeatability and accuracy of results, we performed all assays an average of three times.

References

1. Sawyer, R. H. & Knapp, L. W. 2003 Avian skin development and the evolutionary origin of feathers. *J. Exp. Zool. Part B Mol. Dev. Evol.* **298B**, 57–72. (doi:10.1002/jez.b.26)

2. Alibardi, L. & Sawyer, R. H. 2002 Immunocytochemical analysis of beta keratins in the epidermis of chelonians, lepidosaurians, and archosaurians. *J. Exp. Zool.* **293**, 27–38. (doi:10.1002/jez.10145)

3. Greenwold, M. J. & Sawyer, R. H. 2013 Molecular evolution and expression of archosaurian β-keratins: diversification and expansion of archosaurian β-keratins and the origin of feather β-keratins. *J. Exp. Zool. B. Mol. Dev. Evol.* **320**, 393–405. (doi:10.1002/jez.b.22514)

4. Strasser, B., Mlitz, V., Hermann, M., Tschachler, E. & Eckhart, L. 2015 Convergent evolution of cysteine-rich proteins in feathers and hair. *BMC Evol. Biol.* **15**, 82. (doi:10.1186/s12862-015-0360-y)

5. Fraser, R. D. & Parry, D. A. 2011 The structural basis of the filament-matrix texture in the avian/reptilian group of hard beta-keratins. *J Struct Biol* **173**, 391–405. (doi:S1047-8477(10)00289-3 [pii]10.1016/j.jsb.2010.09.020 [doi])

6. Fraser, R. D. B. & Parry, D. A. D. 2008 Molecular packing in the feather keratin filament. *J. Struct. Biol.* **162**, 1–13.

7. Eglinton, G. & Logan, G. A. 1991 Molecular preservation. *Philos. Trans. R. Soc. Lond. B. Biol. Sci.* **333**, 315–27; discussion 327–8. (doi:10.1098/rstb.1991.0081)

8. Stettenheim, P. R. 2000 The Integumentary Morphology of Modern Birds--An Overview. *Integr. Comp. Biol.* **40**, 461–477. (doi:10.1093/icb/40.4.461)

9. Cai, C. & Zheng, X. 2009 Medium optimization for keratinase production in hair substrate by a new Bacillus subtilis KD-N2 using response surface methodology. *J. Ind. Microbiol. Biotechnol.* **36**, 875–83. (doi:10.1007/s10295-009-0565-4)

10. Holthaus, K. B. et al. 2015 Comparative genomics identifies epidermal proteins associated with the evolution of the turtle shell. *Mol. Biol. Evol.* , msv265. (doi:10.1093/molbev/msv265)

11. Alibardi, L. 2015 Immunolocalization of sulfhydryl oxidase in reptilian epidermis indicates that the enzyme participates mainly to the hardening process of the beta-corneous layer. *Protoplasma* **252**, 1529–36. (doi:10.1007/s00709-015-0782-9)

12. Schweitzer, M. H., Watt, J. A., Avci, R., Knapp, L., Chiappe, L., Norell, M. & Marshall, M. 1999 Beta-keratin specific immunological reactivity in feather-like structures of the Cretaceous Alvarezsaurid, Shuvuuia deserti. *J. Exp. Zool.* **285**, 146–157. (doi:10.1002/(sici)1097-010x(19990815)285:2<146::aid-jez7>3.0.co;2-a)

13. Schweitzer, M. H., Watt, J. A., Avci, R., Forster, C. A., Krause, D. W., Knapp, L., Rogers, R. R., Beech, I. & Marshall, M. 1999 Keratin Immunoreactivity in the Late Cretaceous Bird Rahonavis ostromi. *J. Vertebr. Paleontol.* **19**, 712–722.

14. Manning, P. L. et al. 2013 Synchrotron-based chemical imaging reveals plumage patterns in a 150 million year old early bird. *J. Anal. At. Spectrom.* **28**, 1024–1030. (doi:10.1039/C3JA50077B)

15. Lindgren, J. et al. 2015 Molecular composition and ultrastructure of Jurassic paravian feathers. *Sci. Rep.* **5**, 13520. (doi:10.1038/srep13520)

16. Schweitzer, M. H. 2011 Soft Tissue Preservation in Terrestrial Mesozoic Vertebrates. *Annu. Rev. Earth Planet. Sci.* **39**, 187–216. (doi:doi:10.1146/annurev-earth-040610-133502)

17. Davis, P. G. & Briggs, D. E. G. 1995 Fossilization of feathers. *Geology* **23**, 783–786. (doi:10.1130/0091-7613(1995)023<0783:fof>2.3.co;2)

18. Lucas, A. M. & Stettenheim, P. R. 1972 *Avian Anatomy - Integument*. Washington, DC.

19. Hitchcock, E. 1841 *Final Report on the Geology of Massachusetts: In Four Parts: I. Economical Geology. II. Scenographical Geology. III. Scientific Geology. IV. Elementary Geology. With an Appended Catalogue of the Specimens of Rocks and Minerals in the State Collection, Vol*. J.S. & C. Adams. [cited 2014 Jul. 10].

20. Osborn, H. F. 1911 A dinosaur mummy. *Am. Museum J.* , 7–11.

21. Carvalho, I. de S., Novas, F. E., Agnolín, F. L., Isasi, M. P., Freitas, F. I. & Andrade, J. A. 2015 A new genus and species of enantiornithine bird from the Early Cretaceous of Brazil. *Brazilian J. Geol.* **45**, 161–171. (doi:10.1590/23174889201500020001)

22. de Souza Carvalho, I., Novas, F. E., Agnolín, F. L., Isasi, M. P., Freitas, F. I. & Andrade, J. A. 2015 A Mesozoic bird from Gondwana preserving feathers. *Nat. Commun.* **6**, 7141. (doi:10.1038/ncomms8141)

23. Navalón, G., Marugán-Lobón, J., Chiappe, L. M., Luis Sanz, J. & Buscalioni, Á. D. 2015 Soft-tissue and dermal arrangement in the wing of an Early Cretaceous bird: Implications for the evolution of avian flight. *Sci. Rep.* **5**, 14864. (doi:10.1038/srep14864)

24. O'Connor, J. & Zhou, Z. 2015 Early evolution of the biological bird: perspectives from new fossil discoveries in China. *J. Ornithol.* (doi:10.1007/s10336-015-1222-5)

25. Vinther, J. 2015 A guide to the field of palaeo colour: Melanin and other pigments can fossilise: Reconstructing colour patterns from ancient organisms can give new insights to ecology and behaviour. *BioEssays* **37**, 643–656. (doi:10.1002/bies.201500018)

26. Schweitzer, M. H., Lindgren, J. & Moyer, A. E. 2015 Melanosomes and ancient coloration re-examined: A response to Vinther 2015 (DOI 10.1002/bies.201500018). *BioEssays* , n/a–n/a. (doi:10.1002/bies.201500061)

27. Allentoft, M. E. et al. 2012 The half-life of DNA in bone: measuring decay kinetics in 158 dated fossils. *Proc. Biol. Sci.* **279**, 4724–33. (doi:10.1098/rspb.2012.1745)

28. Willerslev, E. & Cooper, A. 2005 Ancient DNA. *Proc. Biol. Sci.* **272**, 3–16. (doi:10.1098/rspb.2004.2813)

29. Willerslev, E., Hansen, A. J. & Poinar, H. N. 2004 Isolation of nucleic acids and cultures from fossil ice and permafrost. *Trends Ecol. Evol.* **19**, 141–7. (doi:10.1016/j.tree.2003.11.010)

30. Lindahl, T. 1993 Instability and decay of the primary structure of DNA. *Nature* **362**, 709–15. (doi:10.1038/362709a0)

31. Eliason, C. M., Bitton, P.-P. & Shawkey, M. D. 2013 How hollow melanosomes affect iridescent colour production in birds. *Proc. Biol. Sci.* **280**, 20131505. (doi:10.1098/rspb.2013.1505)

32. Shawkey, M. D., D'Alba, L., Xiao, M., Schutte, M. & Buchholz, R. 2015 Ontogeny of an iridescent nanostructure composed of hollow melanosomes. *J. Morphol.* **276**, 374–384. (doi:10.1002/jmor.20347)

33. Greenwold, M. J., Bao, W., Jarvis, E. D., Hu, H., Li, C., Gilbert, M., Zhang, G. & Sawyer, R. H. 2014 Dynamic evolution of the alpha (α) and beta (β) keratins has accompanied integument diversification and the adaptation of birds into novel lifestyles. *BMC Evol. Biol.* **14**, 249. (doi:10.1186/s12862-014-0249-1)

34. Ng, C. S. et al. 2012 The chicken frizzle feather is due to an alpha-keratin (KRT75) mutation that causes a defective rachis. *PLoS Genet* **8**, e1002748. (doi:10.1371/journal.pgen.1002748 [doi]PGENETICS-D-11-02513 [pii])

35. Chen, C.-F., Foley, J., Tang, P.-C., Li, A., Jiang, T. X., Wu, P., Widelitz, R. B. & Chuong, C. M. 2015 Development, regeneration, and evolution of feathers. *Annu. Rev. Anim. Biosci.* **3**, 169–95. (doi:10.1146/annurev-animal-022513-114127)

36. Symondson, W. 1999 Amplified detection, using a monoclonal antibody, of an aphid-specific epitope exposed during digestion in the gut of a predator. *Insect Biochem. Mol. Biol.* **29**, 873–882. (doi:10.1016/S0965-1748(99)00063-6)

37. Goldstein, G., Flory, K. R., Browne, B. A., Majid, S., Ichida, J. M. & Burtt Jr., E. H. 2004 Bacterial Degradation of Black and White Feathers. *Auk* **121**, 656–659.

38. Gunderson, A. R., Frame, A. M., Swaddle, J. P. & Forsyth, M. H. 2008 Resistance of melanized feathers to bacterial degradation: Is it really so black and white? *J. Avian Biol.* **39**, 539–545. (doi:10.1111/j.0908-8857.2008.04413.x)

39. Briggs, D. E. G. 1995 Experimental taphonomy. *Palaios* **10**, 539–550. (doi:10.2307/3515093)

40. Briggs, D. E. G. 2003 The role of decay and mineralization in the preservation of soft-bodied fossils. *Annu. Rev. Earth Planet. Sci.* **31**, 275–301. (doi:doi:10.1146/annurev.earth.31.100901.144746)

41. Flemming, H.-C. & Wingender, J. 2010 The biofilm matrix. *Nat. Rev. Microbiol.* **8**, 623–633. (doi:10.1080/0892701031000072190)

42. Pacton, M., Fiet, N. & Gorin, G. E. 2007 Bacterial Activity and Preservation of Sedimentary Organic Matter: The Role of Exopolymeric Substances. *Geomicrobiol. J.* **24**, 571–581. (doi:10.1080/01490450701672042)

43. Moyer, A. E., Zheng, W., Johnson, E. A., Lamanna, M. C., Li, D.-Q., Lacovara, K. J. &

Schweitzer, M. H. 2014 Melanosomes or microbes: testing an alternative hypothesis for the origin of microbodies in fossil feathers. *Sci. Rep.* **4**, 4233. (doi:10.1038/srep04233)

44. Chiappe, L. M., Norell, M. A. & Clark, J. M. 1998 The skull of a relative of the stem-group bird Mononykus. *Nature* **392**, 275–278. (doi:10.1038/32642)

45. Whitman, W. B., Coleman, D. C. & Wiebe, W. J. 1998 Prokaryotes: the unseen majority. *Proc. Natl. Acad. Sci. U. S. A.* **95**, 6578–83.

46. Dent, B. B., Forbes, S. L. & Stuart, B. H. 2004 Review of human decomposition processes in soil. *Environ. Geol.* **45**, 576–585. (doi:10.1007/s00254-003-0913-z)

47. Westall, F., de Wit, M. J., Dann, J., van der Gaast, S., de Ronde, C. E. J. & Gerneke, D. 2001 Early Archean fossil bacteria and biofilms in hydrothermally-influenced sediments from the Barberton greenstone belt, South Africa. *Precambrian Res.* **106**, 93–116.

48. Notbohm, H., Mosler, S., Bodo, M., Yang, C., Lehmann, H., Bätge, B. & Muller, P. K. 1992 Comparative study on the thermostability of collagen I of skin and bone: Influence of posttranslational hydroxylation of prolyl and lysyl residues. *J. Protein Chem.* **11**, 635–643. (doi:10.1007/BF01024964)

49. Collins, M. J., Walton, D. & King, A. 1998 The Geochemical Fate of Proteins. In *Nitrogen-Containing Macromolecules in the Bio- and Geosphere*, pp. 74–87. American Chemical Society. (doi:doi:10.1021/bk-1998-0707.ch006)

50. Fujii, T. & Li, D. 2008 Preparation and properties of protein films and particles from chicken feather citation export. *J. Biol. Macromol.* **8**, 48–55.

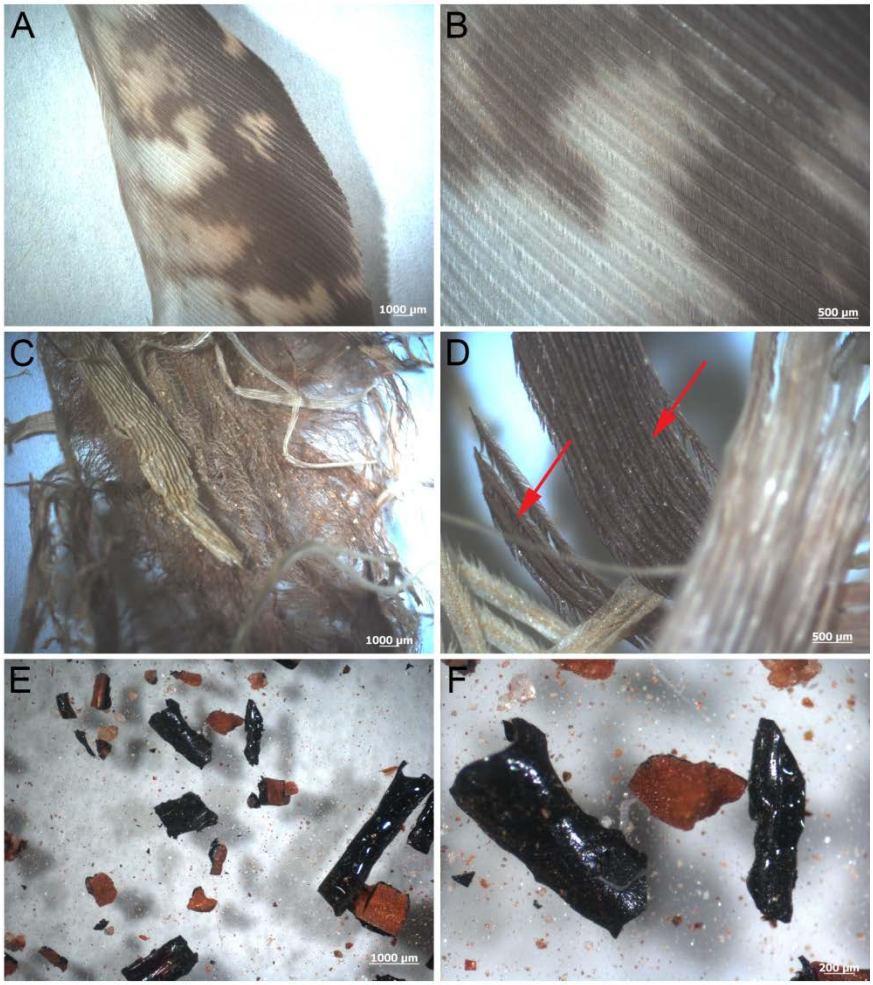

Figure 1. Feathers after 10 year exposure to several different environmental conditions. (A-B) Room temperature control feathers. Pigmented (reddish-brown) and non-pigmented (white to beige) patterning is visible with no signs of degradation. (C-D) Wet burial (60°C) feathers show signs of degradation and color change. Bands of pigmentation are still visible (arrows), although the white-beige parts appear more yellow and the patterning observed in control feathers are obscured. (E-F) 350°C feather pieces appear as small shiny black fragments which are associated with reddish-brown sediment. The pieces are not able to be identified to specific parts of the feather.

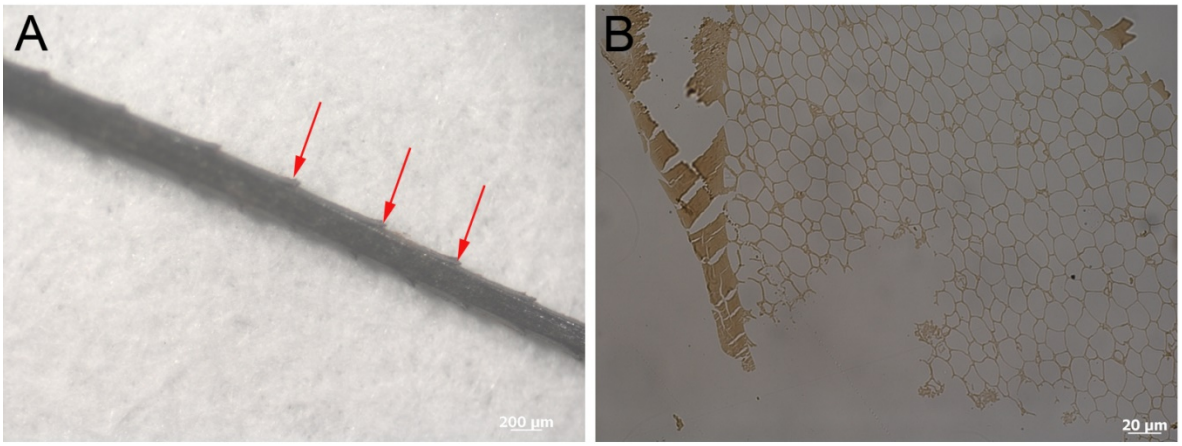

Figure 2. Barb fragment from 350°C feather. (A) Barb ramus retaining barbule protrusions (arrows) allows definitive identification as a barb fragment. Only the most proximal parts of the barbules can be observed where they branch from the ramus. (B) Transmitted light image of a 200nm thin section of a barb from the 350°C treated feather (similar to A) shows presence of external cortex (arrowhead) and inner pith observed as honey-comb texture.

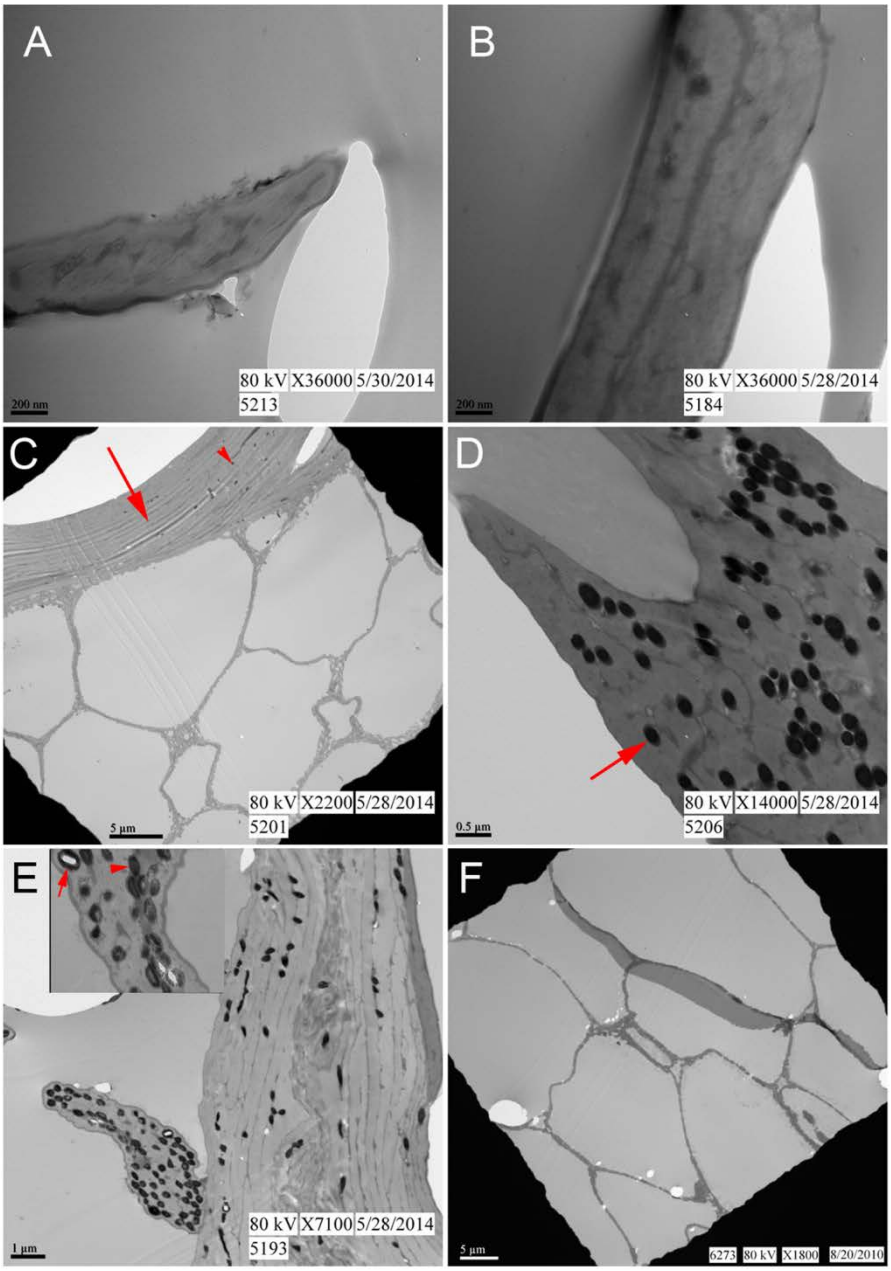

Figure 3. TEM images of feathers from varied conditions. (A-B) Represent unpigmented barbs from the control feather and 60°C feather respectively. (C- D) Brown barb and barbule from control feather. (C) Represents barb where cortex (arrow) and inner pith are visible. Note melanosomes (arrowhead) are sparse but present only in barb cortex. (D) Barbule with melanosomes (arrow) from control feather. (E) 60°C brown barb with barbule extending from the left side. Melanosomes are concentrated in the barbule and appear partially degraded as indicated by the less dense (arrowhead) and even 'hollow' (arrow) centers observed in the inset. (F) Pith from a rachis taken from the 60°C condition, embedded and sectioned separately (see Methods). Note: Whether pith derives from the rachis (F) or barb (C) is impossible to determine at this level of magnification.

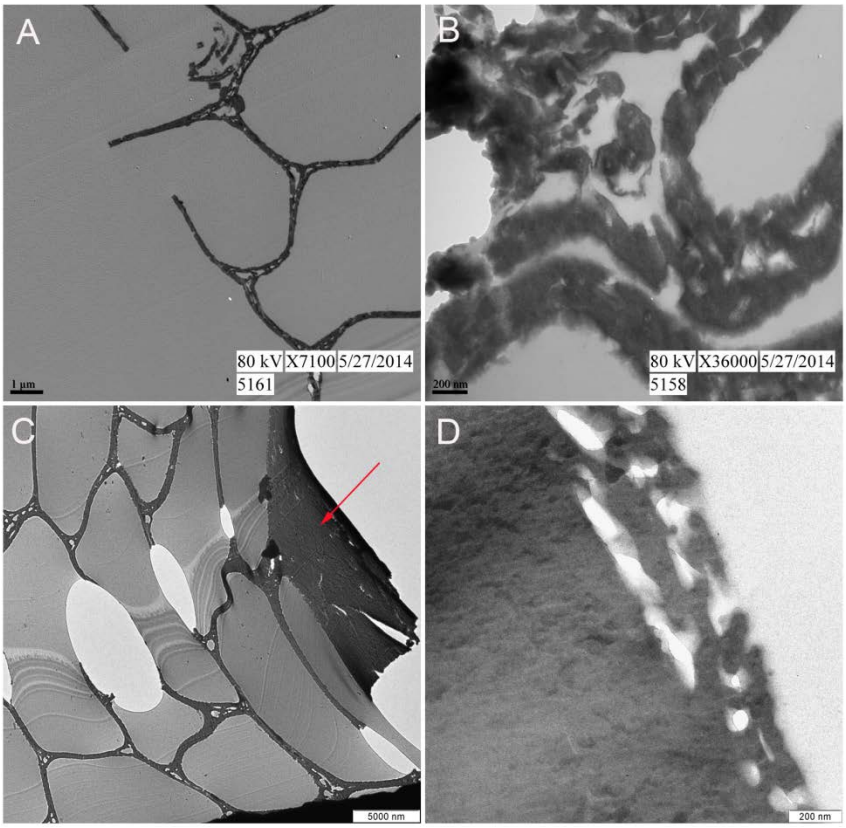

Figure 4. TEM images of 350°C feather fragments. (A-B) Unidentifiable piece of 350°C feather at lower and higher magnification, respectively. The honey-comb structure observed in (A) indicates it is the pith of either a barb or rachis. (C-D) Feather fragment positively identified as barb. (C) External cortex (arrow) and internal pith are observed. (D) At higher magnification no electron dense microbodies consistent with melanosomes are observed in the cortex.

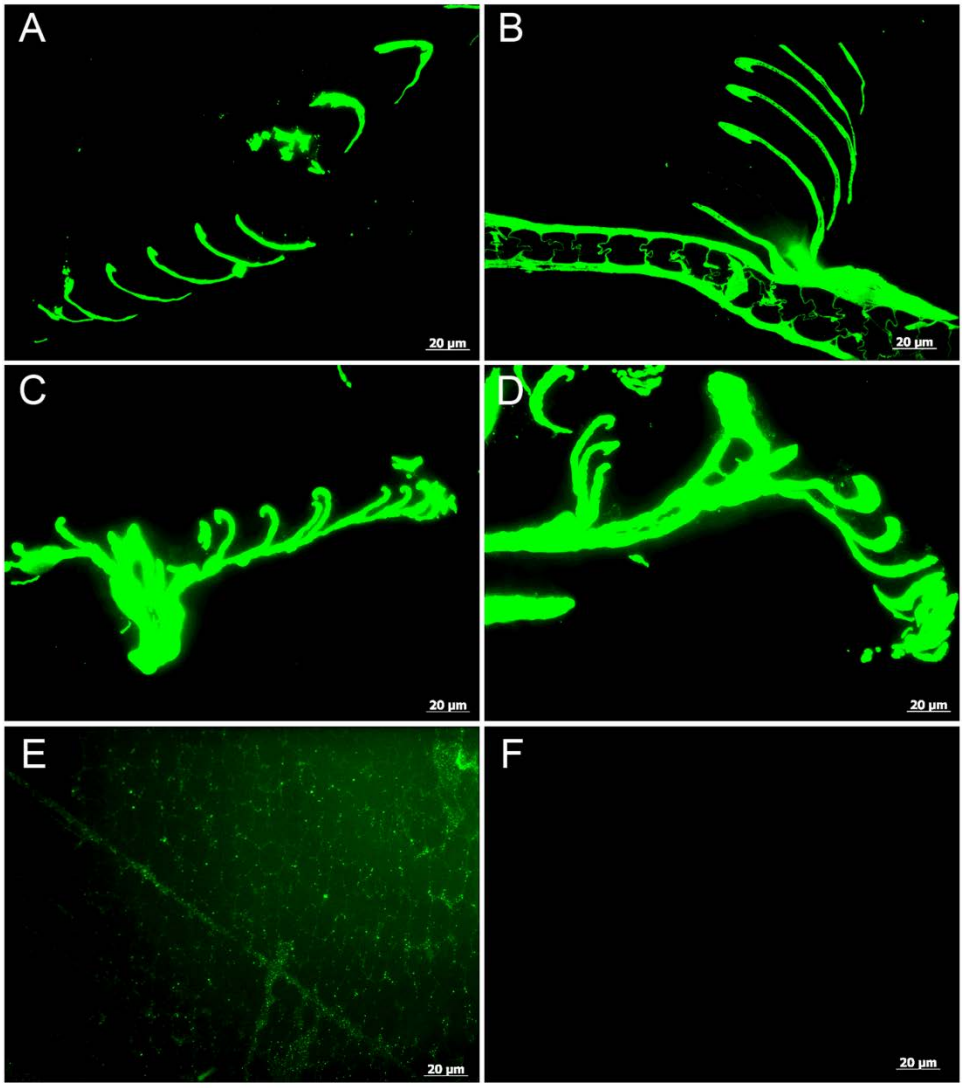

Figure 5. Localization of antibody antigen (ab—ag) complexes *in situ* on feathers exposed to varied conditions. (A-B) Control, (C-D) 60°C, and (E-F) 350°C feathers. White barbs (A and C) are compared with brown barbs (B and D) for both the control and 60°C conditions. There are no noticeable differences in strength of binding between the pigmented and non-pigmented barbs in either condition. Antibodies bind with greater avidity in the feathers treated at 60°C, consistent with what we have observed in samples from other experiments that are partially degraded. (E) Background signal in the 350°C condition is weak and diffuse but binding is greater than the secondary antiserum only negative control (F) and localized to the keratinous 'struts' within the pith.

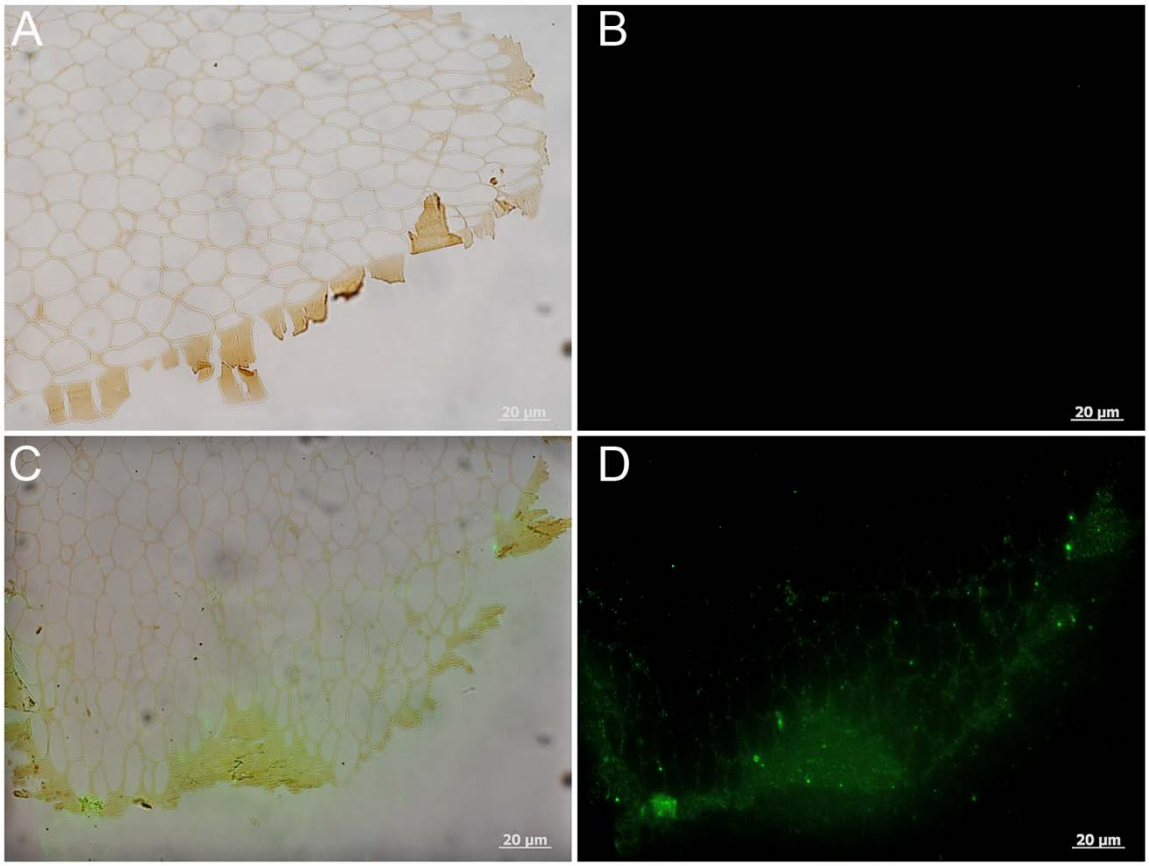

Figure 6. Localization of antibody antigen (ab—ag) complexes *in situ* on 350°C barb. (A-B) Secondary antibody only control shows no signal in the absence of the primary antiserum. (C-D) Positive binding of primary antibodies to the 350°C feather barb. Note that the diffuse signal is localized to the cortex (C-D) and the adjacent lattice structure of the pith.

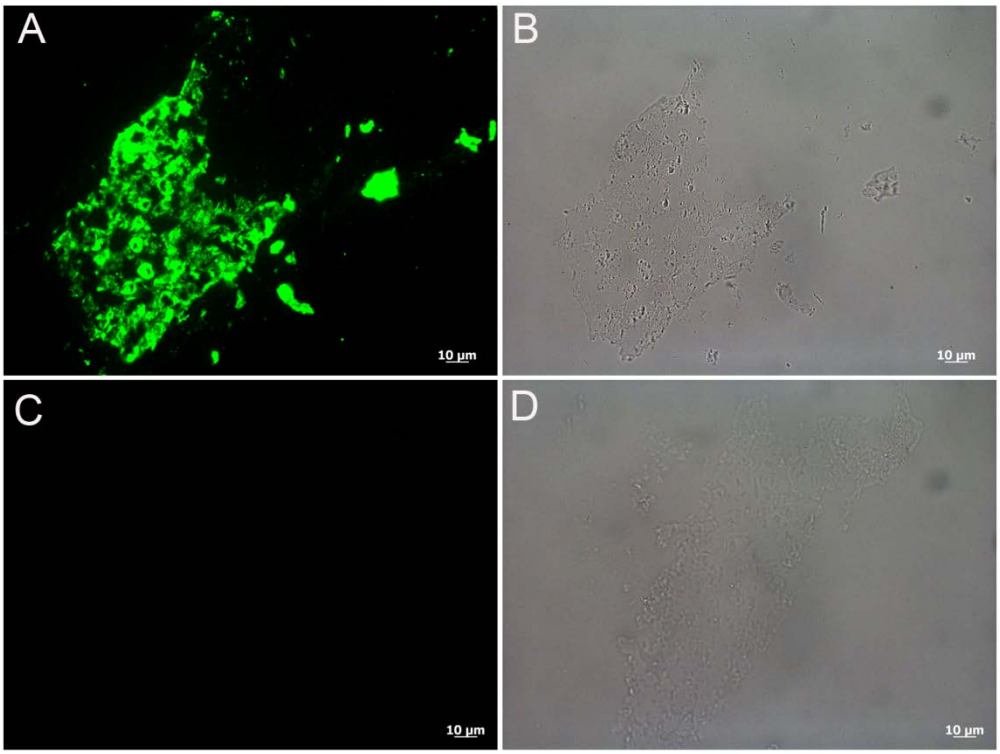

Figure 7. Localization of antibody antigen (ab—ag) complexes *in situ* on *Shuvuuia deserti* (IGM 100/977) filament. (A) Shows positive binding of the anti-chicken feather antiserum to the fossil tissue as indicated by the green fluorescent signal. (B) Demonstrates that the binding in A) is localized specifically to the tissue. (C and D) Secondary antiserum only control is negative and shows that the positive signal in A) is not due to spurious antibody binding.

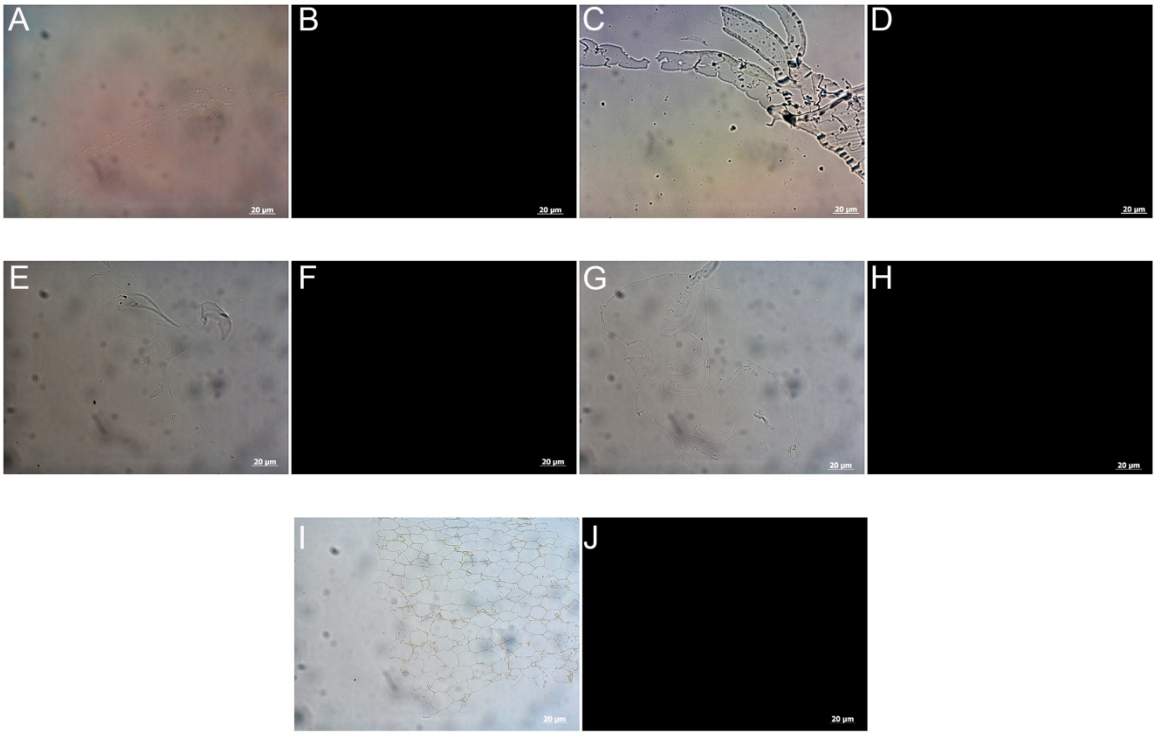

Figure S1. Immunological staining results for the secondary antibody only (negative) controls of feathers exposed to varied conditions. (A-D) Room temperature control feathers. (E-H) 60°C wet burial feathers and (I-J) 350°C dry burial. White barbs (A and B, E and F) and brown barbs (C and D, G and H) are both shown. The brightfield filter (A, C, E, G) reveals the presence of the tissue and the FITC filter (B, D, F, H, J) demonstrates the absence of fluorescence indicating a negative result. Because all other conditions were identical (for the same tissues tested in Fig 5), this controls for non-specific binding of the secondary antibody to the tissues. No signal observed in this control supports that the binding observed in Fig 5 is specific to the tissue recognized by the anti-feather primary antiserum.

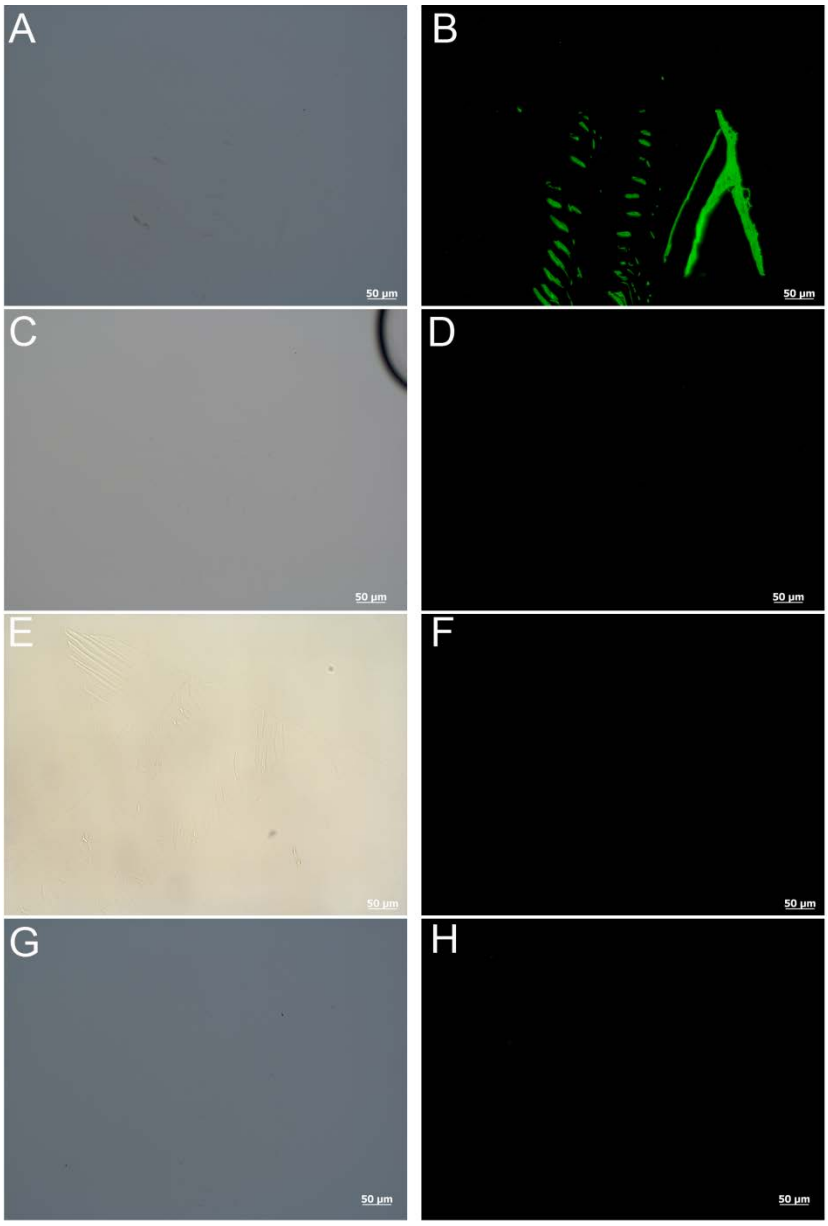

Figure S2. Immunological staining results from the specificity controls of the primary antibody on extant tissue. (A and B) The positive control using brown chicken feather tested against the anti-chicken feather primary antiserum (1:200 dilution). (C and D) Brown chicken feather subjected to the primary anti-chicken feather antibody after inhibition by incubating with extracted chicken feather protein (1:200 dilution, See Methods). The absence of binding, observed as the lack of fluorescence in D), shows that the antigen retrieval is specific to the keratinous tissue, because all binding sites were occupied by the specific antigen prior to exposure. (E and F) Feather incubated with anti-human elastin. As expected, binding is negative and negates the possibility that positive binding of the anti-chicken feather antibody is spurious or non-specific. (G and H) Negative control in which only the secondary antibody was applied, no primary antiserum, showing no binding as expected. Note: the artefact observed in the top right corner of image C is an air bubble.

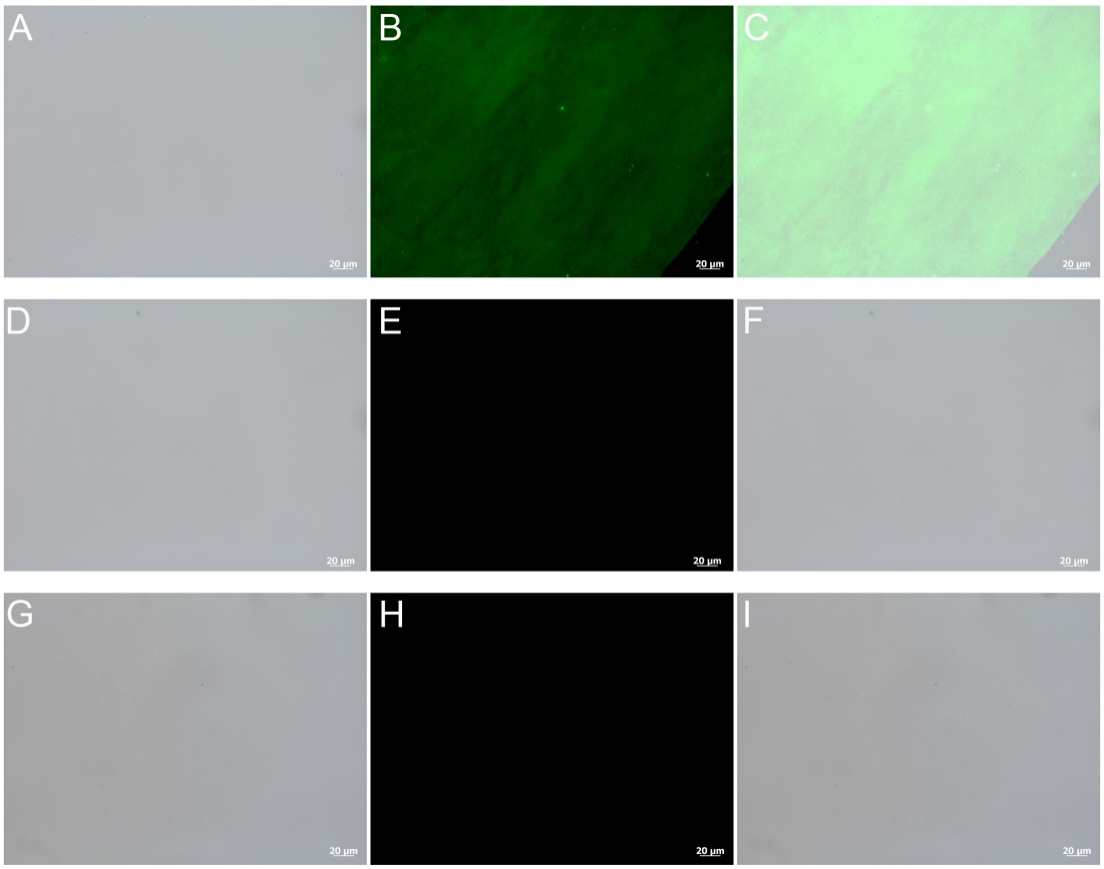

Figure S3. Immunological staining results from human fingernail tissue. (A-C) Sectioned human fingernail tissue tested against anti-rabbit alpha-keratin as a positive control. (E-F) Fingernail tissue tested against the anti-rabbit chicken feather protein. (G-I) Negative control in which 'secondary only' antibody applied. This test demonstrates that the custom made anti-chicken feather protein antibody does not bind human alpha-keratin thus ruling out a positive response due to human contamination.

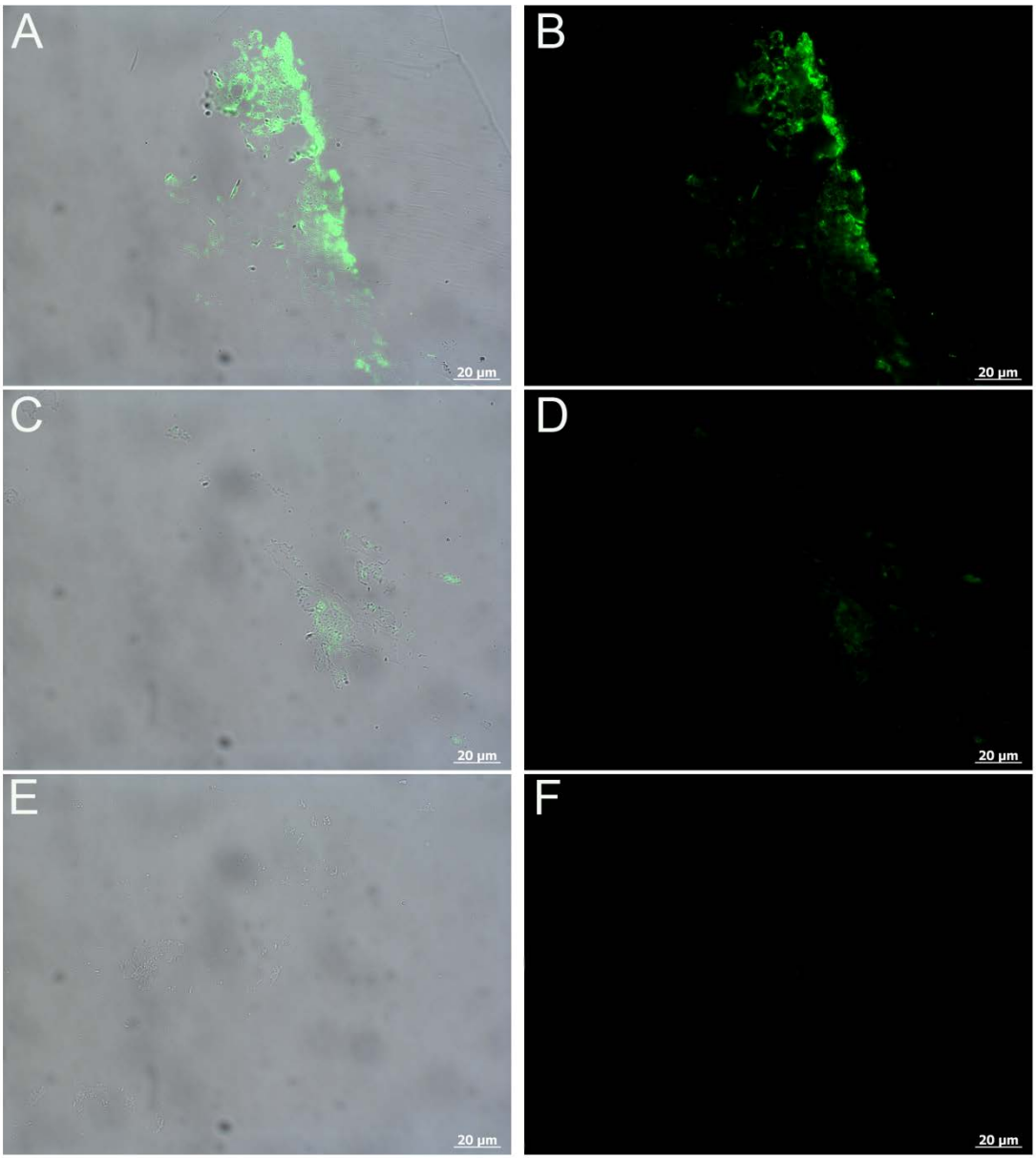

Figure S4. Immunological staining results from the inhibition control of the primary antibody on *S. deserti* tissue. (A and B) Positive control of fossil tissue tested against the primary anti-chicken feather antiserum (1:200 dilution). (C and D) Inhibition control where fossil tissue was incubated with the primary antiserum after it had been exposed to pure chicken feather antibodies (1:200 dilution) to block the active binding sites. Binding is greatly reduced demonstrating the positive binding observed in A and B is specific to epitopes consistent with beta-keratin proteins. (E and F) Negative control in which no primary antiserum, secondary antiserum only, was applied to the tissue.

CHAPTER 6 - Microscopic and immunohistochemical analyses of the claw of the nesting dinosaur, *Citipati osmolskae*

Abstract

Arguably one of the most well recognized Cretaceous fossils is *Citipati osmolskae* (MDC-P 100/979), an oviraptorid dinosaur discovered in brooding position on a nest of unhatched eggs. The original description of the specimen includes mention of a thin lens of white material extending from the manual claw of one of the digits. This material was proposed to be the remains of the original keratinous sheath covering the ungual. Keratin is not biomineralized, thus its three-dimensional presence suggested that original proteinaceous material may remain. Here, we use multiple techniques to test this hypothesis. Fossil material compared favorably in morphology and location to claw sheath tissues from extant birds, and microstructural organization similar to extant bird claw sheath was demonstrated using light microscopy and scanning and transmitted electron microscopy. In living birds, claw sheath material consists primarily of two structural proteins; alpha-keratin, expressed in all vertebrates, and beta-keratin, found only in reptiles and birds (sauropsids). Therefore, we employed immunological techniques using antibodies raised against avian feathers, which are comprised almost entirely of beta-keratin, to demonstrate that fossil tissues respond with the same specificity and as those from living birds. Controls were negative for binding. Furthermore, we show that calcium chelation greatly increased antibody reactivity, suggesting a role for calcium in the preservation of this fossil material.

Introduction

In 1995, paleontologists unveiled a remarkable specimen of an oviraptorid dinosaur (MDC-P 100/979) excavated in the Djadokhta Formation, Ukhaa Tolgod locality, Mongolia, preserved in an upright position over a nest of unhatched eggs [1,2]. In 2001, this specimen (MDC-P 100/979) became the referred specimen for *Citipati osmolskae* [3]. Its arms extend and are wrapped around the nest while the hindlimbs are tucked underneath the body and lie parallel to the eggs [1]. The specimen is entombed by amorphous, massive sandstone. A dune-originated sandslide event was interpreted to be the proximal cause of death, based upon the sedimentary context of the Djadokhta Formation and the upright position of the specimen [4]. The Ukhaa Tolgod site is estimated to be upper Campanian in age [4,5].

In the description of this specimen [1,2] a thin lens of material was described as extending from the manual digit (figure 1a). It differed in texture and color from both the surrounding sandstone matrix and the bone, and was proposed to be remnants of the claw sheath, which in living animals covers the ungual bone and consists primarily of keratin proteins. Unlike bone, keratinous structures are not biomineralized, thus the preservation of this material suggested the possibility that original organic material persisted.

Here we test this hypothesis using multiple techniques, including scanning electron microscopy (SEM) coupled with energy dispersive X-ray spectroscopy (SEM-EDS), transmission electron microscopy (TEM), and *in situ* immunohistochemistry (IHC). If original, endogenous keratinous material persists, we predict microstructural features similar to those of comparable extant tissues will be retained. Additionally, if original molecules are preserved in these tissues, they will show reactivity when exposed to antibodies raised against keratin proteins similar to modern claw sheath material.

There are two major families of keratins: alpha- and beta-keratins. Alpha-keratins are intracellular proteins derived from intermediate filaments originating from the cytoskeleton [6], and are widely distributed across all vertebrates, consistent with an early origin of this gene family. Alpha-keratin is comprised of an alpha-helical central rod, a 10nm intermediate filament [7].

The beta-keratin multigene family is expressed only in reptiles and birds (sauropsids) [8–10], suggesting that this gene family originated after the divergence of sauropsids from other vertebrates [6,11–13]. It is likely its evolution correlates with niche filling after the transition of animals out of the water and onto land [14]. The sauropsid beta-keratins consist of chains of twisted (beta) pleated sheets in a non-uniform (both parallel and anti-parallel) direction [15,16].

These beta-keratins are insoluble, rigid, fibrous structural proteins distinct from the alpha-keratins produced by all vertebrates, including mammals. Monomeric beta-keratin forms filaments or microfibrils 3 nm in diameter [15]. All beta-keratin proteins share a ~30 amino acid core which conveys hardness to the molecule and is highly hydrophobic due to the presence of amino acids such as proline and valine [8,15,17,18].

All keratins contain the amino acid cysteine, and thus are high in sulfur, which distinguishes them from other structural proteins [19]. Although alpha-keratins exist as both low sulfur proteins, (“soft” keratins like skins), and high sulfur proteins, (“hard” keratins like hair

and nails) [7,19,20], beta-keratins incorporate high levels of the sulfur-containing amino acid, cysteine, and thus have a sulfur content and amino acid composition more similar to the hard alpha-keratins [12,19]. In mature form these become highly cross-linked through formation of disulfide bonds [16], which also confers rigidity and hardness to the proteins.

The claw sheath of modern birds is composed primarily of keratinous structural proteins. The outermost cornified layer is comprised mostly of beta-keratin, which is underlain by a more pliable and softer layer where primarily alpha-keratin is expressed [21–23]. Some scientists in recent publications refer to these beta-keratin proteins as 'corneous beta proteins' however[24–26] the majority of scientists in the literature continue to characterize them as beta-keratins and therefore we employ the commonly used term throughout this paper.

As demonstrated in two earlier studies [27,28], and suggested by others [29–31], the composition and structure of beta-keratin makes it amenable for use in analyzing fossil material. Furthermore, because this protein is not found in humans and is vertebrate specific, its identification using the methods we employ cannot be ascribed to human or microbial contamination, and when used with adequate controls is a good indicator of endogeneity.

We performed scanning and transmission electron microscopy to compare microstructure and histology of the fossil material from MDC-P 100/979 with homologous extant claw sheath from emu and ostrich. An affinity purified, custom-made primary antibody raised against protein extracted from chicken feathers (comprised primarily of beta-keratin in mature form [32,33]) was employed to localize antibody-antigen complexes to dinosaur tissue in *in situ* immunohistochemical studies.

Results

In addition to location and gross morphology, microstructural similarities between the fossil claw material and the extant emu and ostrich claws supported the hypothesis that original keratinous tissue has been preserved in the *Citipati* specimen. The purported fossil claw tissue was observed as the white material (figure 1b, c, arrow) surrounded by reddish sandstone grains (figure 1b, c, arrowheads). SEM images of this white material indicated the presence of thin, plate-like layers similar to those observed in the extant emu claw sheath (figure 2). In both fossil and extant claw, a rugose texture covering the entire surface was observed. In the emu claw (figure 2a) the rugosity was observed as a mat of finger-like projections. Similar projections were observed in a smaller region of the *Citipati* claw but were much less pronounced (figure 2b,

arrow) than the modern comparison. See below for discussion of the origin of this textured appearance.

Energy dispersive X-ray spectroscopy (EDS) data indicated the fossil dinosaur claw material had an elemental composition dominated by oxygen and calcium (figure 3), unlike the extant emu claw in which no calcium was detected (figure 4). Although the EDS scan was performed at a higher magnification (1000x) for the emu claw than the scan on *Citipati* claw (250x), a scan performed at 250x on an uncoated spot of the superficial surface of the emu claw resulted in the same elemental observations (data not shown). Carbon, oxygen and sulfur were the most abundant elements in the emu claw (figure 4), representing ~97% of the X-rays detected. Although carbon was much higher in the emu claw, reflecting the highly organic composition of this material, carbon was also the third most abundant element in fossil material as well. The other elements detected in the fossil claw were carbon, phosphorous, zirconium and silicon, along with oxygen and calcium which represented ~97% of the X-rays detected (figure 3). Quantitative data (Table 1) showed the amount of calcium in the sediment surrounding the fossil claw (figure S2) was greatly reduced relative to that seen in the fossil claw material.

Parallel-oriented fibers were observed in both fossil and extant claw tissues when compared under TEM (figure 5). The fibers occasionally separated to form irregularly spaced openings (figure 5a, b, yellow outlines) that did not reflect sectioning artifact but were part of the original structure.

Primary antiserum was shown to bind to keratinous tissues from both groups of living archosaurs, chicken and alligator (figure S4). Binding was also localized to the *Citipati* tissue, but was decreased from that observed in extant counterparts, which may have resulted from incorporation of less tissue in sections of the fossil sample relative to extant ostrich claw tissue and/or preservation of fewer epitopes. Furthermore, the binding in the alligator skin was localized to the outermost layer of the epidermis, stratum corneum, where beta-keratin dominates [17], and not the underlying layers which are composed primarily of alpha-keratin (and other non-keratinous proteins) [23].

No binding was observed in any of the negative controls (figures S5-S7) used to demonstrate antibody specificity.

The secondary antibody only controls were uniformly negative for all tissue and antisera tested, indicating that the secondary antibodies did not react in an unspecific manner to the tissues tested.

Discussion

We tested the hypothesis that original claw components were preserved in the *Citipati* specimen using microstructural and biochemical methods.

Histological micro- and ultrastructure of the *Citipati* claw material observed in both SEM and TEM was consistent with that of extant emu and ostrich claw sheath. It is likely the rugosity and structures observed in the SEM images of the *Citipati* claw and ventral surface of the emu claw served to increase surface area, forming greater adhesion to the underlying bone for this proteinaceous tissue. Such rugosity on bony surfaces is often used as an osteological correlate to infer the presence of a keratinous covering in fossil specimens without soft tissue preservation, e.g. on the rostrum of dinosaurs with beaks [39–41], or covering the bony shield of the epiparietals in ceratopsians (e.g. [42,43]).

The similar voids observed in the TEM images of the ostrich claw and *Citipati* claw may resemble remnants of what were originally lipid droplets. The presence of lipid droplets in forming keratinous tissues cause fibers to compensate by forming such rounded openings which remain even after cornification [44]. The presence of lipid droplets and their remnants have been demonstrated in the skin and claw of modern ostrich tissue [44,45] as well as in a developing claw of an Australian skink [46] and scutate scale of a White Leghorn chick embryo [47].

Determining the mode of preservation is beyond the scope of this paper, but several aspects of our study suggest calcium may have played a role in the preservation of this dinosaur claw material. Calcium was not detected in emu claw sheath, and was detected at a much reduced amount in the sediment immediately surrounding the fossil relative to the fossil claw material. However, calcium was present as a calcium carbonate lens in the depositional environment in which the dinosaur was buried [48]. Thus, microbially mediated mobilization of either biological (i.e. from the underlying bone [27]) or environmental (from this lens) calcium may be stabilizing this keratin sheath before complete degradation can occur [49]. Future taphonomic experiments may elucidate the mechanisms and role of calcium in the preservation of claw tissue.

Although calcium may have played a role in preserving the organic residues detected by our methods, its *removal* was required to obtain positive immunohistochemical results as has been demonstrated in other experiments with heavy metal ions associated with fossil soft tissues [50]. Taphonomic experiments performed on extant blood vessels from ostrich showed that vessels exposed to iron were stable at room temperatures without further treatment for time periods orders of magnitude greater than vessels without such exposure. In that study, the use of an iron chelator treatment on dinosaur tissue increased the signal using immunohistochemistry, similar to the data presented here, where antibody binding was enhanced after chelation of calcium from the dinosaur claw tissue [50].

Because beta-keratin is not produced by mammals, nor are any keratin proteins produced by microbes [51], specific binding and localization of beta-keratin epitopes to these fossil tissues strongly supports the hypothesis that endogenous protein components are preserved in *Citipati*.

To test binding specificity, antiserum was applied to controls not expected to possess beta-keratin (e.g. decalcified ostrich bone); and, to control for spurious, nonspecific binding of primary antibodies, we show no reactivity when fossil claw was exposed to a non-relevant antibody, human elastin, which is not present in any keratinous tissue. Elastin antibodies do not react to extant (figure S5a, b) or fossil material (figure S6a, b), refuting the possibility that our antibodies were binding randomly, or that secondary antibodies were binding non-specifically. When antiserum was inhibited with purified keratin used as the immunogen, antibodies no longer bound to the tissue, resulting in negative binding and support the specificity of these antibodies for keratin epitopes present in the tissue (figures S5c,d and S6c, d).

When we tested this antiserum against decalcified ostrich bone, which does not contain keratin protein, no reactivity was seen (figure S7c, d). This lack of reactivity is not the result of damage to bone proteins, because chicken collagen antibodies demonstrated localized binding to the decalcified ostrich bone tissue (figure S7a, b).

Furthermore, localization of antibody-antigen complexes to the outermost layer of the alligator skin indicates that our custom-made antibody is specific to and cross-reacts with beta-keratin epitopes but not alpha-keratin (also see Fig S3 in Moyer et al. 2016 in review).This testifies to the use of antibodies to delineate compositional differences in tissue.

Keratinous tissues preserved with fossils are rare, and in general the amount of available working material is much less than that recovered from fossil bone or other biomineralized

remains. This limits the methods that can be employed to analyze samples, and requires applying the most specific methods possible that use the least amount of material. This in turn precludes chemical extraction of bulk tissues to recover proteins for use in electrophoretic separation methods, and/or mass spectrometry analyses to ultimately obtain sequence information. However, *in situ* immunohistochemical analyses demonstrate localization of specific epitopes within fossil tissues, and, when used with appropriate controls, can also be utilized to argue for endogeneity over contaminant signal. Furthermore, when antibodies support the presence of endogenous proteins, mass spectrometry techniques can be coupled with immunoprecipitation experiments, to isolate and concentrate proteins, to analyze the binding characteristics of the primary antibody which can elucidate specific information on epitope retrieval.

Because these keratinous tissues are often preserved as small, thin structures (compared to skeletal material), they are susceptible to destruction during preparation; our study calls for an increased awareness on the part of both paleontologists and preparators that these proteinaceous structures may be preserved, particularly when other aspects of the specimen, including articulation and three-dimensional preservation as seen in this *Citipati* specimen, indicate that exceptional taphonomic conditions prevailed. Molecular remains, even associated with minute tissues, have potential to elucidate aspects of the biology of these extinct animals that are otherwise unapproachable. Although conventional wisdom challenges the preservation of endogenous molecular remains, our combined data support the presence of original, proteinaceous material associated with this specimen, and add to the growing body of literature supporting molecular preservation in fossil materials across geological time.

Conclusions

Our study supports the preservation of original claw material in this approximately 75 million year old oviraptorid dinosaur, *Citipati osmolskae* (MDC-P 100/979), using electron microscopy and *in situ* immunofluorescence. Using extant emu and ostrich claw tissues as modern comparisons, we have shown that the fossil claw material retains microstructure consistent with keratinous tissues. Antiserum specific for sauropsid beta-keratins demonstrates positive binding to these fossil tissues, while all appropriate controls are negative. This study adds to the growing number of publications demonstrating that beta-keratins are an ideal target for molecular paleontological studies. Although, often, the amount of fossil material available to work with associated with keratinous remains is minute, as technology advances and sample

preparation methods improve we will be able to elucidate the early evolutionary history of beta-keratin which remains uncertain when only data from extant material are studied.

Methods and materials

For our analyses, fossil samples were handled at all times using gloves and sterile materials and instruments, and only in lab space designated for experimentation of ancient specimens (separated from all modern tissues used as controls). Dinosaur claw samples were compared with extant emu and ostrich claw sheath. For efficiency, we employed emu for scanning electron microscopy analyses and ostrich for transmission electron microscopy and immunohistochemical analyses. Little variation between ostrich and emu claw samples was expected because of their close relationship (both 'ratite' members of the superorder Paleognathae) [34], similar cursorial life style [35] and similar gross morphology.

Experimental parameters between ancient and modern samples were identical, but samples were always treated in separate lab space.

Scanning electron microscopy (SEM) coupled with energy dispersive X-ray spectroscopy (EDS)

A fragment of the fibrous material associated with the *Citipati osmolskae* (MDC-P 100/979) ungual (figure 1b-c) was subjected to SEM prior to embedding for analyses and compared with a ~2mm fragment of emu claw sheath, taken from the dorsal proximal region of emu claw (figure 1d). The ventral surface adjacent to the bone (more protected from contamination) was analyzed.

Samples were mounted on double-sided carbon tape and imaged using a JEOL JSM-6010LA analytical SEM controlled by JEOL InTouchScope version 1.05A software. The mount and forceps used for the fossil sample were cleaned by sonicating in an acetone (100%) bath for 5 minutes, followed by a five minute ethanol (100%) bath. Fossil material was not coated but emu claw images were captured after applying a 3–6 nm gold/palladium coating for charge compensation.

All EDS data were collected at 20 and 10 kV accelerating voltage (for extant and fossil material, respectively), a working distance of 10 mm and for 100–120 seconds.

Transmission electron microscopy (TEM)

After SEM imaging, the same *Citipati* fragment was embedded in LR white for TEM analyses. A sterile hypodermic needle and ethanol (100%) were used to remove sediment grains

from the fossil sample prior to embedding. The fossil material was then incubated in 3 changes of LR white resin, 24 hours each, placed in a gelatin capsule with fresh LR white (Hard grade acrylic resin, London Resin Company Ltd., Lot# 140916, Batch# 409081), capped to exclude oxygen, and allowed to harden at 60°C. This embedding polymer was chosen because it is permeable to antibody solutions (see IHC methods below).

In a separate room, ostrich claw sheath was fixed in 10% neutral buffered formalin, washed in phosphate buffered saline (PBS), and dehydrated in two changes of 70% ethanol. Sample was then incubated in (2:1) LR white: 70% ethanol to equilibrate then infiltrated by incubating in three changes of LR white embedding medium. The specimen and embedding medium were placed in a gelatin capsule, capped, and allowed to polymerize for 48 hours at 60°C. Samples were sectioned to 90nm using A Leica EMUC6 ultra-microtome with dedicated diamond knife (separate knives for fossil and extant tissues). Sections were mounted on 200 mesh copper grids and imaged with a Zeiss Leo 912 TEM. Images were taken at 100KV accelerating voltage with a Proscan 2048X2048 CCD camera and processed with Olympus Soft Imaging System.

Extant ostrich claw sheath sections were stained with 15% methanolic uranyl acetate and Reynold's lead citrate prior to imaging. Fossil material was visualized without staining.

In situ immunohistochemistry (IHC) – Immunofluorescence (IF)

To achieve positive IF results for the *Citipati* sample (figure S3a), it had to be demineralized overnight in 0.5M EDTA pH 8.0 (ethylenediaminetetraacetic acid) to chelate the calcium (see Discussion below). What remained after demineralization (figure S3b) was carefully collected and washed in PBS.

Note that demineralized fossil tissue was used only for immunohistochemical analyses. SEM and TEM analyses were performed on a sample that was not demineralized.

In a separate room, all extant tissues analyzed in this study (ostrich claw sheath, decalcified ostrich bone, alligator skin) were fixed in 10% neutral buffered formalin for a minimum of one hour follow by a PBS wash.

All samples were then embedded in LR white resin as described above.

Using the ultra-microtome and dedicated diamond knives (as described above) 200 nm sections were taken. Sections were transferred to a 6-well Teflon coated slide, dried on a plate warmer (45°C) and then allowed to fully dry overnight at 42°C.

The primary antiserum for this study is an affinity purified polyclonal rabbit anti-chicken feather antibody produced by Bio-Synthesis, Inc (Lot Number: AB1312-1). Full details on the production of the custom-made antiserum as well as additional specificity controls are described in Moyer et al. 2016 (in review). In brief, protein extracted from a mature chicken feather was dialyzed for purification and concentration, then used to immunize two laboratory rabbits at Bio-Synthesis, Inc. The resultant polyclonal antiserum was purified using a protein bounded affinity column. Because mature feathers are composed of 80-90% beta-keratin [9,36,37], it can confidently be assumed that the original extraction resulted in a protein solution composed almost entirely of beta-keratin; therefore, the antibodies directed against this protein solution will respond specifically to epitopes that share a three-dimensional conformation with feather beta-keratin.

In situ immunohistochemistry (IHC) (immunofluorescence) was conducted to localize binding of the beta-keratin antibody to epitopes within the fossil sample. Binding patterns and avidity were compared to modern tissue. All incubations were performed at room temperature unless noted otherwise and separated by 2x5 minute washes using IHC phosphate buffered saline (PBS). To expose epitopes, sections were incubated for 15 min with 25 µg/µL Proteinase K in 1X PBS at 37˚C, followed by 3x10 minutes with 0.5 M EDTA pH 8.0, which participates in antigen retrieval in addition to chelation of any remaining calcium. Sections were incubated for 2x10 min with 1mg/mL $NaBH_4$, also an antigen retrieval method as well as to reduce autofluorescence, then with 4% normal goat serum (NGS) in IHC PBS for four hours to block nonspecific binding sites. The primary antiserum was diluted in primary dilution buffer (1% bovine serum albumin (BSA), 0.1% cold fish skin gelatin, 0.5% Triton X-100, 0.05% sodium azide, 0.01M PBS (pH= 7.2-7.4)) at 1:500, applied to all test samples and incubated overnight at 4°C. Controls consisting of identical tissues sectioned and treated as above were incubated with buffer containing no primary antibodies in tandem with and under identical conditions as the test samples. This controlled for non-specific binding of secondary antibodies or detection agents.

After incubation with the primary antiserum and all remaining incubations were followed by two washes in PBS with 5% Tween20 wash buffer for 10 minutes and then by 2x10 minutes washes in PBS to remove unbound antibody. All sections, including controls, were then incubated with secondary antibody (biotinylated goat anti-rabbit IgG(H+L) from Vector Laboratories, BA-1000, Lot-Y1228) diluted 1:500 in secondary dilution buffer (0.01M PBS

(pH= 7.2), 0.05% Tween 20) for 2 hours, and binding detected after incubating in Fluorescein Avidin D (Vector laboratories, A-2001, Lot-W1124), diluted 1:1000 in secondary dilution buffer for 1 hour in the dark. Slides were mounted with Vectashield mounting media (Vector laboratories, H-1000, Lot-Y0417), coverslips were applied, and sections were visualized using a Zeiss Axioskop 2 plus biological microscope and images captured using an AxioCam MRc 5(Zeiss) with 10x ocular magnification on the Axioskop 2 plus using Axiovision software package (version 4.7.0.0).

Before testing against fossil claw material, the primary antiserum was exposed to keratinous tissues from chicken feather and alligator skin (figure S4). If positive binding was observed in both chicken and alligator tissues, Extant Phylogenetic Bracketing [38] allows the first order assumption that dinosaur tissue would also react and antibodies would bind in a similar manner, if similar epitopes were preserved.

Controls for non-specific binding and specificity of antigen retrieval included application of an irrelevant primary antibody (anti-human elastin (courtesy of R. Mecham), 1:500) not expected to have epitopes cross-reacting with feather antibodies. A second control used the primary antiserum as described above, after incubating the antiserum with excess extracted chicken feather proteins (1:200, in a protein solution with ~1.75 mg of protein determined using a Pierce® BCA protein assay kit (Thermo Scientific, Product# 23227, Lot# OI193596)). This served to block the antibody binding sites specific for keratin, thus diminishing binding to epitopes in tissue. The inhibited antiserum was applied to sections as described above, and binding was greatly reduced, demonstrating again the specificity of the serum for keratin-derived epitopes (figures S5 and S6).

To show that our custom antiserum does not cross-react with collagen or any other bone protein, it was tested against decalcified ostrich bone; no reactivity was observed (figure S7). However, when ostrich bone was tested against a polyclonal antibody raised against chicken collagen I (US Biological, C7510-13B) strong and localized reactivity was observed, as expected. This control shows that the lack of binding to keratin antibodies is not due to the lack of epitopes in bone, rather that epitopes present in bone do not bind keratin antibodies; both collagen and keratin antibodies are specific to their respective immunogens.

Secondary antiserum, without application of specific primary antibodies, was applied to tissues to control for spurious binding of the secondary antibody and always run in parallel as negative controls. No binding was visualized.

References

1. Norell, M. A., Clark, J. M., Chiappe, L. M. & Dashzeveg, D. 1995 A nesting dinosaur. *Nature* **378**, 774–776. (doi:10.1038/378774a0)
2. Clark, J. M., Norell, M. & Chiappe, L. M. 1999 An oviraptorid skeleton from the late Cretaceous of Ukhaa Tolgod, Mongolia, preserved in an avianlike brooding position over an oviraptorid nest. *Am. Museum Novit.* **3265**, 1–36.
3. Clark, J. M., Norell, M. A. & Barsbold, R. 2001 Two new oviraptorids (Theropoda: Oviraptorosauria), Upper Cretaceous Djadokhta Formation, Ukhaa Tolgod, Mongolia. *J. Vertebr. Paleontol.* **21**, 209–213. (doi:10.1671/0272-4634(2001)021[0209:TNOTOU]2.0.CO;2)
4. Dingus, L., Loope, D. B., Dashzeveg, D., Swisher, C. C., Minjin, C., Novacek, M. J. & Norell, M. A. 2008 The Geology of Ukhaa Tolgod (Djadokhta Formation, Upper Cretaceous, Nemegt Basin, Mongolia). *Am. Museum Novit.* **3616**, 1. (doi:10.1206/442.1)
5. Dashzeveg, D., Dingus, L., Loope, D. B., Swisher, C. C., Dulam, T. & Sweeney, M. R. 2005 New Stratigraphic Subdivision, Depositional Environment, and Age Estimate for the Upper Cretaceous Djadokhta Formation, Southern Ulan Nur Basin, Mongolia. *Am. Museum Novit.* **3498**, 1. (doi:10.1206/0003-0082(2005)498[0001:NSSDEA]2.0.CO;2)
6. Wu, D.-D. & Zhang, Y.-P. 2008 Molecular evolution of the keratin associated protein gene family in mammals, role in the evolution of mammalian hair. *BMC Evol. Biol.* **8**.
7. Moll, R., Divo, M. & Langbein, L. 2008 The human keratins: biology and pathology. *Histochem Cell Biol* **129**, 705–733. (doi:10.1007/s00418-008-0435-6 [doi])
8. Greenwold, M. J. & Sawyer, R. H. 2013 Molecular evolution and expression of archosaurian β-keratins: diversification and expansion of archosaurian β-keratins and the origin of feather β-keratins. *J. Exp. Zool. B. Mol. Dev. Evol.* **320**, 393–405. (doi:10.1002/jez.b.22514)
9. Greenwold, M. J., Bao, W., Jarvis, E. D., Hu, H., Li, C., Gilbert, M., Zhang, G. & Sawyer, R. H. 2014 Dynamic evolution of the alpha (α) and beta (β) keratins has accompanied integument diversification and the adaptation of birds into novel lifestyles. *BMC Evol. Biol.* **14**, 249. (doi:10.1186/s12862-014-0249-1)
10. Wu, P. et al. 2015 Topographical mapping of α- and β-keratins on developing chicken skin integuments: Functional interaction and evolutionary perspectives. *Proc. Natl. Acad.*

Sci. **112**, E6770–E6779. (doi:10.1073/pnas.1520566112)

11. Alibardi, L., Toni, M. & Dalla Valle, L. 2007 Hard cornification in reptilian epidermis in comparison to cornification in mammalian epidermis. *Exp. Dermatol.* **16**, 961–976. (doi:10.1111/j.1600-0625.2007.00609.x)
12. Vandebergh, W. & Bossuyt, F. 2012 Radiation and functional diversification of alpha keratins during early vertebrate evolution. *Mol Biol Evol* **29**, 995–1004. (doi:msr269 [pii]10.1093/molbev/msr269 [doi])
13. Greenwold, M. & Sawyer, R. 2010 Genomic organization and molecular phylogenies of the beta (beta) keratin multigene family in the chicken (Gallus gallus) and zebra finch (Taeniopygia guttata): implications for feather evolution. *BMC Evol. Biol.* **10**, 148.
14. Greenwold, M. J. & Sawyer, R. H. 2011 Linking the molecular evolution of avian beta (β) keratins to the evolution of feathers. *J. Exp. Zool. Part B Mol. Dev. Evol.* **316B**, 609–616. (doi:10.1002/jez.b.21436)
15. Fraser, R. D. B. & Parry, D. A. D. 2008 Molecular packing in the feather keratin filament. *J. Struct. Biol.* **162**, 1–13.
16. Fraser, R. D. & Parry, D. A. 2011 The structural basis of the filament-matrix texture in the avian/reptilian group of hard beta-keratins. *J Struct Biol* **173**, 391–405. (doi:S1047-8477(10)00289-3 [pii]10.1016/j.jsb.2010.09.020 [doi])
17. Dalla Valle, L., Nardi, A., Gelmi, C., Toni, M., Emera, D. & Alibardi, L. 2009 Beta-keratins of the crocodilian epidermis: composition, structure, and phylogenetic relationships. *J Exp Zool B Mol Dev Evol* **312**, 42–57. (doi:10.1002/jez.b.21241 [doi])
18. Gregg, K. & Rogers, G. E. 1986 Feather Keratin: Composition, Structure and Biogenesis. In *Biology of the integument* (eds J. Bereiter-Hahn A. G. Maltosy & K. S. Richards), pp. 667–694. Berlin: Springer-Verlag.
19. Fraser, R. D. B., MacRae, T. P. & Rogers, G. E. 1972 *Keratins: their composition, structure, and biosynthesis*. Springfield, Ill.: Thomas.
20. Marshall, R. C., Orwin, D. F. G. & Gillespie, J. M. 1991 Structure and biochemistry of mammalian hard keratin. *Electron Microsc. Rev.* **4**, 47–83. (doi:10.1016/0892-0354(91)90016-6)
21. Alibardi, L. 2008 Microscopic analysis of lizard claw morphogenesis and hypothesis on its evolution. *Acta Zool.* **89**, 169–178. (doi:10.1111/j.1463-6395.2007.00312.x)

22. Alibardi, L. 2015 Immunolocalization of sulfhydryl oxidase in reptilian epidermis indicates that the enzyme participates mainly to the hardening process of the beta-corneous layer. *Protoplasma* **252**, 1529–36. (doi:10.1007/s00709-015-0782-9)
23. Alibardi, L. 2003 Immunocytochemistry and keratinization in the epidermis of crocodilians. *Zool. Stud.* **42**, 346–356.
24. Alibardi, L. 2015 Review: mapping epidermal beta-protein distribution in the lizard Anolis carolinensis shows a specific localization for the formation of scales, pads, and claws. *Protoplasma* (doi:10.1007/s00709-015-0909-z)
25. Holthaus, K. B. et al. 2015 Comparative genomics identifies epidermal proteins associated with the evolution of the turtle shell. *Mol. Biol. Evol.* , msv265. (doi:10.1093/molbev/msv265)
26. Strasser, B., Mlitz, V., Hermann, M., Tschachler, E. & Eckhart, L. 2015 Convergent evolution of cysteine-rich proteins in feathers and hair. *BMC Evol. Biol.* **15**, 82. (doi:10.1186/s12862-015-0360-y)
27. Schweitzer, M. H., Watt, J. A., Avci, R., Forster, C. A., Krause, D. W., Knapp, L., Rogers, R. R., Beech, I. & Marshall, M. 1999 Keratin Immunoreactivity in the Late Cretaceous Bird Rahonavis ostromi. *J. Vertebr. Paleontol.* **19**, 712–722.
28. Schweitzer, M. H., Watt, J. A., Avci, R., Knapp, L., Chiappe, L., Norell, M. & Marshall, M. 1999 Beta-keratin specific immunological reactivity in feather-like structures of the Cretaceous Alvarezsaurid, Shuvuuia deserti. *J. Exp. Zool.* **285**, 146–157. (doi:10.1002/(sici)1097-010x(19990815)285:2<146::aid-jez7>3.0.co;2-a)
29. Moyer, A. E., Zheng, W., Johnson, E. a, Lamanna, M. C., Li, D.-Q., Lacovara, K. J. & Schweitzer, M. H. 2014 Melanosomes or microbes: testing an alternative hypothesis for the origin of microbodies in fossil feathers. *Sci. Rep.* **4**, 4233. (doi:10.1038/srep04233)
30. Schweitzer, M. H., Lindgren, J. & Moyer, A. E. 2015 Melanosomes and ancient coloration re-examined: A response to Vinther 2015 (DOI 10.1002/bies.201500018). *BioEssays* , n/a–n/a. (doi:10.1002/bies.201500061)
31. Manning, P. L. et al. 2013 Synchrotron-based chemical imaging reveals plumage patterns in a 150 million year old early bird. *J. Anal. At. Spectrom.* **28**, 1024–1030. (doi:10.1039/C3JA50077B)
32. Ng, C. S. et al. 2012 The chicken frizzle feather is due to an alpha-keratin (KRT75)

mutation that causes a defective rachis. *PLoS Genet* **8**, e1002748. (doi:10.1371/journal.pgen.1002748 [doi]PGENETICS-D-11-02513 [pii])

33. Alibardi, L. 2013 Immunolocalization of alpha-keratins and feather beta-proteins in feather cells and comparison with the general process of cornification in the skin of mammals. *Ann. Anat.* **195**, 189–98. (doi:10.1016/j.aanat.2012.08.005)
34. Phillips, M. J., Gibb, G. C., Crimp, E. A. & Penny, D. 2010 Tinamous and moa flock together: mitochondrial genome sequence analysis reveals independent losses of flight among ratites. *Syst. Biol.* **59**, 90–107. (doi:10.1093/sysbio/syp079)
35. Baker, A. J., Haddrath, O., McPherson, J. D. & Cloutier, A. 2014 Genomic support for a moa-tinamou clade and adaptive morphological convergence in flightless ratites. *Mol. Biol. Evol.* **31**, 1686–96. (doi:10.1093/molbev/msu153)
36. Stettenheim, P. R. 2000 The Integumentary Morphology of Modern Birds—An Overview. *Am. Zool.* **40**, 461–477. (doi:10.1093/icb/40.4.461)
37. Cai, C. & Zheng, X. 2009 Medium optimization for keratinase production in hair substrate by a new Bacillus subtilis KD-N2 using response surface methodology. *J. Ind. Microbiol. Biotechnol.* **36**, 875–83. (doi:10.1007/s10295-009-0565-4)
38. Witmer, L. M. 1995 The extant phylogenetic bracket and the importance of reconstructing soft tissues in fossils. In *Functional Morphology in Vertebrate Paleontology*, pp. 19–33.
39. Lautenschlager, S., Witmer, L. M., Altangerel, P. & Rayfield, E. J. 2013 Edentulism, beaks, and biomechanical innovations in the evolution of theropod dinosaurs. *Proc. Natl. Acad. Sci. U. S. A.* **110**, 20657–62. (doi:10.1073/pnas.1310711110)
40. Norell, M. A., Makovicky, P. J. & Currie, P. J. 2001 Palaeontology. The beaks of ostrich dinosaurs. *Nature* **412**, 873–874. (doi:10.1038/35091139 [doi]35091139 [pii])
41. Ostrom, J. H. 1961 Cranial Morphology of the Hadrosaurian Dinosaurs of North America. *Bull. Am. Museum Nat. Hist.* **122**, 33–186.
42. Sereno, P. C., Shichin, C., Zhengwu, C. & Chenggang, R. 1988 Psittacosaurus meileyingensis (Ornithischia: Ceratopsia), a new psittacosaur from the Lower Cretaceous of northeastern China. *J. Vertebr. Paleontol.* **8**, 366–377. (doi:10.1080/02724634.1988.10011725)
43. Horner, J. R. & Goodwin, M. B. 2008 Ontogeny of cranial epi-ossifications in Triceratops. *J. Vertebr. Paleontol.* **28**, 134–144. (doi:10.1671/0272-

4634(2008)28[134:OOCEIT]2.0.CO;2)

44. El-Gendy, S. A. A., Derbalah, A. & El-Magd, M. E. R. A. 2012 Macro-microscopic study on the toepad of ostrich (Struthio camelus). *Vet. Res. Commun.* **36**, 129–38. (doi:10.1007/s11259-012-9522-1)
45. Zaghloul, D. & El-Gendy, S. 2014 Anatomical, light and scanning electron micr oscopical study of ostrich (Struthio camelus) integument. *J. Vet. Anat.* **7**, 33–54.
46. Alibardi, L. 2008 Cornification in developing claws of the common Australian skink (Lampropholis guichenoti) (Squamata, Lacertidae). *Ital. J. Zool.* **75**, 327–336.
47. Carver, W. E. & Sawyer, R. H. 1988 Avian scale development: XI. Immunoelectron microscopic localization of alpha and beta keratins in the scutate scale. *J Morphol* **195**, 31–43. (doi:10.1002/jmor.1051950104 [doi])
48. Dingus, L., Loope, D. B., Dashzeveg, D., Swisher, C. C., Minjin, C., Novacek, M. J. & Norell, M. 2008 The geology of Ukhaa Tolgod (Djadokhta Formation, Upper Cretaceous, Nemegt Basin, Mongolia) ; American Museum novitates, no. 3616.
49. Briggs, D. E. G. 1995 Experimental Taphonomy. *Palaios* **10**, 539–550.
50. Schweitzer, M. H., Zheng, W., Cleland, T. P., Goodwin, M. B., Boatman, E., Theil, E., Marcus, M. A. & Fakra, S. C. 2014 A role for iron and oxygen chemistry in preserving soft tissues, cells and molecules from deep time. *Proc. Biol. Sci.* **281**, 20132741. (doi:10.1098/rspb.2013.2741)
51. Fuchs, E. 1995 Keratins and the skin. *Annu. Rev. Cell Dev. Biol.* **11**, 123–53. (doi:10.1146/annurev.cb.11.110195.001011)

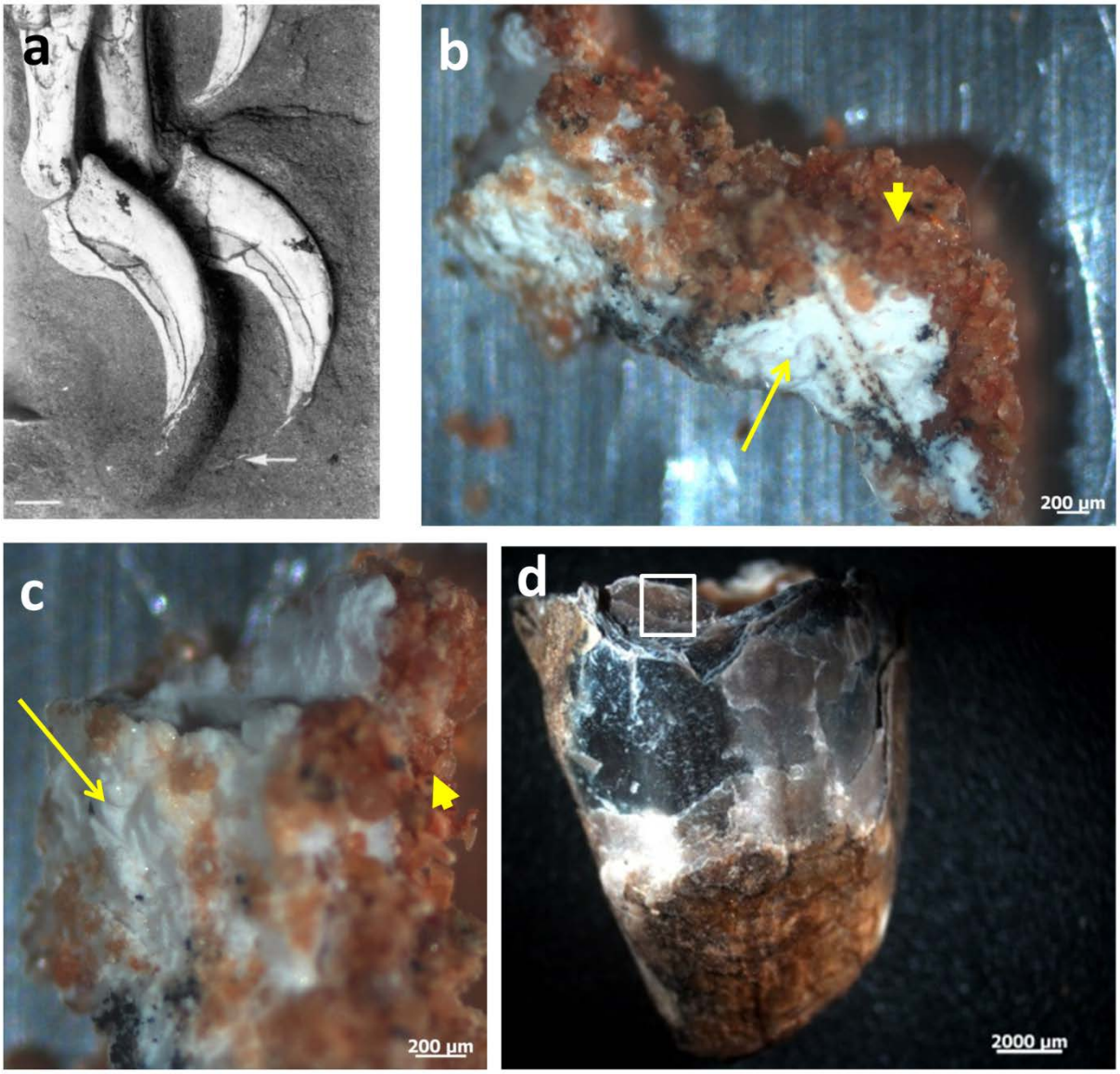

Figure 1. Fossil and extant claw material. (a) Photograph from the initial description of *Citipati osmolskae* (MDC-P 100/979) demonstrating the purported preserved keratinous claw sheath (white arrow) observed as a thin lens of white material extending off the phalanx of one of the manual digits. Reprinted with permission from Macmillan Publishers Ltd: [NATURE] [1], copyright (1995). Fossil claw sheath in a), b) lower and c) higher magnification. Claw material can be differentiated from surrounding sediment based on color and texture; sand (arrowheads) is red and granular, sheath (arrow) is white, dense and cohesive. (d) Macroscopic image of the entire emu claw sheath. Boxed region shows the approximate location and piece (ventral surface) that was extracted for SEM analysis.

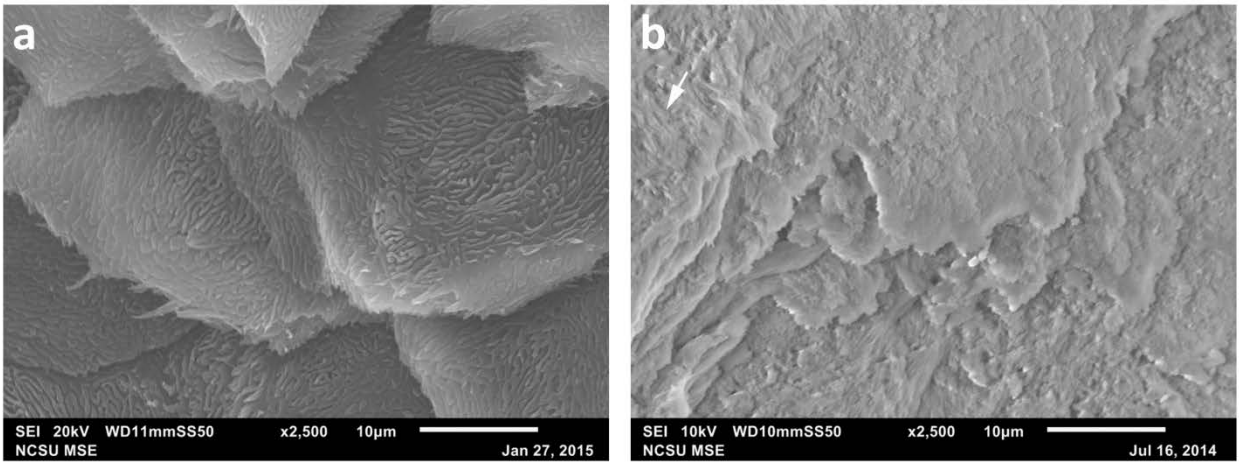

Figure 2. SEM images of extant emu (a) and *Citpati* (b) claw material. Both specimens show plate-like layering in a similar pattern as well as a rugose texture covering the surface. In the emu claw, this is the ventral surface adjacent to the bone. The rugosity is observed as a mat of finger-like projections, and is likely how the keratinous tissue formed to help adhere the claw sheath to the underlying bone (see text for details). A similar texture is observed in the fossil material (arrow), but much less pronounced compared to the extant tissue.

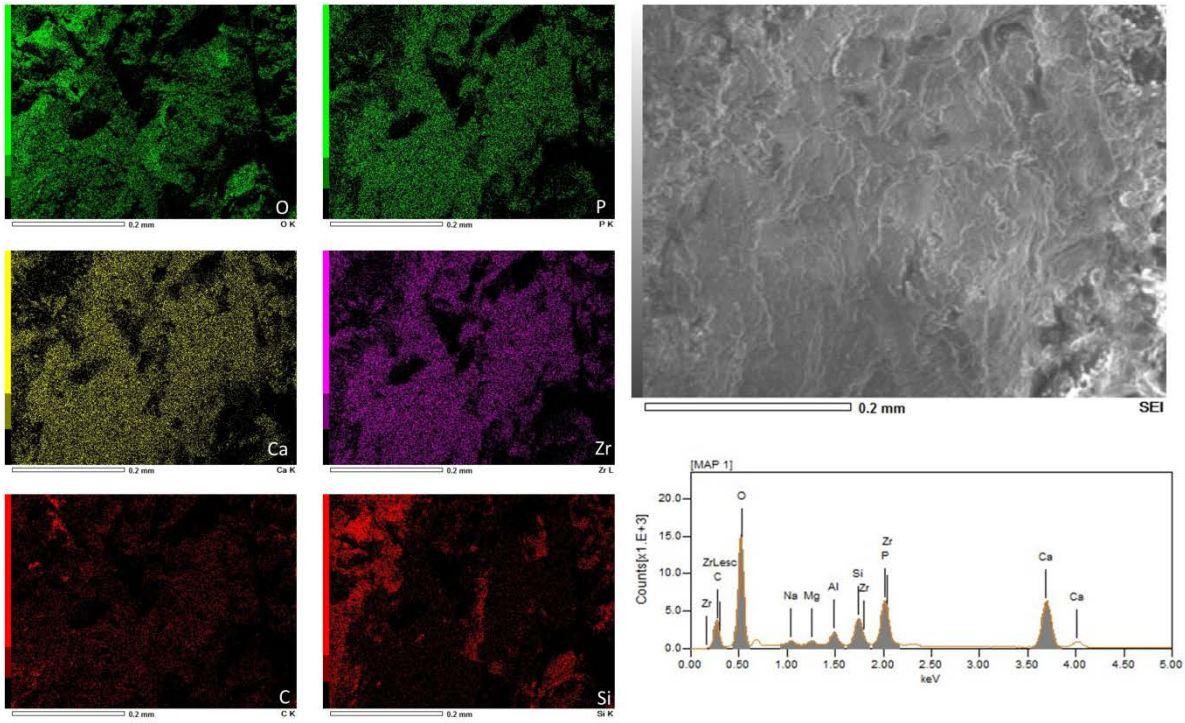

Figure 3. SEM-EDS results for *Citipati* claw material (white material near arrow in Figure 1c). These six elements represent ~97% (by mass) of the X-rays detected in this sample area. Quantitative data show oxygen to be the most dominant element in both white claw material and sediment; however there was a relatively greater amount of calcium detected in the claw material than in the sediment. No calcium was detected in the emu claw. See Table 1 for quantitative data.

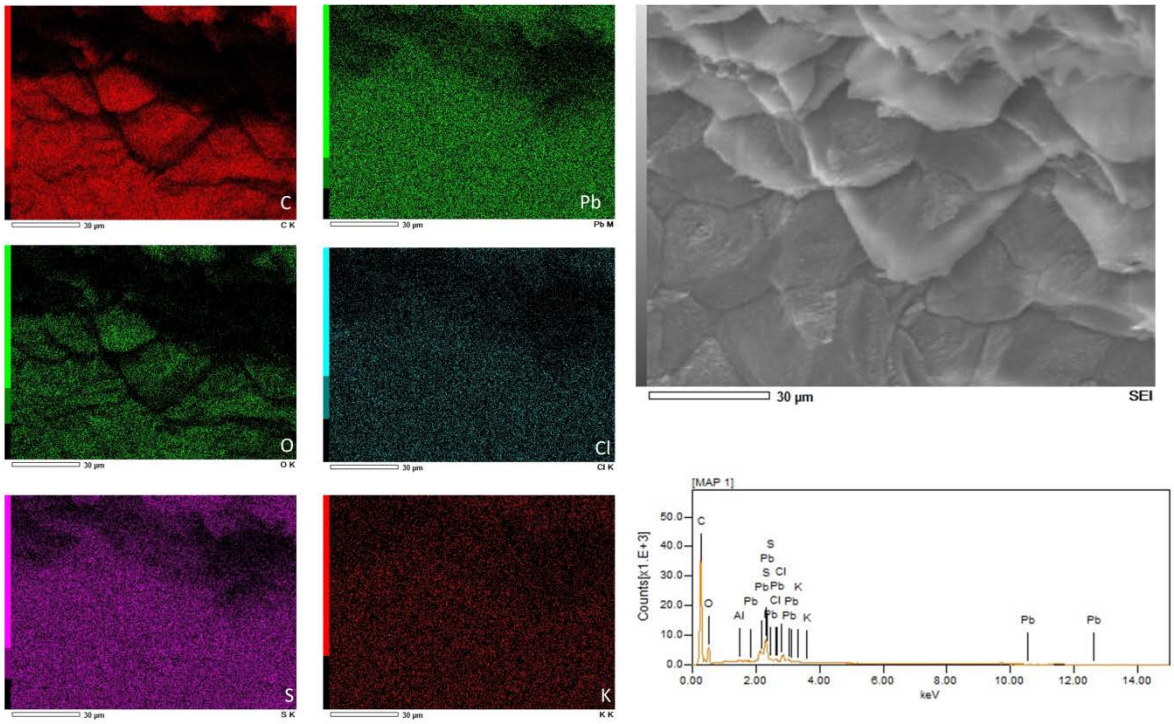

Figure 4. SEM-EDS results for emu claw tissue. Carbon, oxygen and sulfur were the primary elements composing the claw and represent ~97% (by mass) of all X-rays detected. Lead, chlorine and potassium, and aluminum (not shown) were detected in trace amounts. The black region observed along the upper regions of the elemental maps represents an area that was blocked from the detector. Although this EDS scan was performed at a higher magnification (1000x) than the fossil scan (250x), a scan performed at 250x on an uncoated spot of the superficial surface of the emu claw resulted in the same elemental observations (data not shown). See Table 1 for quantitative data.

Emu	ms%	mol%	***Citipati***	ms%	mol%	**Sediment**	ms%	mol%
C	74.75	82.24	O	34.53	47.67	O	41.39	44.49
O	19.36	15.99	**Ca**	**29.26**	16.12	C	24.68	35.34
S	3.1	1.28	C	11.7	21.51	Si	18.64	11.41
Pb	1.79	0.11	P	9.66	6.89	Al	7.2	4.59
Cl	0.62	0.23	Zr	7.54	1.83	**Ca**	**2.37**	**1.02**
K	0.26	0.09	Si	4.41	3.46	Fe	2.04	0.63

Table 1. SEM- EDS quantitative data for the emu claw (Figure 4), fossil *Citipati* claw (Figure 5), and the sediment associated with the fossil claw (Figure S2), in decreasing abundance. Percentages are presented by mass (ms%) and (mol%).

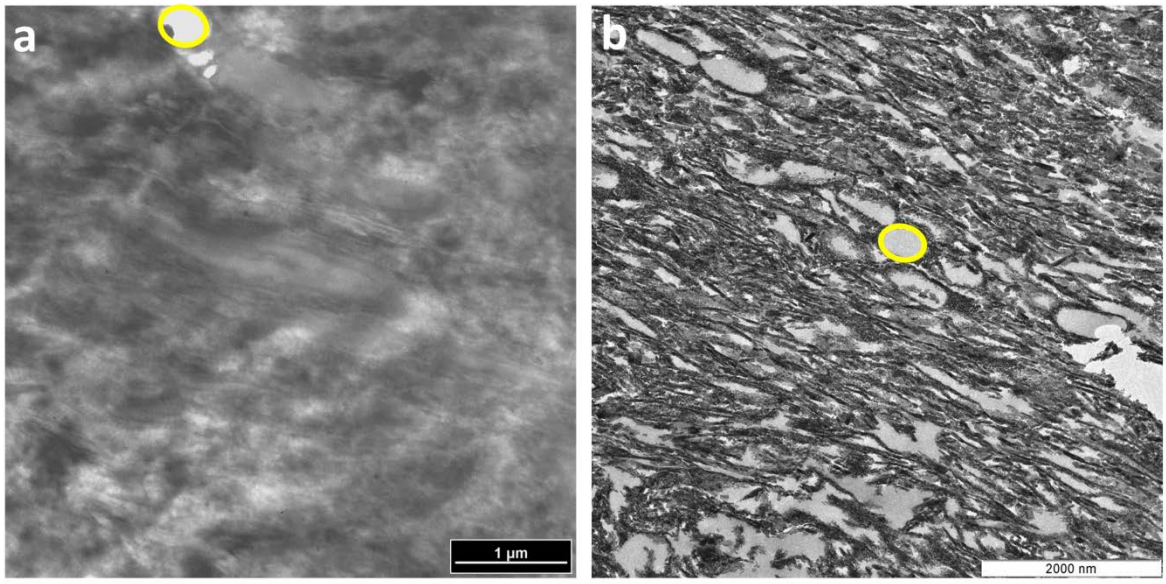

Figure 5. TEM micrographs of (a) ostrich claw tissue and (b) *Citipati* claw material. In both samples, parallel fibers can be seen running diagonally, and identical voids (yellow outlines) were observed amongst the fibers in both samples. These may represent structural remnants of what were originally lipid droplets in developing claw tissue [44,45].

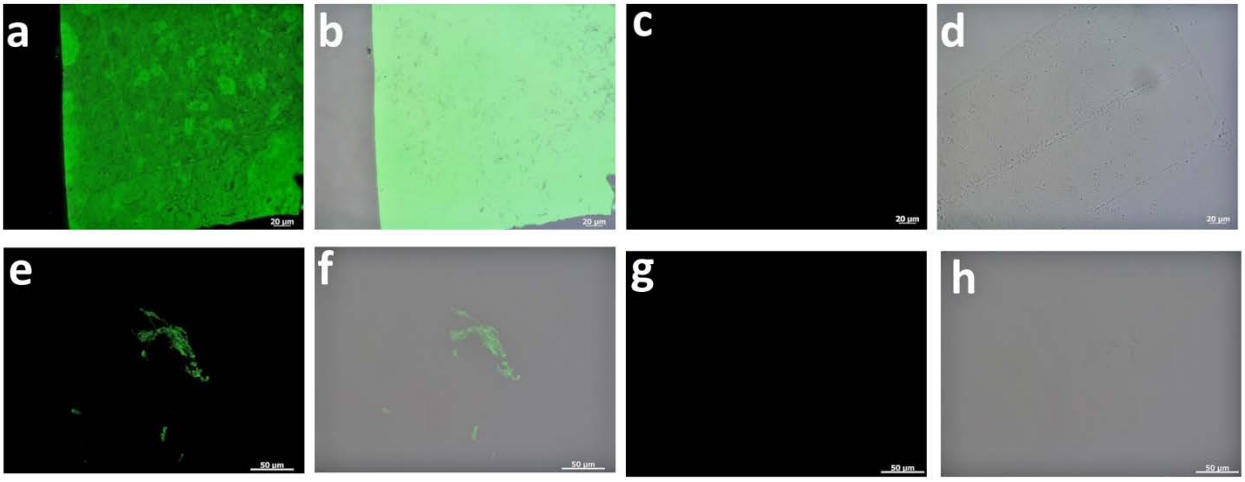

Figure 6. Immunohistochemical staining results for (a-d) ostrich claw and (e-h) *Citipati* claw exposed to the custom-made antiserum. Positive binding and localization of antibody-antigen complexes are indicated by the green fluorescent signal. Controls using secondary antibody only are negative for both (c-d) ostrich and (g-h) fossil material.

Figure S1. *Citipati osmolskae* specimen MDC-P 100/979. Reprinted with permission from Macmillan Publishers Ltd: [NATURE] (Norell et al. 1995), copyright (1995). The sample used in this study (figure 1 b, c) was collected from the region encircled.

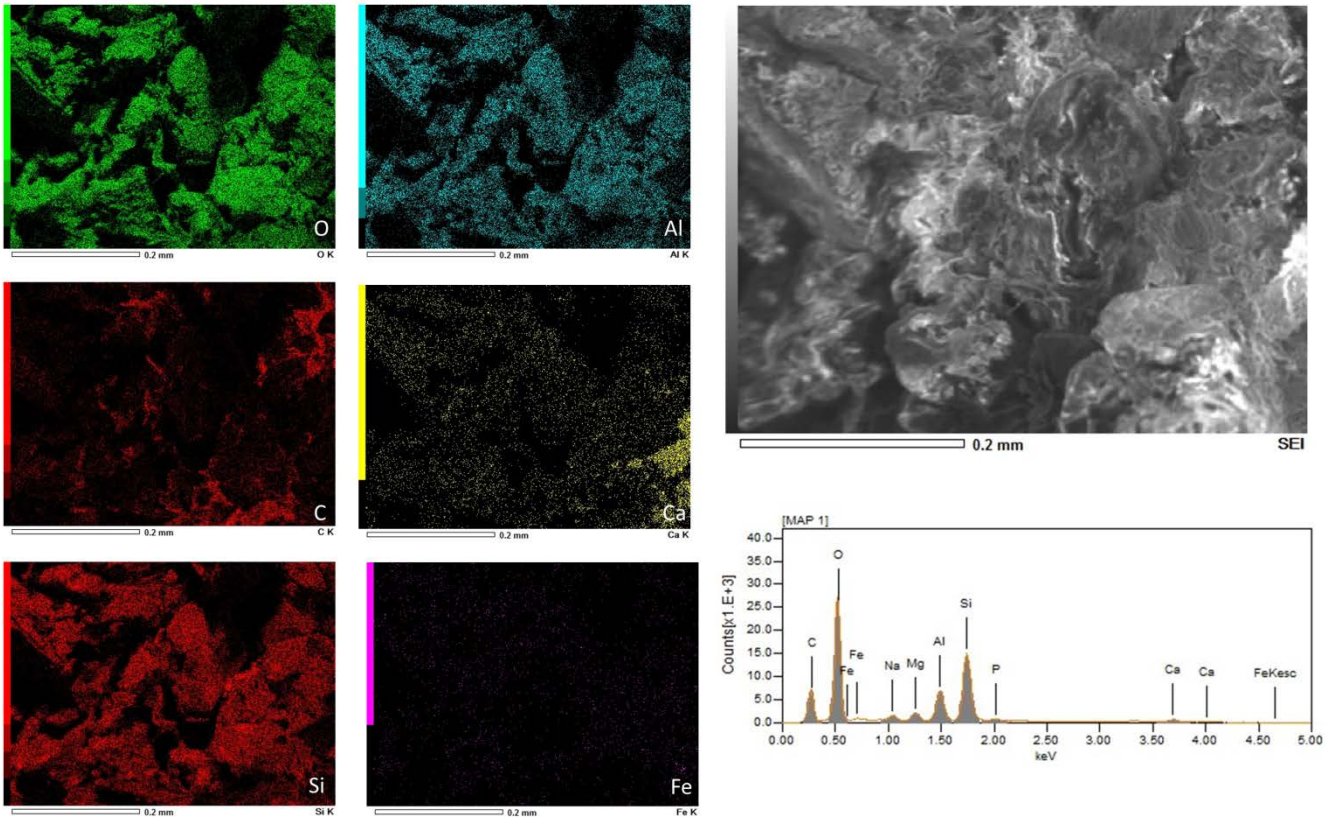

Figure S2. SEM-EDS results of sediment surrounding the claw material from *Citipati*. These six elements represent ~96% of the X-rays detected (by mass). See Table 1 for quantitative data.

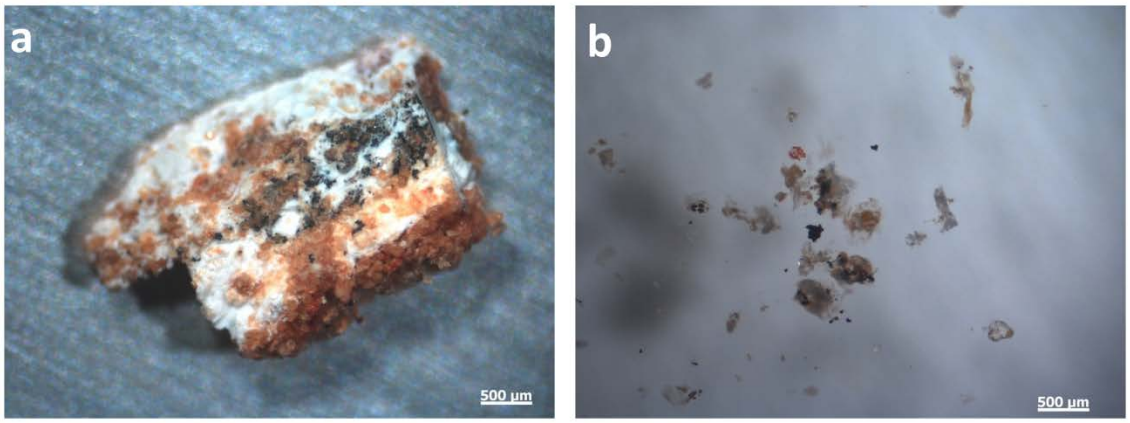

Figure S3. *Citipati* claw (a) before and (b) after EDTA demineralization. The material remaining after demineralization was embedded and used for all *in situ* IF tests.

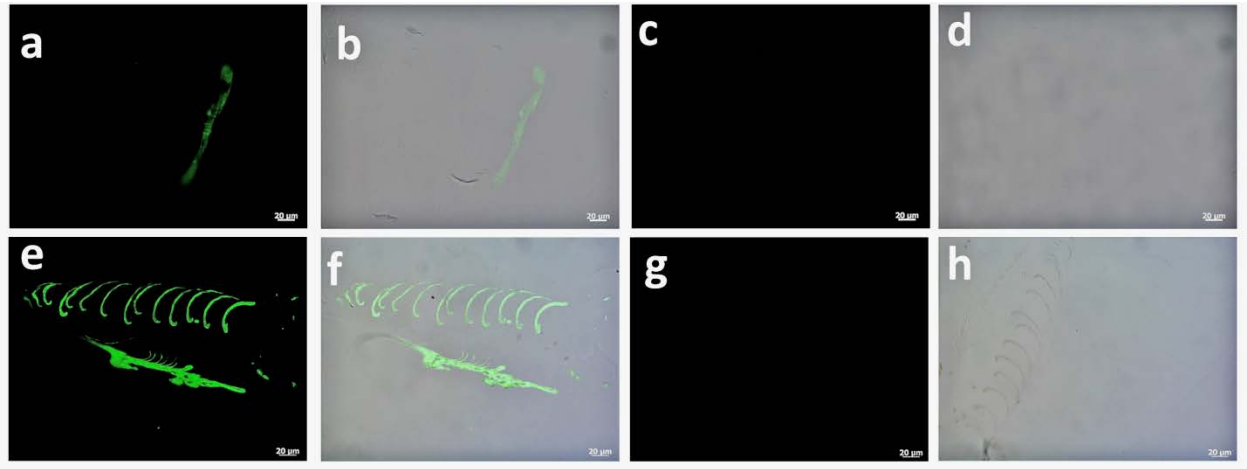

Figure S4**.** Immunohistochemical staining results. (a-d) Alligator skin and (e-h) chicken feather exposed to anti-feather antibodies. (a,b and e, f) The green fluorescent signal indicates positive binding of the primary antiserum to epitopes in the tissue, which is specific in both tissues. Note the antibody-antigen complexes are localized only to the outermost layer, stratum corneum, of the alligator skin. Controls were performed in parallel in which (c-d) alligator skin and (g-h) chicken feather were exposed to secondary antibody only, and as expected were negative.

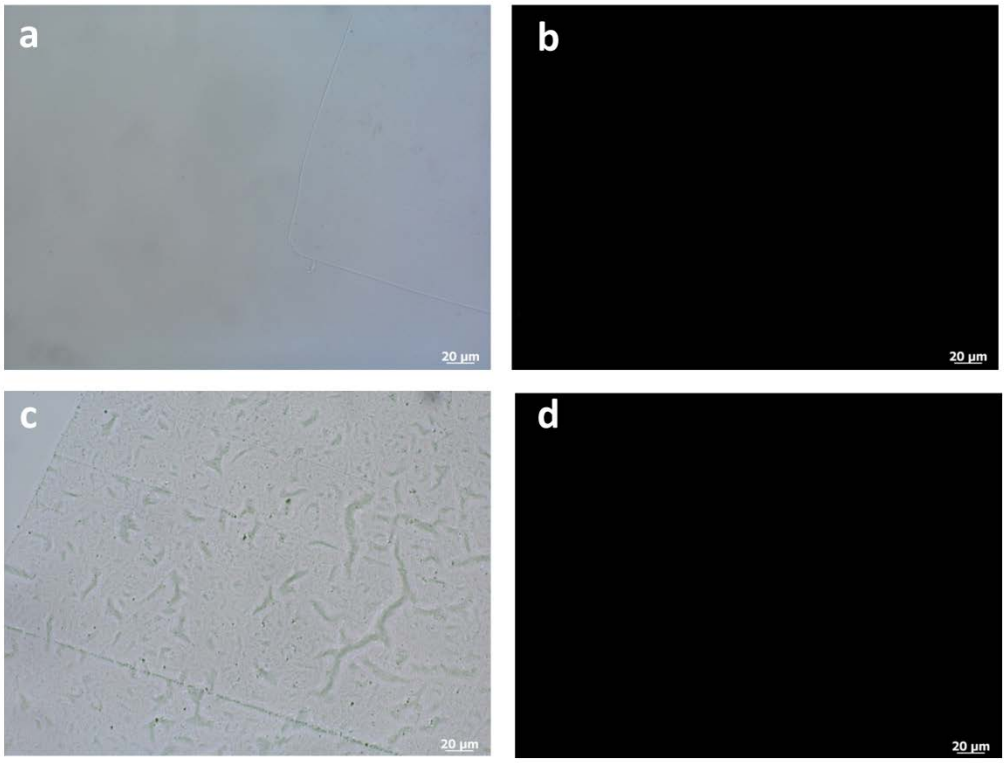

Figure S5. Primary antiserum specificity controls for ostrich claw. (a-b) Tested against an irrelevant antibody, anti-human elastin. (c-d) Inhibition of the primary antiserum using extracted feather protein. The lack of binding in both controls indicates that the binding is specific to the epitopes expressed in the tissue.

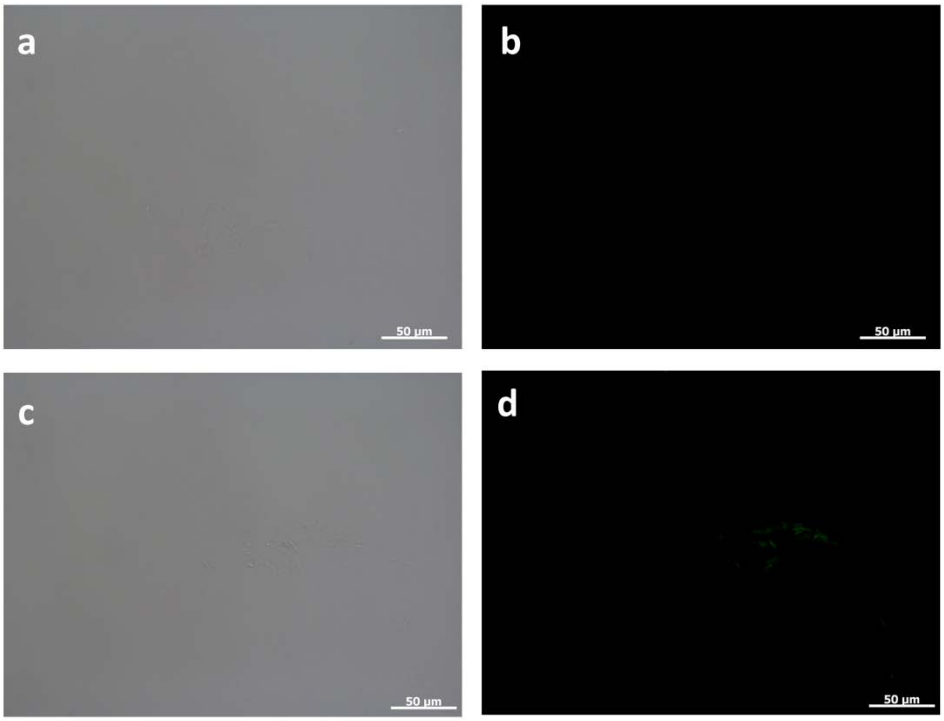

Figure S6. Primary antiserum specificity controls for *Citipati* tissue. (a-b) Tested against an irrelevant antibody, anti-human elastin. (c-d) Inhibition of the primary antiserum using extracted feather protein. As expected, binding is negative in the control using an irrelevant antibody, and greatly reduced in the inhibition control.

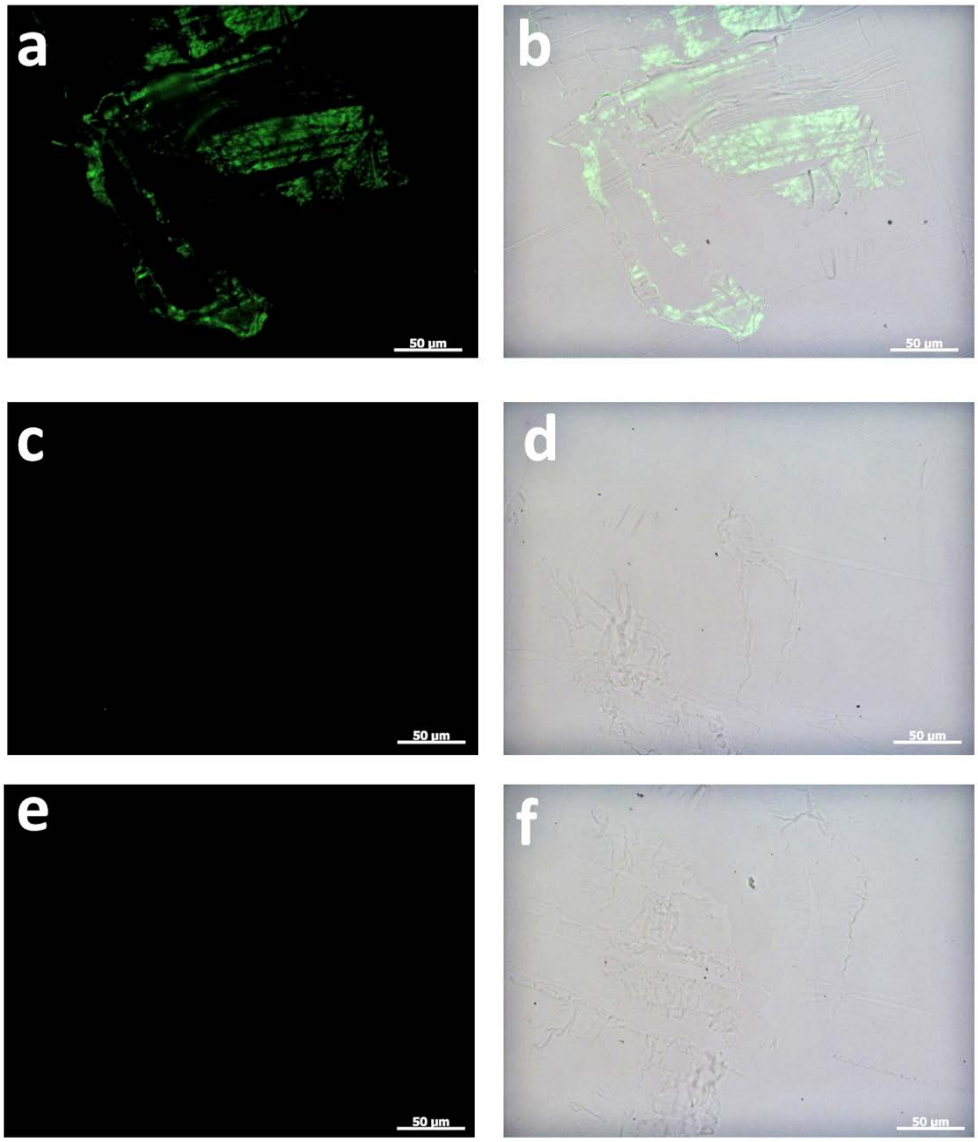

Figure S7. Immunological staining results for decalcified ostrich bone. (a-b) Positive control using anti-chicken collagen I. (c-d) Testing our custom-made antiserum against decalcified ostrich bone. (e-f) Secondary antibody only control. These results show that our antiserum does not cross-react with bone epitopes.

CHAPTER 7 - Testing the Hypothesis of Biofilm as a Source for Soft Tissue and Cell-Like Structures Preserved in Dinosaur Bone

PLOS | ONE

RESEARCH ARTICLE

Testing the Hypothesis of Biofilm as a Source for Soft Tissue and Cell-Like Structures Preserved in Dinosaur Bone

Mary Higby Schweitzer[1,2☯]*, **Alison E. Moyer**[1☯], **Wenxia Zheng**[1☯]

1 Department of Biological Science, North Carolina State University, Raleigh, North Carolina, United States of America, 2 North Carolina Museum of Natural Sciences, Raleigh, North Carolina, United States of America

☯ These authors contributed equally to this work.
* schweitzer@ncsu.edu

OPEN ACCESS

Citation: Schweitzer MH, Moyer AE, Zheng W (2016) Testing the Hypothesis of Biofilm as a Source for Soft Tissue and Cell-Like Structures Preserved in Dinosaur Bone. PLoS ONE 11(2): e0150238. doi:10.1371/journal.pone.0150238

Editor: Leon Claessens, College of the Holy Cross, UNITED STATES

Received: August 27, 2015

Accepted: February 11, 2016

Published: February 29, 2016

Data Availability Statement: All relevant data are within the paper.

Funding: This research was funded by grants to MHS from the David and Lucile Packard Foundation (30533), to MHS and WZ from the National Science Foundation INSPIRE program (EAR-1344198), and to AEM from the National Science Foundation GRFP (DGE-1252376). The EAR-1344198 was given to only MHS as PI. WZ is funded off of this grant, but she is not a PI. The funders had no role in study design, data collection and analysis, decision to publish, or preparation of the manuscript.

Abstract

Recovery of still-soft tissue structures, including blood vessels and osteocytes, from dinosaur bone after demineralization was reported in 2005 and in subsequent publications. Despite multiple lines of evidence supporting an endogenous source, it was proposed that these structures arose from contamination from biofilm-forming organisms. To test the hypothesis that soft tissue structures result from microbial invasion of the fossil bone, we used two different biofilm-forming microorganisms to inoculate modern bone fragments from which organic components had been removed. We show fundamental morphological, chemical and textural differences between the resultant biofilm structures and those derived from dinosaur bone. The data do not support the hypothesis that biofilm-forming microorganisms are the source of these structures.

Introduction

Apparent blood vessels, osteocytes, intravascular contents, and fibrous matrix were recovered from demineralized fragments of long bones of *Tyrannosaurus rex* (MOR 1125) [1], and subsequently, from bone of other dinosaurs and other fossil vertebrate remains [2–4]. However, despite evidence from morphological, microstructural, immunological and mass spectrometry data supporting the hypothesis that these structures were endogenous to the dinosaur, an alternative hypothesis was proposed; that these materials were the result of recent invasion of these dinosaur remains by biofilm-forming micro-organisms [5].

In our initial experiments, we considered possible alternative sources for these dinosaur-derived materials. For all studies, we chose dinosaur (MOR 1125) bone fragments from which no visible signs of glues or consolidants were observed. A second dinosaur (MOR 2598) [3] that also produced blood vessel- and osteocyte-like structures was collected without any chemicals, glues or consolidants applied; nevertheless, we tested the hypothesis that glues or consolidants could form such structures. Samples of preservatives commonly applied in the field were prepared, washed in acetone or ethanol, or embedded in the same resin used to section these

Competing Interests: The authors have declared that no competing interests exist.

dinosaur- derived structures. The consolidants dissolved instantly under these conditions, and could not be seen microscopically, with or without staining. The vessels treated in tandem were unaffected [1,3,6–8]. These results do not support consolidants or glues as a source for these vessel structures.

We eliminated the possibility that the vessels might represent invasion by fungi based upon morphological dissimilarities. Hyphae do not taper after branching and are usually septate [9,10], and the dinosaur vessels do not show these fungal characteristics (Figure 2 in [1]). The vessels were of greater diameter than known fungal hyphae, and like modern blood vessels, they tapered after branching [9], were not septate [9,10], and contained material within them not consistent with spores or other fungal structures (Figure 1e, f in [3]; Figure 2e-g in [11]; Figure 3c, h, n in [2]). Finally, we attempted to stain the structures with a fungi-specific stain, but no reactivity was seen (Fig 1). Thus, a fungal source for the soft tissue dinosaur materials is not supported.

Here, we test the hypothesis that the vessels and/or osteocyte-like structures might arise from microbial invasion by biofilm-forming organisms. Morphologically, the vessels and osteocytes we recovered were not consistent with biofilm. A biofilm is a population of microorganisms and the exopolymeric substances (EPS) they secrete [12–14], but neither transmission electron microscopy (TEM)[8] nor scanning electron microscopy (SEM)[1,3] revealed distinct microbial bodies (or impressions of these bodies) in association with dinosaur vessels. Additionally, a biofilm may be patchy or uneven in distribution [14–16], with cells detaching and EPS undergoing dissolution once nutrients have been removed [13,17]. Thus, biofilm-forming microorganisms cannot produce the continuous-walled and branching structures of different dimensions that we recovered from fossil bone. Biofilms adhere to substrates, but have no means to maintain shape once that substrate is removed (Fig 2); the dinosaur vessesls maintain a lumen and continuous walls after demineralization of the bone and multiple manipulations (Figs 3 and 4E and 4F). Finally, biofilms are rather amorphous (Fig 2). They may have microscopic internal structure, including pores and channels through which nutrients are exchanged [13,14,18] (and references therein), but they are not morphologically similar to osseous blood vessels.

Furthermore, to our knowledge, modern biofilms have not been *directly* shown to colonize fossil bone, except for one example where fragments of archaeological bone were used as a source to grow biofilms [19]. These bones were relatively recent (thousands of years, vs millions for dinosaurs); thus, it could be expected that they retained organic content, providing a

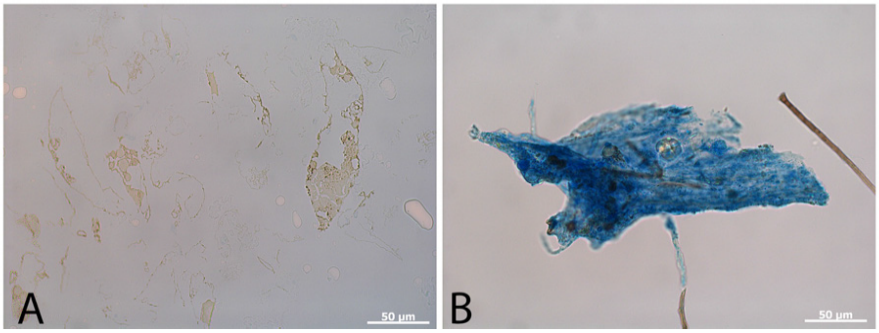

Fig 1. MOR 2598 vessels recovered after demineralization (a) compared with a hyphal mat (b) both stained with the fungal stain cotton blue (see methods). This histochemical stain reacts with fungal components to produce a vivid blue, but dinosaur vessels are unstained.

doi:10.1371/journal.pone.0150238.g001

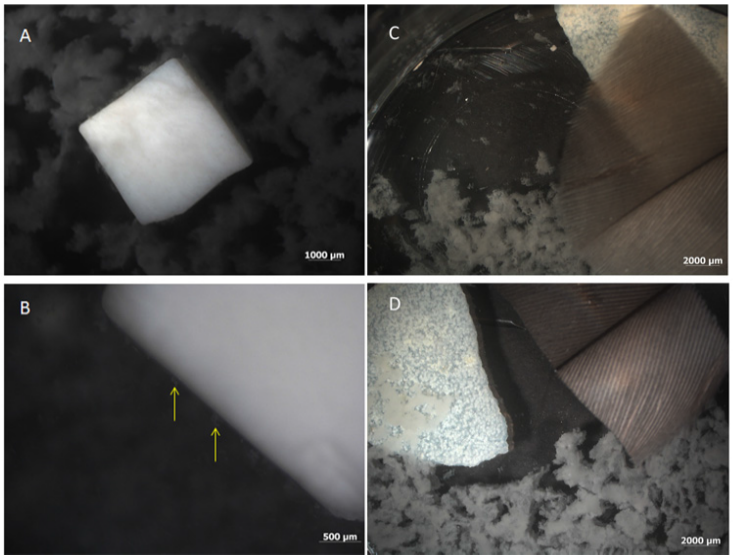

Fig 2. Biofilm growing on cow bone from which organics had been removed (see methods), 48 hours after inoculation. (A) *B.cereus* has colonized the bone and can be seen growing on and around the bone at low magnification. (B) *S.epidermidis* at higher magnification. Note the interaction of the biofilm with the surface of the bone (yellow arrows). Similar observations were made for both organisms. (C) Feather (tan) and ostrich eggshell (white) in the presence of *B. cereus* shows biofilm growth on tissues and in surrounding medium. (D) Feather and eggshell surrounded by biofilm from *S. epidermidis*, as above.

doi:10.1371/journal.pone.0150238.g002

nutrient source for invading microbes. Microbes colonize substrates primarily to obtain nutrients; when the nutrients are no longer available, they detach and the EPS dissipates [17]. Despite recent data to the contrary (e.g. [3,4,6,7]) it is assumed by many that extinct dinosaur bone no longer retains endogenous organics, either DNA or protein (e.g. [20–24]); if devoid of organics, they would not be optimal substrates for microbial growth.

Here, we test the hypotheses that 1) biofilm will colonize and grow within bone from which organics have been removed, as proposed to be the case for dinosaur bone, and 2) biofilm is capable of giving rise to structures similar in morphology to blood vessels. We designed a model system using bovine bone fragments from which organics had been removed, for repeatability and to discount a taxon-specific effect, and to best approximate what is presumed to be the case in dinosaur bone. After organics were removed from modern bone, the remaining bone was either placed in sterile water, or in a medium designed to favor biofilm growth (see methods). We used two different types of microorganisms known to form biofilm, *Bacillus cereus* and *Staphylococcus epidermidis*, to inoculate the bone, again for repeatability and to show that this pattern is not organism-specific (i.e., a property of only one type of biofilm or microorganism). We chose these two microorganisms because both are known to produce biofilm; both are rather common in many environments (e.g. [16,25], and both are readily available. After an incubation period of ~2 weeks, bone fragments were demineralized and remaining biofilm was subjected to both scanning (SEM) and transmission (TEM) electron microscopy. Biofilm was also tested against a range of antibodies (see methods), and reactivity compared with recovered dinosaur vessels exposed to the same antibodies.

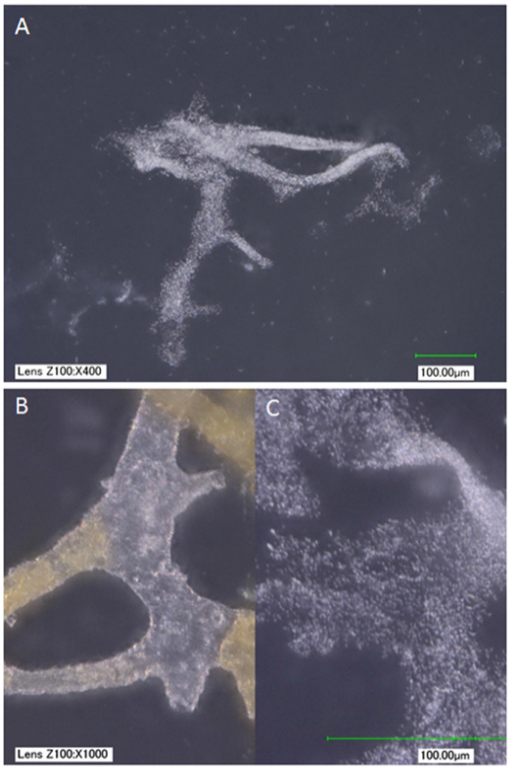

Fig 3. (A) *B.cereus* biofilm grown in cow bone from which organics had been removed (see methods). (B, C) Side-by-side comparison of vessels from MOR 2967-C5-1, a second *Brachylophosaurus* specimen from similar deposits (B), and (C) *B. cereus* biofilm recovered from cow bone at the same magnification. At low magnification, the biofilm mimics vessel shapes; higher magnification reveals that the biofilm is not hollow, as are the vessels, but rather amorphous clusters of cells. In addition, a red substance is clearly visible and differentially distributed within the hollow dinosaur vessels; no similar features are seen in the biofilm. Images taken with a KEYENCE VHX-2000 digital microscope, scale bar as indicated.

doi:10.1371/journal.pone.0150238.g003

Results

Our first attempt to completely remove organics from relatively large (~2cm x 2cm) pieces of bone was unsuccessful. Even after repeated cycles of extreme heat (~200°C), bleach, and enzyme treatment spanning a period of ~3 months, demineralization of the apatite phase of the bone left visible intact vessels and fibrous matrix. It was important to successfully remove all traces of organics, and thus a nutrient source for microbes, to accurately model conditions within dinosaur bone, because it has been proposed that organics do not persist into the fossil record [20–22]. Intriguingly, if organics persist, microbes *will* invade to obtain nutrients; thus biofilm growth may be independent support for organic preservation in bone. However, even after repeated cycles of harsh treatment, collagen matrix and other components persisted; we

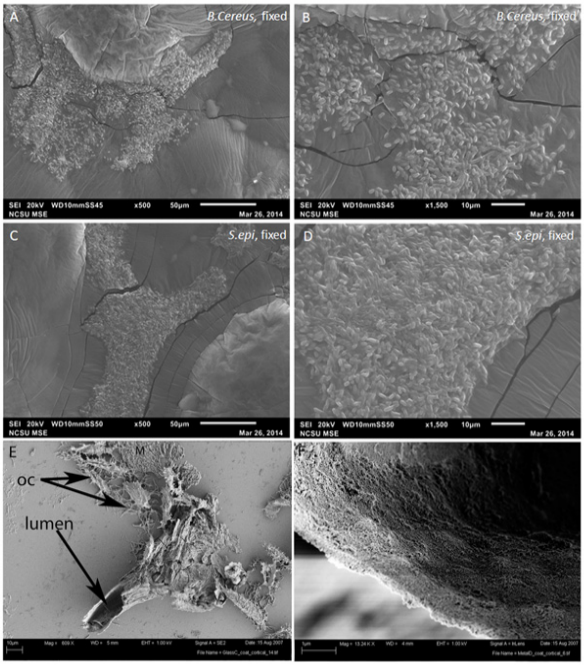

Fig 4. SEM images of (A-B) *B.cereus*; (C-D) *S.epidermidis*, grown in cow bone from which organics had been removed, and fixed with 10% neutral buffered formalin. At low magnification (A, C) the biofilms are roughly in the shape of the bone channels, but higher magnification demonstrates that they are a rather unorganized mass of cells. These are compared with low (E) and higher magnification (F) of vessels recovered from demineralized dinosaur (MOR 2598) bone. E) Dinosaur-derived vessel, arrows indicate the open vascular lumen and remnant osteocytes (OC) recovered in association with vessels during demineralization. Also associated with the vessel are fragments of fibrous matrix (M). The vessel is hollow, and the lumen continues through the length of the vessel. F) High magnification of vessel wall, showing solid fabric and relatively uniform thickness, neither of which are characteristics of biofilm.

doi:10.1371/journal.pone.0150238.g004

could only achieve complete removal of organics after the bone fragments were sufficiently reduced in size (~1cm cubes), and cycles of treatment were significantly prolonged.

Once organics were successfully removed, leaving a bioapatite scaffold to which biofilm-forming organisms could attach, the bone cubes were placed in either sterile water or nutrient broth containing microbes (see methods) and then demineralized to determine 1) if biofilm would form; 2) if this biofilm would retain coherence and morphology of vessels obtained from dinosaur; and 3) if any remnant biofilm would show antibody binding to the same antibodies, and in the same pattern, as observed for vessels recovered from dinosaur bone.

Fig 2A shows that when bone is placed in a nutrient medium, biofilm-producing microbes and biofilm will form, using the bone as a substrate. Both test organisms showed similar results, producing a flocculent biofilm on the surface and in the surrounding medium (Fig 2A and 2B). Higher magnification shows that biofilm is deposited on and interacts with the bone surface (Fig 2B, arrows). However, without the addition of nutrients to facilitate microbial growth, no biofilm was observed. We included feather, a non-biomineralized tissue, and eggshell,

biomineralized but not bone, to show that biofilms from both organisms will grow similarly, regardless of tissue type (Fig 2C and 2D), if nutrients are present.

After full colonization of the bone by both organisms in nutrient broth, the mineralized bone scaffold was removed by calcium chelation using ethylenediaminetetraacetic acid (EDTA). Fig 3A shows that the biofilm product superficially resembles blood vessels at low magnification in both chemically fixed and unfixed samples. However, these structures were never observed to possess a lumen and showed complete loss of integrity when manipulated, or even with simple rinsing. Both samples disintegrated (Fig 3C), in contrast to vessel structures recovered from dinosaur bone (Fig 3B), which were intact and retained shape, texture and hollow lumen, even after being manipulated multiple times [1,2].

Scanning electron microscopy (SEM) reveals further differences between the morphology of the bone-grown biofilm and vessels retrieved from dinosaur bone. Because unfixed biofilm samples did not retain their shape, we applied chemical fixatives to biofilm produced by *B. cereus* (Fig 4A and 4B) and *S. epidermidis* (Fig 4C and 4D) (see methods). These show that while the general shape of vessels is retained in low magnification (Fig 4A–4C), higher magnification images (Fig 4B and 4D) show a rather patchy distribution of microbial bodies, clearly discernible within or associated with an amorphous matrix. The structures are flat and two-dimensional, with no evidence of a lumen, which is consistently present in dinosaur vessels. Fig 4E and 4F show vessels isolated from demineralized bone of a *Brachylophosaur canadensis*, MOR 2598 [3]. These were not treated with fixatives, or any chemicals other than the EDTA used to demineralize the bone, yet the vessels retain shape and integrity and clearly differ in microstructure from the biofilm-produced material. Lower magnification shows branching of a portion of a vessel recovered from this dinosaur bone, with lumen visible at one end (Fig 4E, arrow). Fracturing from exposure of the fragile vessel to high vacuum used to image shows that the vessel is hollow throughout its length. High magnification of another dinosaur vessel shows that the wall of the vessel is smooth and solid, whereas biofilms are not generally uniform in structure, and are patchy in distribution (Fig 4B) [12,18]; their distribution is correlated to nutrient sources. In addition, SEM of dinosaur vessels has never shown what could pass for microbial bodies associated with the soft tissue structures. In fact, in the only work to show biofilm residing in relatively recent human bone [19], SEM imaging presents as a rather foamy appearance, with occasional microbial bodies visible (see [19], Figs 1 and 2), not a coherent structure with discernible shape as observed in these dinosaur materials.

Fig 5 compares TEM images of biofilm grown in bone with those of isolated vessels from the *Tyrannosaurus rex* MOR 1125 [1]. Little structure can be seen in biofilm samples, even after staining, and there is no visible lumen. Fig 5A shows *B. cereus* biofilm, fixed with neutral buffered formalin before demineralization of inoculated modern bone (methods). Fig 5B shows a higher magnification of this material, while Fig 5C shows biofilm from modern bone that has not been fixed prior to imaging. Fig 5D shows two isolated blood vessel sections from demineralized *Tyrannosaurus rex* (MOR 1125) bone visualized using TEM. The vessel walls are distinct, relatively uniform, and surround a lumen. Fig 5E shows another fragment of vessels, again with distinct wall and visible lumen. Fig 5F is a high magnification view of the material in the box in 5e. Elemental analyses [6,8] show that the vessels are infused with nanoparticles of iron, evidenced by the darker band in Fig 5F.

We show that these microbial structures, in both cases, are chemically distinct from dinosaur vessels as well. Antibodies to proteins present in, but not necessarily exclusive to vertebrate vasculature, bind specifically to vessels retrieved from dinosaur bone, but do not bind to biofilms grown in bone. Polyclonal antibodies raised against actin, a eukaryotic protein that forms the cytoskeleton of vertebrate cells [26,27], bind to the vessel walls of both dinosaurs (Fig 6E–6H), but do not react to biofilms prepared in the same manner (Fig 6A–6D). Similarly,

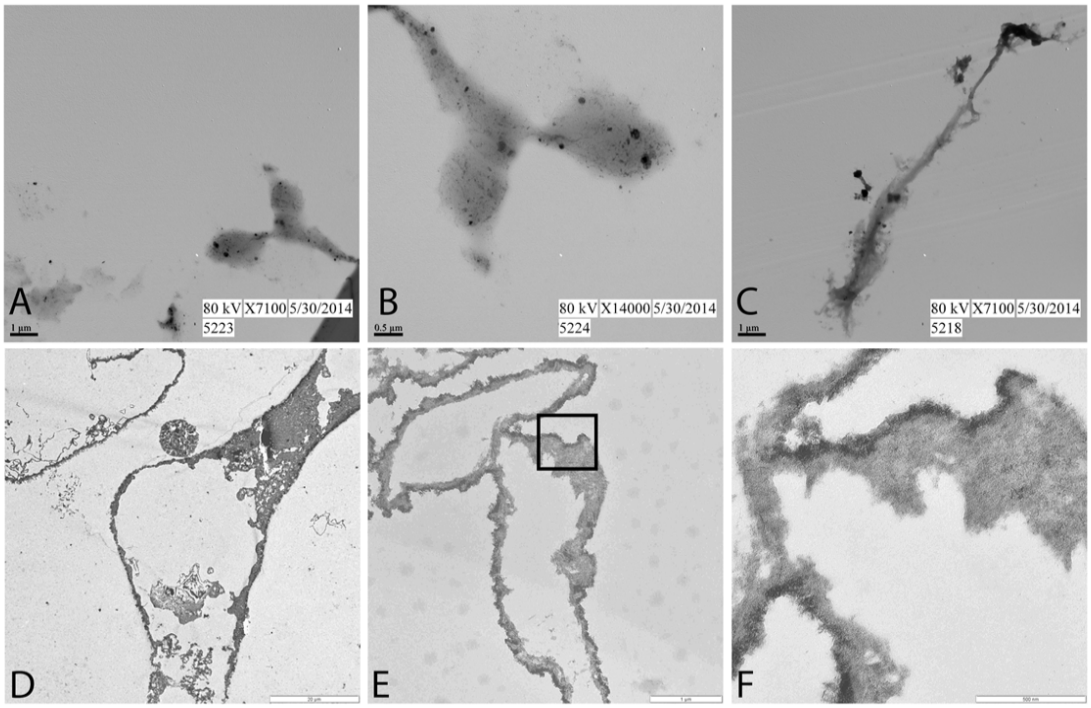

Fig 5. TEM images of biofilm recovered from modern bone from which organics had been removed (A-C), compared with representative vessels recovered from dinosaur bone (D-F). A, low and B, higher magnification of biofilm from bone that has been chemically fixed in 10% formalin. C. *B. cereus* biofilm, grown in bone but not chemically fixed (see methods). D. isolated vessel from *Tyrannosaurus rex* (MOR 1125). Vessel is naturally stained, most likely because of the intimate association of iron with these vessels [8]. E, low and F, higher magnification of a separate preparation of dinosaur vessels, showing open lumen and regular vessel wall structure.

doi:10.1371/journal.pone.0150238.g005

antibodies raised against elastin (Fig 7), a highly durable protein found in the walls of virtually all vertebrate blood vessels [28,29], and hemoglobin (Fig 8), the protein that functions to carry oxygen to tissues and the main protein found in red blood cells [30–32] also bind with specific reactivity to the dinosaur vessels (Figs 7E–7H and 8E–8H) but again, do not react with either biofilm when visualized using identical parameters (Figs 7A–7D and 8A–8D). Finally, antibodies to peptidoglycan, a glycosaminoglycan produced exclusively by bacteria [33], bind to the biofilms grown in bone (Fig 9A–9D), but do not bind to the dinosaur vessels under identical treatment conditions (Fig 9E–9H).

Discussion

The idea that original molecular components can survive across geological time is controversial [22,35,36] (but see [37,38]). The persistence of still-soft and flexible materials like blood vessels and bone cells in dinosaur bone is even more so. It has been predicted that DNA has limited stability [22,39], and will degrade to single bases under best-case conditions in about 6 million years. These time estimates are based upon decreased DNA recovery in a series of Holocene

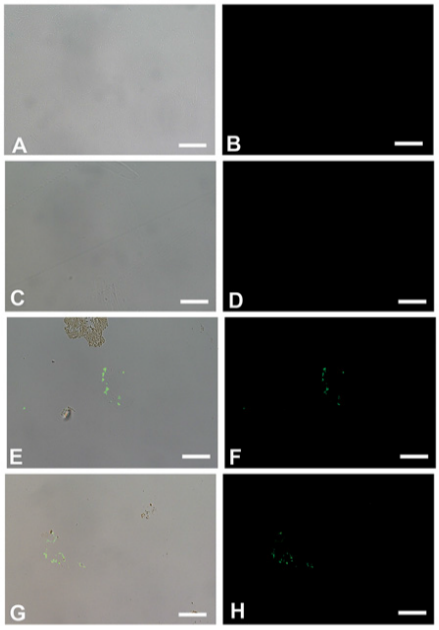

Fig 6. *In situ* immunohistochemistry of biofilms (A-D) and dinosaur vessels (E-H) exposed to polyclonal antibodies raised against actin, a cytoskeletal protein (see methods for details). A, C, E, G are overlay images, showing where on the tissue the antibodies bind; B, D, F, H are fluorescent images showing only antibody binding, as represented by the green fluorescence of the FITC label. A, B represent *B.cereus* biofilm grown in bone; C,D is *S. epidermidis* biofilm; E, F is vessels from *B. canadensis* (MOR 2598 [3]), G, H, vessels from *T. rex* (MOR 1125 [1]). Scale bar for all images = 20 μm

doi:10.1371/journal.pone.0150238.g006

fossil and subfossil materials dating to ~7500 years, then extrapolation of these data to longer time frames [22]. Alternatively, determining breakdown rates of 'naked' DNA in solutions has also been used as a proxy for time [39,40]. Verifiable and accepted DNA sequences have yet to be published from bones older than 1Ma.

Protein survival rates vary depending upon the protein tertiary/quaternary structure and burial history, among other factors [24], but in general, are predicted to outlast DNA. Even so, conventional wisdom states that proteins also will not survive into deep time [24]. Therefore, structures derived from proteins, such as the soft tissues we reported, were proposed to be derived from contamination [5], because if constituent molecules cannot persist in geological time, how can the structures they comprise do so?

We argued for endogeneity of these structures based upon the following lines of evidence: 1) Morphology was inconsistent with other alternatives, but consistent with vessels and osteocytes; 2) Textural differences between the structures were maintained at sub-micrometer levels (i.e., fibrous matrix was distinct, both from osteocytes embedded within it [7], and from vessels); 3) Chemical differentiation between adjacent structures was supported by color differences between vessels, osteocytes, osteocyte filopodia and fibrous matrix (e.g. [2,3]); 4) The materials showed differential response to antibodies raised against eukaryotic or vertebrate proteins [3,6,7,11]; and 5) Molecular sequence data supported a vertebrate source [3,41–43].

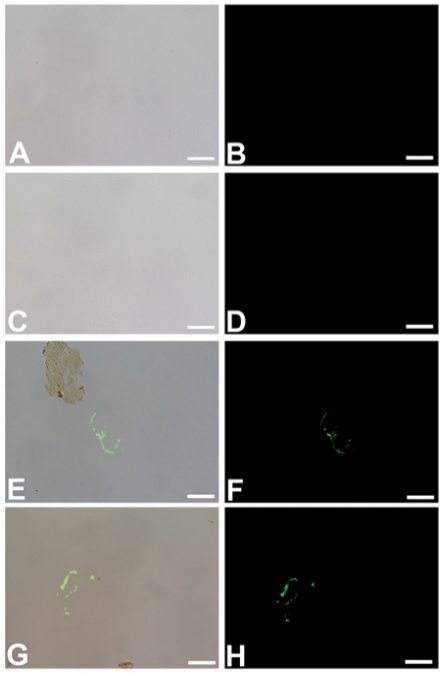

Fig 7. *In situ* immunohistochemistry of biofilms (A-D) and dinosaur vessels (E-H) exposed to polyclonal antibodies raised against elastin, a highly conserved, robust protein found in vascular walls [28,34] (see methods for details). As above, A, C, E, G are overlay images; B, D, F, H are fluorescent images showing only antibody binding, as represented by the green fluorescence of the FITC label. A, B represent *B.cereus* biofilm grown in bone; C,D is *S. epidermidis* biofilm; E, F is vessels from *B. canadensis* (MOR 2598 [3]), G, H, vessels from *T. rex* (MOR 1125 [1]). The specificity of these antibodies is illustrated by the binding to the isolated vessel in E, but not the portion of fibrillar matrix that is naturally stained and visible in the upper left. These antibodies do not bind to either biofilm. Scale bar for all images = 20 μm

doi:10.1371/journal.pone.0150238.g007

Here, we present additional data that *disproves* the hypothesis that these structures derive from biofilm, using actualistic experiments and data from the literature characterizing biofilms and their interactions with substrates.

Microbes most certainly were associated with degrading dinosaur tissues, just as surely as they are found in association with *all* degrading organic matter today. Their presence in the sediments surrounding dinosaur skeletal elements, or even their signature within the bone itself, does not preclude endogenous materials from also being present. Biofilms and bacteria coexist with living organisms, both as contributors to pathology (e.g. [44,45]) and to health (e.g. [46] and references therein). But when an organism dies, the body's defense mechanisms no longer keep these in check, and they proliferate. This, in addition to microbial invasion from the environment, contributes to breakdown and degradation of organics.

However, microbial invasion in bone is easily traced by histological markers, such as Wedl tunneling or focal destruction (e.g. [47,48] and references therein). No such traces were visible in histological sections of dinosaur bone used in this (Fig 10) or other studies. Additionally, although microbial invasion can occur through the vasculature, canaliculi containing osteocyte

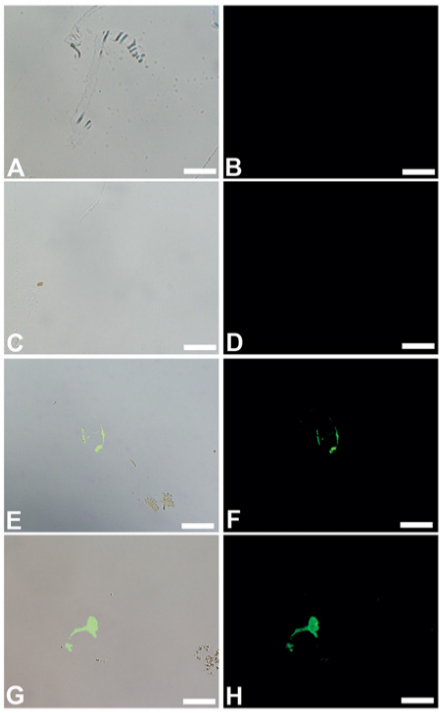

Fig 8. Overlay and fluorescent images of *B. cereus* (A, B), *S. epidermidis* (C, D) *B. canadensis* vessels (E, F) and *T. rex* vessels (G, H) exposed to antiserum raised against purified ostrich hemoglobin. No binding of these antibodies to either biofilm is visualized, but specific binding to vessels from both dinosaurs is seen. Scale bar for all images = 20 μm

doi:10.1371/journal.pone.0150238.g008

filopodia are smaller in diameter than single microbes, making transmission via the lacuno-canalicular network difficult ([7] and references therein).

Here, we have shown that it is difficult to fully remove organics from bone while leaving the mineral phase intact, despite harsh treatment. This result was surprising, and has implications for our understanding of the "fossilization" of organic remains. These labile components, when encased within dense cortical bone, may be much more resistant to degradative processes than previously thought.

Because microbes colonize surfaces where organic nutrient sources are available, the removal of organics is important. It is well known and tested that biofilm will employ living tissues as a substrate for growth (e.g. [12,14,16,49]), but here, we test the hypothesis that biofilm will colonize dinosaur bone if no organics remain. To do this, we could either use synthetic apatite, containing no organics, or remove organics from existing bone. We chose the latter, because synthetic apatite is not as porous as bone; therefore it could be argued if biofilm did not grow, that it was not an accurate system to mimic invasion of dinosaur bone.

We show that, if bone pieces are sufficiently small (with correspondingly great surface area), and if they are placed in a nutrient broth containing molecules needed for growth, microbes

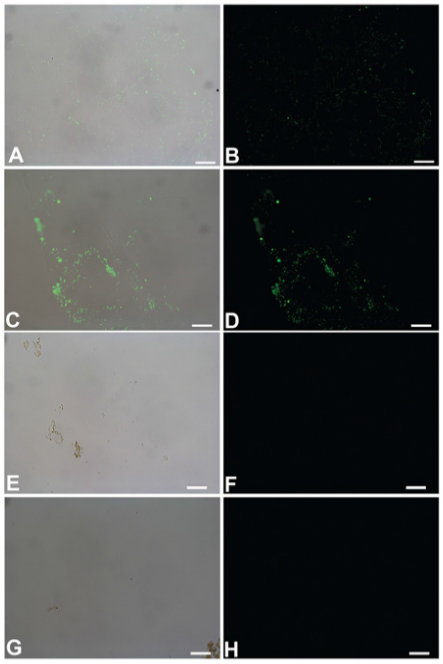

Fig 9. Overlay and fluorescent images of *B cereus* (A, B), *S. epidermidis* (C, D) biofilms, *B. canadensis* (E, F) and *T. rex* (G, H) vessels, exposed to antibodies raised against peptidoglycan, a bacterially produced glycosaminoglycan that is a component of both bacterial cell walls and the EPS they secrete [33]. Binding of these antibodies is evident in both biofilm products, but no binding is seen of these antibodies to either dinosaur vessel. Scale bar for all images = 20 μm

doi:10.1371/journal.pone.0150238.g009

and their associated biofilm will interact with bone surfaces when organics are removed. Controls of bone with organics removed, then inoculated with microbes, did *not* produce biofilm when placed in sterile water, but required nutrient broth (methods); thus bone alone could not supply these microbes with sufficient nutrients to produce a biofilm. These data have implications for analyses of Cretaceous bone; if modern biofilm can be shown definitively to occupy fossil bone, it may imply retention of original organics as a nutrient source for these microbes.

We have also shown that, if fixatives are applied to the biofilm before removing the bone lattice through demineralization, biofilm can bear superficial resemblance to blood vessels prior to any manipulation. However, unlike vessels, the microbial structures do not possess a lumen, but rather are 2-dimensional casts of the channels in bone. Even when fixatives are applied, these biofilm structures do not hold their shape under manipulation, as do vessels derived from dinosaur bone. This illustrates the need for chemical data, not just morphology, when claiming original microstructural components can be recovered from fossil organisms.

Finally, we show that antibodies raised against eukaryotic proteins not present in microbes bind to dinosaur vessels, but do *not* bind to biofilms grown in bone. Conversely, antibodies raised against microbial peptidoglycan *do* bind to the biofilm grown in bone, but do not bind to dinosaur vessels. These data, together with those put forth in previous publications (e.g. [1–

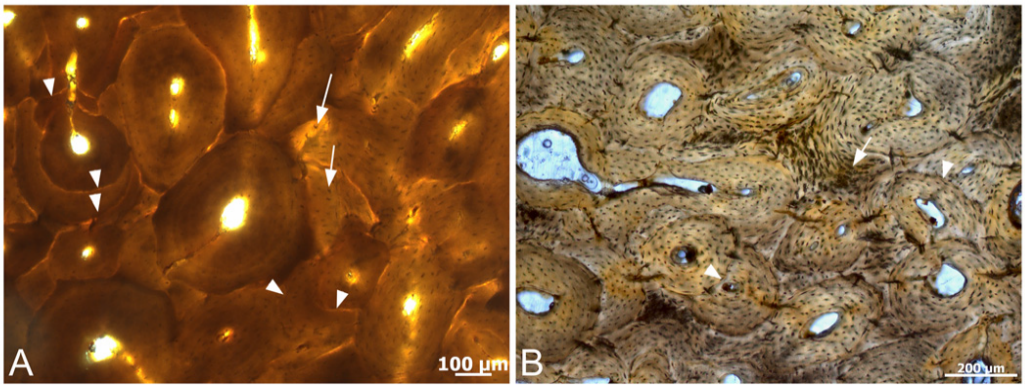

Fig 10. Histological ground sections of A). *T.rex* cortical bone and B) *B. Canadensis* cortical bone, from which the vessels in this study derive. No evidence of focal destruction Wedl tunneling, or other signs of microbial invasion are visualized. However, histological detail, including multiple generations of secondary osteons (arrowheads) and osteocyte lacunae with cannalicular extensions (arrows) are visible in both samples, attesting to histological integrity. The lack of cement lines (indicating remodeling) in *B. canadensis* bone support a younger ontogenetic age for this dinosaur.

doi:10.1371/journal.pone.0150238.g010

3,6,7,41–43] refute the hypothesis that the vessels, osteocytes, and fibrous matrices derived from dinosaur and other fossil bone tissues are solely derived from microbial invasion. Furthermore, sequence data from chemically extracted dinosaur bone [3,41,42] and isolated dinosaur vessels [50] refutes a microbial source.

It should be noted that microbes do indeed play an important role in the fossilization of organic remains (e.g. [51,52]). To enter the rock record, labile organics or the tissues they comprise must be stabilized before degradation is complete[53]. Although microbes are the main agent of degradation, they have been shown to also play an important role in stabilization by mediating, either passively or actively, rapid mineralization of organic materials [54–58], thus imparting stability. The co-existence of microbes or their products with original organic components has been demonstrated repeatedly ([59,60] and references therein); thus both microbial and vertebrate signal may be detected in fossil studies.

When all data are taken into consideration, an endogenous source for these dinosaur-derived tissues is best supported. Determining the endogeneity of soft tissue dinosaur remains opens new avenues of investigation and supports the hypothesis that original molecules, including proteins and perhaps DNA, may persist in fossil bone. This in turn, may provide alternative ways of testing evolutionary hypotheses. Additionally, understanding the chemical alterations of original organics at the molecular level may have implications for fields as far removed as human health.

Materials and Methods

Bovine cortical bone (from local Food Lion grocery) were cut into ~2 cm x 2cm fragments (first round). There was no information on the provenance; it is presumed to derive from a local (NC) feedlot. The bone was purchased fresh, but kept frozen until used in this study. Bone was subjected to sequential digestion using 1) 0.5mg/ml proteinase K (PCR grade, Roche 03115879001) solubilized in 30 mM Tris·Cl; 30 mM EDTA; 5% Tween 20; 0.5% Triton X-100; 800 mM GuHCl, pH 8.0 (product information at www.5Prime.com; proteinase K manual_5-prime_1044725_032007.pdf) and employed at a working temperature of 50C for 5 days;

Trypsin (2 mg/ml, Worthington Biochemical Corp LS003703) solubilized in water with 0.1% calcium chloride, pH 7.8. working temperature 37C [61]; 3) Collagenase A (2mg/ml, Roche 11088785103) solubilized in Dulbucco's phosphate buffered saline, working temperature 37C) for ~48 hours (At the beginning of each digestion, bone was incubated with enzyme solutions in a vacuum oven at room temperature (RT) for 2–3 hours for better infiltration. After sequential digestions, bone was rinsed in E-Pure water to remove enzyme, baked at 200C for 2 days, then incubated with 10% bleach solution for 3 days). Baking and bleaching steps were repeated two more times to complete one cycle. After repeated sequential treatment for a period of ~3 months, demineralization of bone showed continued presence of vessels, cells and matrix, morphologically unaffected by this treatment. Therefore, this treatment sequence was repeated on smaller blocks of bone (~ 1cm x 1 cm), until demineralization left no trace of organic remains, approximately 8 months. Between bleach and enzyme cycle, bone was washed at least 10 times with E-pure water to remove all chemicals. After all organic material were removed, "naked" bone pieces were washed thoroughly again with e-pure water and air-dried before inoculation with biofilm forming organisms. For handling and treatment of dinosaur vessels please see SOM in references[1–3,6,8].

Cotton Blue Staining

B. canadensis (MOR 2598) vessels were embedded for TEM in LR white embedding medium (see below) and 200nm sections were taken and dried onto microscope slides. Modern fungus were not nembedded but dried directly on microscope slides. Both dinosaur vessels sections and fungi were stained using the Lactophenol Cotton Blue Solution protocol from the manufacturer (Fluka Analytical 61335). A drop of Lactophenol Blue Solution was added to each sample, coverslips were applied. Stain was allowed to incubate with both samples for ~ five minutes at room temperature, then samples were imaged using a Zeiss Axioskop 2 plus biological microscope.

Inoculation and growth of biofilm in organic-free bone

Pieces of bone (organics removed) were inoculated with pure cultures consisting of *Bacillus cereus* (ATCC 14579) or *Staphylococcus epidermidis* (ATCC 49134) in 5% tryptic soy broth (TSB). Pieces of bone were also incubated in sterile E-pure water and sterile E-pure water inoculated with bacteria as negative controls; no biofilm was recovered from these. Setups were maintained in 6-well cell culture plates, rocking at room temperature (~20–22°C) for approximately two weeks. The experiment was halted by fixing the pieces of bone in 10% neutral buffered formalin, washing off excess formalin with E-pure water then demineralizing in 0.5% EDTA (pH = 8.0). The experiment was repeated but without the final fixation step, so that artefact induced by fixation would be recognized.

Scanning electron microscopy (SEM)

Samples were washed in 3 changes of E-pure water, allowed to air dry mounted on double sided carbon tape, then coated with ~10nm of gold/palladium. Samples were imaged with a JEOL JSM-6010LA analytical SEM controlled by JEOL InTouchScope version 1.05A software.

Transmission electron microscopy (TEM)

Samples were fixed in 10% neutral buffered formalin, then washed with 1X phosphate buffered saline (PBS) for TEM. Washed samples were dehydrated in 2 changes of 70% ethanol for 30 minutes each, followed by 1 hour incubation in LR white: 70% ethanol (2:1). Samples were

then incubated in 3 changes of undiluted LR white for 1 hour each, then embedded in gelatin capsules and polymerized for 24 hours at 60°C. A Leica EMUC6 ultra-microtome with a Diatome 45° knife was used to cut 90nm sections which were mounted on 200 mesh copper grids. Samples were stained with 15% methanolic uranyl acetate (5 minutes), washed in E-pure water, Reynold's lead citrate (8 minutes) with a final wash. Sections were imaged using Erlangshen ES1000W Model 785 TEM coupled to a CCD 11Megapixel High-speed Digital Camera, and analyzed using Gatan Microscopy Suite (GMS) software.

Dinosaur materials

Dinosaur bone was provided by the Museum of the Rockies, Bozeman, MT, and include *Tyrannosaurusrex* (MOR 1125) *Brachylophosaurus canadensis* (MOR 2958) and a second *Brachylophosaurus* (MOR341 2967-C5-1). All necessary permits for dinosaur collection were obtained for the described study by the Museum of the Rockies, and complied with all relevant regulations. No additional permits were required for the current study, which complied with all relevant regulations. Specimens are currently reposited at the Museum of the Rockies, Bozeman, MT, USA 59717. These specimens were recovered from federal lands and are publicly reposited, and available to others to study with permission from the curator.

TEM of MOR 1125 vessels

Vessels were liberated from dinosaur femora cortical bone using EDTA, pH 8.0 (see methods in references [1,2,6]), then either fixed in a solution of 2% paraformaldehyde: 0.01% gluteraldehyde, or left unfixed. Vessels were then rinsed and embedded in 6% agar (Sigma). Samples were rinsed, then dehydrated in ethanol series from 50% to 100%. Some material was post-fixed in 1% OsO4 for 1 hour. Samples were infiltrated with acetone, followed by 1:1 acetone: Spurrs embedding medium, then 100% Spurrs to infiltrate under vacuum overnight. Sections were cut to 60–90 nm and placed on Au 200 mesh EM grids. Some sections were post-stained in uranyl acetate:lead citrate, others were not stained. Sections were imaged using a ZEISS LEO 912 with an acceleration voltage of 100 kV, coupled to a Proscan 2048–2048 digital CCD camera.

In situ Immunohistochemistry (IHC)

Using the same embedded LR white bullets and ultra-microtome used for TEM prep, 200nm sections of either dinosaur vessels, recovered as described, or biofilm, were cut and mounted on 6-well (8mm) Teflon-printed slides and dried overnight at 42°C. Sections were etched with 25 μg/mL Proteinase K in 1X phosphate buffered saline (PBS) buffer at 37˚C for 15 minutes, followed by 0.5 M ethylenediaminetetraacetic acid (EDTA) pH 8.0 (3x10 minutes) and lastly with $NaBH_4$ (2x10 minutes). Incubations were separated by two five-minute washes in PBS. Following these steps to accomplish epitope retrieval and quenching of autofluorescence, 4% normal goat serum (NGS) in PBS was applied to occupy non-specific binding sites and prevent spurious binding. Sections were incubated in primary antibody (Polyclonal Rabbit anti-Chicken actin 1:75 (Capralogics, Inc. P00851), polyclonal Rabbit anti-Bovine elastin 1:75 (Courtesy of R. Mecham), Polyclonal Rabbit anti-ostrich Hb 1:200 (GenScript 70594), Monoclonal Mouse anti- peptidoglycan 1:75 (AbD Serotec, 7263–1006)) in primary dilution buffer overnight at 4°C. All sections were then incubated with secondary antibody (biotinylated goat anti-rabbit IgG(H+L) (Vector BA-1000) diluted 1:500 for rabbit primary antibodies, biotinylated goat anti-mouse IgG (H+L) (Vector BA-9200), diluted 1:500 for monoclonal mouse anti-peptidoglycan, for 2 hours at room temperature. Sections were then incubated Fluorescein Avidin D (FITC, Vector Laboratories A-2001) for 1hr at RT. All incubations were separated by

sequential washes (2 times for 10 minutes each) in PBS w/Tween 20 followed by two 10minute rinses in PBS. Finally, sections were mounted with Vectashield H-1000 mounting media, and coverslips applied. Sections were examined with Zeiss Axioskop 2 plus biological microscope and captured using an AxioCam MRc 5(Zeiss) with 10x ocular magnification on the Axioskop 2 plus in the Axiovision software package (version 4.7.0.0).

Dinosaur bone petrographic section

Dinosaur bone was examined for microstructural alteration, including evidence of Wedl tunneling or focal destruction[62]. Cortical bone fragments were embedded in Silmar resin, cut, and ground following previous protocols[63] for histological analyses. Transmitted light images were taken on a Zeiss AxioSkop 2 and cross-polarized images were taken on a Zeiss Axioskop 40.

Acknowledgments

This research was funded by grants to MHS from the David and Lucile Packard Foundation and NSF INSPIRE program (EAR-1344198), and NSF (DGE-1252376) to AEM. We thank Jack Horner and the Museum of the Rockies field crews for access to fossil specimens used in this study. We also thank N. Equall (ICAL facility) and S. Brumfield (Plant Pathology), of Montana State University, and T. Tung (Materials and Science Engineering) of NCSU for electron microscopy assistance. No permits were required for the described study, which complied with all relevant regulations.

Author Contributions

Conceived and designed the experiments: MHS AEM WZ. Performed the experiments: AEM WZ. Analyzed the data: MHS AEM WZ. Contributed reagents/materials/analysis tools: MHS. Wrote the paper: MHS AEM WZ.

References

1. Avci R, Schweitzer MH, Boyd RD, Wittmeyer JL, Arce FT, Calvo JO. Preservation of bone collagen from the late cretaceous period studied by immunological techniques and atomic force microscopy. Langmuir. 2005 APR 12; 21(8):3584–90. PMID: ISI:000228218700055.
2. Schweitzer MH, Wittmeyer JL, Horner JR. Soft tissue and cellular preservation in vertebrate skeletal elements from the Cretaceous to the present. Proc R Soc Lond B. 2007; 274:183–97.
3. Schweitzer MH, Zheng W, Organ CL, Avci R, Suo Z, Freimark LM, et al. Biomolecular characterization and protein sequences of the Campanian hadrosaur *Brachylophosaurus canadensis*. Science. 2009; 324:626–29. doi: 10.1126/science.1165069 PMID: 19407199
4. Lindgren J, Uvdal P, Engdahl A, Lee AH, Alwmark C, Bergquist K-E, et al. Microspectroscopic evidence of Cretaceous bone proteins. PLoS One. 2011; 6(4):e19445. doi: 10.1371/journal.pone.0019445 PMID: 21559386
5. Kaye TG, Gaugler G, Sawlowicz Z. Dinosaurian soft tissues interpreted as bacterial biofilms. PLoS One. 2008; 3(7):e2808. doi: 10.1371/journal.pone.0002808 PMID: 18665236
6. Schweitzer MH, Suo Z, Avci R, Asara JM, Allen MA, Teran Arce F, et al. Analyses of soft tissue from Tyrannosaurus rex suggest the presence of protein. Science. 2007; 316:277–80. PMID: 17431179
7. Schweitzer MH, Zheng W, Cleland TP, Bern M. Molecular analyses of dinosaur osteocytes support the presence of endogenous molecules. Bone. 2013; 52:414–23. Epub October 17 2012. doi: 10.1016/j.bone.2012.10.010 PMID: 23085295
8. Schweitzer MH, Zheng W, Cleland TP, Goodwin M, Boatman E, Theil E, et al. A role for iron and oxygen chemistry in preserving soft tissues, cells and molecules from deep time. Proceedings of the Royal Society, Series B. 2014; 281(20132741):1–10. Epub 27 November 2013.
9. Harris SD. Branching of fungal hyphae: regulation, mechanisms and comparison with other branching systems. Mycologia. 2008; 100(6):823–32. PMID: 19202837

10. Bartnicki-Garcia S, Bracker CE, Gierz G, López-Franco R, Lu H. Mapping the Growth of Fungal Hyphae: Orthogonal Cell Wall Expansion during Tip Growth and the Role of Turgor. Biophys J. 2000; 79(5):2382–90. PMID: 11053117

11. Schweitzer MH, Wittmeyer JL, Horner JR, Toporski JK. Soft-tissue vessels and cellular preservation in Tyrannosaurus rex. Science. 2005 MAR 25; 307(5717):1952–5. PMID: ISI:000227957300054.

12. Donlan RM. Biofilms: Microbial Life on Surfaces. Emerging Infect Dis. 2002; 8(9):881–90. PMID: 12194761

13. Singh R, Paul D, Jain RK. Biofilms: implications in biofilm remediation. Trends Microbiol. 2006; 14 (9):389–97. PMID: 16857359

14. Stoodley LH, Costerton JW, Stoodley P. Bacterial biofilms: from the natural environment to infectious diseases. Nat Rev Microbiol. 2004; 2:95–108. PMID: 15040259

15. Stoodley P, Sauer K, Davies DG, Costerton JW. Biofilms as complex differentiated communities. Annu Rev Microbiol. 2002; 56:187–209. PMID: 12142477

16. Costerton JW, Cheng KJ, Geesey GG, Ladd TI, Nickel JC, Dasgupta M, et al. Bacterial biofilms in nature and disease. Annu Rev Microbiol. 1987; 41:435–64. PMID: 3318676

17. O'Toole G, Kaplan HB, Kolter R. Biofilm formation as microbial development. Annu Rev Microbiol. 2000; 54:49–79. PMID: 11018124

18. Stoodley P, Boyle JD, Dodds I, Lappin-Scott HM. Consensus model of biofilm structure. In: Wimpenny JWT, Handley PS, Gilbert P, Lappin-Scott HM, Jones M, editors. Biofilms: community interactions and control. Cardiff, UK: Bioline; 1997. p. 1–9.

19. Pitre MC, Correia PM, Mankowski PJ, Klassen J, Day MJ, Lovell NC, et al. Biofilm growth in human skeletal material from ancient Mesopotamia. J Archaeol Sci. 2013; 40:24–9.

20. Gutierrez G, Marin A. The most ancient DNA recovered from an amber-preserved specimen may not be as ancient as it seems. Mol Biol Evol. 1998 JUL; 15(7):926–9. PMID: ISI:000074477200016.

21. Willerslev E, Cooper A. Ancient DNA. Proceedings of the Royal Society of London Series B-Biological Sciences. 2005 JAN 7; 272(1558):3–16. PMID: ISI:000226838000001.

22. Allentoft ME, Collins MJ, Haile D. H OC J, L., Hale ML, et al. The half-life of DNA in bone: measuring decay kinetics in 158 dated fossils. Proceedings of the Royal Society B. 2012; 279(1748):4724–33. Epub October 10, 2012. doi: 10.1098/rspb.2012.1745 PMID: 23055061

23. Hofreiter M, Serre D, Poinar HN, Kuch M, Paabo S. Ancient DNA. Nature Reviews Genetics. 2001 MAY; 2(5):353–9. PMID: ISI:000168467800012.

24. Wadsworth C, Buckley M. Proteome degradation in fossils: investigating the longevity of protein survival in ancient bone. Rapid Commun Mass Spectrom. 2014; 28(605–615).

25. Stewart PS, Franklin MJ. Physiological heterogeneity in biofilms. Nat Rev Microbiol. 2008; 6:199–210. doi: 10.1038/nrmicro1838 PMID: 18264116

26. Tanaka Y. Architecture of the Marrow Vasculature in Three Amphibian Species and Its Significance in Hematopoietic Development. Am J Anat. 1976; 145:485–98. PMID: 1083670

27. Tanaka-Kamioka K, Kamioka H, Ris H, Lim S-S. Osteocyte Shape Is Dependent on Actin Filaments and Osteocyte Processes Are Unique Actin-Rich Projections. J Bone Miner Res. 1998; 13:1555–68. PMID: 9783544

28. Mecham RP. Elastin synthesis and fiber assembly. Ann N Y Acad Sci. 1991; 624(1):137–46.

29. Vito RP, Dixon SA. Blood vessel constitutive models-1995-2002. Annual Reviews of Biomedical Engineering. 2003; 5:413–39.

30. Coates M, Riggs A. Perspectives on the Evolution of Hemoglobin. Tex Rep Biol Med. 1980; 40:9–22. PMID: ISI:A1980MK40300003.

31. Czelusniak J, Goodman M, Hewettemmett D, Weiss ML, Venta PJ, Tashian RE. Phylogenetic Origins and Adaptive Evolution of Avian and Mammalian Hemoglobin Genes. Nature. 1982; 298(5871):297–300. PMID: ISI:A1982NX38600062.

32. Hardison R. Hemoglobins from bacteria to man: Evolution of different patterns of gene expression. J Exp Biol. 1998 APR; 201(8):1099–117. PMID: ISI:000073772900006.

33. Vollmer W, Blanot D, De Pedro M. Peptidoglycan structure and architecture. FEMS Microbiol Rev. 2008; 32(2):149–67. doi: 10.1111/j.1574-6976.2007.00094.x PMID: 18194336

34. Rosenbloom J, Abrams WR, Mecham RP. The elasatic fiber. FASEB J. 1993; 7:1208–18. PMID: 8405806

35. Buckley M, Larkin N, Collins MJ. Mammoth and mastodon collagen sequences: survival and utility. Geochim Cosmochim Acta. 2011 (75:):2007–16.

36. Collins MJ, Nielsen-Marsh CM, Hiller J, Smith CI, Roberts JP. The survival of organic matter in bone: a review. Archaeometry. 2002; 44:383–94.
37. Collins MJ, Gernaey A, Nielsen-Marsh CM, Vermeer C, Westbroek P. slow rates of degradation of osteocalcin: green light for fossil bone protein? Geology. 2000; 28(12):1139–42.
38. Sykes GA, Collins MJ, Walton DI. The significance of a geochemically isolated intracrystalline organic fraction within biominerals. Org Geochem. 1995; 23:1059–65.
39. Lindahl T. Instability and decay of the primary structure of DNA. Nature. 1993; 362:709–15. PMID: 8469282
40. Lindahl T. Recovery of antediluvian DNA. Nature. 1993; 365:700. PMID: 8413647
41. Asara JM, Garavelli JS, Slatter DA, Schweitzer MH, Freimark LM, Phillips M, et al. Interpreting sequences from mastodon and Tyrannosaurus rex. Science. 2007; 317:1324–25. PMID: 17823333
42. Asara JM, Schweitzer MH, Phillips MP, Freimark LM, Cantley LC. Protein sequences from mastodon (Mammut americanum) and dinosaur (Tyrannosaurus rex) revealed by mass spectrometry. Science. 2007; 316:280–85. PMID: 17431180
43. Organ CL, Schweitzer MH, Zheng W, Freimark LM, Cantley LC, Asara JM. Molecular phylogenetics of mastodon and Tyrannosaurus rex. Science. 2008; 320:499. doi: 10.1126/science.1154284 PMID: 18436782
44. Elkaim R, Dahan M, Kanter D, Kretz JG, Tenenbaum H. Prevalence of periodontal pathogens in subgingival lesions, atherosclerotic plaques and healthy blood vessels: a preliminary study. J Periodontal Res. 2008; 43:224–31. PMID: 18326058
45. Rhoads DD, Wolcott RD, Percival SL. Biofilm in wounds: management strategies. J Wound Care. 2008; 17(11):502–8. PMID: 18978690
46. Neish AS. Microbes in gastrointestinal health and disease. Gastroenterology. 2009; 136(1):65–80. doi: 10.1053/j.gastro.2008.10.080 PMID: 19026645
47. Child AM. Microbial tahonomy of arcaheological bone. Studies in conservation. 1995; 40(1):19–30.
48. Child AM. Towards an Understanding of the Microbial Decomposition of Archaeological Bone in the Burial Environment. J Archaeol Sci. 1995 MAR; 22(2):165–74. PMID: ISI:A1995RB29600004.
49. Donlan RM. Biofilms and device-associated infections. Emerging Infect Dis. 2001; 7(2):277–81. PMID: 11294723
50. Cleland TP, Schroeter ER, Zamdborg L, Zheng W, Lee JE, Tran JC, et al. Mass spectrometry and antibody-based characterization of blood vessels from *Brachylophosaurus canadensis*. J Proteome Res. 2015; 14:5252–62. doi: 10.1021/acs.jproteome.5b00675 PMID: 26595531
51. Raff EC, Andrews ME, Turner FR, Toh E, Nelson DE, Raff RA. Contingent interactions among biofilm-forming bacteria determine preservation or decay in the first steps toward fossilization of marine embryos. Evol Dev. 2013; 15(4):243–56. doi: 10.1111/ede.12028 PMID: 23809699
52. Raff EC, Schollaert KL, Nelson DE, Donoghue PCJ, Thomas C-W, Turner FR, et al. Embryo fossilization is a biological process mediated by microbial biofilm. Proceedings of the National Academu of Science. 2008; 105(49):19360–5.
53. Briggs DEG. The role of decay and mineralization in the preservation of soft-bodied fossils. Annual Review of Earth and Planetary Sciences. 2003; 31:275–301. PMID: ISI:000185093700008.
54. Briggs DEG. The Role of Decay and Mineralization in the Preservation of Soft-Bodied Fossils Annu Rev Earth Planet Sci. 2003; 31:275–301.
55. Briggs DEG. The role of biofilms in the fossilization of non-mineralized tissues. In: Krumbein WE, editor. Fossil and Recent Biofilms. Dordrecht: Springer Science and Business Media; 2003. p. 281–90.
56. Riding R. Microbial carbonates: the geological record of calcified bacterial-algal mats and biofilms. Sedimentology. 2000; 47:179–214.
57. Peterson JE, Lenczewski ME, Scherer RP. Influence of microbial biofilms on the preservation of primary soft tissue in fossil and extant archosaurs. PLoS One. 2010; 5(10).
58. Iniesto M, Zeyen N, López-Archilla A, Bernard S, Buscalioni AD, Guerrero MC, et al. Preservation in microbial mats: mineralization by a talc-like phase of a fish embedded in a microbial sarcophagus. Frontiers in Earth Science. 2015; 3.
59. Lindgren J, Moyer AE, Schweitzer MH, Sjövall P, Uvdal P, Nilsson DE, et al. Interpreting melanin-based colouration through deep time: a critical review. Proceedings of the Royal Society, Series B. 2015; 282:20150614.
60. Schweitzer MH, Lindgren J, Moyer AE. Melanosomes and ancient coloration re-examined: A response to vinther 2015. Bioessays. 2015; 37:1–10.

61. Liu J, Feitelson MA. Detection of hepatitis B virus x antigen by immunohistochemistry and Western blotting. In: Hamatake RK, Lau JYN, editors. Hepatitis B and D Protocols. Methods in Molecular Medicine. 1. Totowa, New Jersey: Humana Press; 2004. p. 71–9.

62. Jans MME, Kars H, Nielsen-Marsh CM, Smith CI, Nord AG, Arthur P, et al. In situ preservation of archaeological bone: a histological study within a multidisciplinary approach. Archaeometry. 2002; 44 (3):343–52.

63. Boyd C, Cleland T, Novas F. Osteogenesis, homology, and function of the intercostal plates in ornithischian dinosaurs (Tetrapoda, Sauropsida). Zoomorphology. 2011; 130(4):305–13.

CHAPTER 8 – Summary

This dissertation focuses on the preservation of soft tissues, primarily keratinous tissues, in the fossil record. I compared microscopic and molecular analyses of both fossil and extant samples, and, to test proposed modes of preservation, particularly the role microbes may play early in diagenesis of these labile tissues, I employed taphonomic experiments on modern, homologous and analogous, tissues. Most of the previously published research on soft tissue preservation has focused on cells and tissues preserved within bone [1–9]. I chose to focus on epidermally derived and non-mineralized tissues composed of keratin proteins. Such tissues have been documented in association with vertebrate fossils since the 1840s [10]. Keratinous structures are epidermally derived and function in homeostasis, defense, protection, feeding, and display, among others, and thus are essential to survival of the organism. The importance of soft tissue recovery in fossils for elucidating the paleobiology of these long extinct animals is inversely proportional to their abundance and frequency of discovery but provide insight into evolutionary features and strategies used by the relatives of present-day archosaurs.

I employed electron microscopy and immunohistochemical methods to analyze my samples. In Chapter 2, I addressed a current controversy in the field debating whether microbodies observed in fossil materials, particular feathers, are intracellular melanin containing organelles, melanosomes, or remnants of microbes involved in degradation [11]. This was approached by growing biofilms on extant feathers and comparing observations from this experiment with observations from fossils. Chapters 3 and 4 addressed this debate in more detail by reviewing the literature on interpreting melanin-based color in the fossil record and analyzing a fossil fish eyespot as a case study (Chapter 3) and also rebutting a recent review on ‘the field of paleo-colour’ (Chapter 4) [12,13]. In Chapter 5, I analyzed feathers from a 10 year taphonomic experiment for the retention of microscopic and molecular components. These data show the durability of keratin, particularly feather keratin, and support the likelihood that these persist in the rock record. I then analyzed fossil samples in the same manner: feather-like filament from the alvarezsaurid *Shuvuuia deserti* (Chapter 5) and claw material from the oviraptorid *Citipati osmolskae* (Chapter 6). In Chapter 7, similar to Chapter 2 with feathers, we tested the hypothesis that biofilm was the source of the soft tissues and vessel-like structures preserved in dinosaur bone [14]. Following is a summary of each Chapter in more detail.

The research presented in Chapter 2 arose in response to the many recent publications, starting in 2008 [15], that claim to have determined the coloration of ancient avian and non-avian dinosaurs based upon the hypothesis that microbodies associated with fossil feathers are pigment containing eukaryotic organelles, melanosomes [16–23]. However, the original hypothesis, that these bodies are fossilized microbes [24], had not been disproven in any of the studies. Therefore, the hypothesis that the observed fossil microbodies represent bacterial overgrowth as part of the degradation process was tested, using extant chicken and guineafowl feathers as models for ancient preserved feathers[11].

Scanning electron microscopy (SEM), field emission SEM (FESEM) and transmission electron microscopy (TEM) were used to examine untreated and uncompromised pigmented and non-pigmented feathers, and compared them with identical feathers exposed to biofilm-producing microbes, in pure and mixed cultures. Although the size and shape of melanosomes were similar to microbes, the distribution was very different: microbes were superficial, usually confluent and sometimes layered; whereas melanosomes were always embedded *within* keratin, rather sparsely distributed, and rarely overlapping. Melanosomes could also be visualized in TEM without staining, but microbes required a heavy metal stain. Based upon these characteristics, the data supported a microbial origin, as originally proposed, rather than 'melanosome' origin for microbodies in fossil feathers. The shape and distribution of bacteria growing across the surface of the feather in the experiments were more consistent with published images of purported fossil 'melanosomes'.

In addition, SEM coupled with energy dispersive X-ray spectroscopy (SEM-EDS), was used to examine a fossil feather ascribed to the Early Cretaceous Chinese bird, *Gansus yumenensis*. Similar to the fossil 'melanosome' studies, 'mouldic impressions' were observed in the fossil specimen. However, these impressions were also detected on the sediment grains associated with but not part of the fossil feather; not reported in any previous studies. Therefore, this observation supported a microbial origin for these structures, not a melanosome origin as concluded in the previous publications.

Distinguishing between these two sources is critical to the study of ancient organisms; therefore the discussion surrounding the melanosome vs. microbe debate was expanded upon in Chapters 3 and 4. Based upon the assumption that these microbodies are fossil melanosomes, and using morphological differences to identify eumelanosomes (elongate melanosomes expressing

grey and black tones) and pheomelanosomes (round melanosomes expressing orange, red or brown tones), inferences have been made about color, behavior, physiology, and ecological interactions of these extinct organisms [17–19,21,23,25–31]. Color determination is complicated because both eu- and phaeomelanin are both present in almost *all* pigmented feathers and it is their relative concentrations that determine color [32–34], and multiple types of pigment [35], which likely do not have the high preservation potential of melanin [36,37], as well as structural coloration can contribute to the color of a single feather [38–40], so overall color cannot be determined on shape of these microbodies alone [32,33,41]. The terms melanosome, melanin and bacteria were defined and criteria proposed that should be met for accepting a melanosome origin for the observed fossil structures.

Color is integral to many aspects of behavior in living animals [42]. Both eumelanin pigment and melanin-containing cellular organelles (melanosomes) can be preserved in fossils [12,26,43–47], and thus may help to resolve aspects of biology and ecology in long-extinct animals, such as feathered dinosaurs and early birds. Nevertheless, recognizing the traces of ancient melanin-based coloration is challenging and wrought with interpretative ambiguity, especially when observations are based on morphological evidence alone [15–21,23]. One of the most problematic assumptions is that all microbodies (or, more often reported, their ‘mouldic impressions’ [19,21,23,29,31]) encountered with fossil animal soft tissues are melanosomes rather than pervasive bacteria, a conjecture that is complicated by the fact that some microorganisms synthesize melanins [48]. Moreover, microbes are known to fossilize, some dating back to the Archean [49–52], and have been demonstrated in association with organic materials across the Phanerozoic (e.g. [24,53–57]).

Therefore in Chapter 3, current knowledge on vertebrate and microbial melanization was summarized and the current conflicts influencing analyses of microbodies associated with fossil animal soft tissues were discussed [12]. Evidence for both the melanosome and microbial hypothesis were presented, starting with distribution, organization and localization; as well as discussed taphonomic experiments that demonstrate the preservation potential of both. Evidence from the literature put forth to support each hypothesis was reviewed. Because much interpretation has been made of the presence of these minute bodies in the fossil record (including behavior, appearance and physiology as mentioned above), resting on the assumption that they are all melanosomes, a critical re-evaluation of the data from both perspectives was put

forth. Types of data that have been used to support both arguments were presented, and we evaluated whether the data are definitive and/or appropriate. The benefits from an integrated morphological and geochemical approach for detecting pigment molecular fingerprints and associated microstructures in fossils was presented through the use of a case study: structural and molecular identification of fossil melanosomes in the 'eye' of a teleost fish (FUM-N-2268) from the early Eocene of Denmark. A sample from the eye was subjected to SEM, TEM and time of flight secondary ion mass spectrometry (ToF-SIMS) and infrared microspectroscopy (IR). The data from each analysis were collectively considered to conclude a melanosome origin for the microbodies observed in the fossil fish 'eyespot' [12].

To my knowledge, only two published studies have applied this suite of techniques to a fossil feather [30,44], however Colleary et al. 2015 did not include TEM analyses [30] and the ToF-SIMS data presented were problematic, and their interpretation challenged (J. Lindgren, personal communication). The study led by Lindgren et al. 2015 provided chemical data to support a melanosome origin for some of the fossil microbodies, as well as some, but not all of the 'mouldic impressions' observed in the fossil feathers [44]. However, in this study other imprints in the matrix were described that did not present evidence for melanin, and therefore could not be assigned to melanosomes. The mouldic impressions figured in this paper were more similar to the ones I observed on the sediment grains associated with the *Gansus yumenensis* fossil feather described in Chapter 2, and suggested a microbial origin [11]. The authors concluded that although some microbodies could parsimoniously be melanosome in origin, others could equally be ascribed to a microbial source. These two studies further advocate for caution in ascribing all fossil microbodies to melanosomes.

Shortly following the publication of our fossil melanin review and case study, another review was published on 'the field of palaeo-colour' [27]. Because it consisted of misinterpretations of my data, as well as a lack of attention to certain aspects of the scientific literature, we wrote a rebuttal (Chapter 4) [13]. In this manuscript, in addition to addressing the misinterpretations and research Vinther failed to consider, we re-examined evidence for melanosomes in light of literature on the preservation potential of microorganisms and their exopolymeric secretions. We also: 1) discussed the need for caution in interpreting "voids" and microbodies associated with degraded fossil feathers; 2) presented evidence that microorganisms are, in most cases, at least an equally parsimonious source for these "voids" as ancient

melanosomes; and 3) suggested methods for differentiating melanosomes from microbial traces in the rock record. Finally, the need for parsimony when inferring organismal color, behavior and biology was addressed.

In Chapter 5, modern feathers from a Hungarian partridge were exposed to several conditions suggested as proxies for time which included: room temperature control, wet burial at 60°C for 3 years (then dried and kept at room temperature until analyses), dry burial at 350°C, and lastly the whole bird, with remaining feathers attached, was buried in a drainage channel. To keep immediate conditions as similar as possible, all feathers except the control were buried in sands taken from a single dinosaur excavation site in the Judith River Formation in northern Montana (USA). The feathers were analyzed using gross observation, light microscopy, TEM to document changes in microstructure, *in situ* immunofluorescence (IF) was employed to test for the durability of keratin epitopes. A custom-made antiserum, raised against extracts of mature modern chicken feathers (anti-chicken feather antiserum) was used in the IF experiments. All appropriate controls were conducted in parallel to demonstrate the specificity and applicability of the antibody. In addition, I repeated an experiment published almost two decades ago [58], confirming the preservation of feather-like molecules in a fossil filament collected from *Shuvuuia deserti*, a 75 million year old dinosaur [59].

These experiments had duration of over 10 years before the microscopic and molecular methods were applied. The temperature conditions in this study were chosen because 1) temperature has been suggested in the literature to be a proxy for time in the degradation of organic molecules with the trend that warmer and wetter conditions result in the most destruction [60,61], 2) destruction of all microscopic and molecular components of the feathers was predicted, particularly for the 350°C condition, but this was not observed, 3) the 60°C condition with an influence of water would be similar to conditions in the Cretaceous [62], and 4) these temperatures were available and could be maintained for an extended amount of time at the facility where the experiment was being conducted.

This study showed that feather microstructure and keratin epitopes remain detectable, though for the 350°C feathers, they were greatly reduced. These data have profound implications for the preservation of keratinous material frequently observed in association with non-avian dinosaurs. This is especially applicable to the debate discussed above, whether the preservation of microbodies associated with fossil feathers are preserved pigment containing organelles,

melanosomes, or the remnants of bacteria. Further analyses are required to determine if melanin 'leached' during degradation and thus may still be present in the sample (J. Lindgren personal communication); however, in this study, keratin epitopes persisted but melanosomes did not. If the structures observed in other studies are indeed fossil melanosomes, the matrix in which they are embedded should be keratin, and we show that keratin should be detectable using appropriate methods.

In Chapter 6, electron microscopy and *in situ* immunohistochemistry methods were used to demonstrate the microscopic and molecular preservation of ~75 million year old fossil claw material from the well-recognized brooding oviraptor (IGM 100/979). During the initial preparation and description of this specimen, the original authors noted the presence of a white material extending from one of the manual digits that was distinct from the surrounding matrix and underlying bone [63,64]. They hypothesized that this material represented remains from the original keratinous claw sheath covering the bone. I tested this hypothesis using multiple methods to compare textural, microstructural and immunological response of these fossil tissues to those of claw sheath from extant ratites, ostrich and emu.

The results supported the initial hypothesis, by showing micro- and ultrastructural similarities between the fossil and modern claw materials. Immunohistochemical analyses add to the growing literature supporting the preservation of proteins over deep time, which have primarily focused on bone. I showed the presence of endogenous epitopes to beta-keratin proteins in the fossil claw. Because beta-keratin is not produced by either mammals or microbes, the two most obvious sources of contamination, the likelihood that these signals arose from contamination is greatly reduced.

Chapter 7 focused on research that again addresses the presence and role of bacteria in the preservation of soft tissues [14]. In 2005, the first reports of still-soft, blood vessel-like networks with intravascular contents, and osteocytes recovered after demineralization of dinosaur bone were published [1], and because of morphological, histological, molecular and microscopic data, it was proposed that they were endogenous to the dinosaur. These materials have since been recovered in a variety of fossil specimens (e.g. [3,9,65]) and recently, peptide sequences consistent with the proteinaceous composition of vertebrate blood vessel were recovered using high resolution mass spectrometry methods [65].

Despite multiple studies and publications supporting the endogeneity of these structures, it has been proposed that these materials arise from contamination by biofilm forming organisms [66]. The biofilm hypothesis was directly tested by removing organics from modern bone, placing these mineral (apatite) blocks in diluted nutrient broth, and inoculating with biofilm-forming organisms to attempt to grow biofilms. After demineralizing the bone, biofilms were recovered and analyzed using the same methods as for dinosaur materials. The data showed clear differences in morphology and antibody response between biofilm grown in bone and vessels recovered from dinosaurs, thus refuting the biofilm hypothesis. Although biofilm does not explain the presence of blood vessels, cells or organic matrix in bone, we have shown in the above experiments (Chapters 2 and 7) that because of their propensity to grow on and interact with flat surfaces, they most likely play a role in stabilizing superficial keratinous structures (i.e. feathers, skin) through secretion of easily mineralized extracellular polymeric substances (EPS) [67,68].

To further examine this role, I also degraded feathers in sediment collected from the Neuse River. These degradation experiments resulted in observations that mimic what is seen in the rock record. In one experiment, a black halo was observed surrounding the degrading feather which resembles the black 'carbonaceous' films described for fossil feathers (Figure 1). In another, the rachis of the feather was completely degraded away before any other parts of the feather (Figure 2). Often the rachis cannot be discerned in fossil feathers (e.g., Figure 5 of *Gansus yumenensis* feather in Chapter 2), which has been a challenge for determining the evolutionary steps involved in ancestral states of these complex epidermal appendages [69]. Further analyses are necessary to not only determine what remains in these samples but also the processes responsible for producing these results. Nonetheless, the preliminary findings from these relatively simple degradation experiments demonstrate how fundamental taphonomic experiments are to our understanding of fossilization. These data will be submitted for publication in post graduate work.

Future Directions

My dissertation has only 'scratched the surface' of our understanding of soft tissue preservation and the role microbes may play in their preservation. My research has demonstrated that beta-keratin proteins and the tissues they comprise are good targets for molecular paleontological studies. But, I have only looked in depth at feathers and claw sheaths. Therefore,

more studies need to be undertaken to analyze other types of keratinous fossils and to model taphonomic conditions under which they may have been preserved, which in turn will facilitate our searches for other fossils preserved in this manner. As discussed in Chapter 1, the early evolution of beta-keratin and which organisms first expressed this protein remains to be determined. Testing more fossils with epidermally derived structures for the retention of keratinous remnants would aid in elucidating this evolutionary challenge, one that cannot be met by studying only extant species.

To my knowledge, there has only been one study on the microscopic and molecular preservation of dinosaur skin [70] (see [26] for analyses of fossil marine 'reptile' skin). This study analyzed the skin from a hadrosaur mummy (specimen MRF-03, *Edmontosaurus sp.)* from the Hell Creek Formation of North Dakota. This study identified remnants of organic molecules; however the origin of these organics cannot be identified due to limitation of the methods utilized [2,70]. It was proposed that the soft-tissue of this specimen was replaced by mineral precipitation resulting in the partial preservation of the epidermis [70].

Most dinosaur skin fossils are described as impression fossils (e.g., [71–74]). This term suggests that no original tissue remains, but rather that these are preserved as imprints in a sediment matrix surrounding the skin, much like a footprint in beach sands [75–77]. However, an alternative matrix and mode of preservation may be a biofilm covering the skin as has been demonstrated in other fossils, e.g. encasement of fish [78]. My preliminary data (not included in this dissertation) on fossilized skin from an *Edmontosaurus annectens* specimen (NCSM 23119) suggest that the skin is not a true impression because it differs in texture (Figure 3) and composition (SEM-EDS data not shown) compared to the surrounding sediment. Whether actual skin remnants have been retained or the skin is preserved as a cast and mold fossil in a mineral film and/or a biofilm requires further analyses, but if original components remain, this dissertation shows that beta-keratin of archosaurs is a good target. Keratinous fossils are not only rarer and thus more difficult to acquire permission for destructive analyses than are bony elements, but usually the samples are extremely limited and minute. Therefore, they require very different sample preparation techniques, which vary not only from those used with bone but also between each type of keratinous fossil. For example, the fossil claw material analyzed in Chapter 6 was preserved in three-dimensions and able to be separated from the surrounding coarse sand grains, which is required for most destructive analytical methods. Fossil feather samples, on the

other hand, are more two-dimensional and intimately associated with the surrounding sediment (similar to the *Gansus yumenensis* feather in Chapter 2). More work needs to be conducted on sample preparation methods to optimize separation of fossil material from sediments and subsequently results for each type of fossil. This will also be crucial for testing significantly older fossils, as discussed above, to determine in which lineage beta-keratin arose. Preliminary trials suggest that subjecting keratinous fossils to hydrofluoric acid (HF) aids in separating the fossil material from the surrounding sediment. I selected to try HF because of its ability to break done silica products but *not* sulfur-containing organics, which include the sulfur containing residues of beta-keratins. This method is frequently employed to isolate palynomorphs (e.g. [79]) and coal research studies (e.g. [80]).

The small sample size of most fossil keratin samples also precludes studies requiring whole protein extract, such as enzyme-linked immunosorbent assay (ELISA), Western Blot and mass spectrometry. Instead, mass spectrometry coupled with immunoprecipitation assays can be conducted to further characterize the antibody and determine more specifically what proteins the antibody is binding.

Lastly, the importance and need for actualistic experiments must be emphasized (as mentioned above). Fossils are the end product of a natural experiment lasting tens of millions of years. Every fossil represents a disruption of normal degradation processes. However, we know very little about how those processes are altered and the mechanisms leading to soft tissue preservation. But because degradation must be halted early in the decay process, this means taphonomic studies on soft tissue preservation are amenable to being tested in the lab. Understanding the transition of tissues from the biosphere to geosphere will provide data necessary for addressing many paleontological discussions, especially controversial topics.

References

1. Schweitzer, M. H., Wittmeyer, J. L., Horner, J. R. & Toporski, J. K. 2005 Soft-Tissue Vessels and Cellular Preservation in Tyrannosaurus rex. *Science* **307**, 1952–1955.
2. Schweitzer, M. H., Avci, R., Collier, T. & Goodwin, M. B. 2008 Microscopic, chemical and molecular methods for examining fossil preservation. *Comptes Rendus Palevol* **7**, 159–184. (doi:10.1016/j.crpv.2008.02.005)
3. Cadena, E. & Schweitzer, M. 2012 Variation in osteocytes morphology vs bone type in turtle shell and their exceptional preservation from the Jurassic to the present. *Bone* **51**, 614–620.
4. Zheng, W. & Schweitzer, M. H. 2012 Chemical analyses of fossil bone. In *Forensic Microscopy for Skeletal Tissues: Methods and Protocols, Methods in Molecular Biology* (ed L. S. Bell), pp. 153–72. [cited 2015 Mar. 23]. (doi:10.1007/978-1-61779-977-8_10)
5. Schweitzer, M. h, Starkey, J. R., Cano, R. J. & Horner, J. R. 1994 Evidence for preservation of collagens, DNA and other biomolecules in undemineralized bone from Tyrannosaurus rex. *Matrix Biol.* **14**, 363–364.
6. Mary Higby, S., Johnson, C., Zocco, T. G., Horner, J. R. & Starkey, J. R. 1997 Preservation of Biomolecules in Cancellous Bone of Tyrannosaurus rex. *J. Vertebr. Paleontol.* **17**, 349–359.
7. Schweitzer, M. H., Wittmeyer, J. L. & Horner, J. R. 2007 Soft tissue and cellular preservation in vertebrate skeletal elements from the Cretaceous to the present. *Proc. R. Soc. B Biol. Sci.* **274**, 183–197. (doi:10.1098/rspb.2006.3705)
8. Mary Higby, S., Suo, Z., Avci, R., Asara, J. M., Allen, M. A., Arce, F. T. & Horner, J. R. 2007 Analyses of Soft Tissue from Tyrannosaurus rex Suggest the Presence of Protein. *Science* **316**, 277–280. (doi:10.2307/20036013)
9. Schweitzer, M. H., Zheng, W., Cleland, T. P. & Bern, M. 2013 Molecular analyses of dinosaur osteocytes support the presence of endogenous molecules. *Bone* **52**, 414–23. (doi:10.1016/j.bone.2012.10.010)
10. Hitchcock, E. 1841 *Final Report on the Geology of Massachusetts: In Four Parts: I. Economical Geology. II. Scenographical Geology. III. Scientific Geology. IV. Elementary Geology. With an Appended Catalogue of the Specimens of Rocks and Minerals in the State Collection, Vol*. J.S. & C. Adams. [cited 2014 Jul. 10].

11. Moyer, A. E., Zheng, W., Johnson, E. A., Lamanna, M. C., Li, D.-Q., Lacovara, K. J. & Schweitzer, M. H. 2014 Melanosomes or microbes: testing an alternative hypothesis for the origin of microbodies in fossil feathers. *Sci. Rep.* **4**, 4233. (doi:10.1038/srep04233)
12. Lindgren, J. et al. 2015 Interpreting melanin-based coloration through deep time: a critical review. *Proc. R. Soc. B Biol. Sci.* **282**, 20150614. (doi:10.1098/rspb.2015.0614)
13. Schweitzer, M. H., Lindgren, J. & Moyer, A. E. 2015 Melanosomes and ancient coloration re-examined: A response to Vinther 2015 (DOI 10.1002/bies.201500018). *BioEssays* , n/a–n/a. (doi:10.1002/bies.201500061)
14. Schweitzer, M. H., Moyer, A. E. & Zheng, W. 2016 Testing the Hypothesis of Biofilm as a Source for Soft Tissue and Cell-Like Structures Preserved in Dinosaur Bone. *PLoS One* **11**, e0150238. (doi:10.1371/journal.pone.0150238)
15. Vinther, J., Briggs, D. E. G., Prum, R. O. & Saranathan, V. 2008 The colour of fossil feathers. *Biol. Lett.* **4**, 522–525. (doi:10.1098/rsbl.2008.0302)
16. Vinther, J., Briggs, D. E. G., Clarke, J., Mayr, G. & Prum, R. O. 2010 Structural coloration in a fossil feather. *Biol. Lett.* **6**, 128–131. (doi:10.1098/rsbl.2009.0524)
17. Zhang, F., Kearns, S. L., Orr, P. J., Benton, M. J., Zhou, Z., Johnson, D., Xu, X. & Wang, X. 2010 Fossilized melanosomes and the colour of Cretaceous dinosaurs and birds. *Nature* **463**, 1075–1078. (doi:http://www.nature.com/nature/journal/v463/n7284/suppinfo/nature08740_S1.html)
18. Carney, R. M., Vinther, J., Shawkey, M. D., D'Alba, L. & Ackermann, J. 2012 New evidence on the colour and nature of the isolated Archaeopteryx feather. *Nat. Commun.* **3**, 637. (doi:10.1038/ncomms1642)
19. Li, Q., Gao, K. Q., Vinther, J., Shawkey, M. D., Clarke, J. A., D'Alba, L., Meng, Q., Briggs, D. E. & Prum, R. O. 2010 Plumage color patterns of an extinct dinosaur. *Science* **327**, 1369–1372. (doi:science.1186290 [pii]10.1126/science.1186290 [doi])
20. Clarke, J. A., Ksepka, D. T., Salas-Gismondi, R., Altamirano, A. J., Shawkey, M. D., D'Alba, L., Vinther, J., DeVries, T. J. & Baby, P. 2010 Fossil Evidence for Evolution of the Shape and Color of Penguin Feathers. *Science* **330**, 954–957. (doi:10.1126/science.1193604)
21. Li, Q. et al. 2012 Reconstruction of Microraptor and the Evolution of Iridescent Plumage. *Science* **335**, 1215–1219. (doi:10.1126/science.1213780)

22. Vitek, N., Vinther, J., Schiffbauer, J., Briggs, D. G. & Prum, R. 2013 Exceptional three-dimensional preservation and coloration of an originally iridescent fossil feather from the Middle Eocene Messel Oil Shale. *Paläontologische Zeitschrift* , 1–11. (doi:10.1007/s12542-013-0173-5)
23. Li, Q., Clarke, J. A., Gao, K.-Q., Zhou, C.-F., Meng, Q., Li, D., D'Alba, L. & Shawkey, M. D. 2014 Melanosome evolution indicates a key physiological shift within feathered dinosaurs. *Nature* (doi:10.1038/nature12973)
24. Davis, P. G. & Briggs, D. E. G. 1995 Fossilization of feathers. *Geology* **23**, 783–786. (doi:10.1130/0091-7613(1995)023<0783:fof>2.3.co;2)
25. Manning, P. L. et al. 2013 Synchrotron-based chemical imaging reveals plumage patterns in a 150 million year old early bird. *J. Anal. At. Spectrom.* **28**, 1024–1030. (doi:10.1039/C3JA50077B)
26. Lindgren, J. et al. 2014 Skin pigmentation provides evidence of convergent melanism in extinct marine reptiles. *Nature* (doi:10.1038/nature12899)
27. Vinther, J. 2015 A guide to the field of palaeo colour: Melanin and other pigments can fossilise: Reconstructing colour patterns from ancient organisms can give new insights to ecology and behaviour. *BioEssays* **37**, 643–656. (doi:10.1002/bies.201500018)
28. Vinther, J. 2015 Fossil melanosomes or bacteria? A wealth of findings favours melanosomes: Melanin fossilises relatively readily, bacteria rarely, hence the need for clarification in the debate over the identity of microbodies in fossil animal specimens. *Bioessays* **38**, 220–5. (doi:10.1002/bies.201500168)
29. Xu, X. et al. 2015 A bizarre Jurassic maniraptoran theropod with preserved evidence of membranous wings. *Nature* **521**, 70–3. (doi:10.1038/nature14423)
30. Colleary, C. et al. 2015 Chemical, experimental, and morphological evidence for diagenetically altered melanin in exceptionally preserved fossils. *PNAS* , 1509831112–. (doi:10.1073/pnas.1509831112)
31. Huang, J., Wang, X., Hu, Y., Liu, J., Peteya, J. A. & Clarke, J. A. 2016 A new ornithurine from the Early Cretaceous of China sheds light on the evolution of early ecological and cranial diversity in birds. *PeerJ* **4**, e1765. (doi:10.7717/peerj.1765)
32. McGraw, K. J. 2006 Mechanics of Melanin-Based Coloration. In *Bird Coloration: Mechanisms and measurements* (eds G. E. Hill & K. J. McGraw), pp. 243–294. London:

Harvard University Press.

33. Liu, S. Y., Shawkey, M. D., Parkinson, D., Troy, T. P. & Ahmed, M. 2014 Elucidation of the chemical composition of avian melanin. *RSC Adv.* **4**, 40396–40399. (doi:10.1039/C4RA06606E)
34. Simon, J. D., Hong, L. & Peles, D. N. 2008 Insights into Melanosomes and Melanin from Some Interesting Spatial and Temporal Properties†. *J. Phys. Chem. B* **112**, 13201–13217. (doi:10.1021/jp804248h)
35. Hill, G. E. & McGraw, K. J. 2006 *Bird Coloration: Function and evolution*. Harvard University Press.
36. Hollingworth, N. T. J. & Barker, M. J. 1991 Colour pattern preservation in the fossil record: taphonomy and diagenetic significance. In *The Processes of Fossilization* (ed S. K. Donovan), pp. 105–119. New York: Columbia University Press.
37. Riley, P. A. 1997 Melanin. *Int. J. Biochem. Cell Biol.* **29**, 1235–1239. (doi:10.1016/S1357-2725(97)00013-7)
38. Shawkey, M. D. & Hill, G. E. 2005 Carotenoids need structural colours to shine. *Biol. Lett.* **1**, 121–4. (doi:10.1098/rsbl.2004.0289)
39. Prum, R. O., Dufresne, E. R., Quinn, T. & Waters, K. 2009 Development of colour-producing β-keratin nanostructures in avian feather barbs. *J. R. Soc. Interface* **6**, S253–S265. (doi:10.1098/rsif.2008.0466.focus)
40. Prum, R. O. 1999 The anatomy and physics of avian structural colours. In *Proceedings in 22nd International Ornithology Congress* (eds N. Adams & R. Slotow), pp. 1633–1653. University of Natal: Durban.
41. Cuervo, J. J., Belliure, J. & Negro, J. J. 2016 Coloration reflects skin pterin concentration in a red-tailed lizard. *Comp. Biochem. Physiol. B. Biochem. Mol. Biol.* **193**, 17–24. (doi:10.1016/j.cbpb.2015.11.011)
42. Solano, F. 2014 Melanins: Skin Pigments and Much More—Types, Structural Models, Biological Functions, and Formation Routes. *New J. Sci.* , 1–28. (doi:10.1155/2014/498276)
43. Lindgren, J., Uvdal, P., Sjövall, P., Nilsson, D. E., Engdahl, A., Schultz, B. P. & Thiel, V. 2012 Molecular preservation of the pigment melanin in fossil melanosomes. *Nat Commun* **3**, 1–7.

(doi:http://www.nature.com/ncomms/journal/v3/n5/suppinfo/ncomms1819_S1.html)

44. Lindgren, J. et al. 2015 Molecular composition and ultrastructure of Jurassic paravian feathers. *Sci. Rep.* **5**, 13520. (doi:10.1038/srep13520)
45. Glass, K. et al. 2012 Direct chemical evidence for eumelanin pigment from the Jurassic period. *Proc. Natl. Acad. Sci.* **109**, 10218–10223.
46. Glass, K. et al. 2013 Impact of diagenesis and maturation on the survival of eumelanin in the fossil record. *Org. Geochem.* **64**, 29–37. (doi:10.1016/j.orggeochem.2013.09.002)
47. Simpson, M. J., Glass, K. E., Wilson, J. W., Wilby, P. R., Simon, J. D. & Warren, W. S. 2013 Pump–Probe Microscopic Imaging of Jurassic-Aged Eumelanin. *J. Phys. Chem. Lett.* **4**, 1924–1927. (doi:10.1021/jz4008036)
48. Plonka, P. M. & Grabacka, M. 2006 Melanin synthesis in microorganisms--biotechnological and medical aspects. *Acta Biochim Pol* **53**, 429–443. (doi:20061329 [pii])
49. Buick, R. 1990 Microfossil recognition in Archean rocks; an appraisal of spheroids and filaments from a 3500 m.y. old chert-barite unit at North Pole, Western Australia. *Palaios* **5**, 441–459.
50. Westall, F., de Wit, M. J., Dann, J., van der Gaast, S., de Ronde, C. E. J. & Gerneke, D. 2001 Early Archean fossil bacteria and biofilms in hydrothermally-influenced sediments from the Barberton greenstone belt, South Africa. *Precambrian Res.* **106**, 93–116.
51. Walsh, M. W. 1992 Microfossils and possible microfossils from the early archean onverwacht group, Barberton mountain land, South Africa. *Precambrian Res.* **54**, 271–293. (doi:10.1016/0301-9268(92)90074-X)
52. Schopf, J. W., Kudryavtsev, A. B., Czaja, A. D. & Tripathi, A. B. 2007 Evidence of Archean life: Stromatolites and microfossils. *Precambrian Res.* **158**, 141–155. (doi:10.1016/j.precamres.2007.04.009)
53. Martill, D. M. & Wilby, P. R. 1994 Lithified prokaryotes associated with fossil soft tissues from the Santana Formation (Cretaceous) of Brazil. *Kaupia* , 71–77.
54. Wilby, P. R., Briggs, D. E. G., Bernier, P. & Gaillard, C. 1996 Role of microbial mats in the fossilization of soft tissues. *Geology* **24**, 787–790. (doi:10.1130/0091-7613(1996)024)
55. Liebig, K., Westall, F. & Schmitz, M. 1996 A study of fossil microstructures from the Eocene Messel Formation using transmission electron microscopy. *N. Jb. Geol. Pala¨ont.*

Mh **4**, 218–231.

56. McNamara, M. E., Orr, P. J., Kearns, S. L., Alcala, L., Anadon, P. & Penalver Molla, E. 2009 Soft-tissue Preservation in Miocene Frogs from Libros, Spain: Insights into the Genesis of Decay Microenvironments. *Palaios* **24**, 104–117. (doi:10.2110/palo.2008.p08-017r)
57. Franzen, J. L., Aurich, C. & Habersetzer, J. 2015 Description of a Well Preserved Fetus of the European Eocene Equoid Eurohippus messelensis. *PLoS One* **10**, e0137985. (doi:10.1371/journal.pone.0137985)
58. Schweitzer, M. H., Watt, J. A., Avci, R., Knapp, L., Chiappe, L., Norell, M. & Marshall, M. 1999 Beta-keratin specific immunological reactivity in feather-like structures of the Cretaceous Alvarezsaurid, Shuvuuia deserti. *J. Exp. Zool.* **285**, 146–157. (doi:10.1002/(sici)1097-010x(19990815)285:2<146::aid-jez7>3.0.co;2-a)
59. Chiappe, L. M., Norell, M. A. & Clark, J. M. 1998 The skull of a relative of the stem-group bird Mononykus. *Nature* **392**, 275–278. (doi:10.1038/32642)
60. Notbohm, H., Mosler, S., Bodo, M., Yang, C., Lehmann, H., Bätge, B. & Muller, P. K. 1992 Comparative study on the thermostability of collagen I of skin and bone: Influence of posttranslational hydroxylation of prolyl and lysyl residues. *J. Protein Chem.* **11**, 635–643. (doi:10.1007/BF01024964)
61. Collins, M. J., Riley, M. S., Child, A. M. & Turner-Walker, G. 1995 A Basic Mathematical Simulation of the Chemical Degradation of Ancient Collagen. *J. Archaeol. Sci.* **22**, 175–183. (doi:10.1006/jasc.1995.0019)
62. Hay, W. W. 2008 Evolving ideas about the Cretaceous climate and ocean circulation. *Cretac. Res.* **29**, 725–753. (doi:10.1016/j.cretres.2008.05.025)
63. Norell, M. A., Clark, J. M., Chiappe, L. M. & Dashzeveg, D. 1995 A nesting dinosaur. *Nature* **378**, 774–776. (doi:10.1038/378774a0)
64. Clark, J. M., Norell, M. & Chiappe, L. M. 1999 An oviraptorid skeleton from the late Cretaceous of Ukhaa Tolgod, Mongolia, preserved in an avianlike brooding position over an oviraptorid nest. *Am. Museum Novit.* **3265**, 1–36.
65. Cleland, T. P. et al. 2015 Mass Spectrometry and Antibody-Based Characterization of Blood Vessels from Brachylophosaurus canadensis. *J. Proteome Res.* (doi:10.1021/acs.jproteome.5b00675)

66. Kaye, T. G., Gaugler, G. & Sawlowicz, Z. 2008 Dinosaurian Soft Tissues Interpreted as Bacterial Biofilms. *PLoS One* **3**, 1–7. (doi:10.1371/journal.pone.0002808)
67. Sagemann, J., Bale, S. J., Briggs, D. E. G. & Parkes, R. J. 1999 Controls on the formation of authigenic minerals in association with decaying organic matter: an experimental approach. *Geochim. Cosmochim. Acta* **63**, 1083–1095. (doi:http://dx.doi.org/10.1016/S0016-7037(99)00087-3)
68. Ferris, F. G. 2000 Microbe-metal interactions in sediments. In *Microbial Sediments* (eds R. Riding & S. M. Awramik), pp. 121–126. Springer Berlin Heidelberg.
69. Chen, C.-F., Foley, J., Tang, P.-C., Li, A., Jiang, T. X., Wu, P., Widelitz, R. B. & Chuong, C. M. 2015 Development, regeneration, and evolution of feathers. *Annu. Rev. Anim. Biosci.* **3**, 169–95. (doi:10.1146/annurev-animal-022513-114127)
70. Manning, P. L. et al. 2009 Mineralized soft-tissue structure and chemistry in a mummified hadrosaur from the Hell Creek Formation, North Dakota (USA). *Proc. Biol. Sci.* **276**, 3429–37. (doi:10.1098/rspb.2009.0812)
71. Schweitzer, M. H. 2011 Soft Tissue Preservation in Terrestrial Mesozoic Vertebrates. *Annu. Rev. Earth Planet. Sci.* **39**, 187–216. (doi:doi:10.1146/annurev-earth-040610-133502)
72. Bell, P. R. 2012 Standardized Terminology and Potential Taxonomic Utility for Hadrosaurid Skin Impressions: A Case Study for Saurolophus from Canada and Mongolia. *PLoS One* **7**, e31295.
73. Czerkas, S. 1994 The History and Interpretations of Sauropod Skin Impressions. *GAIA* , 173–182.
74. Davis, M. 2012 Census of dinosaur skin reveals lithology may not be the most important factor in increased preservation of hadrosaurid skin. *Acta Palaeontol. Pol.* **59**, 601–605. (doi:10.4202/app.2012.0077)
75. Currie, P. J., Nadon, G. C. & Lockley, M. G. 1991 Dinosaur footprints with skin impressions from the Cretaceous of Alberta and Colorado. *Can. J. Earth Sci.* **28**, 102–115. (doi:10.1139/e91-009)
76. Vila, B., Oms, O., Fondevilla, V., Gaete, R., Galobart, A., Riera, V. & Canudo, J. I. 2013 The latest succession of dinosaur tracksites in Europe: Hadrosaur ichnology, track production and palaeoenvironments. *PLoS One* **8**, e72579.

(doi:10.1371/journal.pone.0072579)

77. Gatesy, S. M., Middleton, K. M., Jr, F. A. J. & Shubin, N. H. 1999 Three-dimensional preservation of foot movements in Triassic theropod dinosaurs. **399**, 141–144. (doi:10.1038/20167)

78. Carpenter, K. 2007 How to make a fossil: Part 2 - dinosaur mummies and other soft tissue. *J. Paleontol. Sci.* **1**, 1–10. (doi:JPS.C.07.0001)

79. Higgs, K. T. & Jones, G. L. 2000 Palynological evidence for Mesozoic karst at Piltown, Co. Kilkenny. *Proc. Geol. Assoc.* **111**, 355–362. (doi:10.1016/S0016-7878(00)80091-7)

80. Vaccaro, S. 2011 Demineralization and Desulfurization Process to Generate Clean Coal. *Chem. Eng. Trans.* **21**, 1489–1494. (doi:10.3303/CET1021249)

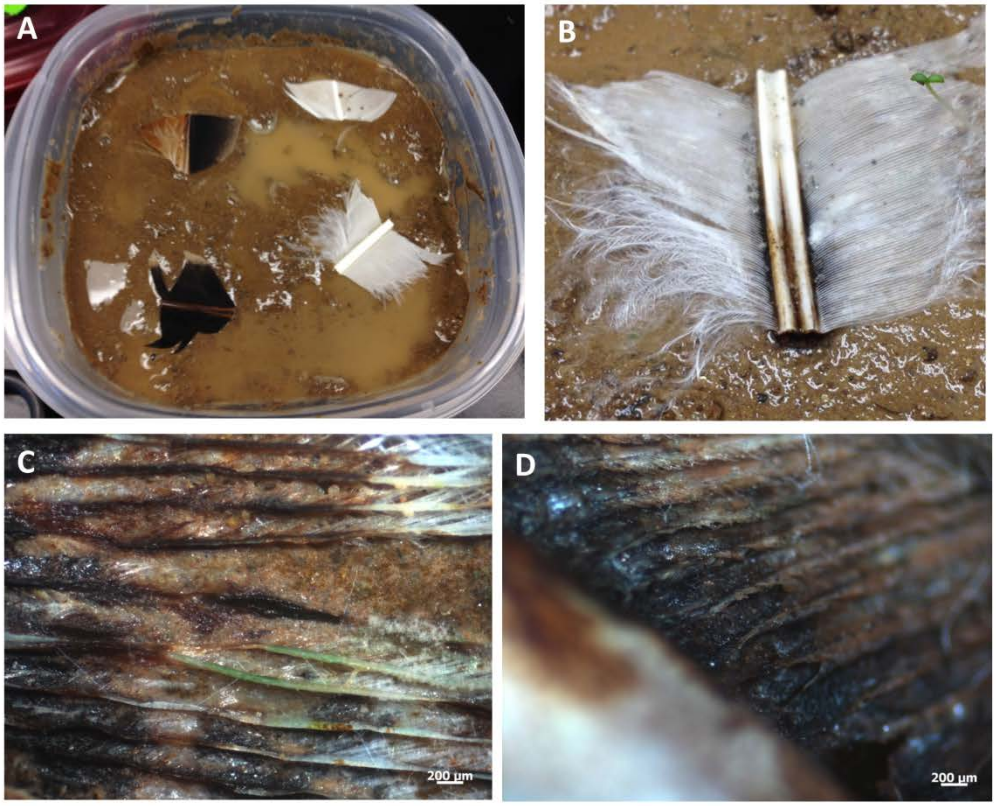

Figure 1. Feather degradation experiment that resulted in the production of a black ‘film’ under and surrounding both pigmented (reddish-brown and black) and unpigmented (white) chicken feathers. A) The initial setup of the experiment using sediment (fine-grained) from the Neuse River. B) Image of one of the white feather pieces after 4 weeks of degradation. Note the presence of a blackened film surrounding the rachis not observed in the initial setup. After 10 weeks of degradation, C) this film could be observed surrounding the barbs of the white feather, D) and the brown barbs (top left feather piece in A). At this magnification, it is impossible to determine what color the original feather was because of the diagenetic changes.

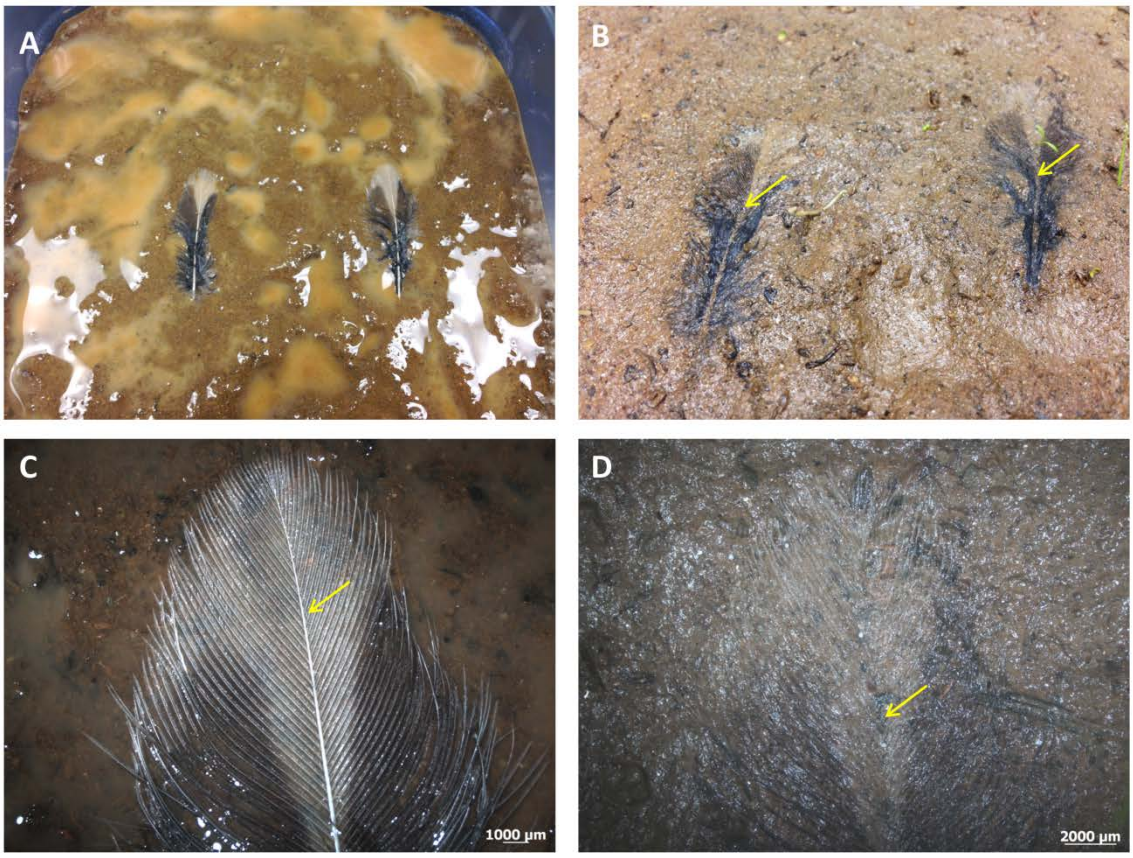

Figure 2. Feather degradation experiment that resulted in the degradation of the rachis before any other parts of the feather. A) Initial setup of feathers with pigmented and unpigmented regions and white rachises, in sediment (coarse-grained) from the Neuse River. B) After 4 weeks of degradation, the white rachises were completely degraded (yellow arrows). C and D) Higher magnification of the distal part of the feather (right feather in A), C) at initial setup and D) after 4 weeks of degradation. Note: The magnifications are the same in C and D.

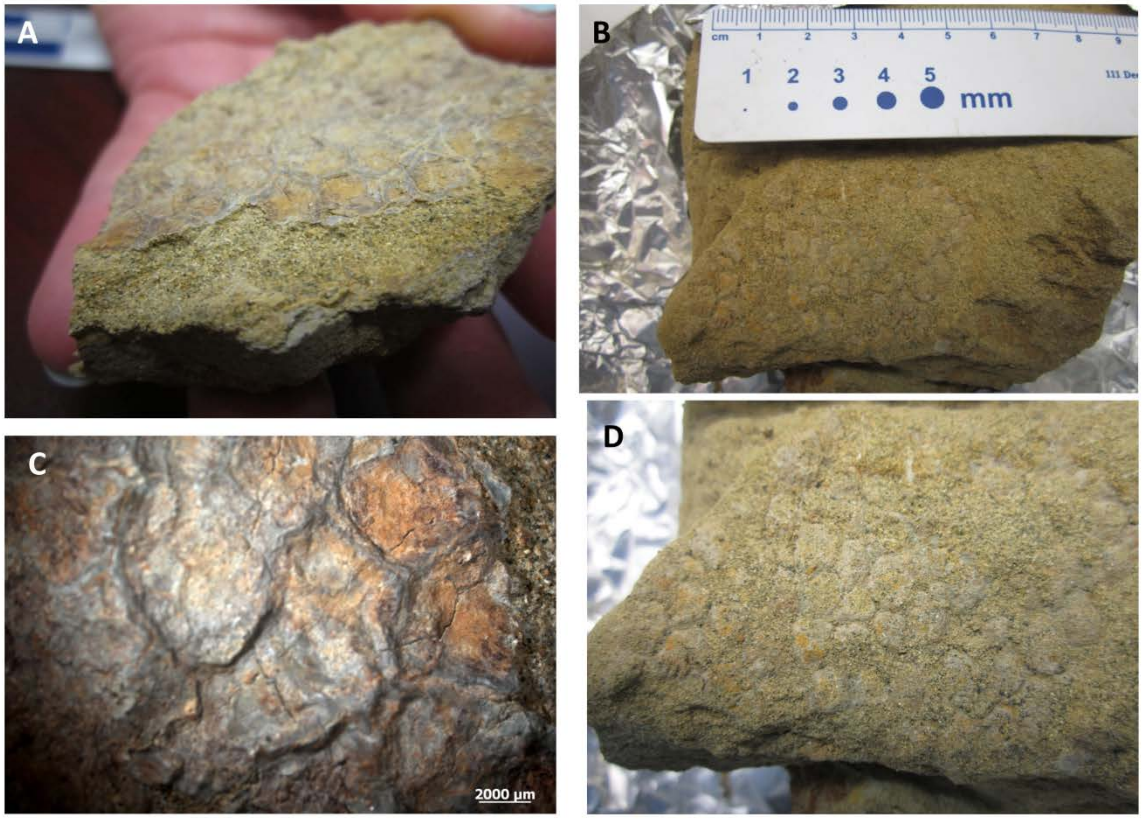

Figure 3. Fossil skin samples from *Edmontosaurus annectens* (NCSM 23119). A and C) A distinct layer with apparent scale 'impressions' is different in color and texture from the underlying sediment. B and D) A second sample of fossil skin from a different region of the specimen demonstrates a different preservational mode, but the skin pattern still differs in texture and color from the sediment.